Archaeological Prospection for Ring-Midden Features in Southeastern New Mexico Using Lidar Data: An Experimental Study

By Michael Heilen, Monica Murrell, Timothy Mills, Nahide Aydin, Phillip Leckman, and Adam Byrd

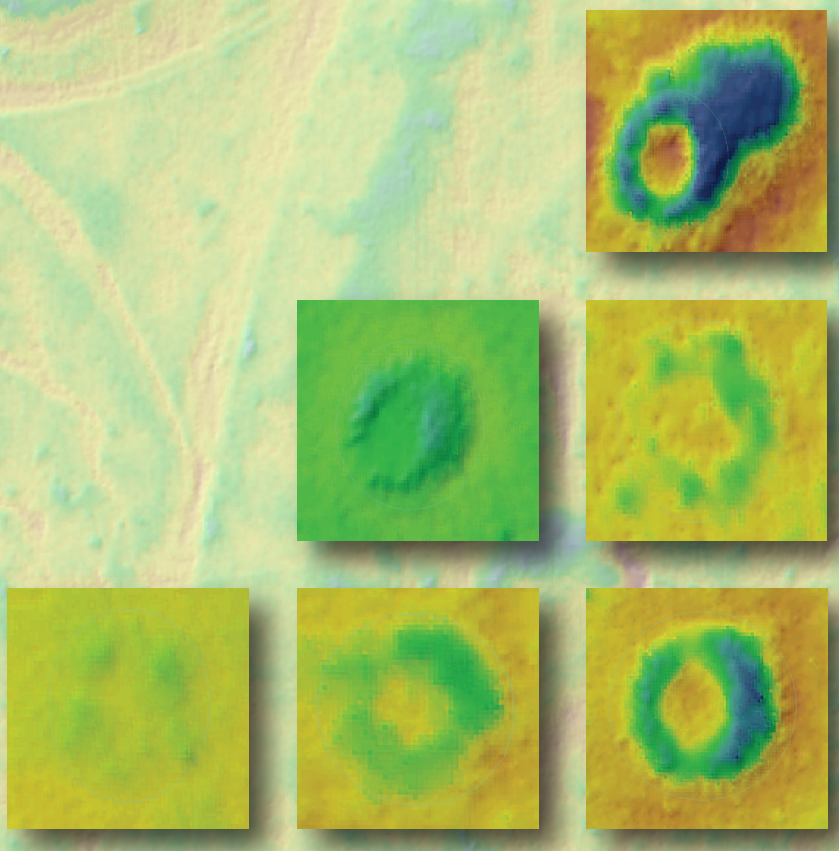

Submitted to

Bureau of Land Management
Carlsbad Field Office
620 E. Greene St.
Carlsbad, NM 88220

Contract No. L08PC90395
Task Order No. L13PD01347

Technical Report 15-33
Statistical Research, Inc.
Albuquerque, New Mexico

Archaeological Prospection for Ring-Midden Features in Southeastern New Mexico Using Lidar Data: An Experimental Study

By Michael Heilen, Monica Murrell, Timothy Mills, Nahide Aydin, Phillip Leckman, and Adam Byrd

Submitted to

Bureau of Land Management
Carlsbad Field Office
620 E. Greene St.
Carlsbad, NM 88220

Contract No. L08PC90395
Task Order No. L13PD01347

Technical Report 15-33
Statistical Research, Inc.
Albuquerque, New Mexico

July 2015

CONTENTS

LIST OF FIGURES

LIST OF TABLES

EXECUTIVE SUMMARY

The U.S. Bureau of Land Management (BLM) contracted with Statistical Research, Inc. (SRI), to conduct an archaeological survey for ring-midden features using lidar data (Contract No. L08PC90395 and Task Order No. L13PD01347). The survey was to be conducted in three localities located in the foothills of the Guadalupe Mountains and Sacramento Mountains of southeastern New Mexico: Azotea Mesa (140 km^2), Box Canyon (166 km^2), and Upper Rio Felix (658 km^2). All three study areas contain a large proportion of land administered by the BLM's Carlsbad Field Office (CFO), but only 8 percent of Azotea Mesa, 6 percent of Box Canyon, and 1 percent of Upper Rio Felix have been inventoried using pedestrian survey methods. Among the most common archaeological features found at sites identified in Azotea Mesa and Box Canyon are ring-midden features. Prior to the current project, ring-midden features had not been identified in Upper Rio Felix. Ring-midden features in southeastern New Mexico consist, in part, of a pile of discarded material (a midden) that is shaped like a ring or doughnut. These feature are interpreted to result from the repeated use of an earth oven to cook food in an earth-covered pit using heated rocks. Each time an earth oven was used, fractured rocks and sediment were removed from the oven and raked out of the way, resulting in the formation of a large, doughnut-shaped (or annular) ring of fire-affected rocks surrounding the earth oven.

The unique shape and prominence of ring middens suggested to the BLM that these features could potentially be identified using remote sensing data rather than attempting to find them through pedestrian survey (which would take decades of effort to complete). Lidar data are remote sensing data that are obtained by systematically scanning a surface with a laser and analyzing the laser's reflection to compute the elevation of a measured surface. These data can be used to create high-resolution topographic maps that can be analyzed in a geographic information system (GIS) to identify and map archaeological and other features across a landscape surface. Under contract with SRI, Surdex collected lidar data for the three project areas between February 14 and March 14, 2014, using an airborne lidar system outfitted with a Leica ALS70-HP SP3 sensor. These data were classified by Surdex following standards developed by the American Society of Photogrammetry and Remote Sensing. Surdex provided both the raw and classified data to SRI for used in the digital survey, along with an acquisition report.

The classified lidar data were used by SRI, along with data on the locations of recorded ring-midden features, to develop an approach to identifying ring-midden features in digital lidar data using GIS software. The locations of recorded sites with ring-midden features were used to develop an approach to visualizing (or recognizing) in a GIS ring-midden features using the lidar data and to create a locational model predicting where within the three study areas ring middens were more or less likely to be located. Observations made on the size and shape characteristics of recorded ring middens were then used to create an automated GIS method for identifying in the lidar data features with shapes and sizes similar to those of ring middens.

Based on results of the locational model, a sample of survey areas was selected from the three study areas and subjected to systematic digital survey. The surveyed area covered a total of 32,965 acres (13,340 ha) and consisted of approximately 19.8 percent of the Azotea Mesa, 17.2 percent of Box Canyon, and 10.0 percent of Upper Rio Felix. The digital survey was conducted within a GIS by an experienced archaeologist who systematically inspected the lidar data for each survey area using a variety of visualization techniques. Each location identified as potentially containing a ring midden using our automated feature identification method was also closely inspected during the survey. Potential ring-midden features identified during digital survey were delineated as polygon features in a GIS and characterized according to key attributes.

Digital survey resulted in the identification of 511 potential ring-midden features (254 identified during digital survey in the Azotea Mesa study area, 155 in the Box Canyon study area, and 102 in the Upper Rio Felix study area), as well as 25 features that could be confused with ring middens because of similarities in

morphology. Thirty-three (6.5 percent) of the potential ring-midden features identified during sample survey were located within previously recorded sites. The remainder were located in areas where sites have yet to be recorded.

Once the survey was complete, a sample of areas where potential ring-midden features had been identified was chosen for field verification. These efforts focused on ground-truthing clusters of features that were of diverse sizes, shapes, and conditions to evaluate how effective the digital survey was in identifying ring-midden features. The results of the field verification confirmed that each feature digitally identified as a potential ring-midden feature was, in fact, a ring-midden feature. In areas where disturbance was common, however, ring-midden features that had very low relief or had shapes altered by disturbance were not properly identified during the digital survey. Overall, these efforts suggested that digital survey using lidar data to find ring-midden features was effective, but that features that had been disturbed and/or were of limited relief were likely to be missed by digital survey. Since digital survey can miss ring-midden features that have been disturbed or are of low relief, as well as features of other types and artifact scatters, digital survey methods are appropriate for project scoping and landscape-level studies but cannot be considered an alternative to Section 106 inventory. We recommend that the remainder of the three study areas be digitally surveyed following the approach developed for this project. This will result in a more complete inventory of ring middens in southeastern New Mexico, which can then be field-checked, recorded, and sampled.

ACKNOWLEDGMENTS

This project was conceived originally by the U.S. Bureau of Land Management and demonstrates excellent foresight in pioneering the use of lidar for identifying and documenting ring-midden features in southeastern New Mexico. We would like to extend special thanks to Martin Stein of the BLM for their guidance and support. We would also like to thank Cornell Rowan, project manager at Surdex who collected the lidar data for the project under contract with Statistical Research, Inc (SRI). Nahide Aydin, Adam Byrd, and Phillip Leckman of SRI provided significant technical support in processing the data in a geographic information system (GIS), developing Python scripts, and in assisting with in the visualization and characterization of ring midden features using lidar data. Nahide Aydin also provided text on the characteristics and acquisition of lidar data. The digital survey was performed by Monica Murrell of SRI. Ground-truthing efforts were carried out by Monica Murrell and Timothy Mills of SRI. Monica Murrell provided text on the environmental and cultural background of southeastern New Mexico. Timothy Mills provided significant insights and report text regarding the archaeological study of ring midden features. Michael Heilen of SRI was the principal investigator for the project and took the lead in designing the project approach, evaluating the lidar data, generating archaeological models, performing data analysis, and reporting on the project results. Robert Heckman of SRI served as the project manager. The report was produced by SRI's publication department. The report was edited by Beth Bishop and Jennifer Shopland. Report graphics were developed by Andrew Saiz and Jacquelyn Dominguez. The layout of the report was produced by KeAndra Begay. As always, Maria Molina of SRI did an outstanding job overseeing the report production.

CHAPTER 1

Project Background and Approach

Introduction

The western portion of the area managed by the U.S. Bureau of Land Management's (BLM's) Carlsbad Field Office (CFO), in southeastern New Mexico, consists of foothills of the Guadalupe Mountains and Sacramento Mountains. This region corresponds roughly to the Sacramento Section of the Southeastern New Mexico Regional Research Design (SNMRRD) (Hogan 2006) and is dramatically different in geology, topography, elevation, and vegetation from the area covered by the Permian Basin Memorandum of Agreement (BLM 2008). The physiography of this rugged area is characterized by canyons and draws ranging in elevation from 3,200 to 6,500 feet (975 to 1,980 m) above mean sea level (AMSL). Thin sediments blanket dolomite and limestone geological formations and support a variety of plant communities, particularly those that include various species of agave (*Agave*) and sotol (*Dasylirion*).

One of the most common archaeological resources found in this area of southeastern New Mexico is the ring-midden feature. Many sites in the area contain of one or more ring middens. Ring middens are sometimes found in association with features or deposits of other types or, in many cases, have been recorded as individual features or clusters of features indicating recurrent use of a locale for specialized plant-processing activities. As is discussed in more detail below, ring-midden features are understood to result from the repeated use of earth ovens to thermally process materials, principally plant foods, for extended periods. Earth ovens probably were used (1) to make plant foods more digestible and palatable and (2) to conserve scarce fuel resources. Repeated cleaning to recover cooked food items and to remove fractured rocks and sediment used in the earth oven often resulted in the formation of a large, doughnut-shaped (annular) ring surrounding the earth oven. Stockpiles of rocks intended for use as heating elements were also occasionally placed adjacent to earth ovens for anticipated future use. As an earth oven was cleaned out and reused several or many times, the annular ring surrounding it became larger and more obtrusive, increasing both the visibility and the prominence of these features from a surface perspective.

In southeastern New Mexico, agave and sotol appear to be the food resources most commonly processed in ring-midden features, although other resources could have been processed in these features as well. The SNMRRD indicates that ring middens first appeared in the region at approximately 3,500 years B.P. and were used more frequently as of approximately 2,500 years B.P. Ring middens were most intensively used in southeastern New Mexico during the ceramic period; indigenous groups, such as the Mescalero Apache, also relied on them for subsistence during the historical period (Figures 1–3). The appearance of ring middens is taken to be one form of evidence for resource intensification in that their use signifies the attempt to derive a greater quantity of subsistence resources per unit area, often in response to social and environmental pressures, such as population packing. In other words, as the population in the region increased and subsistence resources that were more readily available were depleted, earth ovens were used to make greater use of food resources, such as agave and sotol, that require extended cooking time to be detoxified and rendered digestible (Wandsnider 1997). Moreover, earth ovens conserve fuel by transferring heat created through fuel combustion to rocks placed within the oven that slowly radiate the heat. Sediment used to cover the oven functions to insulate its contents from heat loss. These performance characteristics of earth ovens make the greatest use of limited fuel resources, particularly as these resources are depleted in a region as a result of increased settlement and land use.

Figure 1. "Filling the Pit." Edward S. Curtis, Spring 1906, south of Black River; NAA Neg. No. 76-4670, SIRIS No. NAA INV 3012400; permission pending.

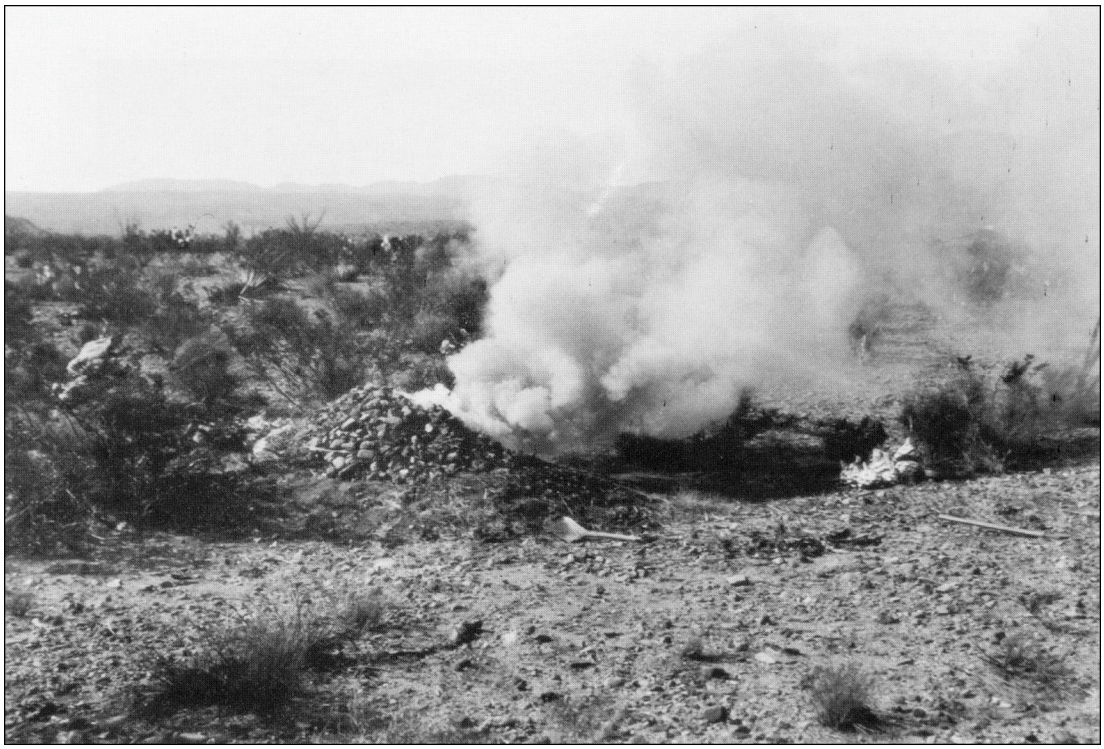

Figure 2. "Heating the stones for cooking the century plants." Pliny E. Goddard, 1914, Calva, AMNH Neg. No. 242716; permission pending.

Figure 3. "The pit containing the century plants while cooking." Pliny E. Goddard, 1914, Calva, AMNH Neg. No. 242720; permission pending.

One of the great advantages in the study of ring middens is that they are highly visible on the landscape and exhibit distinct morphology consisting of an annular midden surrounding a central depression. The topographic prominence and characteristic morphology of ring middens suggested to the BLM that, in the absence of pedestrian survey, ring middens could be identified digitally through examination of high-resolution lidar data. These remote-sensing data are obtained by systematically scanning a surface with a laser and by analyzing the laser's reflection to compute the elevation and other properties of a measured surface. The collection of such data thus permits the creation of high-resolution topographic data sets that can be used to identify and map archaeological and other features across a landscape surface.

The BLM contracted with Statistical Research, Inc. (SRI), to conduct an archaeological survey using lidar in three localities located west and northwest of Carlsbad, New Mexico: Azotea Mesa, Box Canyon, and Upper Rio Felix. The Azotea Mesa study area is approximately 54 square miles (140 km^2), the Box Canyon study area is approximately 64 square miles (166 km^2), and the Upper Rio Felix study area is approximately 254 square miles (658 km^2) (Figure 4). Each of the three study areas contains one or more entire drainages. These include both named and unnamed tributaries of Box Canyon, Rio Felix, and the West Fork Little McKittrick Draw. This report details the approach, methods, and results of this survey.

None of the three study areas, all of which contain a large proportion of land administered by the BLM, has been completely surveyed. In fact, only 8 percent of Azotea Mesa, 6 percent of Box Canyon, and 1 percent of Upper Rio Felix have been surveyed. At the outset of this project, pedestrian survey had identified a total of 127 sites in the Azotea Mesa study area, 84 of them (66 percent) containing one or more ring-midden features. Most of the remaining sites consisted of small fire-cracked rock (FCR) features; a few contained caves or rockshelters. In the Box Canyon study area, 24 sites had been identified; 15 of them (63 percent) contained one or more ring-midden features. Only 8 sites had been identified in the Upper Rio Felix study area; none of these was reported to contain one or more ring-midden features.

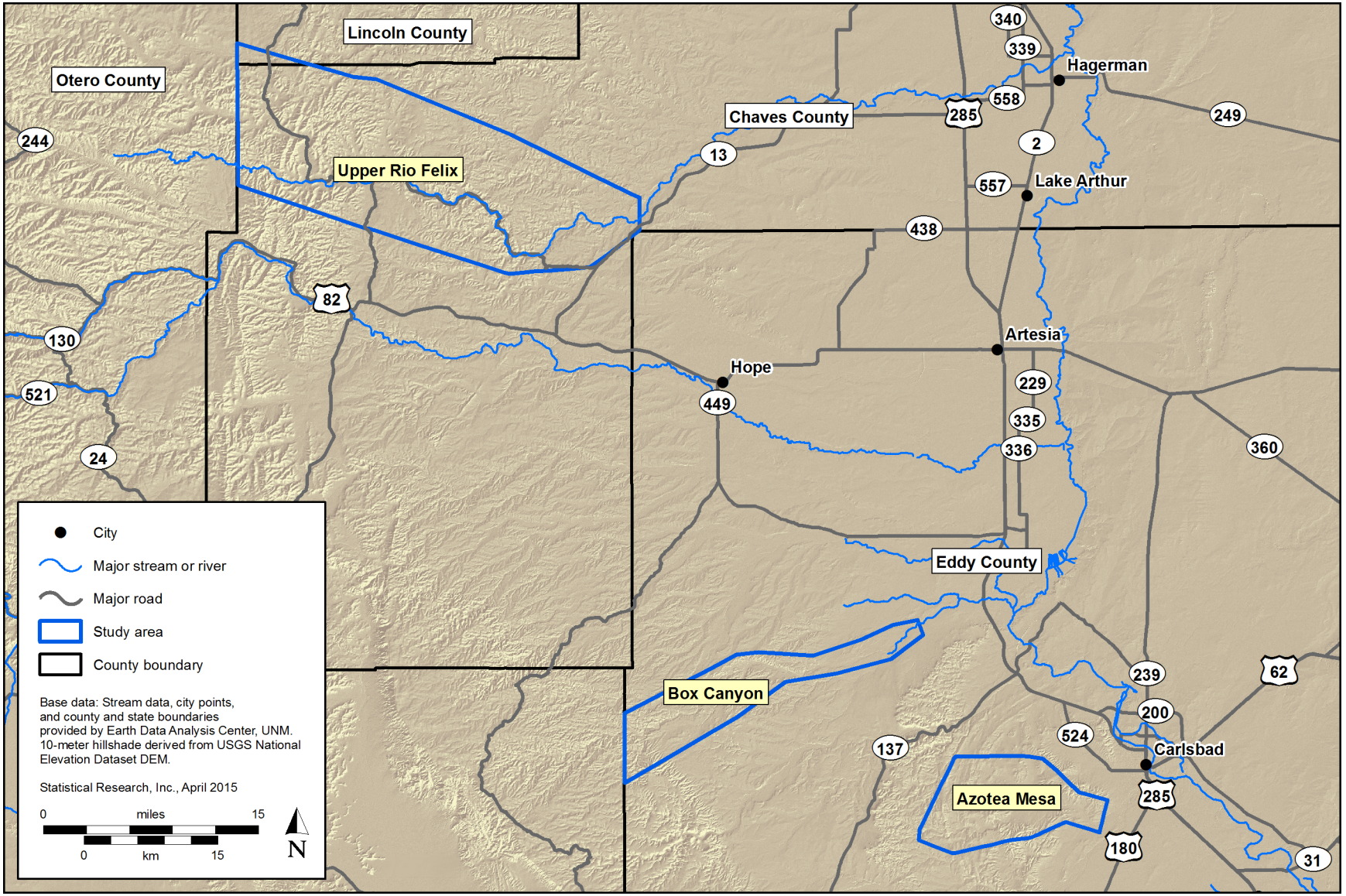

Figure 4. Map of the project location, showing the three study areas: Azotea Mesa, Box Canyon, and Upper Rio Felix.

The remainder of this chapter provides an outline of the project approach and goals, a synopsis of ring-midden research, a description of how lidar data were obtained for the project, a summary of project findings, and a description of how the report is organized.

Project Goals and Approach

The purpose of this project was (1) to collect, for each of the three study areas, lidar data of resolution sufficient for identifying ring-midden features and (2) to conduct digital survey to identify ring-midden features using the lidar data. A field-verification component was included to test the validity of digital identifications. Because of the experimental nature of the project, the degree to which ring middens would be visible in the lidar data and which approaches would work best in identifying ring-midden features through digital survey were unknown at the outset. The project demonstrated that ring-midden features are indeed visible in the lidar data and resulted in the identification of more than 500 ring-midden features. The project also provides a systematic digital approach to visualizing, identifying, and measuring ring-midden features using lidar data. Therefore, the project provides important information on the distribution of ring-midden features in southeastern New Mexico that can be used to improve the preservation and interpretation of this significant and fascinating heritage resource.

To accomplish the goals of this project, we organized our interpretation and inventory of ring middens present within the lidar data into a series of seven iterative stages, as follows:

1. *Identification of ring-midden features within the study area at sites where ring middens have been recorded*. To confidently identify unrecorded ring middens in the lidar data, we first had to determine whether and how we could identify the features in the lidar data at locations where they have been recorded. This was achieved by examining multiple transformations of the lidar elevational data, including hillshade representations, local relief models (LRMs), and topographic-position indexes (TPIs) (see Chapter 3) as well as lidar intensity data in site areas where ring middens have been identified. At the time of this study, a total of 99 sites with one or more ring middens had been recorded in two of the study areas (84 in the Azotea Mesa study area and 15 in the Box Canyon study area), whereas no sites with ring midden(s) had been recorded in the Upper Rio Felix study area. Where possible, site maps and other recorded information were used to verify the identification of ring middens in the lidar data. Features of other types that could be confused with rock rings were also identified for comparison.

2. *Characterization of ring-midden features*. Ring middens identified in the lidar data during Stage 1 (above) were characterized quantitatively in terms of their size, morphology, and topographic setting as well as characteristics of the lidar point cloud corresponding to each feature (i.e., lidar intensity, return number, and location). Characterization enabled parameterization of ring middens as they appear in lidar data, identification of settings where they are likely to be present, and development of a decision-tree model for the classification and identification of ring middens in the lidar data.

3. *Development of a sensitivity model and a decision-tree classification scheme for ring middens.* To better understand where ring middens may be located within the study area and to design our digital survey of the lidar data, we constructed a sensitivity model for ring-midden location using the recorded locations of sites with ring middens. Protocols and geographic information system (GIS) variables that SRI developed recently for the Southern New Mexico BLM Sensitivity Modeling Project (Heilen et al. 2013) were used to develop and validate the model. The model was divided into high- and low-sensitivity zones representing the likelihood, in any part of the study areas, that ring middens would be present. This effort provided a preliminary statistical characterization of where ring middens are more or less likely to be found in unsurveyed areas. The sensitivity model identifies broad zones where ring middens are more or less likely to be present, as determined from their environmental associations. A separate decision-tree classification model was also constructed in an attempt to identify individual

ring-midden features by identifying features in the lidar data that are consistent with the morpohological characteristics of ring middens, as identified in Stage 2 of the project approach.

4. *Digital sample survey.* For the purposes of collecting and organizing lidar data for the project, Surdex (see below) divided each of the three study areas into a grid of square tiles measuring 2,000 by 2,000 feet (610 by 610 m). The tile index supplied by Surdex for the three study areas was used as a sampling frame for selecting land parcels for digital survey using the results of the sensitivity model developed in Stage 3 (above). Survey sample tiles were selected on the basis of the percentage of land area within each tile consisting of high- or low-sensitivity zone.

   For each tile in each of the three study areas, we calculated the percentage of its area covered by high-sensitivity zone and the percentage of its area covered by low-sensitivity zone. We then identified, per study area, which tiles had the largest percentages of high-sensitivity zone and which tiles had the smallest percentages of high-sensitivity zone. We then selected a random sample of tiles based on the percentage of high-sensitivity zone in each tile, such that 75 percent of tiles in each study area's survey sample consisted of tiles with a large percentage of high-sensitivity zone and the remaining 25 percent of the sample tiles consisted primarily of low-sensitivity zone. Tiles that had been inspected during an initial pilot study were removed from consideration to allow us to cover more area and to avoid reinspecting areas that had already been documented for ring middens.

   This sample-selection process resulted in a sample of approximately 19.8 percent for digital survey from the Azotea Mesa study area and a 17.2 percent sample from the Box Canyon study area. Because of its much larger size and low archaeological sensitivity, in comparison to Azotea Mesa and Box Canyon, a 10 percent sample of the Upper Rio Felix study area was selected for digital survey. Overall, in terms of acreage, 32 percent of survey area consisted of high-sensitivity zone and 68 percent consisted of low-sensitivity zone.

   This sampling approach enabled the search effort to focus on areas of the landscape, in each of the three study areas, most likely to contain ring middens and provided an opportunity to test and refine the sensitivity model. Digital sample survey consisted of (1) systematic visual inspection of lidar-derived GIS layers, including hillshades, classified images, and other available remote sensing data (e.g., aerial photographs) and (2) visual inspection and characterization of possible ring-midden features identified by the decision-tree classification model. Potential ring middens investigated during digital survey were represented as polygons and were attributed according to shape characteristics and the degree of feature definition. The high side of each ring midden was also recorded, given that many ring middens are higher on one side.

5. *Evaluation of digital-survey results.* Survey results were evaluated through statistical analysis of the morphology and environmental setting of potential ring middens identified during digital survey. The morphological and locational attributes of potential ring middens identified during Stages 3 and 4 were compared statistically with the attributes of known ring middens identified during Stage 1. This comparison allowed us to detect outliers and anomalous cases and to further define the potential range of variation in ring-midden morphology and location. Evaluation allowed us to categorize ring middens according to size, elevation, and setting for field-verification efforts.

6. *Field verification*. A sample of possible ring middens identified during sample survey was selected for field verification. The sample was chosen to represent the range in variation of possible ring middens identified during the digital survey, taking into account limiting factors such as accessibility and land ownership. Because of practical limitations on the amount of fieldwork that could be conducted with the budgeted field effort, special attention was paid to inspecting clusters of ring middens of variable shape and definition so that more time could be spent examining potential ring-midden features, rather than traveling between widely spaced feature locations. Field-checked locations included recorded sites with known ring middens as well as locations not yet subjected to pedestrian survey and, therefore, where no sites had been recorded. Field-verification efforts involved field identification and inspection of features identified as possible ring middens and measurement of their physical attributes. Ring middens not identified during digital survey but identified during field verification were also recorded; this recording

enabled the identification of conditions and contexts where ring middens are difficult to observe in lidar data. Laboratory of Anthropology site-report forms were completed for sites visited. Field-verification results were evaluated to determine the accuracy of possible ring-midden identifications made during automated feature extraction and digital survey. Except for one case where a feature was considered unlikely to be a ring midden, all features visited in the field were verified as ring-midden features.

7. *Model evaluation and refinement*. The sensitivity model was evaluated using the results of the digital survey. Efforts were made to refine the model during this stage on the basis of the results of the digital survey, but these efforts did not result in a model that performed better than the original model.

The Archaeological Study of Ring Middens

On the whole, the study of ring middens has developed from the more general investigation of burned-rock features. Prewitt (1991:26–27) has described the history of study of burned-rock features in terms of six distinct stages: (1) recognition in the early 1900s, when burned-rock features were initially described in archaeological publications; (2) the pre–Works Progress Administration (WPA) period, when the first systematic excavations took place; (3) early investigations and involvement by academics in the late 1920s; (4) the WPA period, which resulted in an interval of elevated funding and intensified research; (5) a curtailed period of activity from World War II until the 1960s; and (6) the current interval, which is associated largely with federal and state conservation efforts arising since the 1960s with the development of cultural resource management programs and the passage of the National Historic Preservation Act of 1966. Although myriad types of burned-rock features were initially identified and described, throughout all of these periods described by Prewitt (1991) archaeologists generally focused attention on "burned-rock mounds" because of their more significant stature and obvious presence in the landscape. By 1965, Greer (1965:41) noted that "interest was growing concerning a type of archaeological site known as the midden circle or mescal pit." Other names for this feature type in the archaeological literature of the time included *ring midden, doughnut midden, midden mound, circle mound, cooking mound, cooking pit, sotol pit*, and *earth oven*.

From the outset of research efforts, ring middens were almost universally regarded in the context of a cooking facility because of numerous anecdotal and ethnographic accounts attributing a cooking function to similar features (Castetter 1935; Opler 1969). Nevertheless, disagreements arose about the specific function of the cooking facility, and no early attempts were made to draw specific distinctions among the various structural components of these features. Some believed them to be simple trash mounds of accumulated cooking debris, whereas others regarded them as grilling facilities, where meats were cooked atop heated rock mounds. As a seemingly unceasing array of burned-rock-feature typologies developed, Greer (1965) offered one of the earliest functional definitions by describing ring middens as doughnut-shaped deposits of FCR and gray ash that accumulated as a result of repeated cleaning and discarding activities that produced a circular formation of expended hearth debris. In doing so, Greer was also the first to draw a clear contrast between the outlying burned-rock midden and the central ash-pit formation. This realization, subtle as it was, set the stage for a series of more-recent archaeological definitions founded in contrasting theoretical perspectives.

An Archaeological Definition through Formation Processes

Black and Thoms (2014) have been prominent proponents of an archaeological definition grounded in a careful examination of site-formation processes, whereby an ethnographically demonstrable (and universally applied) series of steps is necessary for the construction of a ring midden (Figure 5). Black and Thoms (2014:205) "argue[d] that most closely spaced arrangements of heated stones, including many 'hearth' features, as well as most substantial accumulations of spent cooking stones are manifestations of a single

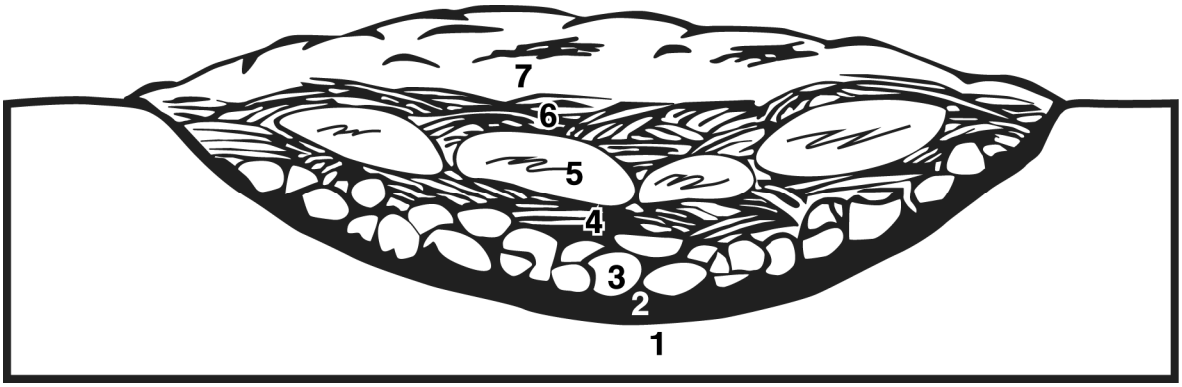

Figure 5. Schematic of an earth oven showing the various components proposed by Black and Thoms (2014): (1) oven pit; (2) fire; (3) hot rocks; (4) plant material (packing); (5) food; (6) plant material (packing); (7) earthen cap. Adapted from Black and Thoms (2014:206).

technology: earth oven cookery." To Black and Thoms (2014), ring middens are but one manifestation of earth-oven technology.

Earth-oven cookery involves a series of steps. First, a shallow earthen pit is dug and is loaded with fuel. The fuel is ignited and is allowed to burn for a predetermined interval before being covered with stones. As soon as the stones become sufficiently hot, they are covered in a layer of moist plant material on which the food to be cooked is placed. The food is subsequently covered with another layer of plant material, which, in turn, is covered with an earthen cap. Once sufficient cooking time has elapsed, the cap is removed and the cooked food product is extracted. Of crucial importance is the fact that the archaeological signature that we regard as the "ring midden" results from the process of repeatedly using an earthen-oven facility. With each reuse episode, spent stones, earth, and ash are cleaned from the oven pit and are deposited at the oven's periphery, giving rise over time to the distinctive raised annular midden surrounding the central cooking feature. Millward (2010:33) reported that, in New Mexico, cooking pits typically range from 1.5 to 3 m in diameter and average approximately 15 cm deep. Discard piles, on the other hand, can range from a small scatter of stones to massive piles consisting of several hundred thousand stones and stone fragments (Miller et al. 2011).

To date, no comprehensive synthesis has been undertaken to evaluate the range of variability in ring-midden dimensions, but several publications provide data based on specific accounts, largely from Texas. Greer (1965:43–45), for instance, stated that Form 1 of his Type 1 circle-midden ranged from 30 to 55 feet (9 to 17 m) in diameter, averaged approximately 3 feet (1 m) high, and had a central depression measuring 12 feet (4 m) in diameter, whereas Form 2 ranged from 40 to 55 feet (12 to 17 m) in diameter and had midden debris 4.0–5.5 feet (1.2–1.7 m) high. Mera (1938) characterized ring middens as ranging from 6 to 10 m in diameter. Simpson (2010:51, cited by Katz and Katz [1985a]) briefly summarized the average dimensions of ring middens as approximately 10 m in diameter, with up to 2 m of mounded rock. Dering (1997) supplied information on ring-midden dimensions in central Texas, noting that they reached a maximum diameter of 25 m between 4200 and 2600 cal B.P. Similarly, Black et al. (1997) described overall dimensions for ring-type middens of the Edwards Plateau as varying between 8 and 20 m but averaging 12 m, with a thickness of 0.5–2 m.

An Archaeological Definition through Structural Recognition

A series of parallel definitions of ring middens naturally arose through excavation efforts (Hester 1999; Hogan 2006:3–7; Katz and Katz 1985a; Miller et al. 2009; Miller et al. 2011; Millward 2010; Quigg et al. 2002; Simpson 2010; Ward and Vierra 2011). Although a range of classificatory accounts exists, three distinct components of burned-rock-midden features have been almost universally described. Many fit within Black and Thoms's (2014) corollaries and, on a practical level, substantiate the existence of a ring midden through archaeological recognition of the requisite structural components: (1) the annular discard midden, (2) a central baking area embracing one or more baking pits, and (3) various ancillary subfeatures indicative of repeated use.

The *discard midden* is the most prominent of the three most commonly accepted components and consists typically of FCR, discarded artifacts, and earth and ash that accumulate as the pit is repeatedly accessed and cleaned after baking. Shapes of discard piles of earth ovens vary from rings and crescents to amorphous mounds and diffuse scatters. Discard middens are accretionary features that grow in size with repeated use, as more rocks used as heating elements are tossed or raked out to form an annular ring. Accumulations from burned-rock discard middens in the Sacramento Mountains vary from a few FCR to thousands of metric tons of fractured rock, ash, and soil, depending on the level and intensity of reuse. Thus, larger rings indicate more-frequent and/or more-intensive use of the feature and suggest a greater time depth to feature use than do smaller discard middens. Individual uses can be separated by decades, or even by centuries or millennia. Katz and Katz (2001) also observed that intersecting rings, which are often inferred to have resulted from rings growing outward from earth ovens and eventually intersecting, are another indicator of time depth.

The idea of the *center-focused pit area*, as outlined by Black and Thoms (2014), anchors the archaeological concept of a ring midden functionally by designating the requirement for a central zone where baking or heating must have repeatedly taken place. As Miller et al. (2011) pointed out, the *central baking area* should not be confused with a *central baking pit* in that the central baking area frequently displays an activity zone containing one or more types of pit, plant debris, tool-processing debris, or ashen materials related to earlier occupational surfaces. In southern New Mexico and western Texas, the central pit area typically consists of a roughly circular carbon-stained area, either surface based or penetrating into earthen basins or shallow subsurface depressions. The ashen deposit can be discrete, mottled, or patchy; some contain unburned organic debris. Stained areas are typically either devoid of FCR or close to secondary deposits. Some depressions are lined with stone; more are not. The morphology of the pits, basins, or depressions varies considerably, presumably because of the nature of prevailing resources or perhaps because of functional or ethnographic considerations not well understood. Overall, unlined pits are more common than those that are lined, although the two types have been noted near each other.

Though not always present, *ancillary subfeatures* are frequently observed within the established boundaries of burned-rock features. These include depressions from soil borrowing, concentrations of unburned plant materials, or secondary deposits of stone or artifacts within or outside the center-focused pit area. Although the function of the subfeatures is not well understood, their presence underscores the uniqueness of ring middens by demonstrating repeated use of the facility. Moreover, it reinforces the notion that the intensity and redundancy of use distinguish ring middens from other types of burned-rock features, such as simple hearths constructed for warmth, light, safety, or expedient cooking needs.

An Archaeological Definition through Arbitrary Size Assignment

With the advent of large-scale field surveys, brought about by efforts at Section 106 compliance, archaeologists and land managers began struggling with the problem of classifying burned-rock features in the field, on the fly, and entirely on the basis of their surface manifestation. This led to the practice of categorizing burned-rock features solely on the basis of size (Quigg et al. 2002:328). Throughout the El Paso region, for instance, arbitrary size-interval classes were assigned to burned-rock features at the following intervals for maximum dimension: (1) less than 1 m, (2) 1–2 m, and (3) more than 2 m. Burned-rock features less than 2 m in maximum dimension were designated simple hearths, whereas features more than 2 m in maximum dimension were assigned a roasting function. In other instances, the weight of the FCR was used to draw

distinctions: concentrations with masses greater than 13 kg were interpreted as roasting pits. Although both methods eventually led to a recognition of the varying levels of effort required to construct individual burned-rock features, particularly the monumental efforts required to amass some of the largest, the practice has failed to offer any clear interpretation of functional differences among burned-rock features as a whole. Indeed, as Black and Thoms (2014) argued, all of the scalar distinctions mentioned above fall within a continuum of earth-oven technology.

Spatial Distribution

A clear understanding of temporal and spatial variation in the use of ring-midden features has been constrained historically by the lack of a universally applicable definition. Broadly speaking, however, ring middens must display evidence of annular midden accumulation around a central hearth feature. Although a range of postdepositional structural configurations for burned-rock/earth-oven features is possible (Petragalia 2002), arguing that a thermal feature is a "ring midden" if it lacks the associated ring-shaped midden deposits that give rise to the term is ultimately problematic. Suhm (1960:68) appears to have been the first to acknowledge this requirement, succinctly arguing that there are two categories of large burned-rock middens: domed and annular. Although the two might be considered functionally equivalent, the archaeological manifestation of an annular discard midden is the practical basis and origin of the term.

Having adopted this distinction, archaeologists in Texas and New Mexico currently recognize that the two types overlap in distribution. Domed middens are generally associated with the region encompassing the eastern portion of the Edwards Plateau of central Texas, whereas the annular variety is more closely associated with the western portion of the Edwards Plateau, the Trans-Pecos Region, and the Lower Pecos River, including the study areas defined for the current project (Figure 6). Some of the most pristine examples can be found on the eastern flanks of the Guadalupe Mountains. The scarcity of rock within the Mescalero Sands environment restricts the size of burned-rock features to simple scatters; a similar but not identical situation exists within the Pecos Valley. In the northern Chihuahua Desert, near El Paso, large earth ovens are documented in elevated areas up to and along the Sacramento Mountains, Organ Mountains, and San Andres Mountains fronts. Elsewhere, in the adjacent Tularosa Basin and Hueco Basin environments, extensive palimpsests of large thermally altered rock and ashen features are common. Some of these may be ring-midden features grossly affected by deflation.

Katz and Katz (2001) observed that sites in southeastern New Mexico that contain more than one ring midden are more frequent in the desert scrub zone (3,200–3,600 feet [975–1,100 m] AMSL). These sites are often large and commonly include ceramic artifacts and are thought to represent a mixture of processing activities and/or base camps. Sites with single rings are more common in the grassland and lower scrub zones (3,600–5,000 feet [1,100–1,525 m] AMSL). Most of these sites are smaller and less complex than sites with ring middens at lower elevations, typically lacking features of other types and containing primarily lithic artifacts and few ceramic artifacts. Single-ring sites are apparently even more common in the upper scrubland zone (5,000–6,100 feet [1,525–1,860 m] AMSL). Where multiple rings are present in the upper scrubland zone, they have been observed in linear distributions that follow ridgelines. All sites in the upper scrubland zone have debitage but lack ceramic artifacts or features of other types. Katz and Katz (2001) interpreted ring-midden sites in the upper scrubland zone as possible staging areas from which hunting and gathering activities were launched while agave was being roasted in the earth oven. In the woodland zone (higher than 6,100 feet [1,860 m] AMSL), the highest-elevation zone in which ring middens have been documented in southeastern New Mexico, ring middens are smaller and rarely have more than a few associated artifacts.

Simpson (2010) noted that ring middens in southeastern New Mexico typically are located in rocky upland environments west of the Pecos River. By contrast, hearth fields consisting of many smaller thermal features with carbon stains and relatively small numbers of FCR are more common east of the Pecos River. Whereas ring middens are thought to have been used in southeastern New Mexico to process agave, sotol, and yucca (*Yucca*) parts and in Texas to process geophytes (see below), these smaller carbon stains are thought to be associated with a different form of cooking: the indirect cooking of small seeds (such as those from amaranth (*Amaranthus*) or goosefoot (*Chenopodium*) for use in flours and gruels.

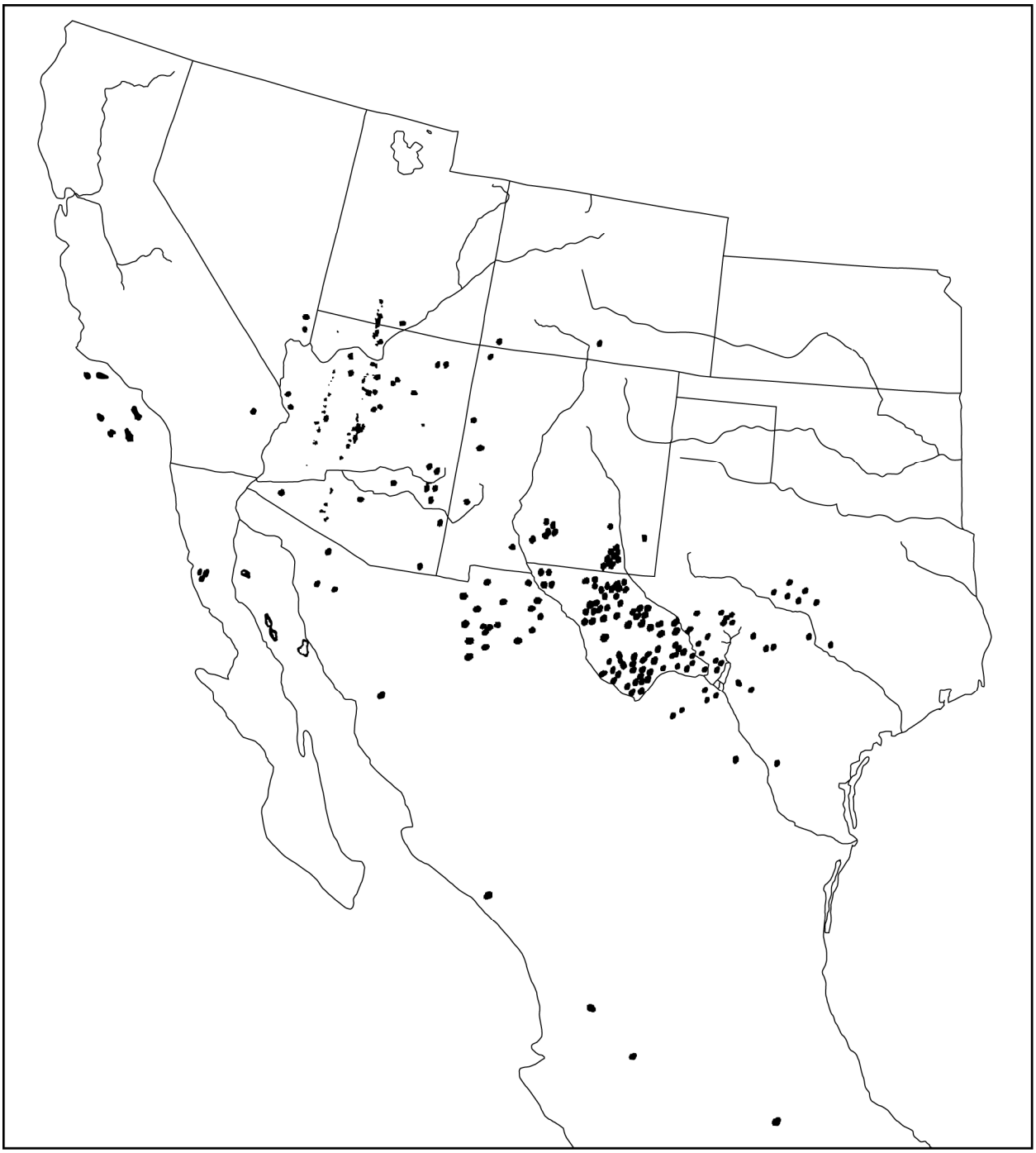

Figure 6. Map detailing the distribution of midden circles and mescal pits. Adapted from Greer (1965:45).

Temporal Variation

Thoms (2009:579) noted that, in western North America, cook-stone technology was present as early as 10,500 B.P. and that the practice was well established by the early Holocene but is poorly documented and often archaeologically invisible. Hammatt (1976:270), on the other hand, suggested that middens and hearths of burned rock provide a clear means of recognizing an Archaic period occupation. In the U.S. Northeast, large, rock-filled earth ovens signal the Early Archaic period (Funk 1978). In general, FCR features, including small earth ovens, appear common in the U.S. Southeast culture area by 9,000 years ago (Anderson and Sassaman 1996; Cable 1996). Burned-rock features, as a whole, enjoy an equally broad temporal distribution in the U.S. Southwest; however, few published examples of Paleoindian period thermally altered rock features appear in the southwestern record (Dering 2007). Consequently, both domed and annular midden deposits are unlikely to predate 6000 B.C. Prewitt (1991:26) stated that, although the full age range remains to be seen, the general age range for the onset of midden construction in the central Texas region is relatively well established to be the Middle Archaic period (roughly 5000 to 2250 B.P.). Black and Creel (1997:274; but see Thoms 2009:581), in a study of 141 published radiometric dates from the same area, reported an increased frequency of dates after A.D. 500.Various published reports document large middens in Texas dating to time intervals as recent as the late prehistoric period.

The first regular appearance of burned-rock features in the U.S. Southwest occurs in the Early Archaic period, followed by a general and gradual increase in the diversity of hearth form throughout the region during the Middle and Late Archaic periods. By the Formative period, burned-rock features are less diversified, hinting at a shift toward either specialization or behavioral conformity. Katz and Katz (2001) indicated that ring middens first appear in southeastern New Mexico during the Archaic 3 period (3000–2000 B.P. [1000 B.C.–A.D. 1]) and become more common during the subsequent Archaic 4 period (2000–1500 B.P. [A.D. 1–500]). Within southeastern New Mexico, the Formative period (most notably between A.D. 500 and A.D. 1450) is generally considered the principal time of use of large earth-oven facilities (Black and Creel 1997:274; Miller et al. 2011:227). Katz and Katz (2001) indicated that, during this time, ring middens are common in all ecozones except the forest ecozone. Although older dates typically are recorded for burned-rock features in general, post–A.D. 1500 dates are rare in the Guadalupe Mountains, but this may reflect sampling bias, as numerous unexcavated Apache sites with burned-rock middens are known in upland settings there (Miller et al. 2011). Miller et al. (2011) proposed an extraregional decline in the use of plant-baking facilities after A.D. 1300, which they attributed to a miscellany of signatures for agriculture-based economies that become especially prominent in the lowlands (see also Miller et al. 2012; Vierra and Ward 2012). Overall, for the time span between A.D. 500 and the end of the Formative period, large burned-rock features in southeastern New Mexico are most frequently found west of the Pecos River and are particularly common in upland areas or alluvial fans lacking residential components. The lack of an association with residential remains, along with ethnographic accounts, provides much of the impetus for ongoing interpretations of ring middens as having been primarily devoted to the processing and cooking of locally obtainable plants.

Borrowing sediment for the earthen cap of an earth oven and the redistribution of deposits removed from a cleaned-out oven result in the mixing of deposits from several periods and activities. Also, ring middens were often reused several to many times; some episodes of use may have been separated in time by centuries or even millennia. The recurrent reuse of ring middens results in a dating conundrum. Because of how they formed and were used, ring middens are difficult to date. For example, Katz and Katz (2001:26) have asked, “Which episode of use is being dated? Does this date the entire feature? Do diverse dates result from dating different episodes, or are some dates aberrant? If the dates are accepted, can they be used to date a related (and deflated) living surface, or just the feature?” A better understanding of ring-midden chronology probably will require large numbers of dates from different deposits within ring middens.

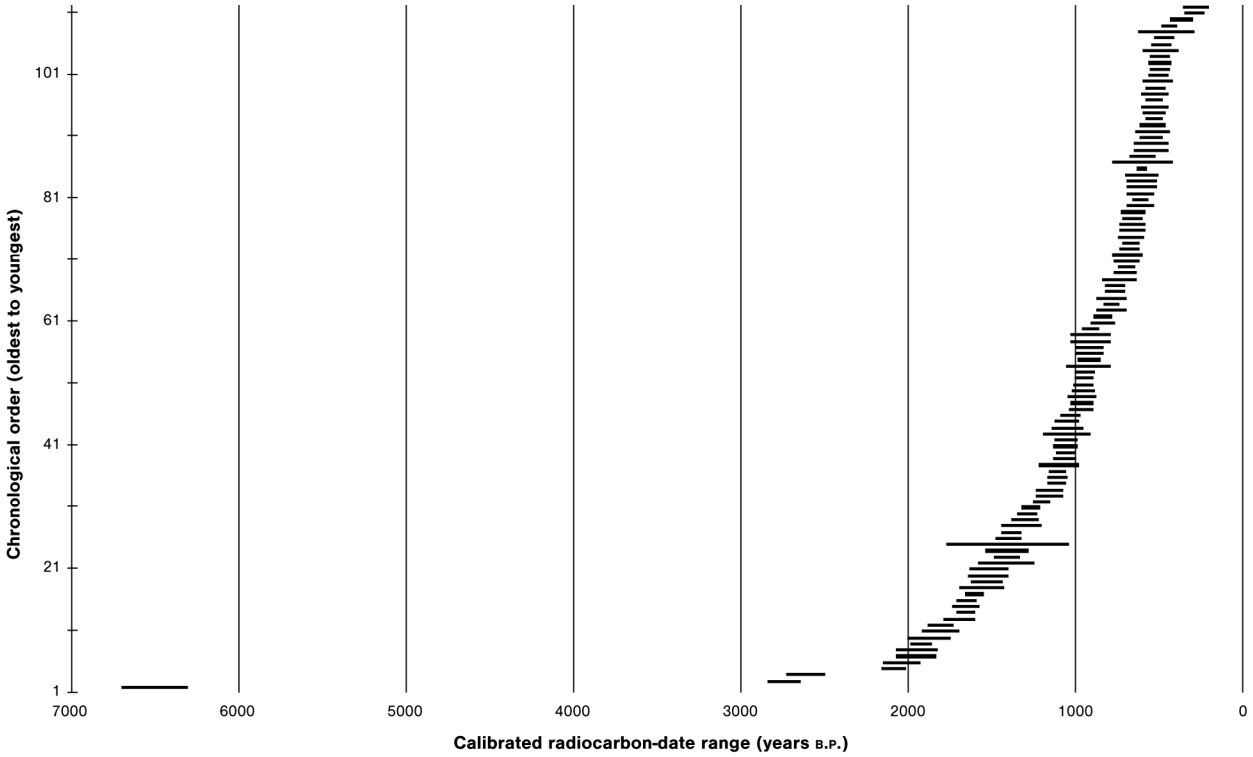

Figure 7. The distribution of dates compiled by Katz and Katz (2001) for radiocarbon-dated ring-midden features in southeastern New Mexico.

Katz and Katz (2001:Table III-35) compiled a table of 111 calibrated radiocarbon assays obtained from ring middens in southeastern New Mexico and from a few in neighboring regions of south-central New Mexico and west-central Texas. Nearly all dates obtained lie within the last 2,000 years (Figure 7), and use of ring middens in southeastern New Mexico was relatively continuous during that period. Analysis of a histogram of the calibrated dates (Figure 8) suggests that ring-midden use increased dramatically after A.D. 800. Katz and Katz (2001) interpreted the distribution of dates as indicating steady use of agave from A.D. 800 through 1400. Finer analysis of the distribution also suggests that there may have been peaks in ring-midden use during the Formative period and that the more pronounced peaks occurred between A.D. 850 and 1000 and between A.D. 1250 and 1400. Perhaps these represent periods of intensification for the use of earth ovens, possibly coinciding with population packing or periods of environmental stress that required more-intensive use of agave and sotol. Alternatively, unless sampling bias is an issue, intensive use of ring middens may not have been sustainable for more than a century, with the result that the system collapsed temporarily and required time for ecological regeneration of resources processed in ring middens.

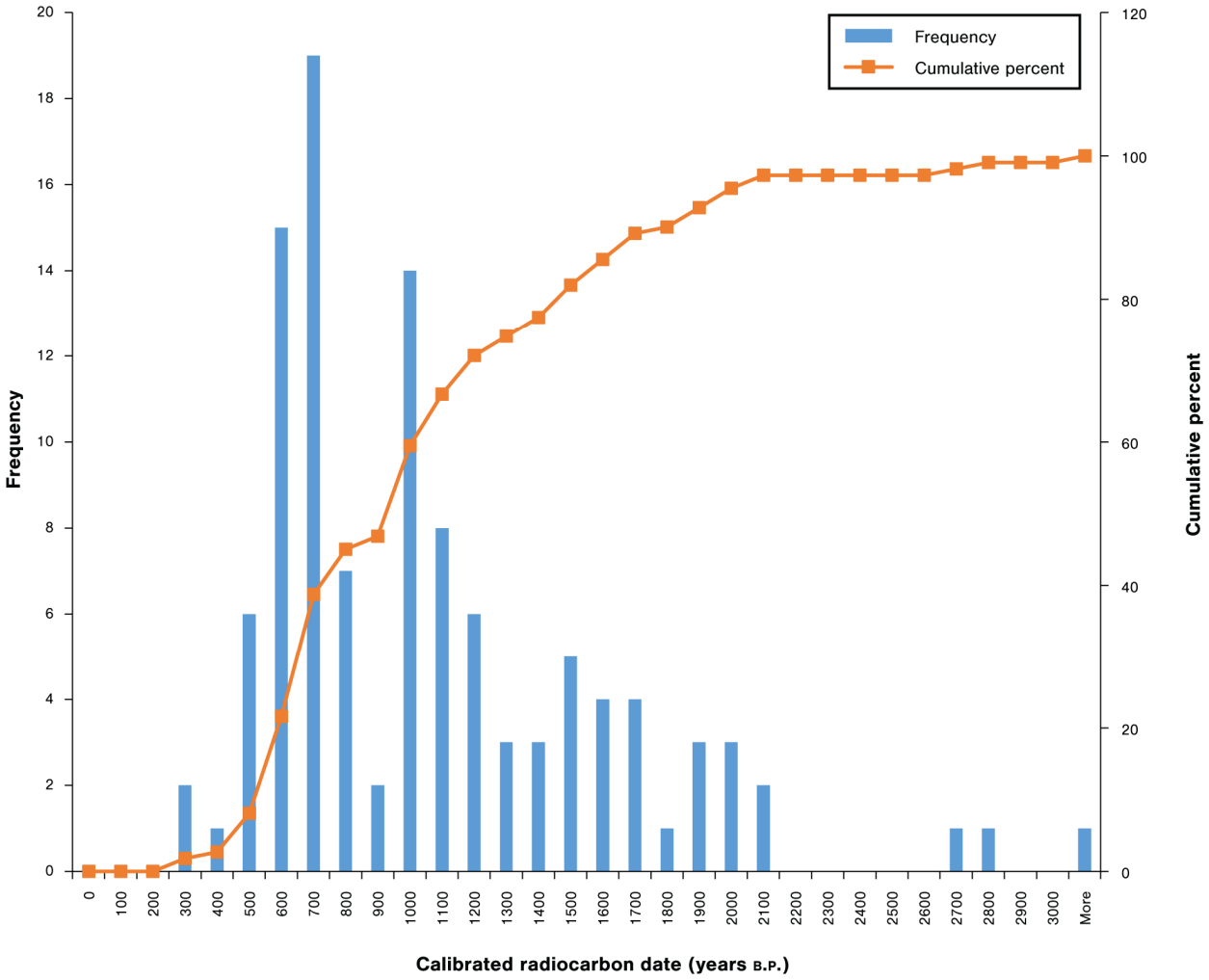

Figure 8. A histogram displaying the frequency of dates compiled by Katz and Katz (2001) for radiocarbon-dated ring-midden features in southeastern New Mexico.

Inference of Ring-Midden Functions

The overlapping geographic distribution of, as well as the wide variation in, the forms of burned-rock features seems to suggest that feature form generally follows feature function. In other words, although the basic elements of earth ovens remain the same, distinctive shapes and sizes probably correspond to what was being cooked. In general, light scatters of burned rock are thought to be associated with stone boiling or the parching of small seeds, perhaps even the grilling of meats over flat stones. Large earthen ovens, on the other hand, are associated with a more specific type of food processing or cooking whereby plant foods are subjected to protracted periods of heating or steaming in a sealed environment. Steaming pits are widely noted in ethnographic records of the Pacific Northwest (Driver and Massey 1957; Thoms 2009). They are not, however, common in archaeological sites in the U.S. Southwest, potentially because of difficulties in distinguishing them from other types of burned-rock features (Thoms 2009:587). Southwestern ethnographic accounts overwhelmingly suggest that earth-oven cooking was employed in order to make plant foods high in lipids or complex carbohydrates digestible.

Geophytes (bulbs, corms, tubers, rhizomes, tuberous roots) and succulent species like agave or sotol are the plant foods most frequently cited in ethnographies as having been cooked in earth ovens and are widely associated with the subsistence activities of protohistoric populations of Mescalero Apache dwelling in the study area. Indeed, in a study of botanical remains from 82 baking pits and burned-rock middens, Miller et al. (2011:323) noted that 31 cases now exist in which vascular fibers, leaf or crown fragments, or spines of species of the agave family (Agavaceae) have been identified from burned-rock discard middens from the Trans-Pecos and southern New Mexico. Nevertheless, globally, earthen ovens are used for cooking a whole range of foods that require extended cooking intervals; a number of foods meet this requirement (Wandsnider 1997). Meats need the shortest time; pithy plant foods, such as roots or succulent species, require relatively long exposures to high temperatures. Thoms (2009:577) proposed that, with respect to North America, earth ovens are typically oriented toward both meat and plant-food processing in the Pacific Northwest, whereas people in the U.S. Southwest and northern Mexico typically used them for cooking plants.

To date, no comprehensive effort has focused exclusively on cataloging plant remains from ring middens. Moreover, as a general rule, ring middens have been found to contain uncharacteristically low levels of identifiable charred macrofossils other than extensive deposits from fuelwoods. Results from macrobotanical, Fourier transform infrared spectroscopy (FTIR), and pollen analyses are often ambiguous and have low sample yields. Nevertheless, several regional studies have attempted to synthesize macrofloral evidence from burned-rock features as a whole. In an analysis of 43 flotation samples from ring middens in the lower piñon/juniper (*Pinus/Juniperus*) belt and juniper savanna of the Sacramento Mountains, Dering (2011) identified 15 samples with edible remains. These consisted mainly of agave, cholla (*Cylindropuntia*) buds, tansy mustard (*Descurainia*) seeds, and prickly pear (*Opuntia*) fruits. The presence of seeds in conjunction with trace amounts of species that do not require earthen-oven treatment led him to conclude that the features had been used in a context where more than one type of cooking had occurred (Dering 2011:248). Likewise, in an analysis of burned-rock features from the Black River area, Millward (2010:100) observed that feature form and function seem to vary with the availability of plant resources. Features were not necessarily species specific but were adapted, in terms of size and shape, to whatever resource might be present. Furthermore, because of the small size of many features included in the study, Millward hypothesized that many features were used expediently. Excavations at three sites on Otero Mesa that included midden deposits led Adams et al. (2011:250) to propose that people living there chose subsistence resources and fuels that were generally available in the surrounding area and that some of their choices were influenced by their season of residence. Howard (1999:66), having reviewed published macrofloral evidence for 225 domed burned-rock middens in Texas, similarly stated that "the variety of plant species represented by the botanical remains recovered, does not suggest a focal economy based on any specific type of food, but may reflect the opportunistic use of a variety of plant foods, varying from area to area under diverse environmental conditions." Alternatively, Creel (1999:42) noted that the distribution of burned-rock middens in west central Texas is closely correlated with the presence of oak (*Quercus*) savanna; the obvious implication is that acorns were the focus of use. Louderback et al. (2013) similarly verified the existence of the so-called Yucca Complex of the Mojave Desert, where yucca fruits, roasted in pit ovens, served as the main seasonal resource for prehistoric economy. In yet another example of specialized use, excavations at Camp Bowie, Texas, seem to suggest a predominant focus on the processing of small geophytes such as wild onion (*Allium*) (Dering 2003). Along the Texas coast, where sizable middens are common, especially in the context of a dependence on marine resources, earth ovens typically are constructed of baked earth. In the northernmost portions of the High Plains of Texas, where populations of succulent species are sporadic at best, earth ovens are regularly observed, but there are no definitive answers to the question of how they were used.

Artifact assemblages in and around burned-rock middens frequently include large numbers of tools that may be associated with plant processing, including marginally flaked tabular tools, large cobbles, steep-sided scrapers, core tools, and hammerstones. The typical size of tools from southeastern New Mexico assemblages suggests the processing of large or bulky materials. Although ground stone is a regular constituent, it is usually highly fragmented, indicating the recycling of ground stone tools as thermal mass rather than their use at the earth-oven facility itself for processing materials. Ceramics are consistently

present in artifact assemblages from burned-rock middens throughout the Jornada, southeastern New Mexico, and Trans-Pecos regions, but no interpretations of the use of ceramic vessels at ring middens are currently accepted. One explanation for their presence is that broken sherds may have been employed for digging or cleaning debris from the central hearth feature of the oven pit. Also, because borrowing of sediment found within and around a ring midden was often necessary to create an insulative earthen cover for an earth oven, artifacts found in ring middens may often have been redistributed from other parts of a site and from site components that were not associated with ring-midden use.

Acquisition of Lidar Data

This project involved an aerial lidar survey to collect the data necessary for identifying ring middens. To collect lidar data, a sensor directs pulses of laser light toward a target and measures the time required for the pulse to return to the sensor (Lillesand and Kiefer 1999) (Figure 9). The return time is then used to calculate the distance between the sensor and the target. Lidar systems can be classified into two groups: stationary and mobile. A stationary system consists of a sensor mounted on a tripod. This kind of system is used for scanning specific stationary targets, such as buildings or bridges, that must be mapped accurately and precisely in three dimensions. Stationary systems are also used in land survey and small-scale terrain mapping, as in the mapping of an individual archaeological site or landscape feature.

By contrast, mobile systems can be mounted on a truck, boat, or airplane and are used to map large areas that cannot be directly accessed with a stationary system (Nayegandhi 2007). Because they are moving through space as measurements are taken, mobile systems must be integrated with navigational systems, so that both the location of the target and the sensor are known for each measurement made by the system. Mobile systems are used for large-scale surveys such as mapping utility corridors, railroads, or shorelines and are particularly useful for conducting high-resolution topographic mapping over large areas, as was performed by Surdex Corporation (Surdex; see below) for the three study areas involved in the current project.

To map the three study areas for the current project, an airborne lidar system (ALS) was used. An ALS has three components: a lidar sensor, an inertial navigation system (INS), and a differential global positioning system (DGPS) (Figure 10). The lidar sensor sends the laser pulse and measures its return time and intensity; the INS measures the direction and speed of the sensor as it moves through space; and the DPGS records the location of the sensor in x, y, and z dimensions. An ALS survey can cover approximately 50 km^2 per hour, depending on the speed and altitude used to conducted the survey (National Oceanographic and Atmospheric Administration Coastal Services Center 2012). Careful flight planning is essential to ensure data quality and to prevent gaps in the survey area where lidar measurements are absent because of either a lack of overlap between flight lines or the occlusion of a portion of the study area by something, such as a tall hill or building, that blocks the sensor from recording a landscape surface.

Lidar measurements result in a dense point cloud consisting of millions of points tied to a specific location, in three dimensions. Accurate recording of the spatial location of each point in the lidar data requires the use of ground control. Several Global Positioning System (GPS) base stations must be established; these continuously record GPS satellite data before, during, and after a flight. These GPS-base-station data that are then used to differentially correct the GPS data collected on board the aircraft by comparing the onboard GPS data with data collected simultaneously by the GPS base stations.

Lidar data are collected in a proprietary format, based on the sensor's manufacturer. Sensor manufacturers have their own postprocessing software. The software spatially corrects, filters (for noise removal), and calibrates the raw data to produce a georeferenced, unclassified lidar file (Figure 11). The LASer (LAS) file format is a public file format developed and maintained by the American Society for Photogrammetry and Remote Sensing (ASPRS) (ASPRS 2008). Though developed primarily for exchange of lidar point-cloud data, this format supports the exchange of any three-dimensional (x, y, z) data. This binary file format is an alternative to proprietary systems or a generic ASCII file interchange system used by many companies. It also includes several attributes such as surface type, intensity, and flight-line information.

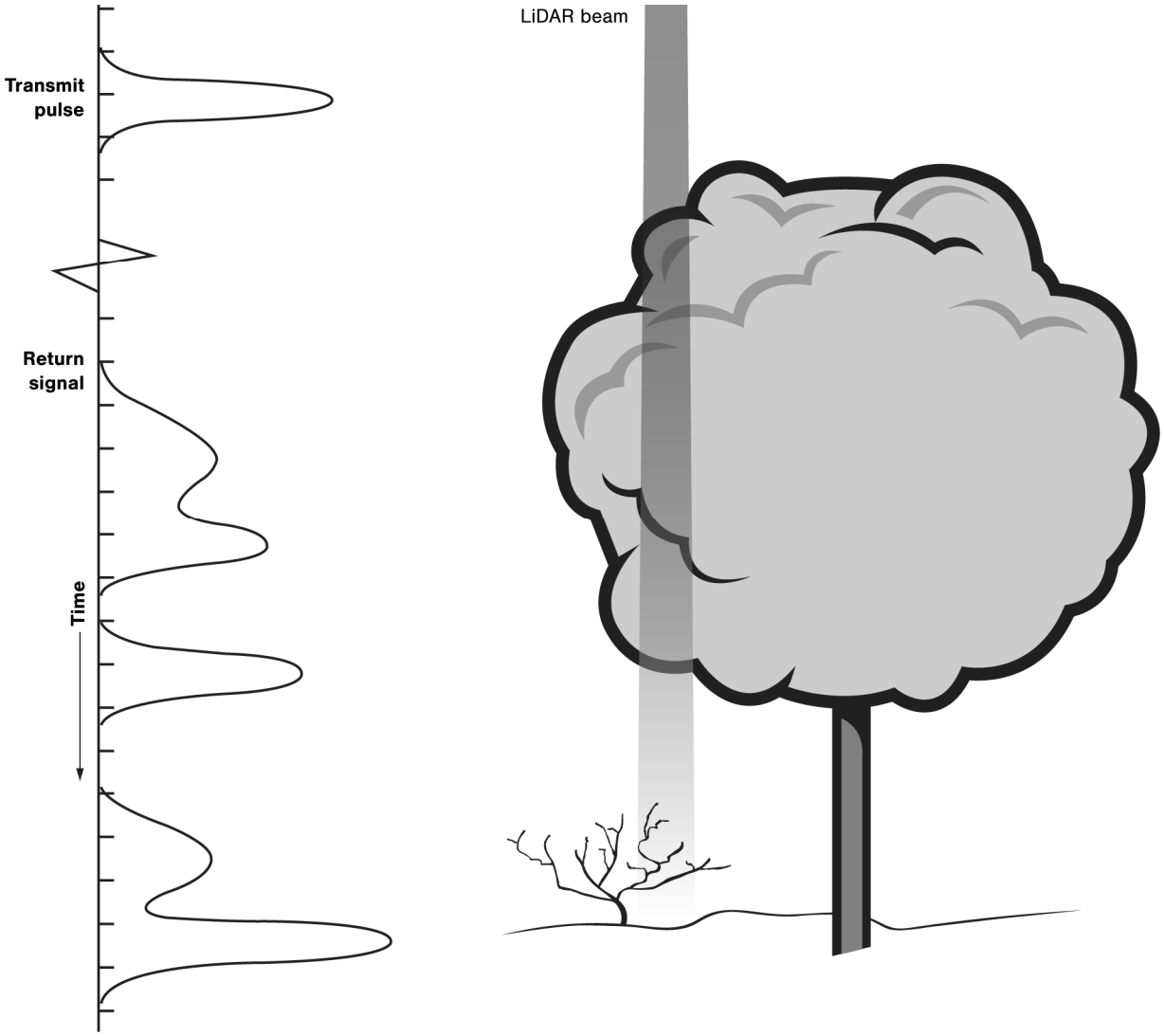

Figure 9. The lidar pulse and return. Adapted from Lillesand and Kiefer (1999).

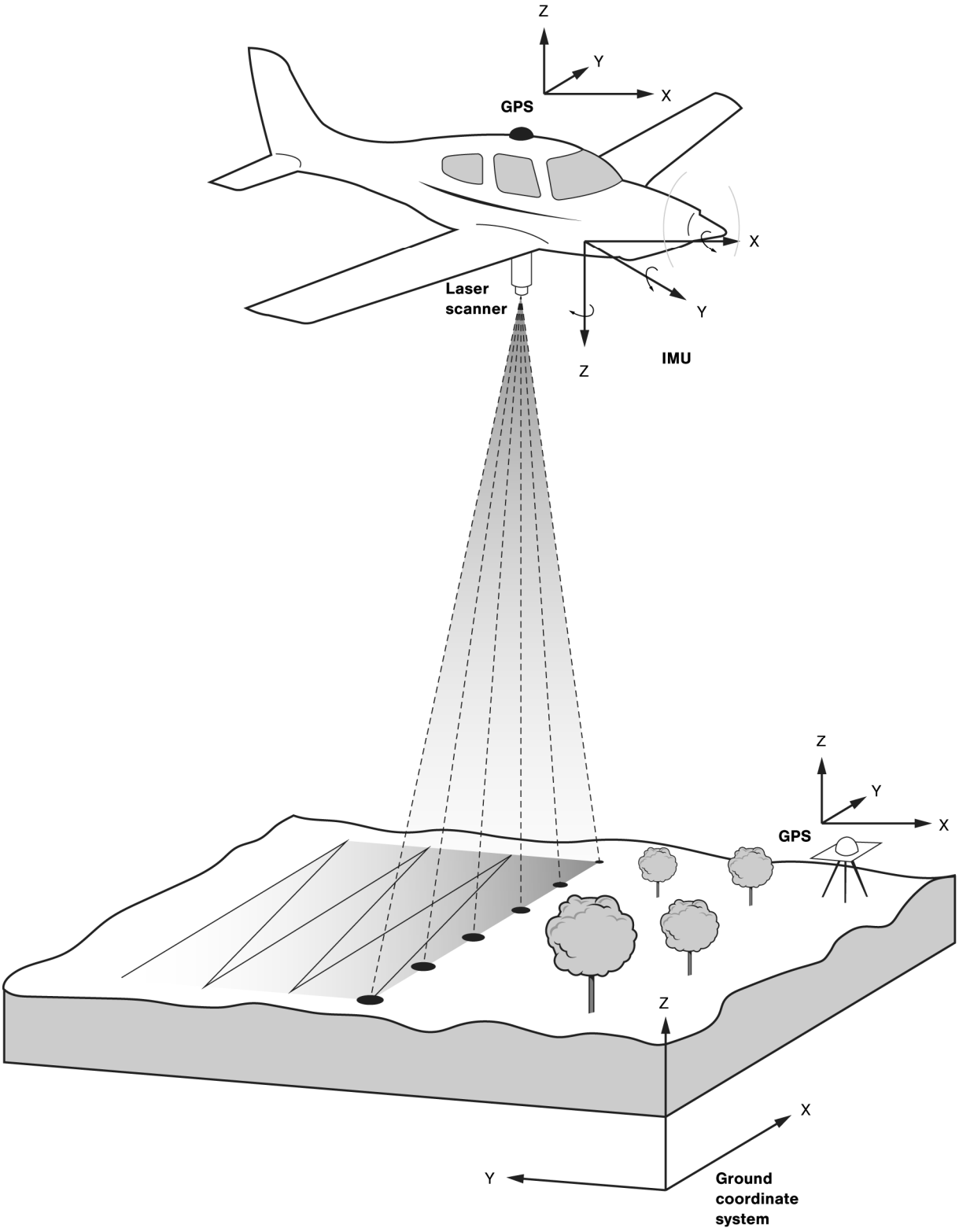

Figure 10. The airborne lidar system (ALS) survey method. GPS = Global Positioning System; IMU = inertial measurement unit. Adapted from Lillesand and Kiefer (1999).

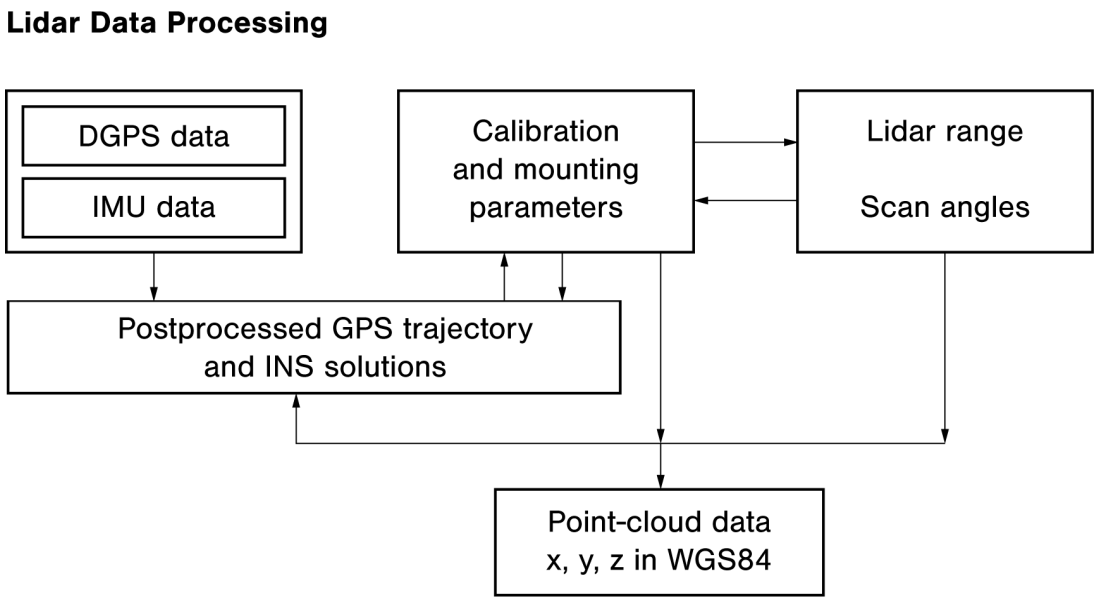

Figure 11. Postprocessing of lidar data. DGPS = differential global positioning system; GPS = Global Positioning System; IMU = inertial measurement unit; INS = inertial navigation system; WGS84 = World Geodetic System 1984. Adapted from Nayegandhi (2007).

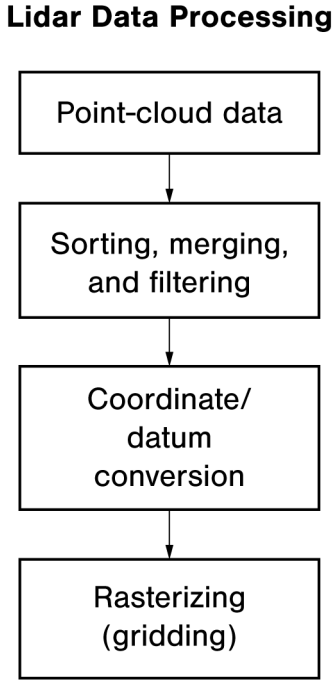

Figure 12. Classification of lidar data for visualization. Adapted from Nayegandhi (2007).

Lidar-data classification is a filtering process by which raw laser data are organized into logical collections based on characteristics of the signal returned to the sensor (Figure 12). The filtering process is based on the point's attributes and on geometric relationships of the laser data in the point cloud (GIS in the Rockies 2012). The ASPRS has developed a series of standard classes for classifying LAS data in terms of the type of surface likely to be measured by each point in a lidar point cloud, such as bare ground, building, water, or low vegetation. Classification of lidar data can also be project specific, and the LAS file format (Version 1.4) is flexible enough to support up to 256 classes (see below).

Lidar data for the project (Subtasks 1 and 2) were collected and processed by Surdex between February 14 and March 14, 2014 (see Appendix A). After receiving the request for quotation (RFQ), Surdex reviewed the specifications and areas of interest provided by SRI for the three study areas. The acquisition plans that were developed follow requirements of the U.S. Geological Survey (USGS) Lidar Base Specification Version 1.0 and the specific requirements detailed in the provided specifications.

Lidar data were acquired by means of Surdex's Leica ALS70-HP SP3 sensor. The ALS70 is capable of pulse rates of 500 kHz and scan rates of 200 kHz. The acquisition plans were created via available terrain model data detailing elevation and surface characteristics. Considering the variable terrain and the point-density and vertical-accuracy requirements, two distinct acquisition approaches were required. Because of relatively consistent terrain, the data acquisition was performed at an approximate altitude of 900 m above ground level with a 55 percent overlap between flight lines to collect a minimum of 15 points per meter (ppm) for all three study areas.

Vertical accuracy is estimated at approximately 11 cm, and a horizontal bare-ground resolution of up to 0.25 m can be supported by the required pulse rate. Acquisition of data for all three study areas required approximately 355 flight lines covering 3,748 flight-line miles (6,032 km). Seventy-two flight hours were required for the project. In addition to a calibration site developed at the local airport base of operations and the established GPS base station, Surdex established approximately 60 GPS ground-control positions. Acquisition included airborne GPS (ABGPS) and inertial measurement unit (IMU) technologies. Lidar processing and classification were accomplished using the Leica and Terrasolid software suite. TerraMatch incorporates least squares adjustment functions contained within the Terrasolid lidar production software suite. The software provides a method for selecting areas between common lidar flight lines to match points. Once the points are measured, the software performs an adjustment of the sensor parameters such as Dx, Dy, Dz, Domega, Dphi, and Dkappa, as well as the time-dependent variability of these parameters. Once resolved, these adjusted parameters are applied to each flight line to remove the identified misfits in the data. Once the data are completely calibrated and meet the project accuracy, automated classification routines are run. Several filter algorithms were employed on the project, given the variances in terrain and scene morphology, to obtain high-yielding results for the project and to minimize the time and cost for manual terrain editing.

The LASer (LAS) file format developed by the American Society of Photogrammetry and Remote Sensing (ASPRS) uses the following classification values in LAS Version 1.2 (values marked with an asterisk were included in the data set for the current project):

0—Created, never classified
1—Unclassified*
2—Ground*
3—Low Vegetation*
4—Medium Vegetation*
5—High Vegetation
6—Building*
7—Low Point (noise)*
8—Model Key-point (mass point)
9—Water
10—*Reserved for ASPRS Definition*
11— *Reserved for ASPRS Definition*
12—Overlap Points*
13–31— *Reserved for ASPRS Definition*

Final deliverables included the following (see Appendix A):

- Flight plan and reports
- GPS control reports
- "All points" lidar data in LAS Version 1.2
- Classified lidar data as described above

Project Findings

In total, 359 lidar tiles, covering a total of 32,965 acres (13,340 ha), were digitally surveyed. The digital survey resulted in the identification of 511 potential ring-midden features (254 identified during digital survey in the Azotea Mesa study area, 155 in the Box Canyon study area, and 102 in the Upper Rio Felix study area), as well as 25 features that could be confused with ring middens because of similarities in morphology (see Chapter 4). Thirty-three (6.5 percent) of the potential ring-midden features identified during sample survey were located within previously recorded sites; most of these were located within the Azotea Mesa study area, where survey has been more extensive and many sites with ring middens have been recorded. The remaining ring middens identified during digital survey were located outside previously recorded site boundaries.

Among the three study areas, feature identification during digital survey demonstrates large differences in ring-midden density: the highest density is in the Azotea Mesa study area and the lowest in the Upper Rio Felix study area. Ring middens also vary considerably in size among the three study area: the largest are in the Azotea Mesa study area and the smallest in the Upper Rio Felix study area. The average, median, and maximum sizes of ring middens are much greater in the Azotea Mesa study area than in the Upper Rio Felix study area. Moreover, the percentage of ring middens with a well-defined appearance was highest in Azotea Mesa, lower in Box Canyon, and lowest in Upper Rio Felix.

Many of the potential ring-midden features identified during the digital survey appear to cluster in space. In other words, potential ring-midden features commonly are located within tens of meters of 1 or more similar features. Statistical analysis of feature locations using nearest-neighbor hierarchical cluster analysis (and a search window distance of 100 m) resulted in the identification of a total of 87 clusters of potential ring-midden features in the digital survey results. Clusters consisted of 2–11 ring-midden features. Roughly 50 percent of potential ring-midden features were located in a cluster of 2 or more features; the remaining 50 percent of features could be considered isolated, though potentially clustering at broader scales. Most clusters consisted of just 2 potential ring-midden features; 93 percent of clusters contained 5 or fewer features. Clustered ring-midden features were comparatively more common in Azotea Mesa, where 59 percent of features were located within a cluster of 2 or more features. By contrast, in both the Box Canyon and the Upper Rio Felix study areas, approximately 41 percent of features were located within a feature cluster. To summarize the data, (1) ring-midden features are often located near one another, (2) these features commonly are present in clusters of 2–5 features but may also be found in clusters with as many as 14 features, (3) clusters are most common in the Azotea Mesa study area, and (4) on average, the largest clusters are located in Azotea Mesa and the smallest in Upper Rio Felix. Nearest-neighbor distances for clustered features are remarkably similar among the three study areas, however: they are nearly identical for Azotea Mesa and Box Canyon (approximately 38 m) and slightly smaller for Upper Rio Felix (34.2 m). This similarity suggests a common pattern in ring-midden placement among the three study areas for areas where more than 1 ring midden are located.

Investigators have noted that ring middens are likely to have one side that is higher than the opposing side, but the potential causes for this pattern are unclear. The location of the high side of a feature varies among the three study areas. In Azotea Mesa, the high side is most likely to be located along the east side of the feature but may be located on the northwest side. In Box Canyon, the high side is most often on the southeast side of the feature. In Upper Rio Felix, the high side is most likely to be on either the southeast or the northwest side of the feature. The aspect of the land surface on which ring middens are situated trends toward the east and southeast in all three study area and ranges from northeast to southwest for most ring-midden locations. In general, these data suggest that the high side of a ring-midden feature is most likely to be on the downslope side of the feature. Perhaps, more materials from earth ovens' heating elements are raked or tossed downslope to create the annular ring than are distributed upslope. However, this possible explanation does not account for why, in the Upper Rio Felix study area, a substantial number of ring-midden features have a high side on the northwest side of the feature, given that most land surfaces on which they are situated trend downward in the opposite direction. The difference in pattern in the Upper

Rio Felix study area may be related to disturbance processes that have preferentially removed or buried downslope portions of a ring-midden feature.

In order to understand more about the morphology of potential ring-midden features identified during digital survey, we selected, from each of the three study areas, a random sample of surveyed tiles that contained potential ring-midden features. The sample consisted of a total of 154 prospective features: 69 in Azotea Mesa, 44 in Box Canyon, and 41 in Upper Rio Felix. Detailed profile graphs were generated for each of these features. These profiles were used to calculate statistics on feature morphology. Based on these data, the average height of ring middens recorded during digital survey ranges from 2.6 cm to 42.0 cm, averaging 10.4 cm. The maximum height of the profiled middens varies from 6.5 cm to 88.4 cm, averaging 24.2 cm. Given that the vertical accuracy of the data is 11 cm (see above), these heights can only be considered ballpark figures. These data suggest that the average height of ring middens is largest in Azotea Mesa and smallest in Upper Rio Felix. Interestingly, feature size, average profile height, maximum profile height, span, and estimated aboveground feature volume all decrease with elevation. For each of these variables, small ring middens with little relief are present at high, middle, and low elevations, but the range and maximum values all decrease as elevation increases.

Ground Truthing

Ground-truthing efforts focused on recording clusters of ring middens with different attributes so that a maximal number of ring middens with different characteristics could be observed and recorded during the allotted field time. SRI visited undocumented clusters of ring-midden features in Box Canyon and in Upper Rio Felix, as well as a previously recorded site in the Azotea Mesa study area (LA 130591), where many ring-midden features have been noted. The two clusters in Upper Rio Felix and Box Canyon were newly recorded during the ground-truthing efforts; the site record for LA 130591 was updated.

In all, 43 features were recorded during the fieldwork efforts (see Chapter 4). Fourteen of the features recorded during the fieldwork were not originally identified during the lidar digital survey. Most of these were at the newly recorded site in the Upper Rio Felix study area (SRI-1). The 11 new features found within the Upper Rio Felix study area were comparatively much smaller (6 m or less) and shorter than the adjacent lidar-identified features. Moreover, 3 of these features could be described only as FCR middens and lacked the morphological and structural characteristics of ring-midden features. All of the newly recorded features in this area were moderately to highly disturbed from floodplain erosion/deposition resulting in displacement and partial burial of the features within alluvium. Similarly, the newly identified feature in Box Canyon was located entirely within a roadbed and was almost completely flattened; all that was left behind was a minimally perceptible circular distribution of FCR on the ground surface. The two features not identified at LA 130591 during the digital survey included raised berms that were only slightly detectable in plan view, rather than completely enclosed circular rings.

Overall, the field-verification efforts indicated that the lidar survey was highly successful in identifying ring-midden features but failed to detect heavily disturbed features and features of very low relief. With the exception of one isolated feature that was visited for comparative purposes and that was revealed not to be a feature, all of the lidar-identified ring-midden features visited during ground truthing were verified as ring-midden features. The field-verification efforts suggested that the failure to detect ring-midden features during digital survey can be attributed to a few factors. As discussed above, most of the features that went unrecognized in the lidar data were disturbed and lacked the relief necessary to be detected confidently by means of lidar data.

Admittedly, the sample of ring middens visited in the field is comparatively small (only 5.7 percent of digitally identified ring-midden features). It is likely that some of the potential ring-midden features identified during digital survey are not, in fact, ring-midden features, but we have no way of documenting this without further field checks. The field-verification efforts suggest that many of the potential ring-midden features identified during digital survey will turn out to be ring middens when field checked, but at least some of the digitally identified features are likely to be revealed as features of other types or, in a few cases, no feature at all.

During the ground-truthing efforts, we had hoped to visit two unusual features that were identified through the lidar data as ring middens with mounded lobes. These were identified during digital survey as well-defined rings with a large mounded area extending several meters beyond the outer edge of the ring, usually on one side of the feature. Some evidence from the lidar data suggests that some of these mounded lobes may consist primarily of mounded rock or bare sediment. In all, 33 such features were identified during digital survey, most of them in either Azotea Mesa or Box Canyon. Unfortunately, roads that could be used to reach the two features of this type selected for visits were impassable. Despite several attempts to reach these features, we were unable to observe an example of these unusual features on the ground to gain a better understanding of feature characteristics.

Report Organization

This report documents the process of ring-midden identification, presents the analysis and interpretation of project results, and provides recommendations for further work. It is organized into five chapters:

1. Project Background and Approach
2. Environmental and Cultural Context
3. Presurvey Ring-Midden Visualization, Characterization, and Modeling
4. Digital Survey, Field Verification, and Model Refinement
5. Conclusions and Recommendations

The report also includes 4 appendixes:

A. Lidar-Acquisition Information
B. Python Scripts
C. Digital Survey Methods
D. Site Descriptions Resulting from Field-Verification Efforts

CHAPTER 2

Environmental and Cultural Context

Introduction

This chapter presents an overview of the environmental context and archaeological background for the Southeastern New Mexico Ring Midden Lidar Survey Project area. The project area is situated entirely in the Sacramento Section physiographic subregion, along the westernmost extent of the Permian Basin of southeastern New Mexico. Study areas investigated during the course of the project include major landforms, such as Box Canyon Draw, the Rio Felix floodplain, and Azotea Mesa, all of which are characterized by the environmental setting of the Chihuahuan Desert. In this chapter, the historical development of the natural environment in the vicinity of the Southeastern New Mexico Ring Midden Lidar Survey Project area is discussed within the context of the Chihuahuan Desert region.

Regional Overview of the Chihuahuan Desert

The Chihuahuan Desert is one of the largest deserts in North America. Straddling the United States–Mexico border, it occupies portions of northern Mexico, central and southern New Mexico, and Texas west of the Pecos River. The Chihuahuan Desert formed over the last 8,000 years and is characterized by shrubby desertscrub species, such as creosote bush, mesquite, and ocotillo, which are situated along large expanses of outwash plains, low hills, and valleys (Brown 1994). Upslope of the shrubby plains, bedrock outcrops and arroyo, *bajada*, and piedmont habitats give way to increasingly rich succulent-scrub communities of leaf-and-stem succulents, including agave, yucca, and sotol, that grade into semidesert grasslands at their upper limits (Brown 1994). Chihuahuan desertscrub vegetation has replaced much of the semidesert grasslands that once covered large portions of southeastern New Mexico, largely as a result of the overgrazing that has occurred during the past 150 years (Figure 13). Adjacent vegetation communities situated to the north and east of the Mescalero Plain retain characteristics of the semidesert- and plains-grassland plant communities, such as the shortgrass and midgrass prairies characteristic of the Southern High Plains (Brown 1994).

Succulent-scrub communities dominate the higher-elevation ecosystems within which sampled ring middens in each of the three study areas were investigated. Leaf-and-stem succulents typically associated with the ring middens include multiple species of agave, yucca, and sotol, in addition to a variety of other succulent species, such as prickly pear, claretcup cactus, rainbow cactus, cholla, and pincushion cactus. Ring middens are commonly interpreted as directly linked to the exploitation of these wild succulent resources. Mesquite, acacia, juniper, creosote bush, and ocotillo also compose the shrub component of these higher-elevation ecosystems, and they served as important sources of fuel associated with the use of large earth-oven features. Creosote bush, agave, and sotol, in addition to other woody species, such as javelina bush, often grow in shallow, stony soils distributed along limestone-bedrock substrates. This is not surprising, given that over 80 percent of species endemic to the Chihuahuan desertscrub vegetation community resides on a limestone-bedrock substrate (Brown 1994). Patterns in vegetation diversity within the succulent-scrub communities correspond to changes in elevation, local relief, and characteristics of surface soils

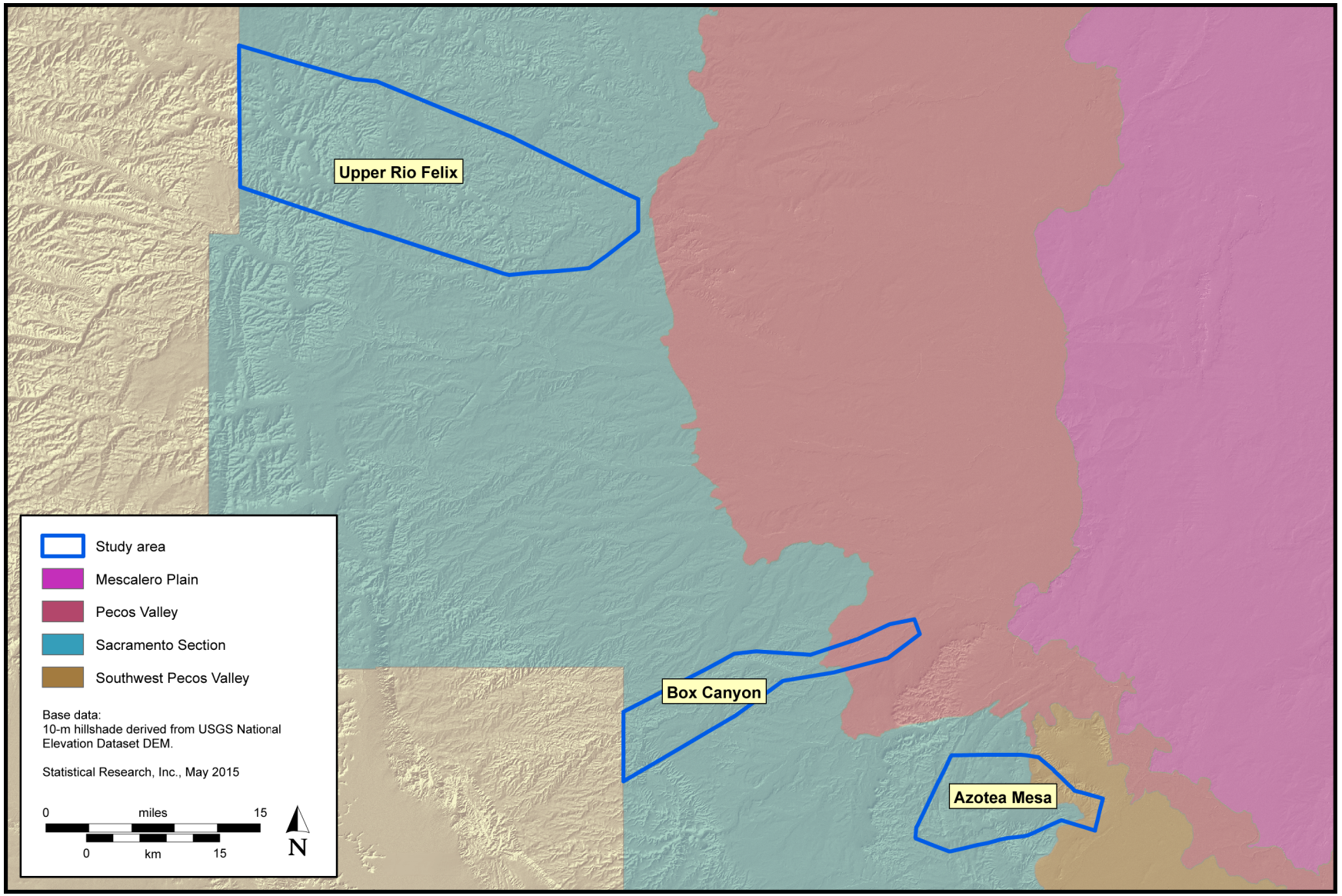

Figure 13. Vegetation communities across the study area.

distributed within each of the three study areas, in that Upper Rio Felix exhibited the least plant diversity, the deepest soils, and the lowest relief and is at the highest elevation, and Box Canyon incorporated the highest diversity of succulent-scrub species, exhibited moderate relief and moderately shallow soils, and is only slightly lower in elevation. Lastly, Azotea Mesa is situated along the lowest elevation investigated among the study areas and exhibited a moderate relief comparable to that of Box Canyon, the shallowest surface soils, and a plant-community diversity that was intermediate between those of Upper Rio Felix and Box Canyon.

The Pecos River constitutes the major watercourse within this portion of the Permian Basin, and named, intermittent tributaries of this drainage system present in the individual study areas include Little McKittrick Draw, Rio Felix, and Box Canyon Draw. Most of the drainage within the Chihuahuan Desert is internal, characterized by bolsons and barren playas that were once pluvial lakes. Dune fields have developed across much of the lowland areas to the east of the study area, as a result of the transportation of dry lakebed deposits by the wind. Aeolian dune and sand-sheet deposits are predominantly composed of quartz or gypsum originating in the calcareous soils that cover much of the region. Playas served as important resources for prehistoric populations within the adjacent lower-elevation areas. Playa settings exhibit a notable diversity of plant species similar to those of wetland communities, such as cattail (*Typha* L. spp.) and bulrush (*Scirpus* L. spp.), and provide important resource patches of seed-bearing annuals that, in turn, also attract a diversity of faunal species, including big game and waterfowl (Haukos 1997). Water availability is the most critical resource issue that impacted the nature of both prehistoric and historical-period land use across the project area. Agricultural pursuits conducted across the area during the historical period relied heavily on irrigation systems developed off major watercourses, including both the Delaware and Pecos Rivers. Ranching activities were also greatly influenced by available water resources.

Lower elevations in the Chihuahuan Desert range from 1,312 feet AMSL, near Langtry, Texas, to as much as 4,900 feet AMSL, near the Rio Grande. The Azotea Mesa, Box Canyon, and Upper Rio Felix study areas are all situated within the higher-elevation hinterlands along the upper reaches of the Permian Basin, at elevations of 3,556, 4,527, and 4,888 feet AMSL, respectively. The Chihuahuan Desert climate is characterized by temperatures that range from lows reaching –22°F and highs in excess of 104°F. Precipitation typically falls during summer rainstorms, influenced by humid air masses originating in the Gulf of Mexico. These localized storms are often of high intensity and short duration, occurring as the result of the intermingling of convection off rocky and sandy surfaces with the moist gulf air (Scurlock 1998; Tuan et al. 1973). Low-intensity fall and winter precipitation usually originates from Pacific Ocean frontal storms. The climate of the area is generally described as warm/temperate, and the growing season includes approximately 200–250 frost-free days. Annual precipitation recorded over a period of more than 70 years at the Carlsbad, New Mexico, weather station (Western Regional Climate Center, http://www.raws.dri.edu/wraws/nmF.html, accessed September 2014) included a low of 2.95 inches and a high of 33.94 inches.

Local Physiography

The Permian Basin of southeastern New Mexico can be divided into at least six distinct physiographic units: the Sacramento Section, the Pecos Valley Section, the Mescalero Plain, the Llano Estacado Section, the Canadian River drainage, and the Portales Valley (Figure 14). The Pecos Valley Section is further divided into three subsections: the Northern Pecos Slopes, the Pecos Floodplain/Terrace, and the Southwest Pecos Slope (Hogan 2006). These different physiographic units can be used to examine adaptive strategies and to isolate differing components of prehistoric settlement-subsistence systems that may have occurred within distinct environmental zones (Hogan 2006; Katz and Katz 2001).

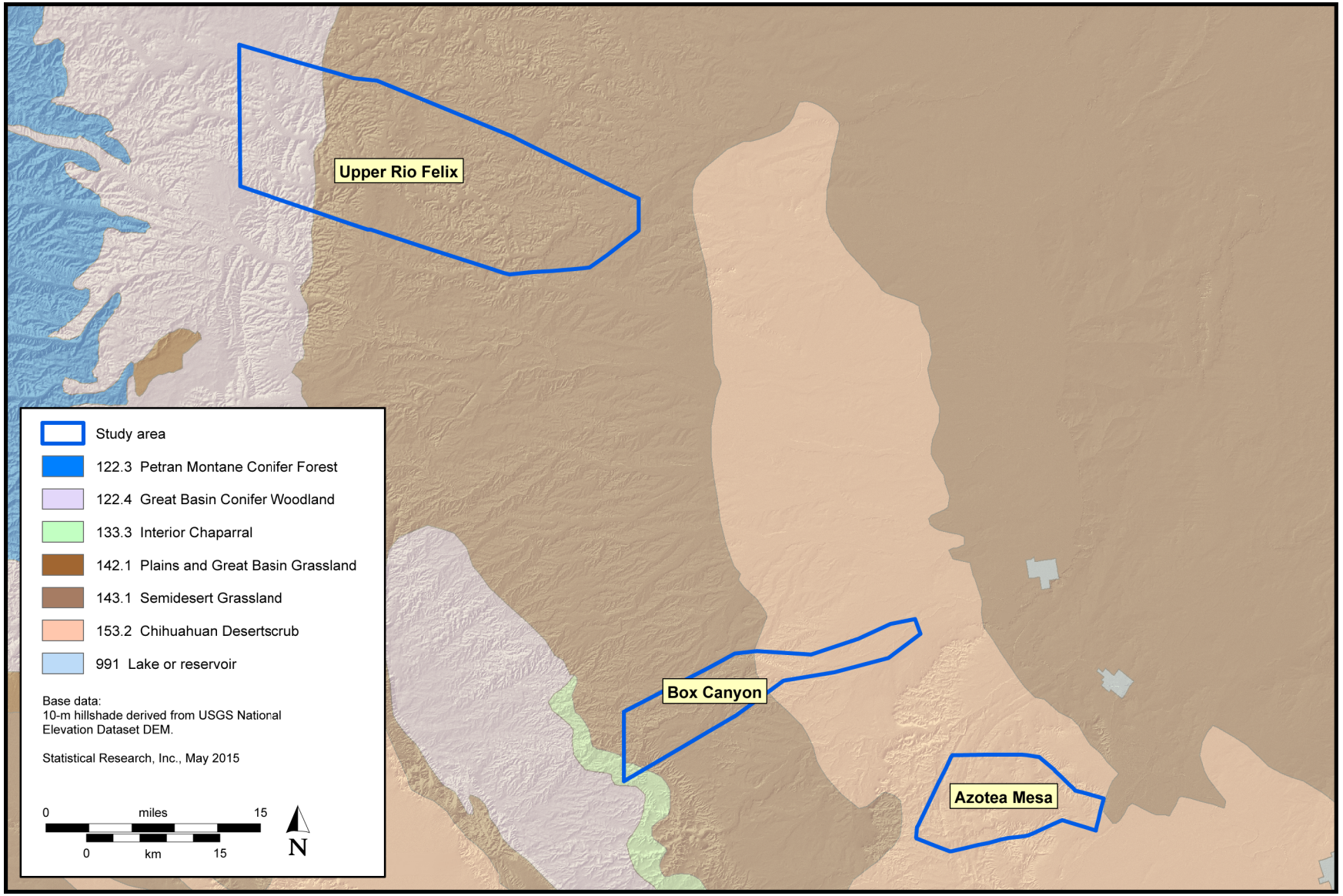

Figure 14. Physiographic subregions in the study area.

Sacramento Section

To the west of the Pecos River are the Sacramento and Guadalupe Mountains, characterized by high tablelands with broad, rolling summit plains and west-facing escarpments; the summit plains are separated by broad, structural basins typical of the Basin and Range Province (Hawley 1986:26). The highlands of the Sacramento and Guadalupe Mountains are composed of a sedimentary sequence of Permian limestone and sandstone interbedded with gypsum. Extensive areas of karst depressions are contained among the summit plains of tablelands and cuestas, where the dissolution of calcium sulfate and carbonate has resulted in the formation of extensive limestone cave systems. The three study areas are within the Sacramento Section.

Azotea Mesa is characterized by a broad, northeast–southwest-trending, heavily dissected tableland immediately west of Carlsbad. The landscape within this study area consists of rolling limestone outcrops interspersed with a series of short and narrow canyon reaches that host small, intermittent drainages. Ring middens visited during the ground-truthing survey were situated along a Holocene-aged terrace formed at the confluence of two intermittent drainages that serve as tributaries to Little McKittrick Draw.

The Box Canyon study area is north of Azotea Mesa and slightly farther west. This study area is generally characterized by a rolling limestone (San Andres Formation) and sandstone (Yeso Formation, Permian red beds) topography. Box Canyon is a narrow west–east-trending canyon enclosed by steep, limestone strath-terrace remnants. Features investigated within this study area are clustered along a Holocene-aged terrace formed along the active floodplain of Box Canyon Draw.

The Upper Rio Felix study area is broadly comparable to the Box Canyon study area and is situated within a much broader, open floodplain bordered by lower-relief Pleistocene-aged strath-terrace remnants. Similar to those in Box Canyon, ring-midden features identified along the Upper Rio Felix are situated along a Holocene-aged terrace at the confluence of an unnamed, intermittent tributary and Rio Felix. Surface soils formed within all the study areas consist of shallow, silty loams and fine sandy loams overlying a limestone-bedrock substrate. Ring middens investigated in the Upper Rio Felix study area are situated along a terrace that appears to have been subjected to periodic inundation during flooding events. Surface deposits are comparatively much deeper along this terrace, as was evident from the thick grass and forb vegetation cover formed in the thick silt deposits covering this area. Features investigated in the Upper Rio Felix study area were also mostly buried by alluvial silt deposits and had been disarticulated by water erosion.

All of the study areas include abundant sources of limestone materials that were used in the earth-oven features. These materials were available from San Andres Formation outcrops present across all of the study areas. Limestone materials were readily available either directly on-site or immediately adjacent (along the strath terraces) to each of the investigated sites.

Pecos Valley Section and Physiographic Subregions

The Pecos Valley Section is bordered on the west by the upland plains and tablelands of the Sacramento Section and on the east by the escarpment of Mescalero Ridge and the caliche caprock of the Llano Estacado. This physiographic section has been traditionally divided into upper and lower subsections based on differential drainage basins (Hawley 1986). A stepped sequence of terraced valleys bordering the Pecos and Canadian Rivers reflects alternating intervals of valley incision and stability during Pleistocene glacial-interglacial cycles. Late Tertiary and Quaternary alluvial fills are located in the broader central-valley areas along the Pecos River, south of Santa Rosa, and in the Portales Valley. Quaternary aeolian deposits blanket older surfaces of the valley border east of the Pecos River (Hawley 1986:27). The Pecos and Canadian River valleys range from broad, flat reaches occupied by floodplains and low terraces to relatively shallow canyons. Bedrock substrates within the Pecos Valley Section include Permian units composed of gypsiferous and saline evaporites, limestone and dolomite, mudstone and shale, and sandstone. Solution-subsidence depressions of varying sizes are common landscape features across this section, because of the dissolution of evaporite and carbonate units (Hawley 1986:27).

Pecos Floodplain/Terrace, Southwest Pecos Slope, and Northern Pecos Slopes

A narrow band mostly conforming to the course of the Pecos River that comprises the inner valleys, canyons, and inset terraces of Quaternary age as well as the broad Blackdom Terrace along the western side of the river near Roswell-Artesia is designated the Pecos Floodplain/Terrace subsection (Hogan 2006). The Southwest Pecos Slope subsection includes a small area of gentle slopes between the Guadalupe Ridge and Reef Escarpment and the Pecos River (Hogan 2006). The Northern Pecos Slopes subsection encompasses erosional remnants of Pliocene and lower Pleistocene alluvial deposits and higher piedmont erosion surfaces transitional to the Sacramento Section highlands, as well as a nearly level plain dipping eastward from the Portales Valley and the Llano Estacado, toward the Pecos River (Hogan 2006).

Mescalero Plain

The Mescalero Plain, though considered part of the Pecos Valley Section, is distinguished by the westward-sloping pediment surface extending from the base of Mescalero Ridge to the Pecos River. It extends southward from the Portales Valley all the way to the New Mexico–Texas border. The Mescalero sand sheet covers approximately 80 percent of this landform. Dunes, drainages, sinks, and rock outcrops provide some local relief across what is predominantly level terrain (Reeves 1972). The majority of the study area is located along the Mescalero Plain.

Canadian River Drainage and Portales Valley

The easternmost extensions of the Pecos Valley Section are defined by the Canadian River drainage and the Portales Valley (Hawley 1986:27). The Canadian River borders the northern margin of the Llano Estacado and is bounded by two prominent escarpments. To the north, the Canadian Escarpment divides the Pecos Valley from the high piedmont plains of the Raton Section, and to the south, the escarpment delineates the boundary of the Llano Estacado Section. At the northern edge of the Mescalero Plain lies the Portales Valley, which divides the westernmost edge of the Llano Estacado into northern and southern lobes. The Portales Valley represents an ancestral channel of the Upper Pecos–Brazos River formed during the middle Pleistocene (Hawley 1986:26).

Llano Estacado Section

A high, isolated pediment surface covering much of the Texas Panhandle and the eastern third of southeastern New Mexico is designated the Llano Estacado Section or the Southern High Plains (Reeves 1972:112–113). The Llano Estacado is bounded on the north by the Canadian River escarpment and on the west by the sand-dune-mantled hillsides, high sandstone cliffs, and caliche caprock of Mescalero Ridge. The Llano Estacado, or Staked Plains, is a nearly flat to undulating, broad mesa with a slight southeastward gradient that ranges in elevation from 5,000 to 3,000 feet AMSL. The resistant caliche-caprock surface of this landform is underlain by Ogallala Formation alluvial and aeolian deposits. The caprock zone of secondary carbonate accumulation rests near or at the surface along the margins of the plateau as well as in areas south of the Portales Valley (Hawley 1986:27). Elsewhere, the caprock is concealed under sandy and clayey deposits. Surface drainage is accommodated by broadly spaced, shallow stream valleys. Thousands of shallow depressions are situated across the Llano Estacado, many of which contain playas bordered by dune ridges along their eastern margins. These depressions were predominantly formed by deflation, but dissolution may also have been related to their formation and enlargement (Hawley 1986:27).

Paleoenvironment

A paleoclimatic model for the Permian Basin recently developed by Cummings and Kováčik (2013) included a detailed reconstruction of precipitation and temperature fluctuations over the past 16,000 years. These data provide a means of interpreting characteristics of the environmental setting, through time, that may have influenced aspects of human occupation across this landscape.

Pleistocene-Holocene Transitions

The Pleistocene-Holocene boundary marks the transition into a much warmer climate and decreased moisture availability. The climate during the late Pleistocene was characterized by wetter and cooler conditions linked to cyclical glacial and interglacial periods. Vegetation zones were displaced 3,000–4,000 feet lower in elevation around 18,000 B.P., when montane coniferous forest and coniferous woodland covered southeastern New Mexico (Dick-Peddie 1993). Pluvial lakes were scattered across much of the Mescalero Plain and the adjacent Llano Estacado during the late Pleistocene and early Holocene. Mollusk-bearing spring and *cienega* deposits also developed along the Mescalero Ridge escarpment during that interval (Hall 2002). The high water table in the Ogallala aquifer during that time fed numerous playas along the Llano Estacado and promoted springs at the foot of the caprock escarpment (Hall 2002).

Temperatures shifted toward hotter and drier summers during the onset of the Holocene, when forest and woodland vegetation retreated to higher elevations. The initial development of the Mescalero sand sheet also coincided with the shift toward xeric conditions (Hall 2002). During that time, the water table also dropped, resulting in the disappearance of playa lakes and springs. Sagebrush also retreated from the grasslands. Desertscrub- and semidesert-grassland vegetation similar to the modern environment was established in the Permian Basin by 8000 B.P.

Middle Holocene

Around 6500 B.P., a warming trend began, and it resulted in increasingly xeric conditions characterized by rising temperatures and decreased annual precipitation, persisting until around 5800 B.P. Temperatures consistently rose throughout that duration of time until the termination of the Medieval Warm Period. Winter precipitation also declined around 5900 B.P. There was a slight rise around 5400 B.P., followed by another drop between 4800 and 4000 B.P. An upward trend in summer precipitation occurred until around 5500 B.P. and was sustained until 4400 B.P., and precipitation declined until around 3300 B.P. Precipitation patterns around 6400 B.P. typically occurred during the late summer, peaking in September, with a smaller spike during the mid-summer, in June. Those patterns shifted to dominant August–September rainfall between 5400 and 4000 B.P. Subsequent to that, rainfall patterns exhibited an annual peak in August over the next 500 years, until another shift to August–September-dominant rainfall. Overall climatic trends during the middle Holocene revealed two major periods of environmental stress from 6500 to 5400 B.P. and around 4000–3000 B.P. (Cummings and Kováčik 2013). Vegetation during that time likely consisted of desert-shrub grassland. The Mescalero sand sheet continued to form a thick mantle over the Berino paleosol (Hall 2002).

Late Holocene

Temperature fluctuations over the last 2,000 years have exhibited less seasonal variability than 5,000 years ago, reflecting modern conditions in the Permian Basin. Annual precipitation over the last 800 years has been slightly higher than during the middle Holocene, averaging approximately 12 inches. Winter precipitation has been historically low in this area, and climate regimes have been dominated by the summer-monsoon pattern. Summer precipitation has exhibited variable fluctuations persisting into

the modern era. Around 2100 B.P., rainfall shifted from a dominant August–September pattern to peaks occurring in May and July. That shift toward late-spring–summer-dominant rainfall patterns diminished after 500 years. For the past 400 years, the seasonality of rainfall has diminished in intensity during the late spring, entirely disappearing for extended periods, and has included a return to a July–August-dominant rainfall pattern. That shift in precipitation patterns corresponded to the Little Ice Age cooling period (Cummings and Kováčik 2013).

Environmental stresses have been less severe than during the middle Holocene but persisted from 2000 to 1600 B.P. and over the past 200 years. The modern environment of the study region has been less hospitable during the historical period than it was during prehistoric occupation of the area (Cummings and Kováčik 2013). A period of landscape stability between 500 and 100 B.P. resulted in the formation of a weak A soil horizon (the Loco Hills soils) along the Mescalero sand sheet. The deflation and concurrent accumulation of coppice and parabolic dunes are the most recent and rapid geologic changes that have occurred along the Mescalero sand sheet. Erosion has presumably been related to changes in historical-period land use—most notably, increased use of the area for grazing livestock, which dramatically impacted the vegetation cover that had developed along the sand sheet during the previous phase of landscape stability (Hall 2002).

Holocene Vegetation Patterns and Prehistoric Land Use

The past 8,000 years has witnessed some dramatic shifts in local vegetation patterns across the study area. Desertscrub- and semidesert-grassland communities developed across the Permian Basin subsequent to the retreat of the coniferous forest and woodland to higher elevations. Although grasslands originally covered much of southeastern New Mexico, the grasses have been replaced with scrubland vegetation as a result of overgrazing during the past 150 years. Table 1 presents a list of plant species currently identified across the three separate study areas.

Macrobotanical remains, phytoliths, and starches recovered from 500 thermal features sampled across the Mescalero Plain and synthesized during a Permian Basin Memorandum of Agreement area research project reflected an emphasis on the use of wild plant species endemic to the Chihuahuan Desert (Cummings and Kováčik 2013). An examination of the macrobotanical remains recovered from features spanning the Middle Archaic period to the Formative and late historical periods indicated a limited variety of wild-plant resources, such as honey mesquite, sumac, barrel cactus, prickly pear, *Chenopodium-Amaranthus* spp., fourwing saltbush, copperleaf or threeseed mercury, sandmat, acacia, acorns, carpetweed, dropseed, goosefoot, juniper, hedgehog cactus, and sunflower (Cummings and Kováčik 2013). Only scant evidence of domesticated food resources (i.e., maize) was identified within the sampled features. Cummings and Kováčik (2013) suggested that the presence of maize within those limited contexts reflected the transport of domesticated resources across the study area, rather than local cultivation. The frequent occurrence of both Cyperaceae sp. and *Commelina* L. sp. (dayflower) phytoliths within a large number of the sampled thermal features was interpreted to reflect human-induced changes to the environment. It was speculated that the occurrence of those weedy species reflected the formation of microhabitat resource patches that resulted from disturbances to the landscape as an unintended consequence of human occupation. Cummings and Kováčik (2013) also suggested that the proliferation of those species may have indirectly enhanced the habitat for quail. Dayflower is a known winter seed resource eaten by quail, and human-induced disturbances to the landscape may have unintentionally promoted the presence of those wild-animal resources within the area.

Table 1. Plant Species Identified during the Ground-Truthing Survey

Genus and Species, by Family	Common Name	Upper Rio Felix	Azotea Mesa	Box Canyon
Agavaceae (agave family)				
Agave parryi spp. *neomexicana*	New Mexico agave, Parry's agave			X
Agave gracilipes	slim-footed agave, slimfoot century plant			X
Agave lechuguilla	lechuguilla		X	
Yucca elata	soaptree yucca	X	X	X
Yucca torreyi	Torrey yucca	X		
Yucca treculeana	Spanish dagger			X
Anacardiaceae (cashew family)				
Rhus microphylla	littleleaf sumac		X	X
Rhus trilobata	fragrant sumac		X	
Asteraceae (sunflower family)				
Acourtia nana	desert holly, perezia	X	X	X
Artemisia ludoviciana	white sagebrush, gray sagewort, prairie sage		X	X
Baccharis salicina	Great Plains falsewillow, willow baccharis	X		X
Erigeron divergens	spreading daisy, spreading fleabane	X	X	
Gaillardia pinnatifida	red-dome blanketflower, slender gaillardia	X		
Gutierrezia sarothrae	broom snakeweed		X	X
Melampodium leucanthum	plains blackfoot daisy		X	
Parthenium incanum	mariola		X	
Senecio flaccidus	Douglas senecio, threadleaf groundsel			X
Viguiera stenoloba	resinbush, skeletonleaf		X	
Berberidaceae (bayberry family)				
Mahonia trifoliolata	agarito, algerita		X	X
Bignoniaceae (catalpa family)				
Chilopsis linearis	desert willow	X		
Boraginaceae (borage family)				
Tiquilia greggii	Gregg's coldenia, plumed crinklemat		X	
Brassicaceae (mustard family)				
Lepidium montanum	mountain pepperweed		X	
Lesquerella fendleri	Fendler bladderpod		X	
Cactaceae (cactus family)				
Echinocereus pectinatus	rainbow cactus	X	X	X
Echinocereus triglochidiatus Engelm.	claretcup cactus	X	X	X
Mammillaria heyderi	Heyder's pincushion, little nipple cactus		X	X
Opuntia imbricata	cane cholla, walkingstick cholla	X	X	X
Opuntia leptocaulis	Christmas cholla, tasajillo	X	X	X
Opuntia phaeacantha	brownspine prickly pear, tulip prickly pear		X	X
Chenopodiaceae (goosefoot family)				
Atriplex canescens	fourwing saltbush		X	
Cupressaceae (cypress family)				
Juniperus monosperma	oneseed juniper		X	X
Euphorbiaceae (spurge family)				

continued on next page

Genus and Species, by Family	Common Name	Upper Rio Felix	Azotea Mesa	Box Canyon
Croton lindheimerianus	three-seed croton	X	X	X
Fabaceae (pea family)				
Astragalus mollissimus	purple locoweed, woolly milkvetch	X		
Fouquieriaceae (ocotillo family)				
Fouquieria splendens	ocotillo		X	
Hydrophyllaceae (waterleaf family)				
Nama hispidum	bristly nama, purple mat, sandbells		X	X
Juglandaceae (walnut family)				
Juglans microcarpa	little walnut	X		
Liliaceae (lily family)				
Allium kunthii	Kunth's onion		X	X
Dasylirion leiophyllum	green sotol		X	X
Nolina texana	basketgrass, Texas sacahuista		X	X
Malvaceae (mallow family)				
Sphaeralcea coccinea	red falsemallow, scarlet globemallow		X	X
Mimosaceae (mimosa family)				
Acacia constricta	whitethorn acacia		X	
Mimosa borealis	fragrant mimosa, pink mimosa		X	X
Prosopis glandulosa	honey mesquite		X	X
Onagraceae (evening primrose family)				
Calylophus hartwegii ssp. *fendleri*	Fendler calylophus	X		
Oenothera pallida	pale evening primrose	X		
Plantaginaceae (plantain family)				
Plantago patagonica	woolly plantain	X	X	X
Poaceae (grass family)				
Pleuraphis mutica	tobosagrass	X		
Polygonaceae (buckwheat family)				
Rumex hymenosepalus	sand dock	X	X	
Rhamnaceae (buckthorn family)				
Condalia ericoides	javelina bush		X	
Scrophulariaceae (figwort family)				
Maurandella antirrhiniflora	climbing snapdragon			X
Verbascum thapsus	woolly mullein	X		
Solanaceae (potato family)				
Lycium berlandieri	silver desertthorn		X	
Quincula lobata	Chinese lantern, purple groundcherry		X	
Verbenaceae (vervain family)				
Glandularia wrightii	Davis Mountain mock vervain, Wright's verbena	X	X	X
Lippia graveolens	Mexican oregano		X	X
Verbena hastata	blue verbena, swamp verbena	X		
Zygophyllaceae (creosote bush family)				
Larrea tridentata	creosote bush		X	

Note: Terminology supplied by the botanist at Carlsbad Caverns National Park.

Archaeological Background

This section provides a cultural-historical overview of the study area. Archaeological sites investigated in the Southeastern New Mexico Ring Midden Lidar Survey Project area all reflect Formative period temporal components. Background information presented in this section is intended to provide a framework for the specific research issues used in evaluating the significance and research potential of the investigated sites.

Paleoindian Period

The earliest evidence of human occupation of the Mescalero Plain and adjacent portions of the Llano Estacado dates to the Paleoindian period (ca. 10,000–6000 B.C.). Paleoindian period populations are traditionally characterized as highly mobile groups that hunted and scavenged extinct megafauna, such as mammoth and a robust form of bison (*Bison antiquus*). The Paleoindian period is typically divided into three main complexes/subphases based on variability in tool kits and projectile point forms.

Clovis Complex

The Clovis complex (ca. 10,000–9000 B.C.), characterized by lanceolate, fluted spear points, represents the first definitive evidence of human occupation in North America (Figure 15). An additional distinctive characteristic of the Clovis complex lithic tradition is a core-and-blade technology that resulted in the production of large, prismatic blades (Collins 1999; Green 1963; Hester 1972; Stanford 1991). Raw materials identified in Clovis complex assemblages typically consist of high-quality cryptocrystalline silicates originating in distant, nonlocal sources consistent with a high degree of residential mobility. However, locally available raw materials were also used by these populations as sources of tool stone (Condon 2006).

Folsom Complex

The Folsom complex (ca. 9000–8000 B.C.) immediately followed the Clovis complex and has sometimes been interpreted to overlap with it. This period in time was host to major environmental changes coinciding with the late Pleistocene–early Holocene transition and the extinction of large megafauna. Folsom adaptations have been invariably linked to a reliance on bison hunting, and numerous mass-kill sites have been documented in the archaeological record for the Southern High Plains (e.g., Lubbock Lake, Blackwater Draw Locality No. 1, Plainview, and Milnesand) (Holliday 1997). Folsom groups were largely confined to the Great Plains and its peripheries. Similar to Clovis points, Folsom points are also characterized by the lanceolate spear point, with a concave base and a wide, shallow flute that extends almost the entire length of the point. Raw-material selection among Folsom assemblages continued to exhibit high-quality nonlocal tool stone as well as locally available materials (Condon 2006). Various researchers have suggested both temporal and technological overlap of Folsom and Midland components (e.g., Amick 1995; Holliday 1997; Sebastian and Larralde 1989). Midland points exhibit a lanceolate form similar to Folsom points but are unfluted.

Late Paleoindian Period

Late Paleoindian period complexes (ca. 8000–6000 B.C.) are generally more varied and less understood than the preceding Folsom complex. Common projectile point styles assigned Late Paleoindian period temporal affinities include a series of unfluted, lanceolate forms, such as Plainview, Plano, Firstview, Hell Gap,

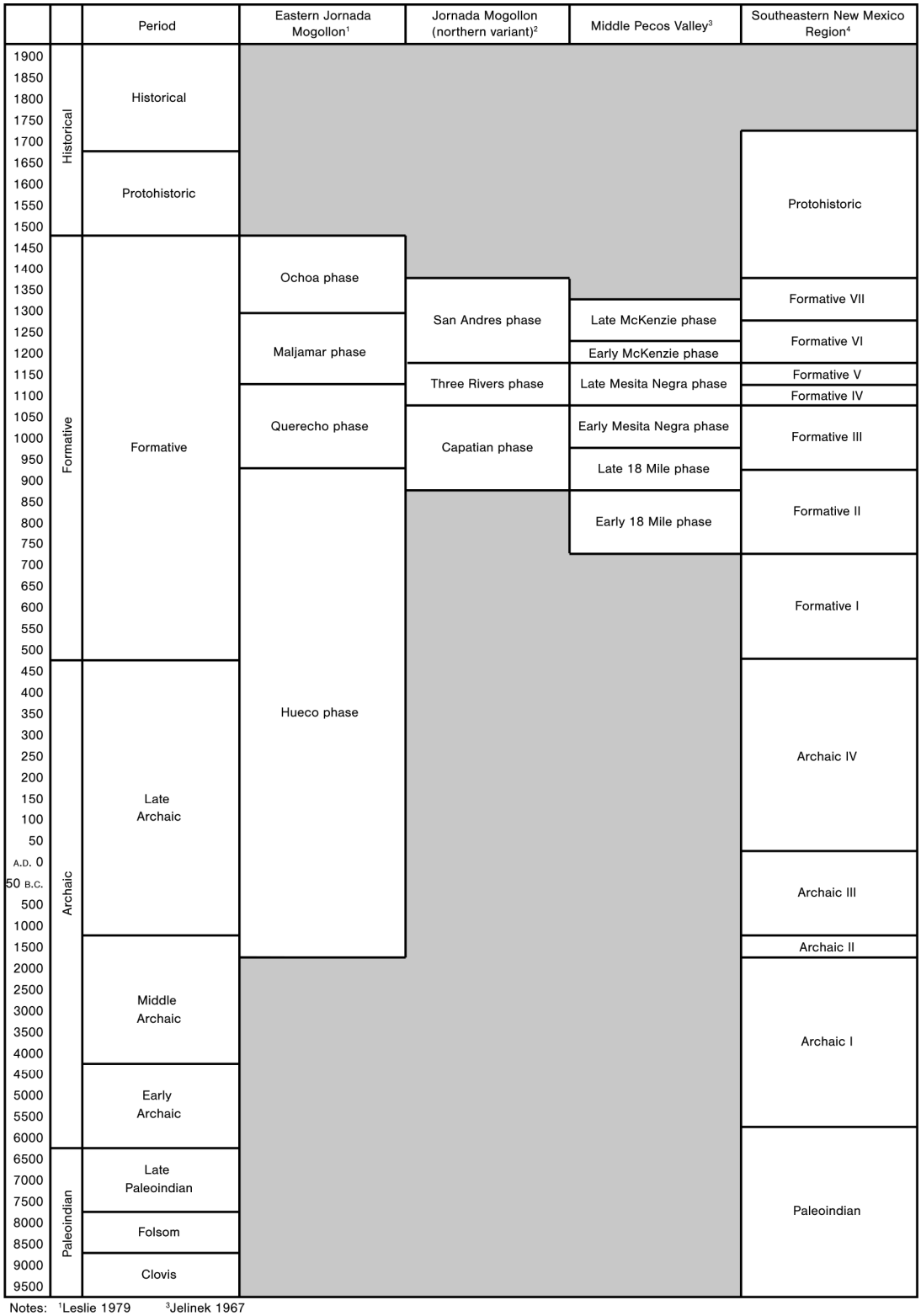

Notes: [1]Leslie 1979 [3]Jelinek 1967
[2]Lehmer 1948 [4]Katz and Katz 1993, 2001

Figure 15. Regional cultural-historical schematics for southeastern New Mexico.

Eden, and Cody (Turner and Hester 1993). Subsistence patterns during this time have been traditionally defined as a continuation of specialized bison hunting but are presumed to reflect a gradual shift toward a more generalized subsistence strategy.

Archaic Period

Researchers typically view the Paleoindian–Archaic period transition as a shift to a broad-spectrum hunter-gatherer settlement configuration that included patterns of seasonal mobility influenced by the availability of specific plant resources (Beckett and MacNeish 1994; Irwin-Williams 1973; MacNeish 1993; Vierra 2005). The Archaic period (ca. 6000 B.C.–A.D. 500) encompassed a wide time depth and has been traditionally divided into Early, Middle, and Late periods based on variations in projectile point typology and paleoenvironmental conditions. Katz and Katz (1993) provided a regionally specific cultural sequence for the Archaic period in southeastern New Mexico that was divided into four generalized phases, as discussed below.

Early Archaic Period

The Early Archaic period (ca. 6000–4000 B.C.) is the first Archaic period phase and is typically defined by a morphologically unique lanceolate projectile point style, commonly referred to as the Jay complex style, characterized by weak shoulders and a long, tapering stem (Irwin-Williams 1973). Although technological aspects of the Jay complex have been identified in southeastern New Mexico, these manifestations have not been associated with a dated context in the region (Katz and Katz 1993, 2001). An additional point style potentially dating to the Early Archaic period is the slender, bipointed Lerma point (Turner and Hester 1993). The Archaic I phase (ca. 5500–1700 B.C.) identified by Katz and Katz (1993) temporally overlaps with the Early Archaic period but encompasses a broad time depth that is too ambiguous for precise interpretations and lacks supporting chronological data.

Vierra et al. (2012) suggested that this period may correspond to the transition from early Holocene warming to middle Holocene xeric conditions and the concomitant movement of Early Archaic period groups into adjacent regions. Bajada phase (4800–3200 B.C.) manifestations, distinguished from Jay complex points by the presence of basal indentation and thinning, well-defined shoulders, and decreasing length, appeared during the terminal Early Archaic period and persisted until the early portion of the Middle Archaic period (Irwin-Williams 1973). That period in time has been interpreted to reflect a mixed spectrum of subsistence activities adapted to the seasonal exploitation of local resources. The presence of Jay and Bajada point types found within the region could reflect limited resource-procurement excursions into desert areas of southeastern New Mexico from the uplands to the north (Vierra et al. 2012).

Middle Archaic Period

The Middle Archaic period (ca. 4000–1200 B.C.) roughly corresponds to the Archaic II sequence (1700–1000 B.C.) identified by Katz and Katz (1993). However, the Archaic II temporal subdivision was based on the dated context of isolated FCR features devoid of associated diagnostic typological assemblages (Hogan 2006). Varieties of diagnostic artifacts associated with the Middle Archaic period have been found in the region, including San Jose–style, contracting-stem (e.g., Langtry), and large side-notched projectile points, which have been interpreted to reflect the movement of groups between the southern desert lowlands and the northern uplands as well as between the desert regions to the west and east and the southern borderlands (Carpenter et al. 2005; Miller and Shackley 1998). San Jose–style projectile points are characterized by basal grinding, serrated blades, and relatively smaller stem-to-blade ratios than are seen in earlier Bajada points, and there was a later development toward increasingly expanded stems and marked serrations (Irwin-Williams 1973). A notable addition to the lithic assemblage during this time was the appearance of milling stones and shallow basin metates, which reflect the intensification of plant-processing activities.

Paleoenvironmental conditions improved after the middle Holocene dry period, and there appears to have been an intensified use of the southern-borderland deserts by Middle Archaic period groups, as evidenced by the increasing number of sites dating to this interval (Amick and Lukowsi 2006; Anderson 1993; Carmichael 1986; O'Laughlin 1980). Aspects of subsistence, settlement, and technological adaptations appear to reflect a greater emphasis on hunting smaller game and wild-plant foraging, which also may have involved an increasing use of upland resources, such as piñon nuts (Vierra 2007). Evidence of ephemeral brush structures during this interval has been found, and large FCR earth ovens and larger groupings of hearths may suggest an increase in the size of specialized-activity groups (Irwin-Williams 1973).

Late Archaic Period

The Late Archaic period (ca. 1200 B.C.–A.D. 500) broadly correlates to the Archaic III and IV phases defined by Katz and Katz (1993). This period heralded the appearance of the earliest-dated maize remains (ca. 1200 B.C.), which were recovered from Tornillo Rockshelter, Fresnal Cave, and Cerro Juanaqueña (Hard and Roney 2005; Tagg 1996; Upham et al. 1987). Projectile points correlating to the Late Archaic period (e.g., Ensor, Palmillas, Maljamar, Marcos, and San Pedro) exhibit a pronounced degree of stylistic variability but are typically characterized by corner-notched and stemmed dart points with large, triangular blades and no basal grinding (Shelley 1994; Turner and Hester 1993).

This interval in time was witness to the use of domesticated-plant resources (i.e., maize), accompanied by a shift toward the use of more-formalized milling technology, although Hard et al. (1996) suggested that there was a low reliance on the use of domesticated food resources by Jornada Archaic period groups. Models of cyclical transhumance have been based on the seasonal availability of plant resources and macrobotanical remains recovered from rockshelter contexts (Anderson 1993). Anderson's (1993) model projected the use of lower-basin settings during the late spring, summer, and early fall to exploit grasses, mesquite, and rabbits and the use of upland alluvial-fan settings for agricultural pursuits. Upland occupations within rockshelters provided resources such as piñon, oak, and deer, which were exploited during summer and fall occupations, and maize was likely cultivated in these areas (Bohrer 2007; MacNeish 1993). Overall patterns of decreased residential mobility, increased complexity in the use of specific environmental zones, and an increasing reliance on maize cultivation typify the Late Archaic period (Anderson 1993).

Formative Period

The Formative period is marked by the introduction of ceramic technology, the appearance of the bow and arrow, the intensification of maize agriculture, and the adoption of a more-sedentary way of life, although these developments did not simultaneously occur across all areas of southeastern New Mexico. The earliest reported instance of Jornada Brown wares, around A.D. 200, was based on radiocarbon dates obtained from Deadman's Shelter (Hogan 2006; Hughes and Willey 1978). Evidence of agricultural intensification and sedentary settlement within the study area has been extremely limited, and there is a traditionally accepted view that there was a continuation of the hunter-gatherer subsistence economy within this region throughout the Formative period.

A number of local phase sequences have been developed for southeastern New Mexico, most of which have limited applicability to this study area, because of the scattered and ephemeral nature of archaeological manifestations in the dynamic aeolian setting of the Mescalero Plain. Lehmer (1948) was the first researcher to recognize the Jornada branch of the Mogollon, as a result of his seminal field investigations conducted in south-central New Mexico. Katz and Katz (1993, 2001) constructed a regional cultural sequence for southeastern New Mexico that was subdivided into seven Formative period phases encompassing generalized date ranges common to multiple local phases. That provisional framework was designed to accommodate broad regional comparisons, but the approach did not include associated developmental changes in artifact types, architectural forms, settlement locations, and subsistence patterns specific to a particular area (Hogan 2006). Another problem with the temporal approach adopted by Katz and Katz (1993, 2001) was

the near impossibility of assigning Ceramic period sites to particular phases based on the presence of temporally diagnostic artifacts (Hogan 2006). Among the various locally specific phase sequences pertaining to southeastern New Mexico, the cultural sequence developed by Leslie (1979) for the eastern extension of the Jornada Mogollon is the most applicable to cultural resources in the Permian Basin. That sequence followed the work of Lehmer (1948) and Corley (1965), which also broadly paralleled general developments associated with the pit-house-to-pueblo transition identified in other major culture areas of New Mexico.

Late Hueco Phase

The earliest phase associated with the local introduction of ceramic technology is referred to as the Hueco phase (pre-A.D. 500–950). This phase overlaps both the Late Archaic and Early Formative periods and is presumed to represent the precursor of Formative period developments (Leslie 1979). It also roughly corresponds to the Formative I phase and the early portion of the Formative II phase identified by Katz and Katz (1993). Only scant evidence of brown ware ceramics and informal ground stone has been associated with late Hueco phase sites. Additional grinding implements added to the Early Formative period milling inventory were bedrock mortars and pestles. Manifestations have mostly consisted of ephemeral campsites with no evidence of structural remains (Leslie 1979). Projectile points associated with this interval in time are Leslie's (1978) Types 5 and 6, as well as regional types, such as Scallorn-style arrow points, and are generally characterized by expanding-base, side- and corner-notched points with triangular blades. A synthesis of radiocarbon dates obtained from various excavations conducted in the Permian Basin revealed a dramatic increase in the occupational intensity of this area beginning in the Late Archaic period and peaking during the Early Formative period (Railey et al. 2009).

Querecho Phase

The Querecho phase (A.D. 950–1100/1150) is considered to be the first ceramic phase associated with Eastern Jornada Mogollon manifestations. Jornada Brown has dominated the ceramic assemblage, sometimes accompanied by Cebolleta and Mimbres Black-on-white trade wares. This period in time also represents the introduction of the bow and arrow, noted by the appearance of corner-notched arrow points that correspond to Leslie's (1978) Types 3A–3F. Grinding implements added to the ground stone assemblage included oval basin metates and convex-faced manos. Most of the known sites from the early part of this phase were nonstructural, but small, rectangular pit rooms and possible surface-room floors configured into loosely aggregated villages have been identified at a handful of late Querecho phase sites (Leslie 1979). A large increase in the presence of logistical gathering sites also appears to have occurred within the large parabolic-dune fields during the Querecho phase. Manifestations assigned to the Querecho phase correspond to the latter half of the Formative II phase and the Formative III phase identified by Katz and Katz (1993).

Maljamar Phase

The Maljamar phase (ca. A.D. 1100/1150–1300) has been suggested to represent a transition into a more-sedentary lifeway characterized by the appearance of pit-house villages with up to 20–30 rectangular structures each (Leslie 1979). Small logistical sites were still established during this phase but were present in smaller numbers. Jornada Brown remained the dominant local ceramic type, and some corrugated wares appeared near the end of the phase. Chupadero Black-on-white, accompanied by small quantities of El Paso Polychrome and Three Rivers Red-on-terracotta, also appeared during this time. Additional nonlocal types occurring during the terminal Maljamar phase included Glaze A, Gila Polychrome, Ramos Polychrome, and Lincoln Black-on-red. Projectile points transitioned from corner-notched to side-notched styles, such as Leslie's (1978) Types 2A and 2B, around A.D. 1200. Leslie (1979) suggested that a large portion of the Eastern Jornada area may have been temporarily abandoned during the latter half of the phase. The Maljamar

phase corresponds to the Formative IV, V, and VI phases described by Katz and Katz (1993). There has been increased evidence of agriculturally based subsistence strategies from the Formative VI phase, and bison remains have been identified in association with Formative VI phase sites.

Ochoa Phase

The Ochoa phase (ca. 1350–1450/1500) is the latest phase associated with Eastern Jornada manifestations. Village sites with 15–30 surface rooms arranged as units or small room blocks and large, shallow pit structures correspond to this phase. Chupadero Black-on-white constituted the dominant decorated ware, accompanied by Ochoa Corrugated brown wares (Leslie 1979). Additions to the lithic assemblage included shaft straighteners, scrapers, and an increase in the presence of obsidian. The projectile points are characterized by the appearance of small, corner- and basal-notched arrow points corresponding to Leslie's (1978) Types 2C–2F. The Ochoa phase parallels the Formative VII phase identified by Katz and Katz (1993) and potentially corresponds to the Little Ice Age cooling period. Although the Protohistoric period is typically conceived as beginning with the first arrival of Spanish explorers, Katz and Katz (1993) pushed back the beginning of this period to coincide with the first appearance of Athapaskans in the region.

Protohistoric Period

Early Spanish explorers travelled through portions of southeastern New Mexico during expeditions conducted around the mid-sixteenth century. The southernmost portion of southeastern New Mexico may have been passed through by Cabeza de Vaca around 1535, along with other survivors of a Spanish shipwreck off the Texas coast, on their way back to Mexico (Pratt et al. 1989). Later entradas, including one by Francisco Vasquez de Coronado in 1541, may have entered the area en route to the Southern Plains, in search of the riches of "Quivera" (Pratt et al. 1989). Antonio de Espejo and Castano de Sosa also led expeditions that followed the Pecos River valley in the late sixteenth century (Williams 1986). The period from 1650 to 1800 was host to several Spanish military expeditions that entered southeastern New Mexico to commercially engage with the Jumanos, as well as for slave raiding (Katz and Katz 1985b; Pratt et al. 1989). Recorders of those expeditions described encounters with Apache groups (referred to as the Querechos, Vaqueros, and Faraones) and the Jumanos, and historical documents mentioned the Siete Rios Apache who inhabited an area near Carlsbad in 1659 (Pratt et al. 1989). Those groups became part of the Mescalero Apaches during the late nineteenth century (Pratt et al. 1989).

Historical Period

Euroamerican settlers attracted by available grazing land had migrated into southeastern New Mexico and established livestock ranches in the area by the mid-nineteenth century. Under the Homestead Act of 1862, a quarter section of land was guaranteed to citizens in the instance that it was settled and improved. The Eddy brothers, along with Joseph S. Stevens, had established the Pecos Irrigation and Investment Company to irrigate the Pecos River valley by the 1880s, to supply much-needed water for farming in the area. In 1891, the Pecos Valley Railroad, running from Eddy to Pecos, was established with the financial backing of John James Hagerman. The residents of Eddy voted to change the name of their town to Carlsbad in 1899, with hopes of attracting tourists to local hot springs. Potash mining became a prominent industry in the area during the 1920s and continues into the present day. The Carlsbad area became the focus of oil and gas development with the establishment of the El Paso Natural Gas Company in 1928, and an emphasis on mining activities has remained a mainstay of the local economy for almost a century.

CHAPTER 3

Presurvey Ring-Midden Visualization, Characterization, and Modeling

Introduction

The current project was designed to take place in a series of iterative stages that would facilitate the identification of ring-midden features, the characterization of their attributes and environmental associations, and the development of models that could facilitate their discovery. In this chapter, we describe our efforts to visualize and characterize ring-midden features using the lidar data collected by Surdex for the project, as well as our efforts to model ring-midden location in the study areas based on the features' recorded distribution and associations with environmental variables. The efforts described in this chapter were subsequently used to guide and inform our digital survey efforts, which are presented in Chapter 4.

Ring-Midden Visualization

Visualization refers to the data and methods used to observe patterns in remotely sensed data, such as lidar data (Devereux et al. 2008). Hillshading is one of the most commonly used techniques for visualizing lidar data for the purpose of archaeological prospection. Hillshade algorithms use a modeled light source to calculate the shading for each cell in a digital elevation model (DEM), producing a raster layer that looks like a natural surface if one were to view a landscape from above, as from a hot-air balloon (Challis et al. 2011:281). As archaeologists increasingly make use of lidar and other remotely sensed data to conduct archaeological prospection, many investigators have come to realize that standard hillshade representations used to visualize terrain are less informative than other visualization techniques. For example, in comparing visualization techniques, Challis et al. (2011:282) concluded that "hill-shading fails to adequately highlight subtle features as well as those aligned close to the azimuth of the illumination source." To make better use of lidar data in archaeological prospection, investigators have been experimenting and comparing different approaches to the visualization of archaeological features, including principal-components analysis (PCA), slope analysis, solar-insolation models, and LRMs (Challis et al. 2011; Hesse 2010; Kokalj et al. 2011, 2013; Štular et al. 2013).

In addition to particular visualization techniques used to identify features in lidar data, decisions need to be made carefully when processing lidar data to produce DEMs and other products. To visualize potential ring-midden features using the lidar data, we first created DEMs for select areas that contain known ring middens, using the lidar data. To create the DEMs, we used returns classified as bare ground as well as those classified as low vegetation, because returns corresponding to the surface of an obtrusive archaeological feature are sometimes misclassified as low vegetation rather than bare ground. So, using only returns classified as bare ground can have the effect of obscuring or erasing the topographic signatures of target archaeological features (i.e., ring middens). Experimentation revealed that the creation of a DEM with a 0.25-m cell resolution, using the minimum elevation return per grid cell and natural-neighbor assignments for cells lacking valid returns, was suited well to identifying small-scale topographic features that are morphologically consistent with ring-midden features. Once the DEM had been created, a hillshade was then created from the DEM. A low sun altitude of 25° and a z factor of 1.5 were used to generate the hillshades, in order to make small changes in surface topography more pronounced and visible.

Using the DEM, we experimented with a variety of ways of visualizing the data, using slope analysis, TPI, and LRMs. Slope analysis was conducted by calculating percent slope, using the Slope tool in ArcGIS. LRMs and TPI appear to have the greatest potential for visualizing ring middens using the lidar data.

TPI was calculated for the DEM by first finding the maximum and minimum elevations within a specified radius and then applying the following formula to the resulting data:

(local elevation – minimum elevation) / (maximum elevation – minimum elevation).

In experimenting with this variable, we found that an effective way to visualize ring middens using TPI was to calculate the minimum elevation within a 2.5-m radius (representing the central depression of a ring-midden feature) and the maximum elevation within a 10-m radius (representing the area within which a ring-midden berm typically falls). An advantage of this approach is that the calculations are made using a circular neighborhood, which conforms to the typical geometry of a ring midden in plan view.

An LRM uses a DEM to create a generalized terrain surface that represents the general trend in terrain at a user-specified scale (Hesse 2010). That generalized terrain surface is then subtracted from a DEM, in order to filter out the general terrain from the DEM and highlight local, or fine-scale, variation in relief. An LRM is an especially valuable tool for identifying archaeological features in lidar data and was designed for that purpose.

The basic process for creating an LRM in a GIS is as follows:

1. Smooth the DEM by applying a low-pass filter.
2. Create a difference model by subtracting the smoothed DEM from the original DEM.
3. Create break lines between the negative and positive values in the difference model by creating contour lines where the elevation equals 0.
4. Create a simplified elevation surface by extracting real elevation values from the original DEM along the break lines.
5. Convert the raster cells in the simplified elevation surface to points.
6. Create a digital terrain model (DTM) by creating a triangulated irregular network (TIN) from the simplified elevation-surface points and then converting the TIN to a raster.
7. Calculate an LRM by subtracting the DTM from the original DEM.

LRMs were calculated using a modified version of the Local Relief Model Toolbox for ArcGIS 10.2 created by David Novák (https://drive.google.com/folderview?id=0Bxw2O48YquY4eG5aTTloSTNWdjg&usp=sharing, accessed November 7, 2014). In attempting to use Novák's tool, which was created in ArcGIS ModelBuilder, we found that the tool consistently crashed when reaching the penultimate step in the process. The final steps of the process could then be completed manually, but because we intended to calculate LRMs for a large number of survey tiles (see Chapter 4), we felt it was necessary to revise the tool so that it could function effectively from start to finish on our computing systems. Adam Byrd, who has extensive experience creating Python applications, rewrote Novák's tool as a Python script, which enabled us to batch process LRMs across our study area (see Appendix B).

The resulting LRM shows where, in an area of interest, the elevation values are above or below the values that would be expected based on the DTM. This process essentially filters out the general terrain surface to allow subtler and finer-scale topographic features, such as ring middens, to "stand out" and be more visually prominent. To visualize ring middens using these data, we developed a standard process of displaying the hillshade with a 60 percent transparency, as described above, over the LRM. This visualization approach greatly enhanced our ability to visually detect potential ring-midden features using the lidar data.

Lidar-intensity data were also used in the attempt to visualize ring middens (Challis and Howard 2013). Some portions of ring-midden features stood out in the lidar-intensity data, but it proved to be quite difficult to isolate consistent variation in lidar intensity with respect to ring middens. Further processing and review

of the lidar-intensity data in the future could potentially improve the utility of lidar-intensity data in identifying ring middens within the study areas, but that was not attempted during the current study.

Presurvey Identification Methods

In order to identify possible ring-midden features using lidar data, we evaluated the site records for previously recorded sites within the lidar study areas where ring middens had been identified as present (Figures 16 and 17). Site records were reviewed to estimate the numbers of ring middens at recorded sites and assess their recorded characteristics and distribution (Table 2). We then created hillshades, TPIs, and LRMs for a series of areas of interest where sites containing ring-midden features had been previously recorded. These areas of interest were then systematically searched for possible ring-midden features evident in the hillshade, TPI, and LRM data. In doing this, we found that it certainly was possible to detect ring-midden features using transformations of the lidar data but also that recorded ring-midden features were difficult to spot in some cases, even at sites where large numbers of ring middens had been recorded.

In a number of cases, possible ring-midden features were located close to, but outside, site polygons. Also, the specific spatial configuration of possible ring-midden features as recognized using the digital data was sometimes inconsistent with the spatial configuration of ring middens as recorded on a site map. Differences between digitally recognized ring-midden distributions and site records often appeared to be idiosyncratic. In general, however, many differences appeared to have resulted from inaccuracies in mapping the location of a site or from cartographic distortions likely introduced during the creation of hand-drawn maps during site-recording episodes. However, it is also likely that topographically subtle ring-midden features may be difficult to recognize in the digital data, as we confirmed later, during the field-verification phase of the project (see Chapter 4).

In examining areas of interest for potential ring-midden features using the digital data, potential ring-midden features were identified within recorded sites as well as in nearby areas where morphologically similar features were evident. When a potential ring-midden feature was identified, a polygon circumscribing the feature was then created, using the Ellipse tool in ArcEditor, and notes were made regarding feature characteristics.

Morphometric Characterization

To characterize the morphology of suspected ring-midden features identified in the digital data prior to digital survey, we identified a series of 59 potential ring-midden features at or near sites in the Azotea Mesa and Box Canyon study areas that had been identified as having documented ring-midden features. Two profiles were created for each potential ring-midden feature, using 3D Analyst in ArcGIS 10.2. Profile lines bisected each feature from one outside basal edge of the ring-midden berm to the outside basal edge on the opposite side of the feature. If a feature was roughly circular in shape, then profile lines were placed to bisect the feature along intercardinal azimuths. If a feature was approximately oval or elliptical in plan, then one profile line was created to bisect the feature along its major axis, and a second 3-D profile line was then created to bisect the feature along its minor axis. However, if portions of the berm appeared to have been disturbed, then profile lines were rotated somewhat to include intact berms on opposing sides of the feature. Profile graphs were then created from the profile lines and the DEM, using the Profile Graph tool in 3D Analyst. The resulting data were then exported to Microsoft Excel as raw x and y coordinates and elevation values, for further analysis.

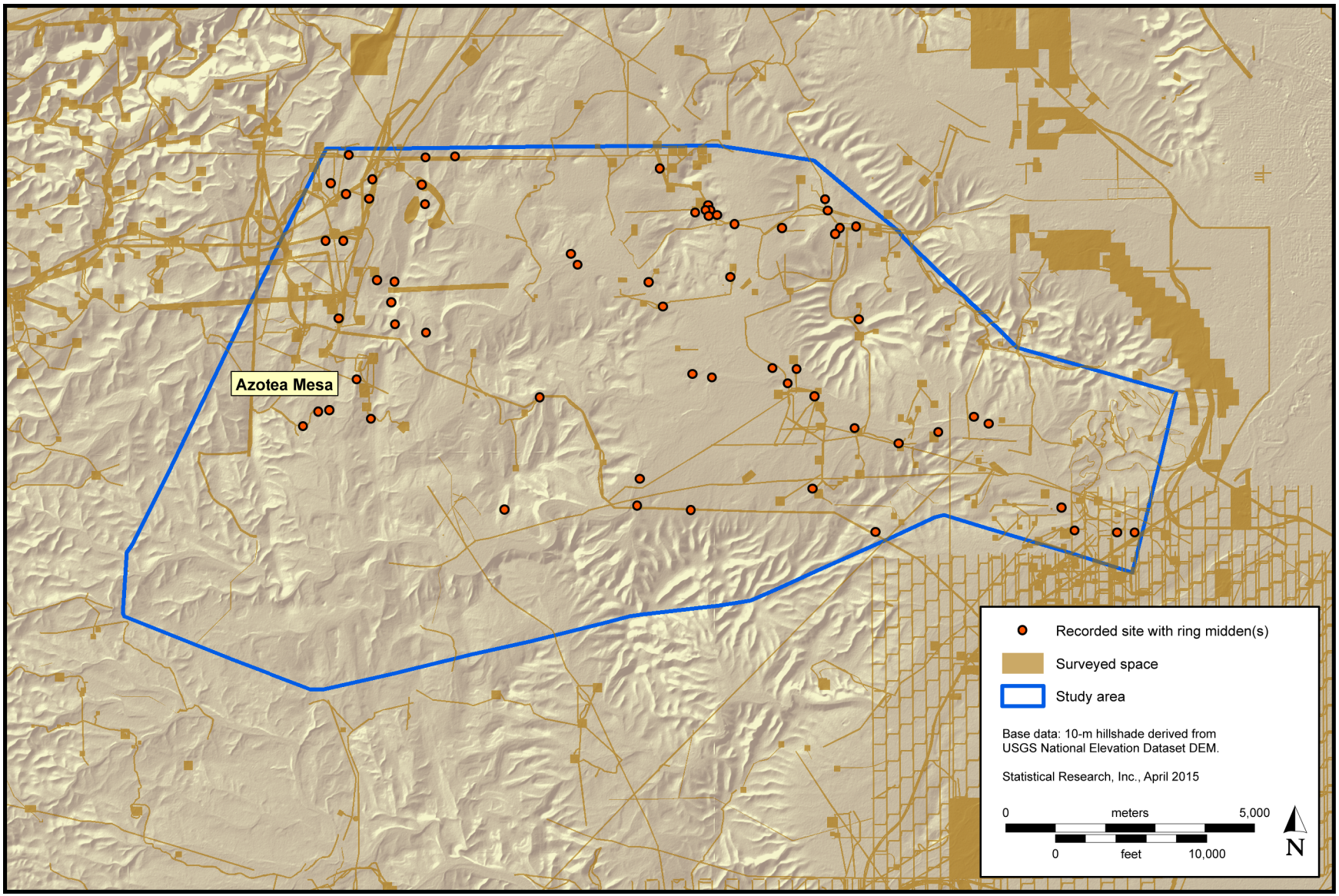

Figure 16. Previously recorded sites with ring middens in the Azotea Mesa study area.

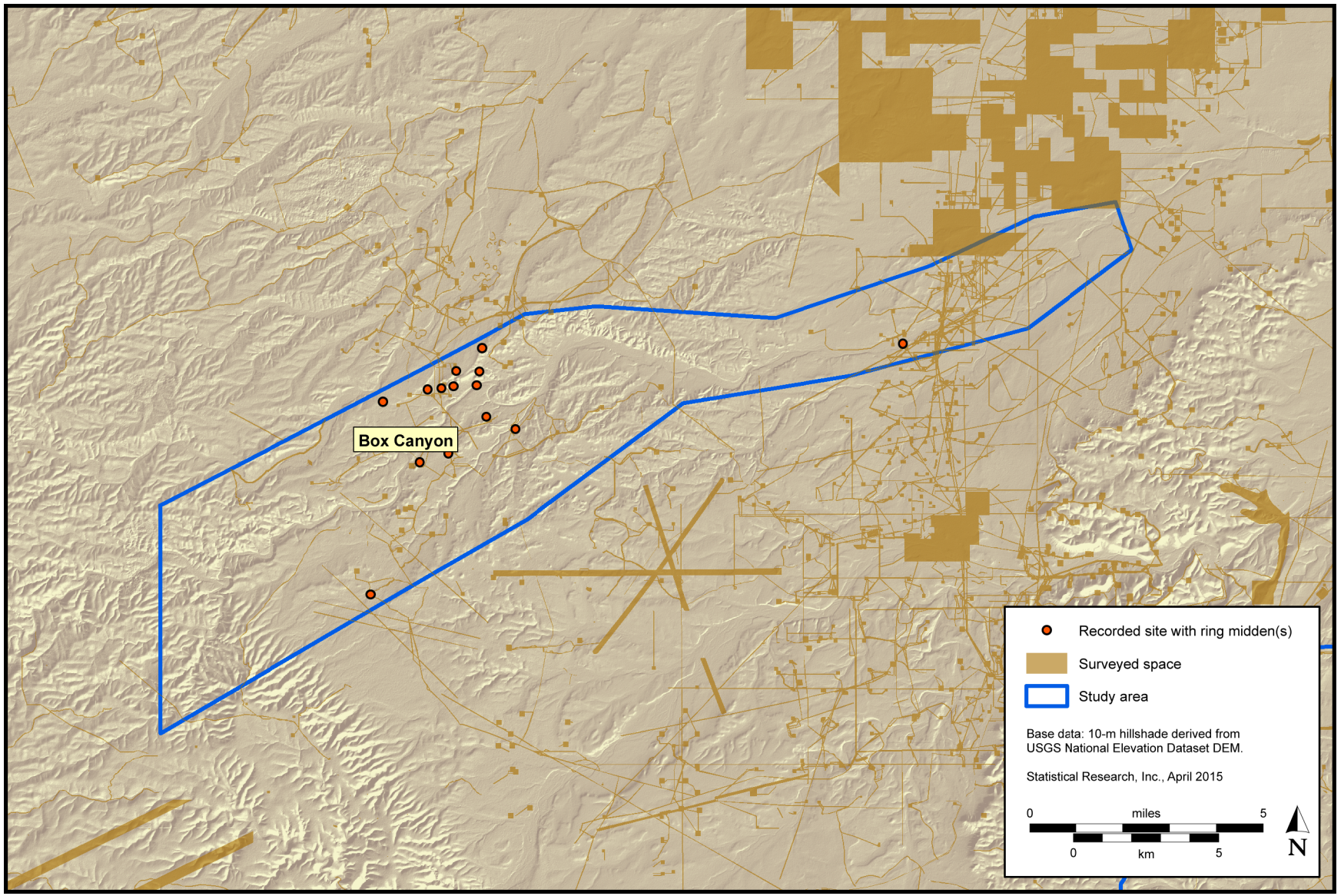

Figure 17. Previously recorded sites with ring middens in the Box Canyon study area.

Table 2. Recorded Sites Examined with the Lidar Data to Characterize Ring-Midden Features and Develop Methods for Feature Visualization and Identification

Site No.	Ring-Midden Count	Map Available?	Condition Data Presented?	Feature Dimensions Reported?
LA 16424	6	yes (poor quality)	no	no
LA 16462	1	no	no	yes
LA 30625	6	yes	yes	yes
LA 38209	2	yes (poor quality)	yes	yes
LA 38210	3	yes	yes	yes
LA 38731	7	yes (poor quality)	yes	yes
LA 43446	5	yes (poor quality)	yes	yes
LA 43450	7	yes (poor quality)	no	no
LA 43451	3	yes (poor quality)	yes	yes
LA 49461	3	yes	yes	yes
LA 49462	5	yes (poor quality)	no	no
LA 51007	13	yes	yes	yes
LA 61246	1	yes (poor quality)	yes	yes
LA 64499	1	yes (poor quality)	no	no
LA 69032	3	yes	yes	yes
LA 82642	2	yes	yes	yes
LA 87012	2	yes	yes	yes
LA 89859	4	yes	yes	yes
LA 89860	4	yes (poor quality)	yes	yes
LA 103228	2	yes	yes	no
LA 107436	4	yes (poor quality)	yes	yes
LA 107437	not reported	yes (poor quality)	no	no
LA 107743	3	yes	yes	no
LA 110660	5	yes	yes	yes
LA 112610	1	yes	yes	no
LA 112613	2	yes	yes	yes
LA 112620	1	yes (poor quality)	yes	yes
LA 112622	1	yes	yes	yes
LA 112627	6	yes	no	no
LA 112629	1	yes	no	no
LA 112633	1	yes	yes	yes
LA 112636	1	yes	yes	yes
LA 115031	6	yes	yes	no
LA 117445	4	yes	yes	yes
LA 121138	1	yes	no	no
LA 129788	3	yes	yes	yes
LA 131367	1	yes	no	no
LA 132632	1	yes	yes	yes
LA 132800	2	yes	yes	yes

Site No.	Ring-Midden Count	Map Available?	Condition Data Presented?	Feature Dimensions Reported?
LA 134390	10	yes	yes	no
LA 134712	1	yes	yes	no
LA 134714	1	yes	yes	yes
LA 134715	1	yes	yes	yes
LA 134716	1	yes	yes	yes
LA 134717	1	yes	no	no
LA 134719	1	yes	yes	yes
LA 134930	6	yes	yes	yes
LA 135284	1	yes	yes	yes
LA 135287	4	yes	yes	yes
LA 139107	10	yes	yes	yes
LA 139951	1	no	no	no
LA 140885	22	yes	yes	yes
LA 140898	5	yes	yes	yes
LA 140944	6	yes	yes	yes
LA 142814	1	yes	no	no
LA 147921	6	yes	no	no
LA 148988	9	yes	yes	yes
LA 148989	19	yes	yes	yes
LA 148990	3	yes	yes	yes
LA 148991	8	yes	yes	yes
LA 148992	1	yes	yes	yes
LA 152305	1	yes	no	yes
LA 152553	1	yes	yes	yes
LA 155040	3	yes	yes	yes
LA 155041	1	yes	yes	yes
LA 161910	1	yes	yes	yes
LA 161911	1	yes	yes	yes
NM-06-0012	1	yes (poor quality)	no	no

Using the raw *x*- and *y*-coordinate data derived from the profile graphs, potential ring-midden features identified in the lidar data were characterized morphometrically, using a series of custom equations and algorithms created in Microsoft Excel for this project. First, raw elevation values were converted to relative elevation values by finding the minimum elevation for a profile and subtracting that from each of the elevations in the profile. This process resulted in relative elevation values ranging from 0 to the maximum relative elevation of a feature profile. Because many of the profiles were affected by the slopes of the land surfaces on which they are situated, profiles were rotated to remove the effects of slope on profile measurements (Figure 18). This was achieved by calculating the slope from the exterior basal edge of a discard midden to the outside bottom edge of the opposing side of the feature. The slope (m) calculated via this method was then used to estimate a slope line, using the equation $y_i = mx_i + b$, where y is the estimated feature height, m is the profile slope, x is the horizontal distance along the profile, and b is the y intercept,

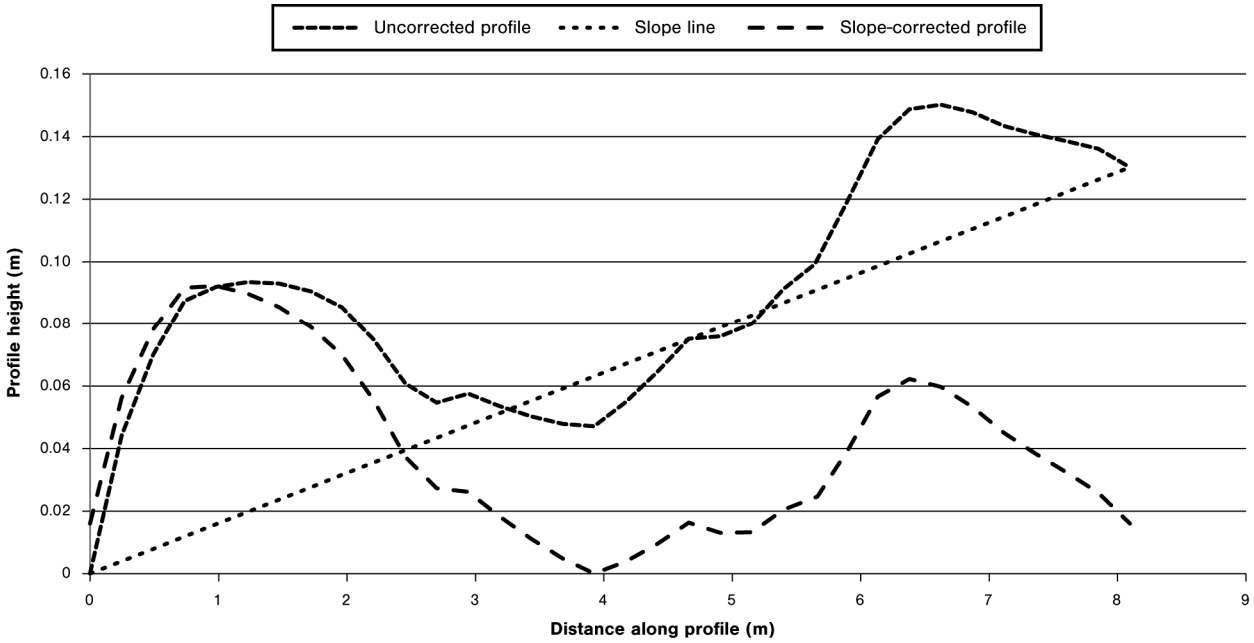

Figure 18. Example of slope correction applied to profiles to standardize profile measurements.

or the elevation at which $x = 0$. The slope line provides an estimate of what the ground-surface height along the profile would be if the feature were absent. At each point along the profile, the elevation along the estimated slope line was subtracted from the relative elevation for the point, to derive a rotated, or slope-corrected, profile (Figure 19). The advantage of rotating the profile in this way is that it allows for a more accurate estimate of feature dimensions, particularly berm height and distance between berms. The slope-corrected profiles exhibited a clear, consistently measurable morphology that conforms to our expectations of ring-midden morphology. A slightly more accurate ring-midden elevation for a rotated profile can be achieved using a complex quadratic equation to estimate the shortest line from the unrotated profile line to the slope line. However, experimentation with this more complex approach suggested that the difference between a simple method for estimating rotated-profile height and the more complex quadratic approach is typically less than 0.01 percent.

Using these slope-corrected relative elevation data, a series of ring-midden statistics was calculated for each profile, to characterize the feature (Figure 20). Statistics calculated for each profile included average height (m), maximum height (m), standard deviation in height (m), span (m), maximum height of the discard midden on each side of the profile (m), horizontal distance between discard-midden maxima (m), difference between maximum discard-midden height and center height (m), feature slope (%), and absolute difference in height between opposing berms in a feature profile (m).

Most of the calculations for these statistics are straightforward, but some require explanation. Span is the profile distance. Center height was calculated using the Index function in Microsoft Excel, by finding the relative elevation in the center point of the profile.

Calculating statistics involving the berm height or the distance between opposing berms requires identifying the maximum elevation on the left- and right-hand sides of a profile, respectively. This was accomplished using an Array function in Microsoft Excel that identified the point representing the maximum height on the left-hand half of the profile and another point representing the maximum height on the right-hand half of the profile. These points were then used to calculate the distance between discard-midden maxima on opposing sides of a ring midden as well as the difference between berm height and center height. Center height was calculated as the difference between the maximum berm height along a profile and the feature center height.

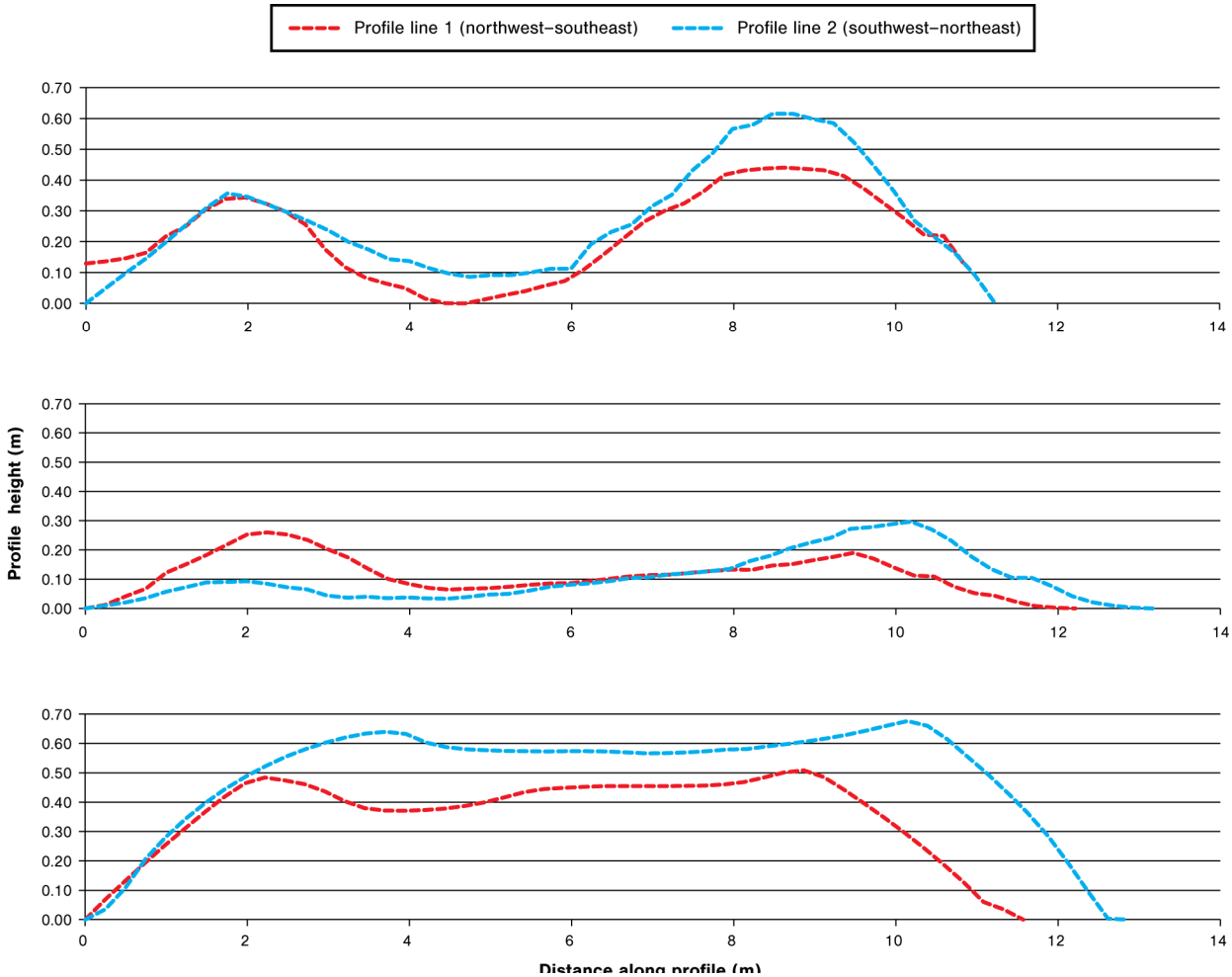

Figure 19. Three examples of ring-midden profiles derived from lidar data (ring-midden Features 70, 87, and 201).

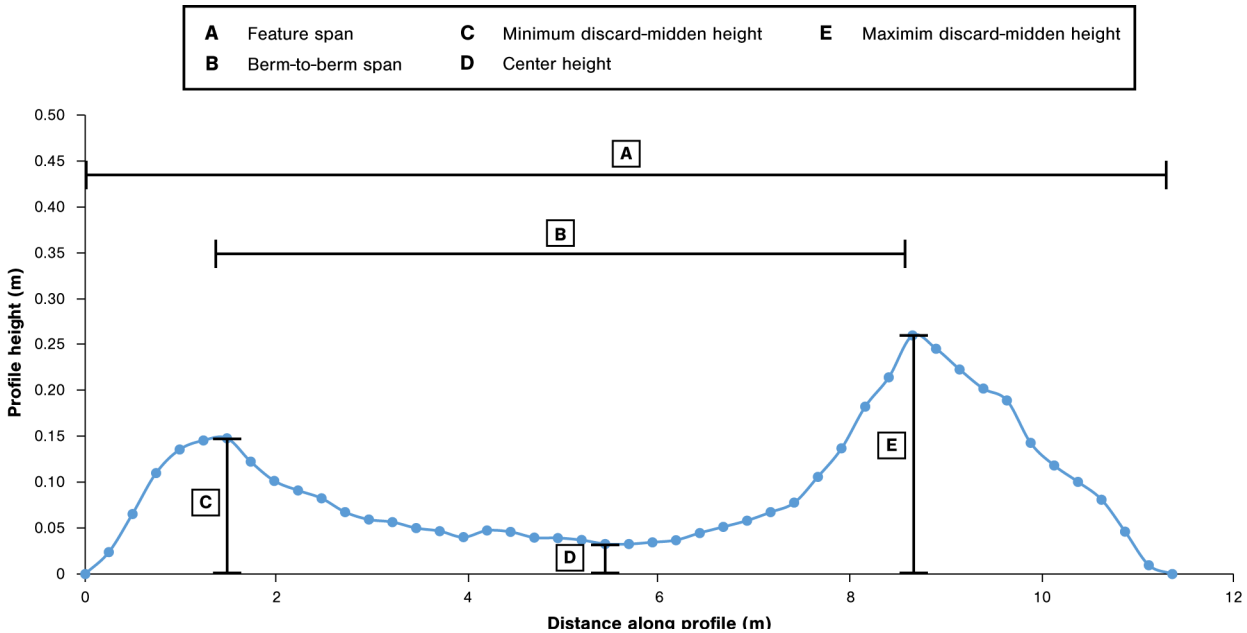

Figure 20. Key measurements obtained from profile data for morphometric characterization.

Feature Statistics

Statistics derived from the two profiles of an individual feature were then combined to calculate statistics for the feature as a whole. Statistics calculated for each of the sampled features were the following:

- maximum height (m),
- center height (m),
- feature span (m),
- maximum difference in elevation between feature berm and feature center (m),
- average berm-to-berm span (m),
- maximal berm-to-berm span (m),
- feature area (m^2),
- interior feature area (from berm to berm) (m^2), and
- feature volume (m^3).

Feature volume was estimated by calculating the area under the slope-corrected profile between each distance measurement along the profile, using the following formula:

$$\text{Profile Area}_{i\text{-}j} = ([\text{profile height}_i + \text{profile height}_j]/2) * (\text{profile distance}_j - \text{profile distance}_i),$$

where $\text{Profile Area}_{i\text{-}j}$ = the area under the profile for a segment of the profile between two adjacent distance measurements, profile height_i = the profile height at distance measurement *i*, profile height_j = the profile height at distance measurement *j*, $\text{profile distance}_j$ = the distance along the profile at distance measurement *j*, and $\text{profile distance}_i$ = the distance along the profile at distance measurement *i*.

To estimate feature volume, we first estimated the area under the slope-corrected profile between each pair of points along the profile. Each of these estimated areas was then multiplied by the circumference of a circle with a radius equaling the distance from the profile section to the center of the feature, to estimate a volume for each profile section. To derive a total volume for a feature, each profile-section volume was then summed for the entire profile and divided by two, because estimates were made across the entire profile. The estimated total volume for each of the two feature profiles was then averaged to derive an estimated volume for the feature.

Evaluation of Feature Statistics

The results indicated that ring middens in the pilot sample tend to be of fairly standard horizontal dimensions (Table 3). Spans ranged from 5.6 to 15.0 m, averaging 10.8 ± 0.5 m. The distribution was highly modal, with low variance and a coefficient of variation of only 16.9 percent. This metric is remarkable in its consistency. Similarly, both average berm-to-berm span and maximum berm-to-berm span for individual ring middens were relatively consistent among features, with a coefficient of variation of 18.0 and 15.1 percent, respectively. In keeping with these results, estimated feature area and berm-to-berm area, though more variable than feature span and berm-to-berm span, were less variable than other metrics corresponding to the size and morphology of ring middens.

The greatest variation in feature metrics has primarily to do with dimensions related to feature height. For example, maximum feature height, center height, and estimated feature volume vary considerably more than do metrics related to a ring-midden feature's horizontal dimensions. In the pilot sample, maximum feature height, for instance, varied from as little as 7 cm to as much as 58 cm, and the difference between maximum berm height and center height varied from less than 1 cm to 30 cm. Similarly, feature volume varied from as little as 1.5 m^3 to more than 45 m^3. This suggests that, in the pilot sample, there was considerably more variation in how high (topographically prominent) a ring-midden feature obtruded above the ground surface than there was in how far the feature extended horizontally in plan view. Possibly, variation in the heights and estimated volumes of ring-midden berms corresponds to variation in the

Table 3. Statistics Derived from Profiles of a Series of 59 Ring Middens Identified during Preliminary Characterization Efforts

Statistic	Average	Median	Standard Deviation	Minimum	Maximum	Coefficient of Variation (%)
Maximum profile height (m)	0.26	0.20	0.15	0.07	0.58	56.1
Center height (m)	0.07	0.04	0.07	0.00	0.30	101.7
Feature span (m)	10.76	10.76	1.81	5.59	15.04	16.9
Maximum discard-midden height (m)	0.14	0.12	0.09	0.02	0.40	66.0
Maximum discard-midden height (m)/ minimum discard-midden height (m)	2.40	2.17	0.79	1.22	4.99	32.9
Maximum discard-midden height (m) – maximum discard-midden height (m)	0.14	0.12	0.09	0.02	0.40	66.0
Maximum discard-midden height (m) – center height (m)	0.20	0.15	0.13	0.04	0.54	65.0
100 * maximum discard-midden height (m) / feature span (m)	2.34	2.23	1.12	0.80	5.19	47.7
Average berm-to-berm span (m)	6.56	6.51	1.18	3.35	8.90	18.0
Maximal berm-to-berm span (m)	7.13	7.12	1.08	3.71	9.34	15.1
Feature area (m^2)	93.18	90.97	31.29	24.57	177.17	33.6
Berm-to-berm area (m^2)	38.67	38.43	12.67	10.73	65.85	32.8
Feature volume (m^3)	13.65	9.52	10.86	1.55	45.72	79.5
Feature slope (%)	2.75	2.50	1.30	0.33	5.81	47.3

intensity or frequency of individual ring-midden use. Alternatively, variation in ring-midden heights and obtrusiveness among features could relate to the degree to which a feature has been buried by depositional processes or truncated as a result of erosion or cultural disturbance processes. Another effect on profile height is the accuracy of vertical measurements obtained for the lidar data. The specific position of the profile line of a feature, particularly where it begins and ends, has an effect on the overall profile height. Many features gradually decrease in elevation near their outer edges. Thus, profile lines that do not completely capture this outermost decline in elevation underestimate the total height of the feature.

An interesting characteristic of ring middens that investigators have noted is that one side of a ring midden is often higher than the opposing side. This analysis supports that interpretation and shows that in the pilot-study sample, the berm on one side of a ring midden tends to be more than twice as high as the berm on the opposite side. On average, there was a 14-cm difference in berm height between opposing berms. Ring middens also tend to be located on a slight slope, ranging between 0.33 and 5.81 percent in slope and averaging 2.75 percent, and more than 90 percent of ring middens are located on a slope of at least 1 percent. In documenting potential ring-midden features that could be identified using the digital data, it appeared that for many ring middens, the highest portions of a berm tend to be located on the downslope side. Perhaps this suggests that as a feature was cleaned out, materials from the center of the ring midden were preferentially redistributed to the downslope side, saving energy and resulting in a higher berm on the downslope side.

Locational Model

Per the scope of work (SRI 2013), we developed a locational model for ring middens, to predict where in the three study areas ring-midden features are more or less likely to occur. The purpose of the model was to use it as a guide for selecting a sample of land parcels within each study area in which to conduct digital survey. Another benefit of the modeling exercise is that it can also be used to help characterize the environmental associations of ring-midden features. Further, the model not only helps to define archaeological sensitivity for ring middens in the three study areas but also defines archaeological sensitivity for ring middens in intervening and adjacent areas, providing the BLM with a broader understanding of the distribution of ring middens across a large portion of southeastern New Mexico.

The methods used to create the sensitivity model were based on the model-construction methods developed for the Southern New Mexico Archaeological Sensitivity Modeling Project (Heilen et al. 2013). Because the modeling area for that project included the current study areas, many of the same environmental variables developed for that project to predict archaeological sensitivity could be used for the current project. However, because the current study area crosscuts two of the modeling units defined for the Southern New Mexico Archaeological Sensitivity Modeling Project, and the environmental variables used in the modeling were created according to modeling units for the previous project, layers representing environmental variables had to be combined from multiple modeling units in order to adequately cover the current study area.

The variables developed for modeling site location in southern New Mexico included sets of variables related to topography, soil attributes, water resources, and vegetation. These variables were conceptualized as proxies for factors that affected how people moved through and used the landscape. It is not expected that ancient dwellers of southern New Mexico measured the slope of a prospective campsite or the distance between a camp and water resources. Instead, they may have placed themselves in relation to specific resources—for example, near enough to potable water to transport it easily in vessels but not so close as to disturb game animals. We can never reconstruct the exact logic used in the past to guide settlement and land use, but if that logic was replicated over time and space, we can expect to discern regularities in the relationships between site location and the environmental and social variables related to settlement and land use. Variables used to generate the model were developed using a 10-by-10-m cell size for a model area

that encompassed the three study areas: Azotea Mesa, Box Canyon, and Rio Felix. The modeling area was approximately 163.9 by 106.7 km in size and consisted of 174,844,335 10-by-10-m grid cells.

Topographic Variables

Variables related to topography, such as slope and aspect, are frequently considered important in predicting site location. For instance, residential sites were often located in areas of relatively low slope or on slopes facing a particular direction, because of the protection they offered from prevailing winds or because of variations in their exposure to solar radiation. Other topographic variables commonly used in predictive modeling include measures of terrain roughness and shelter. Topographic variables were derived in ArcGIS with an enhanced 10-m DEM for the state of New Mexico.

Slope

One of the most common topographic variables used in predictive modeling is slope, as measured either in degrees or percentages, or as a transformation of either scale. Percent slope was calculated for the study area with the 10-m DEM for the state of New Mexico using the Slope tool in ArcGIS.

Aspect

Aspect, or the direction that a slope faces, is a topographic variable commonly used in predictive modeling. Aspect is considered a kind of measure of exposure. For instance, south-facing slopes can offer greater exposure to the sun; in areas where prevailing winds can interfere with daily activities, aspects opposing the direction of prevailing winds can offer protection from them. Conceivably, in some cases, aspect can also relate to visibility, if the aspect of a landform affords or obscures views of the surrounding landscape. When aspect is calculated in ArcGIS, the resulting values correspond to the azimuth of a spherical coordinate system—in other words, the degrees on a compass. One of the issues faced when aspect is used as a variable in predictive modeling, however, is that because of the way in which degrees are scaled, similar aspects, such as 359° and 1°, can be quantitatively distinct, even though there is little qualitative difference between them. One means of addressing this problem is to transform aspect values so that they range in value from 0° to 180° rather than from 0° to 360°. In this way, aspect values can be distributed symmetrically along either a north–south or an east–west axis (Kvamme 1988a, 1988b:337). The advantage of this approach is that it allows one to model aspect relative to cardinal directions and along a continuous scale of measurement while avoiding the quantitative problems associated with using a spherical coordinate system.

North–South Aspect

To calculate the north–south aspect, raw aspect values calculated in ArcGIS were transformed through map algebra such that northerly directions approached 0° (regardless of whether they fell on the east or west side of the compass). In the same manner, southerly directions approached 180°. Strictly east or west directions, in this case, became 90°, rather than 90° and 270°, respectively. Thus, if a landform faces north, the north–south aspect approaches 0°; if the landform faces south, the north–south aspect approaches 180°.

East–West Aspect

The east–west aspect was calculated in a manner similar to the calculation of north–south aspect, but with easterly directions approaching 0° and westerly directions approaching 180°. In this case, strictly north and

south directions both were 90°, rather than 0° and 180°, respectively. Thus, if a landform faces east, the east–west aspect approaches 0°; if the landform faces west, the east–west aspect approaches 180°.

Curvature

Curvature represents the degree of convexity or concavity of a land surface. In ArcGIS, curvature is calculated as the second derivative of an elevation surface, or the slope of the slope. Positive values indicate that a surface is upwardly convex (like an upside-down bowl), and negative values indicate that a surface is upwardly concave (like an upright bowl). ArcGIS also provides options to additionally calculate plan curvature and profile curvature. Plan curvature represents the curvature of a land surface perpendicular to the direction of maximum slope. Profile curvature represents the curvature of a land surface parallel to the direction of maximum slope. Curvature, plan curvature, and profile curvature were calculated using the Curvature tool in ArcGIS.

Relief

Surface texture or roughness is a topographic variable that can be important to site location, because rough terrain can "inhibit day-to-day activities and travel to and from sites" (Kvamme 1988a, 1988b:333). One way to measure terrain roughness is referred to as relief, or the range in elevation within a predefined radius around a raster cell. A large value indicates a large change in elevation within a relatively short distance; a small value indicates little change in elevation within a relatively short distance. Relief was calculated using the Focal Statistics tool in ArcGIS, by calculating the range in elevation within a 200-by-200-m area surrounding each raster cell.

Terrain Texture

Another measure of roughness is referred to as terrain texture, which is defined as the amount of variability in elevation within a predefined radius. Terrain texture was derived using the Focal Statistics tool in ArcGIS, by calculating the standard deviation in elevation within a 200-by-200-m area.

Topographic-Position Index

TPI uses relative elevation to indicate whether a raster cell is located in a lower valley position, at a midslope position, or on a hill or ridgetop. We used the following formula to calculate TPI:

TPI = (local elevation – minimum elevation) / (maximum elevation – minimum elevation).

The index is calculated by first calculating, using the Focal Statistics tool in ArcGIS, the maximum and minimum elevations within a specified area surrounding each raster cell. For developing the preliminary sensitivity model, we used a 200-by-200-m rectangle surrounding each raster cell to calculate the minimum and maximum elevations in the area around the cell. The Map Algebra tool in ArcGIS was then used to calculate TPI, using the above formula. The resulting index ranges from 0 to 1, with 0 representing locations that are low lying compared to the surrounding area, such as valleys or depressions, and 1 representing locations that are prominent, such as hilltops or ridges. Values between 0 and 1 represent different slope positions, such as lower slopes, middle slopes, and upper slopes.

Topographic-Slope Index

In applying TPI in the development of sensitivity models in support of energy development in eastern Ohio for the Gas and Preservation Partnership, Heilen (2014) realized that a similar index could be created using slope as the input value, in place of elevation. Thus, we created an experimental index, called the topographic-slope index (TSI), which employs the same basic formula used to calculate TPI (above), but using slope instead of elevation:

TSI = (local slope – minimum slope) / (maximum slope – minimum slope).

Like TPI, TSI is calculated by first calculating, using the Focal Statistics tool in ArcGIS, the maximum and minimum slopes within a specified area surrounding each raster cell. For this project, we used a 200-by-200-m rectangle surrounding each raster cell to calculate the minimum and maximum slopes in the area surrounding a cell. The Map Algebra tool in ArcGIS was then used to calculate the TSI, using the above formula. The resulting index ranges from 0 to 1, with 0 representing locations that are of low slope compared to the surrounding area and 1 representing locations that are of high slope compared to the surrounding area.

Cost Surface

Topographic data can be used to create a cost surface that represents the relative cost of moving across the landscape. Cost surfaces can be particularly useful for creating variables that measure the distance between a raster cell and the closest resource of a given type. If one calculates the simple straight-line, or Euclidean, distance between a raster cell and a feature of interest, factors affecting movement and energy expenditure (such as variation in slope, surface roughness, vegetation cover, and other potential impediments to movement) are ignored. For instance, on a horizontal plane, only 100 m might separate a location from a water source, but the water source might also be 100 m *below* the location. In such a case, a much greater effort would be required to reach the resource than would be required if there were no difference in elevation between the location and the closest water source.

A cost surface is defined by assigning to each raster cell in a GIS layer a value representing the relative cost of moving across that cell. For instance, if slope is used to create a cost surface, raster cells with high slope values would represent areas that would be relatively more costly to traverse than raster cells with comparatively low slope values. A cost surface can be used as an input layer to calculate, for each raster cell, the cost distance between the cell and a feature of interest, such as the nearest stream or playa. In ArcGIS, this calculation is similar to that used for the Euclidean (or straight-line) distance between a raster cell and a feature of interest. Instead of calculating the straight-line geographic distance between a raster cell and a feature of interest, the cost-distance algorithm calculates the relative cost that would be accumulated by traveling from a raster cell to the closest feature of interest. This "cost distance" is calculated by summing the cost values of the intervening cells. The resulting accumulated cost value can be conceptualized as the relative cost that would be expended if an agent were to traverse an area of the landscape in order to access a given resource.

To create a relatively simple cost surface for the model area that could subsequently be used to calculate the cost distance to features of interest, two measures were used: (1) mean slope within a 100-m radius and (2) standard deviation in elevation within a 100-m radius. These two variables were combined into a single cost metric by adding 1 to each of the variables, taking the natural logarithm of each variable, and then adding the two resulting values together. This results in a cost surface that takes into account both the slope and the texture (or ruggedness) of the area immediately surrounding each raster cell. Areas that have steep slopes and are rugged have the highest cost values; areas that have low slopes and smooth terrain have low cost values. Cost surface was used as the primary measure of the cost to traverse each raster cell in the modeling area.

Soil-Attribute Variables

A useful soils data set for modeling site location is the Natural Resources Conservation Service (NRCS) Soil Survey Geographic (SSURGO) data set. In contrast to state-level State Soil Geographic data, which are mapped at a scale of 1:250,000, SSURGO data are mapped at a much finer scale of 1:24,000. SSURGO contains data on a wide variety of soil attributes (e.g., organic-matter content, available water capacity, and bulk density) that can be extracted from a database and used to attribute individual mapping units. When these data are mapped, detailed variation in soil attributes relevant to soil quality, depositional processes, and geomorphic setting can be used as predictor variables in modeling site location.

Soil-attribute data were extracted from the SSURGO database through a series of complex database queries developed in Microsoft Access in 1997 by Heilen and Homburg (2006, 2007). The queries were initially developed to assess soil quality in ancient agricultural landscapes of southern Arizona but can be applied to many contexts for which soil data are available in the same format. Soil-attribute data were extracted from the SSURGO data by means of the procedure described below. Essentially, the approach involves calculating the weighted average of a variable as derived from soil-horizon- or soil-component-level information and extrapolating those data to a broader-scale mapping unit that encompasses the horizon- and component-level data.

In the SSURGO data, soil-mapping units consist of a series of multiple soil components. Each soil component, in turn, is associated with a characteristic soil profile consisting of a series of representative horizons. In most cases, these individual soil horizons are attributed with soil-quality data that can be useful in predicting site location. To be used for a mapped variable, soil-quality data recorded at the level of soil horizon must be generalized to the level of the component. The resulting component-level data then must be generalized to the level of the mapping unit.

Soil-quality data to be applied to individual mapping units were extracted by following a procedure recommended by the NRCS (U.S. Department of Agriculture 1995). The procedure involves first calculating the weighted average of a variable for each horizon in a representative soil profile. Values for individual horizons are weighted by the relative thickness of the horizon. For instance, the thicker the soil horizon, the more that soil horizon is weighted in computing a component-level average for a variable. In other words, each value for a given variable and soil horizon is multiplied by horizon thickness. The sum of these values for a soil profile is then divided by the total thickness of the profile, to derive a weighted-average value for the soil component represented by the profile. Given that each mapping unit consists of a series of components, weighted-average values for each component also must be calculated. Weighted averages for components are calculated by means of the percentage of the area represented by each soil component in a mapping unit. In other words, the average value calculated for a component is multiplied by the percentage of the area represented by that component in a mapping unit. The sum of these values is then divided by the total percentage of components, to calculate an average value for the mapping unit (in some cases, percentages do not add up to 100, if data are missing from or not applicable to a given component).

To develop the soil-attribute variables for the study area, a large number of SSURGO data sets were downloaded from the NRCS Soil Data Mart (http://soildatamart.nrcs.usda.gov/, accessed June 12, 2013). The queries developed by Heilen and Homburg (2006, 2007) were used to calculate weighted averages that could be used to attribute individual soil-mapping units with soil-quality data. Soil variables that were explored as part of the model-building process were the following:

- available water capacity (inches of water per inch of soil profile),
- calcareousness (percentage of calcium carbonate),
- Kw factor (a soil-erodibility factor that quantifies the susceptibility of soil particles to erosion by water, taking into account the effect of rock fragments),
- texture-modifier index (a texture index developed by Heilen and Homburg [2006, 2007] that quantifies soil rockiness on a scale of 0 to 1 via the texture-description modifier—e.g., gravelly, very gravelly, channery, or very channery), and

- texture index (a texture index developed by Heilen and Homburg [2006, 2007] that quantifies, on a scale of –1 to 1, the degree to which a soil is sand or loamy sand [–1], nonsandy and nonloamy [0], or loamy [1]).

Water-Resource Variables

To model the availability of water resources, water-feature data available in the NHDPlus data set for the project area (U.S. Environmental Protection Agency 2006) were used to create a variety of water-resource variables:

- cost distance to streamlines,
- cost distance to major streams, and
- cost distance to stream-network confluences.

Cost Distance to Streamlines

Drainages, represented by streamlines in the NHDPlus data available for the model area, were considered potential sources of water. Drainages can also influence movement and resource use by affecting topography and the distribution of plants and animals on the landscape. To develop a layer identifying the locations of streams, streamlines were extracted from NHDPlus data. Features identified as pipelines or canals were removed from these data, so that only naturally present linear water features were considered in making calculations. In some parts of the study area, streams typically would have been dry, carrying water principally after periods of rain. However, streams could have offered potential sources of water during flood events, guided movement through the landscape, and provided floral or faunal resources located along stream margins. Cost distance to streamlines was calculated using the Cost Distance tool in ArcGIS and the cost surface described above.

Cost Distance to Major Streams

Initial experimentation with water-resource variables for the Southern New Mexico Archaeological Sensitivity Modeling Project (Heilen et al. 2013) suggested that although streamline data were useful in predicting site location, there were many cases in which sites were clustered around what could be considered "major" streamlines, including segments of the Rio Grande, Pecos, and Upper Gila Rivers, as well as smaller drainages. These were not major drainages, in an absolute sense, but streamlines that had the greatest potential to carry the most water relative to other drainages within the modeling unit. Major drainages were identified using data on the cumulative drainage (the total area drained) for each streamline segment. That was accomplished by first using map algebra to transform the cumulative-drainage raster for each modeling unit into a z-score value. Areas with significantly high cumulative drainage were identified as areas for which z-score values equaled or exceeded 1.64, a z-score value that is significant at the 90 percent confidence interval. Any streamline segment that fell within one of the areas for which cumulative annual drainage was significantly above the mean for the modeling unit was identified as a "major" stream segment. Cost distance to these major stream segments was then calculated using the Cost Distance tool in ArcGIS and the cost surface described above.

Cost Distance to Stream-Network Confluences

Stream-network nodes, such as the confluence of two or more streams (especially major streams), can influence human use of the landscape. The availability of water may be enhanced at stream junctions, and

water may be controlled more readily at such locations along streams. The location of sites near stream confluences may also have enhanced access to different areas of the landscape, should streams and their surrounding environments have functioned as transportation corridors or means of access to critical-resource zones. In an attempt to model stream-network confluence, we isolated points representing stream junctions in ArcGiS. We then calculated the cost distance to stream junctions using the Cost Distance tool in ArcGIS and the cost-distance layer described above.

Modeling Approach

The modeling approach used to develop the ring-midden sensitivity model discussed in this report is a recently developed statistical approach referred to as Random Forests (Breiman 2001; Prasad et al. 2006). Random Forests models have a number of advantages over alternative approaches, such as logistic-regression models, general-additive models, and stochastic-gradient-boosting models. Principal among these advantages is that the Random Forests approach

1. can use a wide variety of variables of different scales of measurement, including categorical variables;
2. is robust to overfitting resulting from intercorrelations among variables;
3. automatically and repeatedly creates test and training samples hundreds or thousands of times and uses them to develop a model; and
4. can make use of all available data to the best possible effect, through an iterative resampling technique referred to as "bootstrapping."

Using many different variables in modeling that are potentially correlated with each other is often considered a problem, because when used together, intercorrelated variables can artificially inflate the statistical performance of a model in complex ways. With other modeling approaches, the use of multiple intercorrelated variables in developing a model can lead to overconfidence in model results. This situation is not considered to present a problem with Random Forests modeling, however.

In addition, Random Forests uses a sampling approach that allows models to be built from all samples iteratively, because the technique creates hundreds of thousands of versions of a model through a randomly derived training set. The remaining test data reserved during each model iteration are used to test the performance of these submodels, ultimately contributing to the construction of a final model. Other approaches, such as logistic-regression approaches, often involve using only some of the data to train a model, and once the model is complete (rather than during the model-building process), the remaining data are used to test the model.

Random Forests is a kind of nonparametric decision-tree statistical-learning technique that falls within a larger class of models known as Classification and Regression Tree (CART) models. CART approaches to modeling perform classification or regression analysis, depending on whether the dependent variable being predicted is continuous or categorical. In the case of archaeological predictive modeling, the dependent variable generally is the presence or absence of an archaeological site—therefore, a categorical, binary variable. Thus, the approach that is applied in this report is a classification analysis.

The decision trees developed in CART models are formed by creating a series of rules that partition independent variables according to different states of the dependent variable—in this case, the presence or absence of an archaeological site. For instance, if a site is present most often when a given variable has a value equal to or above 10 and is absent for values below 10, then a node in the decision tree would be formed with a split for that variable at a value of 10. Based on that split, two child nodes would be formed beneath the node, one corresponding to site presence and the other corresponding to site absence. If further partitioning is possible, these child nodes could themselves become parent nodes and be further split into subsequent child nodes based on splits in other variables. The splitting of parent nodes into child nodes ends when no further gain in predictive power is attained by the creation of additional child nodes.

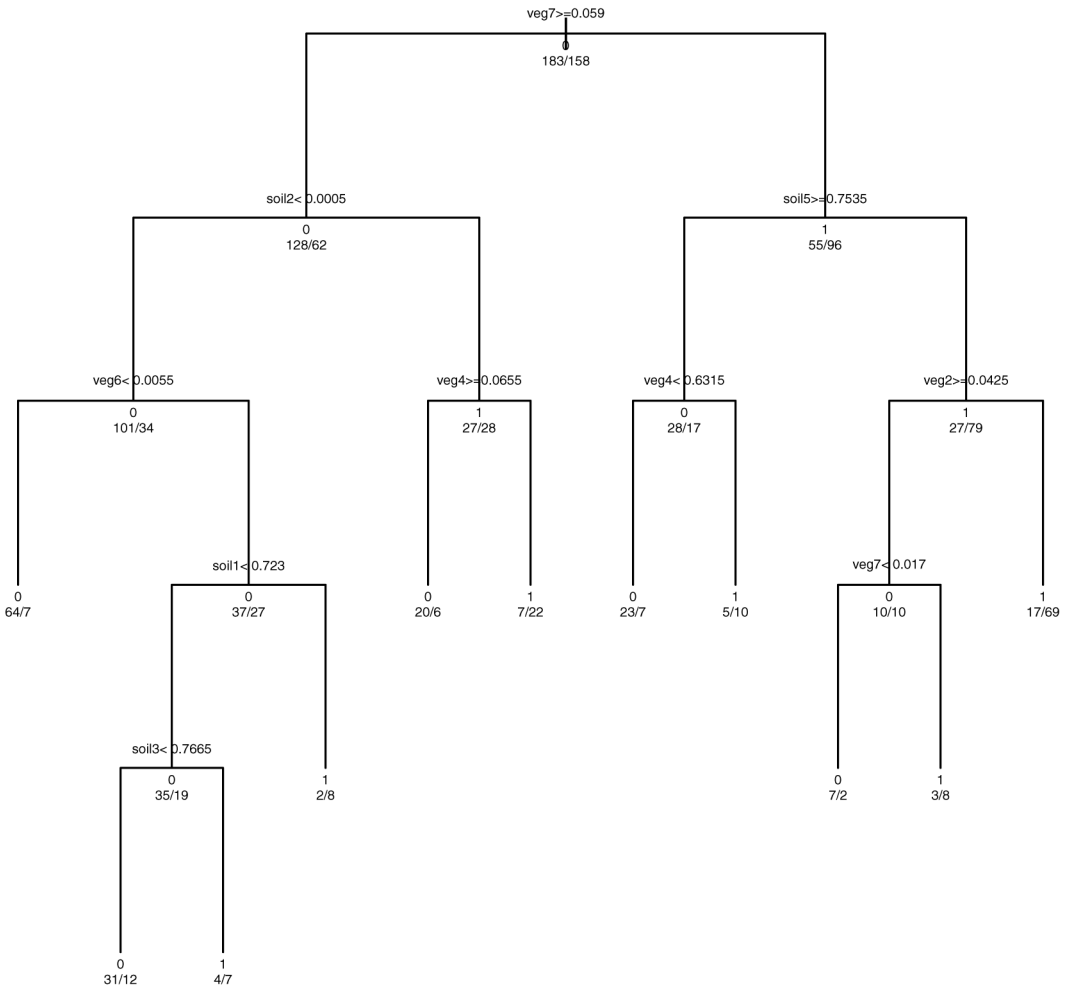

Figure 21. Example of a Random Forests tree graph, showing the variable cases in which parent nodes are split into child nodes for a binary response variable (e.g., site presence or absence).

Random Forests is an approach to CART models that was specifically designed to overcome problems with data overfitting that are common to other multivariate-statistical modeling techniques used to predict archaeological-site locations. In general, models that incorporate large numbers of independent variables relative to the numbers of observations used in the models have a tendency to be overly influenced by minor fluctuations in the data sets (i.e., random error, or "noise"). The consequence of that situation is that a model could "fit" the random particulars of the data set but not the underlying relationships between the dependent and independent variables.

In Random Forests, multiple trees are constructed using bootstrapped samples of both the independent variables and the cases. The CART approach to constructing decision trees, rather than being performed only once, is repeated hundreds or thousands of times in a Random Forests model using a sample of approximately 70 percent of the data. The remaining 30 percent of cases are reserved for testing model predictions. The result is the creation of hundreds or thousands of decision trees, each formed with a randomized set of predictor variables and cases. For instance, if there are 20 variables and 600 cases, each tree would be formed from a random subset of variables (e.g., 7 variables) and a random subset of cases (e.g., 400 cases). Each tree is grown to its maximum size, without pruning (Figure 21).

Error estimates are calculated from the sample of cases withheld from tree formation. Because these estimates are based on cases that were not used to build a decision tree or were not in the group of cases used to train the model, they are referred to as the out-of-bag (OOB) estimates. The repeated formation of independent trees using randomized sets of predictors eliminates the need for creating separate test and training sets, because these sets are continually created, hundreds or thousands of times, through the bootstrapping process. To create the final model, decision trees are melded together by taking a vote across the trees for each node. The most common outcome for that node (or a majority vote) is considered the final result. This process generates a model that is robust to overfitting, diminishes problems with intercorrelations between variables, and reduces bias introduced by individual variables or cases.

A disadvantage of the approach is that it is like a black box: it is not possible to interpret easily how individual trees have contributed to the final model, because hundreds or thousands of trees are created. However, the approach does provide a number of statistical measures that allow for estimation of the importance of each variable in creating the model and in estimating the error rate of the model predictions (the OOB error).

Random Forests models were developed for this project in a program called ModelMap (Freeman and Frescino 2009). ModelMap is available in R, an open-source statistical platform available on the internet (R Development Core Team 2008). ModelMap allows the user to create a Random Forests classification or regression model using a table of cases consisting of a response variable and corresponding values for any number of categorical or continuous predictor variables. The program then allows the user to run internal validation tests and to calculate statistics on model performance, including OOB estimates and the area under the Receiver Operating Characteristic curve. ModelMap also provides graphs of the relative importance of the variables. Once a satisfactory model has been developed and tested internally, a user can call on ModelMap to create a prediction raster using the Random Forests model file created by ModelMap.

Sample Selection

Sample selection is particularly important in archaeological predictive modeling. The sample-selection procedure applied during this project aimed to accomplish five goals:

1. to derive site-positive samples from within the boundaries of sites;
2. to select additional site-positive samples for larger sites, in order to capture environmental variability within sites;
3. to prevent very large sites from being oversampled or overrepresented;
4. to derive site-negative samples from surveyed locations where no sites have been recorded; and
5. to ensure that nonsite samples and site samples were sufficiently distant from each other to be statistically distinguishable from each other according to the values of independent model variables.

The methods involved first selecting samples of points within sites identified as having ring middens as well as from individual ring middens identified, using the lidar data, at or near sites recorded as containing ring middens. Samples representing sites with ring middens were selected in the Azotea Mesa and Box Canyon study areas, but no sample was derived from sites in the Upper Rio Felix study area, because no sites within that study area had been identified as containing ring-midden features. Sites with ring middens were also sampled from within a 256.7-square-mile area immediately adjacent to and northwest of the Box Canyon study area, because a large number of sites with ring middens had been identified in that area. A comparably sized sample of nonsite locations was then selected from locations in surveyed areas within the Azotea Mesa and Box Canyon study areas where ring midden features had not been identified, as well as from the (previously mentioned) additional area immediately northwest of the Box Canyon study area.

Environmental Associations

The site and nonsite samples were then combined into a single ArcGIS point layer and used to obtain the values of environmental variables at each sample-point location, using the Sample tool in ArcGIS Spatial Analyst. A preliminary ring-midden sensitivity model was then calculated in ModelMap using these variables, in order to understand their relative influence in predicting ring-midden location.

Variables tested for association with ring-midden location were the following:

- available water content,
- calcium-carbonate ($CaCO_3$) concentration,
- Kw factor,
- soil texture,
- east–west aspect,
- north–south aspect,
- cost distance to confluence,
- cost distance to USGS National Hydrography Dataset streamline,
- cost distance to major stream,
- curvature,
- profile curvature,
- plan curvature,
- elevation above water,
- relief,
- terrain roughness,
- flow accumulation,
- USGS National Gap Analysis Program vegetation type,
- vegetation richness,
- slope,
- TPI, and
- TSI.

To assess the relative importance of the above variables in influencing the location of sites with ring middens, we used the mean decrease in the Gini measure. Gini is a measure of the relative purity of classifications made based on a given split in a decision tree. In a binary classification, such as the one we used when differentiating sites and nonsite locations at decision-tree nodes, a low Gini indicates that there is a mixture (e.g., of sites and nonsite locations) falling on either side of the split. In other words, for example, if a split at a parent node specifies that sites should be lower than 1,600 m AMSL and nonsites should be higher than 1,600 m AMSL, but a mixture of sites and nonsites falls on either side of that split, then the Gini measure would be low. A high Gini measure indicates that the split results in mostly one class (e.g., sites) falling to one side of the split and mostly the other class (e.g., nonsites) falling to the other side. For example, if sites tend to be located within 10 m above water, and nonsite locations tend to be more than 10 m above water, and nearly all sites and nonsites meet those criteria, then the Gini measure would be high.

Interestingly, the measure indicated that the most important variables had to do with distance to streams or confluences, followed by variables having to do with certain aspects of topography and then variables having to do with vegetation. The least important variables were those having to do with soil attributes. Among the variables having to do with topography, those having to do with surface curvature were of limited importance. In decreasing order of relative influence, the 12 most important variables were cost distance to nearest major stream, cost distance to nearest stream, cost distance to confluence, elevation above water, TPI, east–west aspect, TSI, terrain texture, relief, north–south aspect, vegetation richness, and percent slope.

Analysis of the most important variables indicated that in comparison to nonsite locations, sites with ring middens tended to be closer to streams and confluences and at lower elevations above water. Sites with ring middens also tended more often to be located at lower midslope positions than nonsite locations and to be located in areas of lower relief, terrain roughness, and slope than nonsite locations (Table 4). The greatest differences in locational attributes between sites with ring middens and nonsite locations were observed in cost distance to major streams, cost distance to streams, and elevation above water (Figure 22). Substantial differences in locational attributes between sites with ring middens and nonsite locations were also observed in cost distance to confluence, TSI, and TPI (Figure 23). Among the 12 variables indicated by the Gini scores as having the greatest relative influence on site location, the smallest differences in locational attributes between sites with ring middens and nonsite locations were observed in east–west aspect, north–south aspect, and vegetation richness.

Although elevation was not included as a variable in the preliminary model used to assess the relative influence of environmental variables on ring-midden location, it was used subsequently as a variable in deriving principal components for model refinement (see below). Analysis of this variable in terms of sites and nonsite locations showed that sites with ring middens tended to be located at lower elevations than nonsite locations (Figure 24). Within the sample of sites and nonsite locations evaluated here, elevations ranged from 987 to 1953 m AMSL. However, although both sites with ring middens and nonsite locations were located at a wide variety of elevations below 1,600 m AMSL, only 2 percent of sites with ring middens were located at elevations above 1,600 m AMSL. Contrastingly, 20 percent of nonsite samples were located at elevations in excess of 1,600 m AMSL. A few sites with ring middens were located at elevations higher than 1,600 m AMSL, but it appears that an elevation of 1,600 m AMSL may represent an upper limit in the siting of ring middens in the study area. If this was not the result of sampling vagaries, it could be the case that the kinds of resources typically processed in ring middens were more abundant or accessible at elevations less than 1,600 m AMSL than they were at elevations exceeding 1,600 m AMSL or, perhaps, that elevations below 1,600 m AMSL were more accessible from lowland habitation sites than were higher-elevation portions of the study area.

Principal-Components Analysis

After determining which variables were most important, we then subjected the most important variables to PCA, in order to reduce intercorrelations among predictor variables. It is often recognized that many environmental variables derived from a DEM will be intercorrelated in some fashion. For instance, slope and aspect may both be correlated with elevation as well as with each other. Most multivariate statistics assume that the independent variables (environment) used to predict the dependent variable (site location) are independent of one another. Because many of the variables discussed above could be related in some fashion, it was important to transform them into uncorrelated variables. PCA uses orthogonal transformation to convert a set of correlated variables into a set of uncorrelated variables, termed "principal components." Principal components were derived from the topographic variables and hydrological variables discussed above using the Principal Components tool in the ArcGIS Spatial Analyst toolbox. Because many of these variables are likely to be correlated with elevation, and there may be some limits on the elevation of sites with ring middens, elevation was included as a variable in the PCA of topographic and hydrographic variables. A separate PCA was also performed using the soil-attribute variables discussed above. However, unlike topographic and hydrographic variables, soil-related PCA variables had little influence in subsequent attempts to refine the model and were not ultimately used as predictor variables to create the ring-midden sensitivity model.

Table 4. Statistics for Sites and Nonsite Locations, for Environmental Variables Identified as Important to Predicting Ring-Midden Location

Relative-Influence Rank	Variable	Nonsite Average	Nonsite Median	Nonsite Standard Deviation	Site Average	Site Median	Site Standard Deviation	Difference between Averages of Sites and Nonsite Locations (%)	Difference between Medians of Sites and Nonsite Locations (%)
1	cost distance to major stream	741.71	578.00	654.79	410.40	195.00	508.08	–44.70	–66.30
2	cost distance to stream	405.04	337.00	333.40	205.49	140.00	189.34	–49.30	–58.50
3	cost distance to confluence	1,930.32	1,649.00	1,337.96	1,588.26	1,042.00	1,467.27	–17.70	–36.80
4	elevation above water (m)	16.38	8.34	23.97	7.97	2.72	13.08	–51.30	–67.40
5	TPI	0.48	0.47	0.21	0.40	0.37	0.19	–18.20	–21.30
6	east–west aspect	76.59	71.70	28.01	72.32	69.20	24.34	–5.60	–3.50
7	TSI	0.36	0.32	0.21	0.27	0.22	0.19	–26.30	–31.30
8	terrain texture	4.24	3.10	3.89	3.36	2.79	2.22	–20.80	–10.00
9	relief (m)	18.36	13.94	15.63	15.02	13.13	8.85	–18.20	–5.80
10	north–south aspect	85.02	83.80	31.48	85.61	83.20	29.59	0.70	–0.70
11	vegetation richness	7.09	6.00	2.47	6.50	7.00	1.70	–8.30	16.70
12	slope (%)	9.01	5.88	8.92	6.41	4.98	5.65	–28.90	–15.30

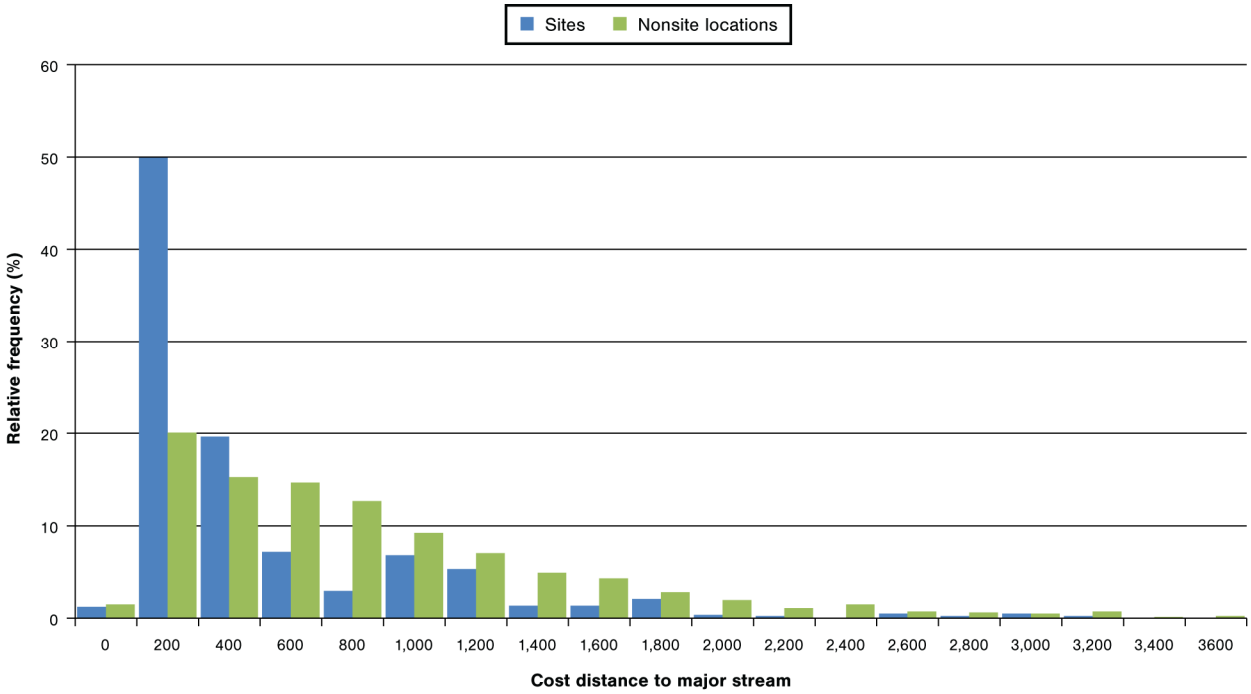

Figure 22. Frequency diagram comparing cost distance to nearest major stream of sample sites and nonsite locations.

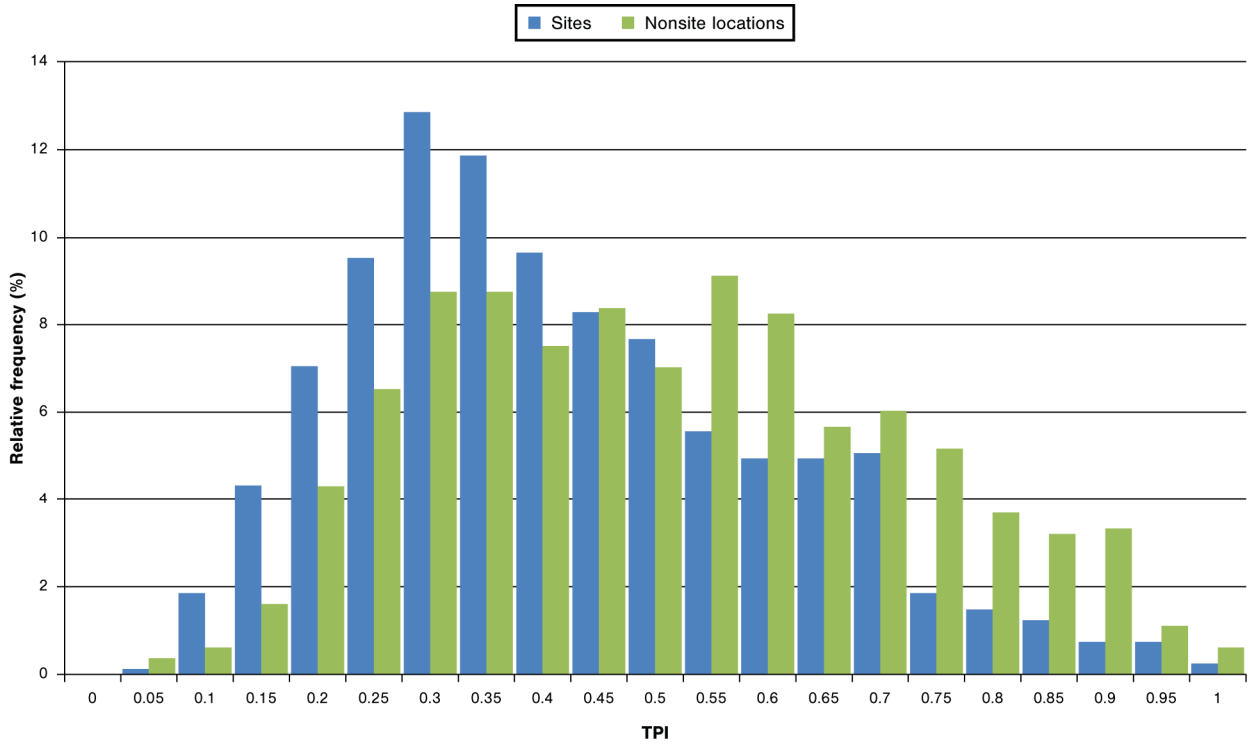

Figure 23. Frequency diagram comparing TPIs of sample sites and nonsite locations.

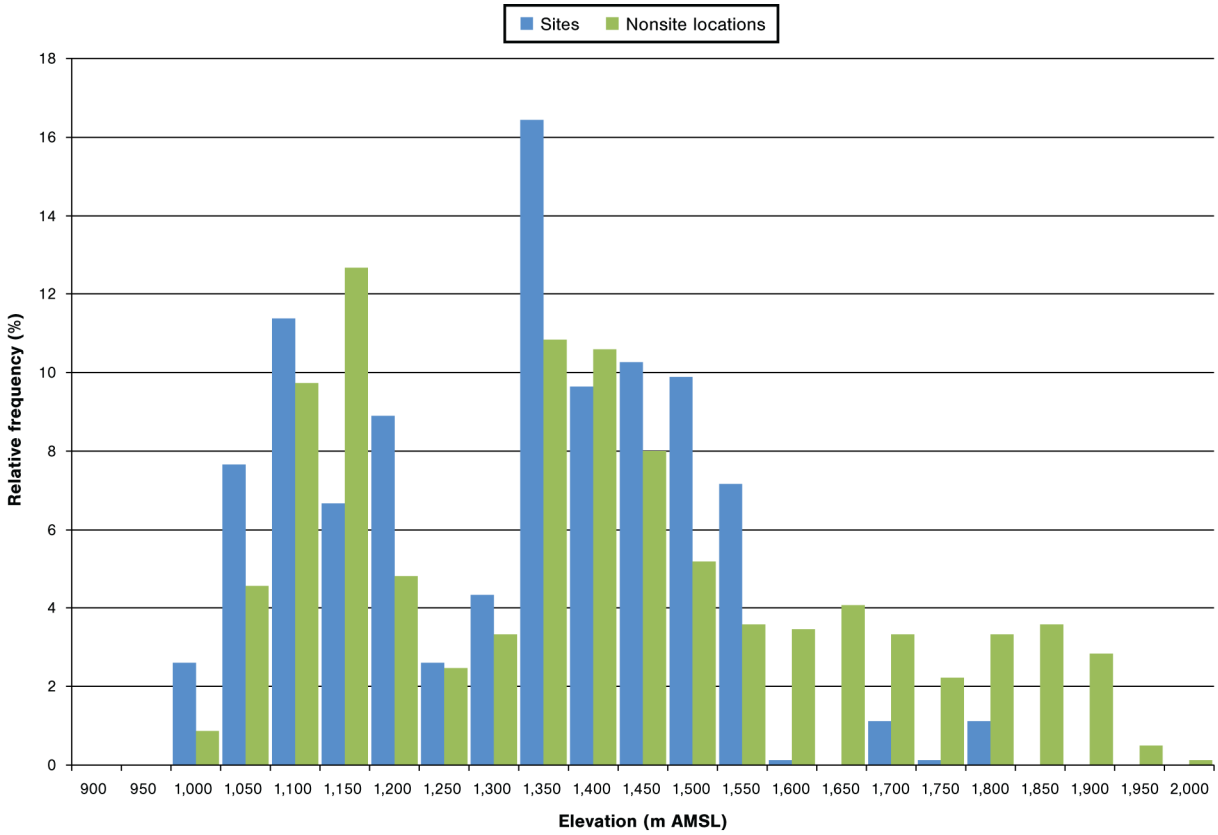

Figure 24. Frequency diagram comparing elevations of sample sites and nonsite locations.

Model Performance

The PCA variables related to topography and hydrology (discussed above), as well as vegetation richness, were used to create a ring-midden sensitivity model to be used in the design of the digital survey and in the development of an automated feature-extraction scheme. Although it is not required to use separate training and testing sets when modeling with the Random Forests algorithm (as discussed above), we nevertheless used a randomly derived 80 percent sample of the overall sample to train the model and reserved the remaining 20 percent of the overall sample for model testing.

The Random Forests model built in ModelMap was used to create a raster map for the model area, using the command, "model.mapmake()". The resulting raster map (created in ModelMap) represents the probability, for each raster cell, that a site containing a ring midden is present. The raster was then reclassified in ArcGIS into a binary sensitivity map based on the optimal threshold probability value supplied by ModelMap, which in this case was 0.54. The high-sensitivity zone was represented by raster cells with probability values that equaled or exceeded the optimal threshold value. The low-sensitivity zone was represented by raster cells with probability values that fell below the optimal threshold value. In the resulting map, the high-sensitivity zone clustered around drainages and drainage confluences—a not-unexpected result, given the strong association of ring middens with land areas close to drainages and confluences (Figures 25–28).

For the model area overall, just 8.6 percent consisted of high-sensitivity zone, and the remaining 91.4 percent consisted of low-sensitivity zone (Figure 29). Archaeological sensitivity for ring middens varied both within and between study areas. Among the three study areas, the largest percentage area of high-sensitivity zone was found within the Azotea Mesa study area (24.8 percent), and the smallest percentage area of high-sensitivity zone was found within the Upper Rio Felix study area (5.8 percent).

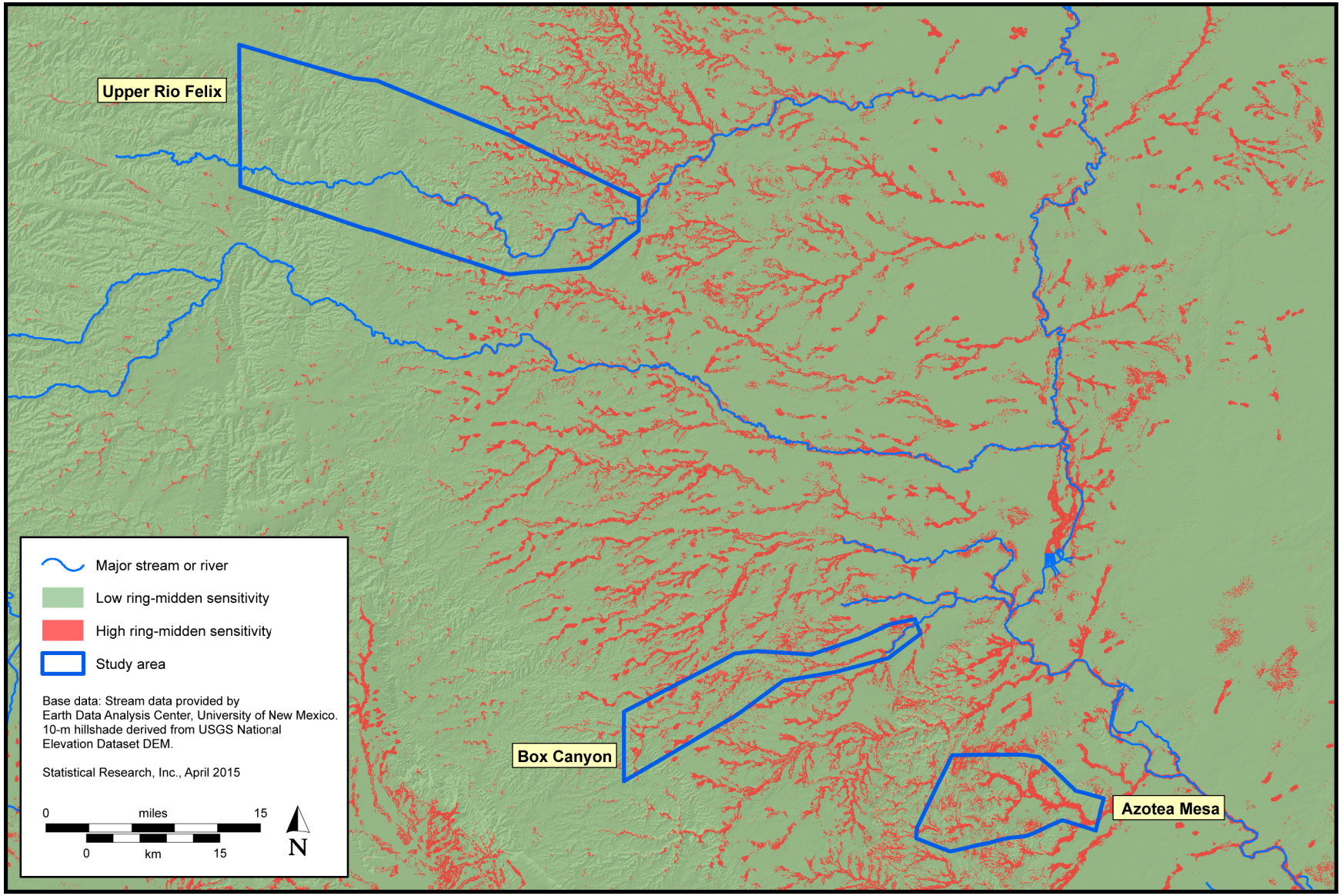

Figure 25. Preliminary sensitivity model encompassing the three study areas.

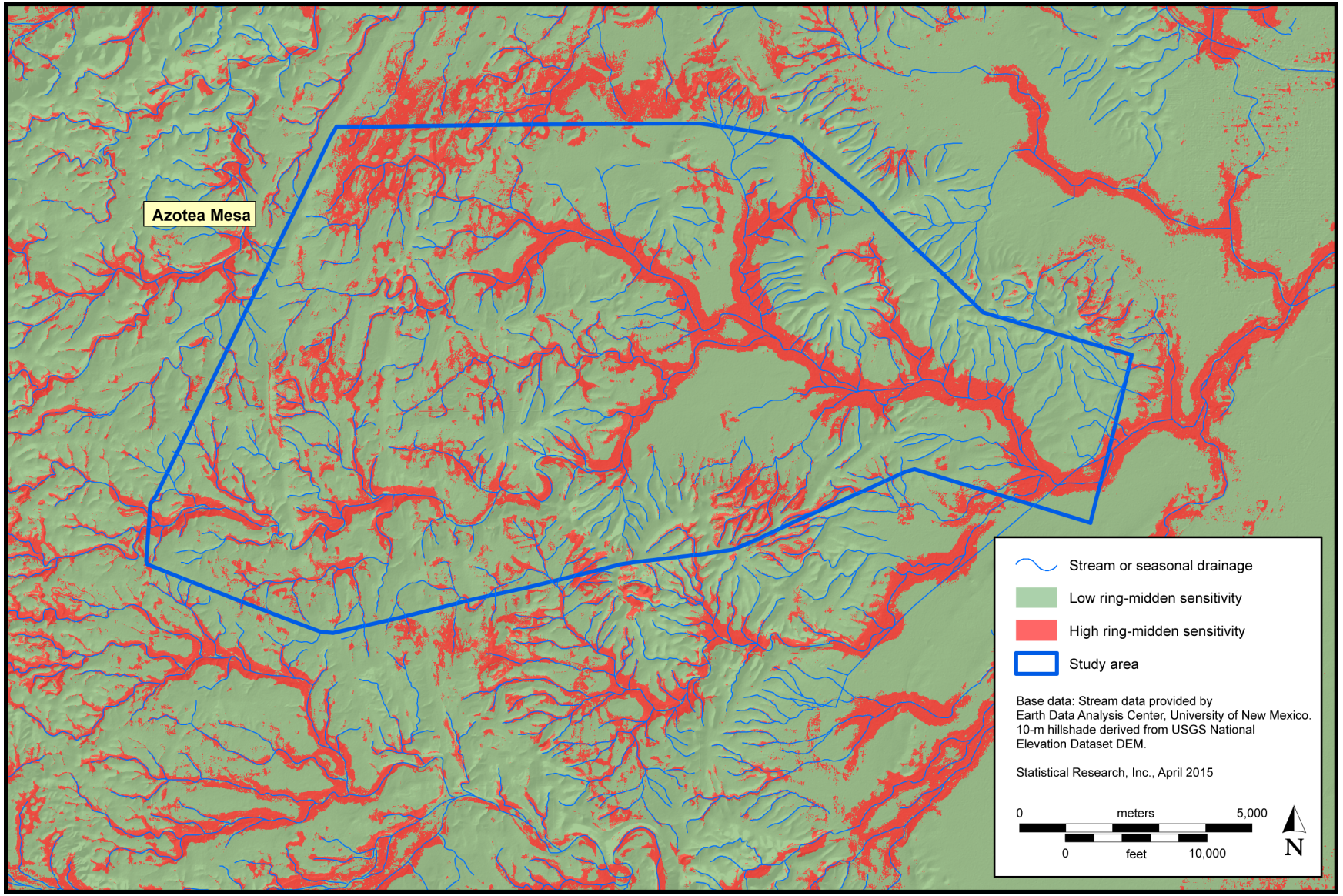

Figure 26. Preliminary sensitivity model in the vicinity of the Azotea Mesa study area.

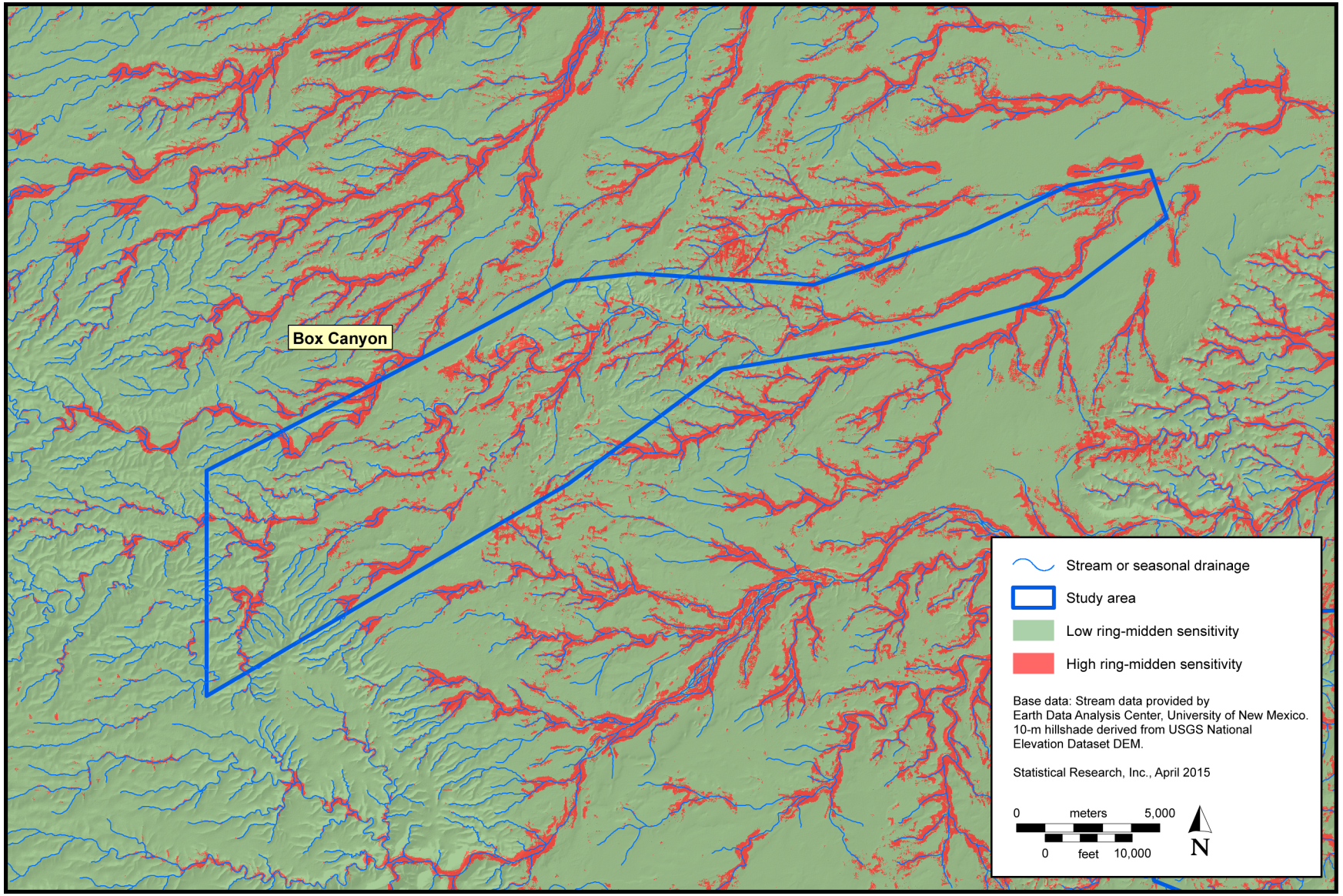

Figure 27. Preliminary sensitivity model in the vicinity of the Box Canyon study area.

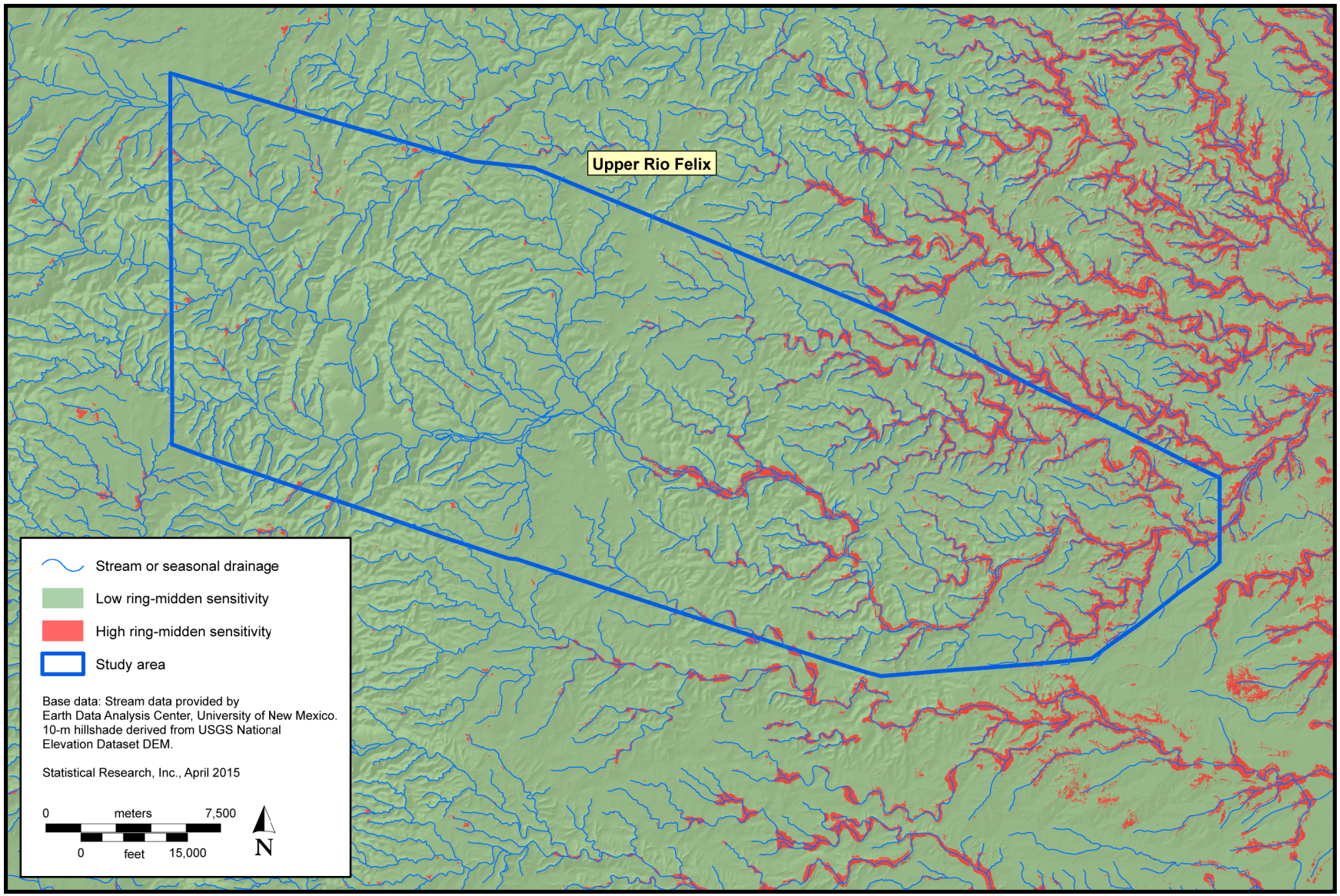

Figure 28. Preliminary sensitivity model in the vicinity of the Upper Rio Felix study area.

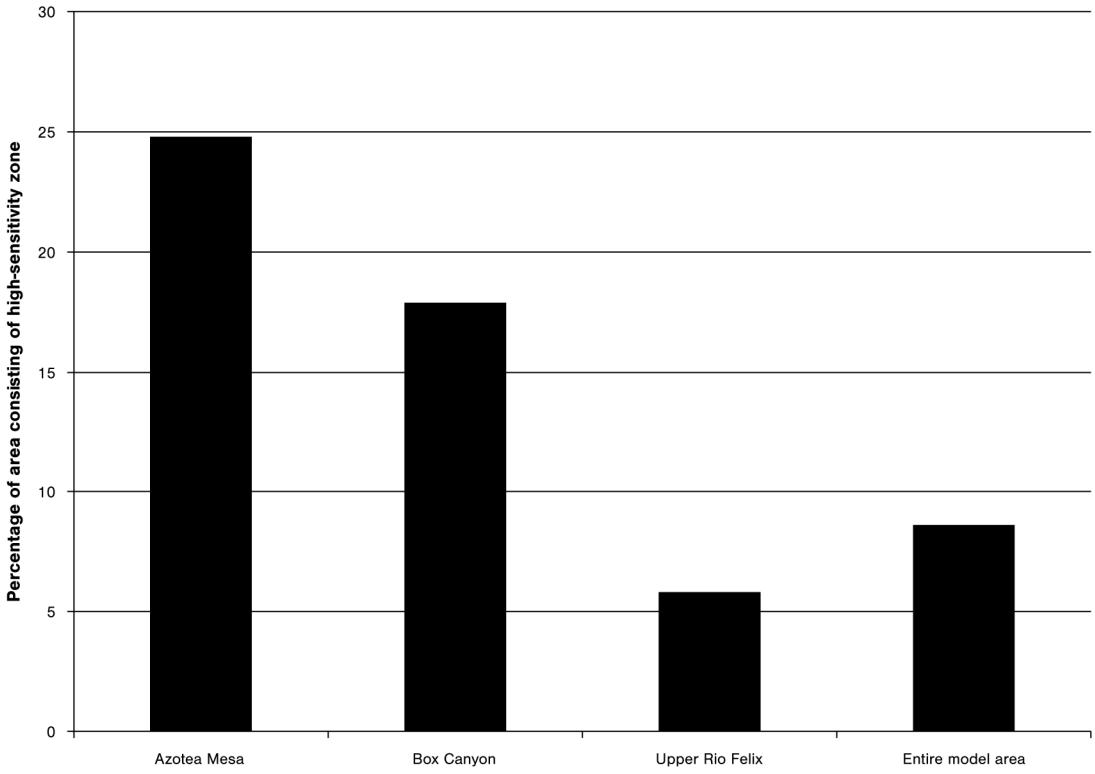

Figure 29. Percentages of areas consisting of high-sensitivity zone for ring-midden location in the three study areas.

Model-Performance Measures Derived from Test Cases

Using the binary sensitivity map and the approximately 20 percent sample of cases reserved from model training, the performance of the model was assessed with a series of metrics: True Positive Rate (TPR), False Positive Rate (FPR), Gain, and Gain Over Random (GOR). Each of these metrics and its derivation and significance are discussed below.

In the case of archaeological sensitivity modeling, the TPR is the number of site-positive cases that are correctly predicted as site locations by the model, divided by the total number of cases representing archaeological site locations. This rate can be converted into a percentage by multiplying by 100. In essence, the TPR indicates how often a model correctly predicts site-positive test cases to be sites rather than nonsite locations. The TPR is an expression of the sensitivity of the model, in that the higher the rate, the more sensitive the model is to correct identification of site locations. Said another way, the higher the number, the better the model is at accurately predicting site locations. A perfectly sensitive model would have a TPR of 100 percent, for instance. For the model discussed here, the TPR was calculated as 83.3 percent, meaning that 83.3 percent of all ring-midden test cases were correctly predicted as located within the high-sensitivity zone.

By contrast, the FPR is the number of site-negative cases incorrectly predicted to be sites by the model, divided by the total number of cases representing nonsite locations. Like TPR, FPR can be converted into a percentage by multiplying by 100. In contrast to TPR, FPR indicates how often site-negative locations are incorrectly predicted to be sites. FPR is an expression of the specificity of the model (FPR = 1 – specificity). The lower the FPR, the more specific (or precise) the model in predicting site location. For instance, if the TPR of a model is 88 percent, the model could be considered to be highly sensitive in predicting site location, because 88 percent of site locations were predicted correctly. If the FPR is 0.33, however, the model could not be considered to be highly specific in predicting site location, because one-third of nonsite

locations were predicted incorrectly to be sites. For the initial model, the FPR was calculated as 18.2 percent, meaning that 18.2 percent of nonsite locations in the sample were incorrectly predicted to be sites. Based on the arbitrary standards set by the Southern New Mexico Archaeological Sensitivity Project, both the TPR and the FPR indicated that the model performed moderately well.

Kvamme (1988b:329, emphasis in original) defined the Gain statistic as indicating whether a predictive model demonstrates "*gain* (e.g., in terms of percent correct predictions) over a purely random model with no predictive capacity." The Gain statistic was calculated as follows, using a random sample from surveyed areas:

Gain = 1 – (percentage of total area covered by model/percentage of total sites within model area).

As the Gain statistic approaches 1, it indicates an increase in a model's predictive capacity. Values near 0 indicate that a model has limited predictive utility, and negative values indicate that a model performs worse than random chance. For instance, if 85 percent of sites are found within 50 percent of the surveyed area (1 – 50/85), the Gain statistic would equal 0.41, indicating a low to moderate gain in predictive capacity. If, by contrast, 85 percent of sites are found within 25 percent of the surveyed area (1 – 25/85), the Gain statistic would equal 0.69, indicating substantial improvement in predictive capacity. When the percentage of surveyed area is close to the percentage of sites found within a model area, the Gain statistic approaches 0 (e.g., 50 percent of sites found in 50 percent of surveyed area), indicating no gain in predictive capacity. A negative Gain indicates that the percentage of sites within a sensitivity zone is smaller than the percentage of survey area covered by the zone. A model with a negative Gain performs worse than a random model. The initial model of ring-midden sensitivity had a Gain of 0.79, a high value. The high Gain was due to the fact that a relatively large percentage of sites (83.0 percent) were found within a small surveyed area that had been identified as high-sensitivity zone (17.2 percent).

GOR is a related statistic that uses the same input variables as the Gain statistic to estimate the difference between the percentage of sites within a model area and the percentage of surveyed area indicated as having medium or high sensitivity, such that

GOR = (percentage of sites within model area – percentage of area covered by model area).

GOR ranges from –100 to 100; negative index values indicate that the model works worse than random chance, low positive values indicate that it works little better than random chance, and high positive values indicate that it accurately predicts site location within a relatively small model area. With the same values used to illustrate the Gain statistic above, the GOR for a case in which 85 percent of sites are found within 50 percent of the surveyed area would be 35 (i.e., 85–50), indicating that the model predicts sites accurately but within a relatively large model area. For a case in which 85 percent of sites are found within 25 percent of the surveyed area, however, the GOR would increase to a value of 60 (i.e., 85–25), indicating substantial improvement in the model's specificity, because most sites were discovered within a model area half the size of the model area in the former case. For the initial model of ring-midden sensitivity, the GOR was calculated as 64.8 percent, representing a relatively high gain in comparison to a random model.

Automated Feature Identification

The locational model described above was designed to predict which portions of the three study areas were more or less sensitive for containing ring-midden features. Because the locational model was based on the associational characteristics of ring middens (i.e., the kinds of environmental settings in which ring middens have been found), it is not intended to identify individual ring-midden features. Rather, it identifies broad zones in which ring middens are more or less likely to be present.

However, a useful tool for identifying landscape features in digital remotely sensed data, such as lidar, is automated feature identification (AFI). Some sophisticated programs have been developed to automatically extract features from lidar data, such as Feature Analyst, a plug-in created by Overwatch Systems, Inc., that can be used with a variety of GIS programs, including ArcGIS (http://www.vls-inc.com/topics/downloads.htm, accessed June 2014), but these are quite costly to license and also have been designed primarily to identify landscape features of more common interest in land-use planning and development, such as roads, buildings, power lines, and water features. Thus, we endeavored to develop a custom application that could use GIS layers derived from the lidar data to locate potential ring-midden features in the digital data based on their unique morphological characteristics.

These kinds of approaches toward AFI tend to be challenging, because they involve experimenting with series of complex transformations of the underlying elevation data and decision-tree-based rules to identify the conditions in which one would expect a feature to conform or not conform. The way we conceptualized the AFI process was based on the fact that, first and foremost, ring-midden features will be recognized by their unique morphology—that is, as roughly circular features, each consisting of a ring-like or doughnut-shaped berm describing its perimeter and a depression in the center. Sometimes, such features can have discontinuous rings, possibly suggesting disturbance, and they typically have diameters in the range of 5–15 m. The central area of a feature is typically lower in elevation than the discard midden, as is the area immediately outside the feature.

We reasoned that this unique morphology could be effectively targeted using layers derived from the DEM, LRM, and TPI and currently available ArcGIS tools for spatial analysis. One of the primary ArcGIS tools used to generate the layers used in the AFI was the Focal Statistics tool available in ArcGIS Spatial Analyst. The Focal Statistics tool calculates one of several statistics for a user-specified area around each cell in a raster (e.g., mean, range, standard deviation, minimum, or maximum). Each cell in the resulting raster represents the statistic as calculated for the specified neighborhood around each raster cell. The user has to specify the shape of the analysis window (circle, rectangle, annulus, or wedge) as well as the size of the window. The Focal Statistics tool is especially suited to identifying topographic characteristics associated with ring middens, because ring middens are typically circular in shape and have annular rings. Ring middens identified in the lidar data using visualization methods (see above discussion) also tended to fall within a characteristic range of sizes. That allowed us to specify various conditions in which we would expect ring middens to occur, based on their characteristic morphology.

To generate the AFI, we first calculated a series of rasters representing conditions that we expected for ring middens (see Appendix B). Because we used the Focal Statistics tool to do this, we were essentially identifying one or more cells in the center of each ring midden that fulfilled the characteristics we expected for a ring-midden feature. To create the conditions raster, we first calculated the TPI, using the LRM. That allowed us to identify, at a fine scale consistent with that of ring middens, whether particular raster cells represented local topographic highs or lows or somewhere between. We expected the rings surrounding ring middens to have relatively high TPIs and the areas immediately outside, or beyond, the rings to have low TPIs. We also expected the center of a ring-midden feature to have a relatively low average TPI, but that came to play in a later step.

To create the conditions raster, we created two rasters using the Focal Statistics tool in ArcGIS. The first was a raster that calculated the mean TPI for an annulus-shaped neighborhood with an inner radius of 3 m and an outer radius of 6 m. This raster was essentially intended to identify any cell surrounded largely by a ring of local topographic highs within a 3–6-m radius around it. The second was a raster that calculated the mean TPI for an annulus-shaped neighborhood with an inner radius of 6 m and an outer radius of 9 m. This raster was intended to identify cells with predominantly low TPI values within a 6–9-m radius.

Based on examination of the values of these two Focal Statistics rasters in the centers of ring middens delineated using the lidar data, we then reclassified the rasters. They were divided into a series of classes, based on ranges of values, and then reclassified. In the reclassification, each class was scored from 0 to 4, with 0 representing a very low probability that a cell represented the center of a ring-midden feature and 4 representing a high probability that a cell represented the center of a ring midden.

The two reclassified rasters were then added together, resulting in a raster with values ranging from a minimum of 0 to a maximum of 8. Examination of this raster revealed that the centers of ring middens typically had values from 6 through 8 in the added raster. Thus, the raster was reclassified such that values from 6 through 8 were reclassified as 1, and values from 0 through 5 were reclassified as 0. In the resulting reclassified raster, a value of 1 corresponded to a cell that may be located within the center of a ring midden, and a value of 0 corresponded to a cell that was likely to be located within the center of a ring midden.

Performing the above transformations of the lidar data resulted in a series of rasterized blobs representing small areas that could be the centers of ring-midden features. Examination of this layer showed that many, but not all, of the centers of previously identified ring middens had been correctly classified as equaling 1. Ring middens that had not been correctly identified tended to be characterized by very subtle topography or had unusual characteristics, such as having been disturbed or abutting other topographically prominent features. At the same time, there were many other blobs in the resulting raster that clearly did not correspond to ring-midden centers and needed to be masked out or removed from consideration.

To mask out false positives to the degree possible, we created a series of three mask rasters representing topographic characteristics inconsistent with ring middens. The first of these had to do with percent slope. Percent slope was calculated using the elevation values in the LRM and the Slope tool in ArcGIS Spatial Analyst. The Focal Statistics tool was then used to calculate the mean slope within a circular neighborhood around each raster cell, using a 9-m radius. We found that cells in the center of a ring midden tended to have focal mean slopes between 2.4 and 12 percent. Cells with higher or lower focal-mean-slope values tended to be located outside ring middens. Thus, the focal-mean-LRM-slope raster was reclassified such that values from 2.4 to 12 equaled 1, and all other values equaled 0.

The second mask raster was based on LRM values. The centers of ring middens tended to have LRM values close to 0. Thus, we reclassified the LRM raster such that values between –0.25 and 0.15 equaled 1, and all other values equaled 0. The 0 values in this raster were then expanded by 2 cells, to generalize the raster.

The third mask raster was based on relief. Many of the false positives occurred in rugged areas on slopes, as a result of slope breaks on steep hills or stream terraces. Thus, we used the DEM derived from the lidar data and the Focal Statistics tool to calculate relief, in order to identify cells located within these rugged areas. This was done by calculating the range in elevation values in the DEM within a circle with a 9-m radius. Ring-midden centers tended to be located in areas where relief was no more than 2 m within a circular neighborhood with a radius of 9 m. Thus, the focal-elevation-range raster was reclassified such that values below 2 m equaled 1, and areas of higher local relief equaled 0.

The three mask rasters described above were then multiplied together, such that areas that fulfilled all the above conditions (with focal-mean-LRM slopes of 2.4–12 percent, LRM elevations close to 0, and focal elevation ranges that were less than 2 m) equaled 1, and all other areas to be masked out equaled 0.

The mask raster was then multiplied by the conditions raster, to generate a final series of rasterized blobs representing possible centers of ring-midden features, where 1 indicated a potential ring-midden center, and 0 indicated no potential ring-midden center. To merge small, disconnected areas within ring middens and avoid double counting of ring-midden features, we then expanded values equaling 1 in the ring-midden-centers raster by 5 cells.

The resulting blobs were then converted into polygons representing possible ring-midden centers. The centroid of each feature was then calculated, to create a point file representing possible ring-midden centers. This process resulted in correct identification of most ring middens but also resulted in a still-large number of false positives. To further reduce the false positives, additional steps were taken and involved calculating the mean TPI for a circular neighborhood with a radius of 2.5 m. We found that the centers of ring middens tended to have focal-mean-LRM-elevation values that were less than 0.35 (often substantially less), and false positives tended to have values of 0.35 or greater. Thus, the raster was reclassified such that values below 0.35 equaled 1, and all other values equaled 0. We used the Extract by Points tool in ArcGIS to obtain the value of this raster for each possible ring-midden point. Points with values of 1 were retained for consideration, and the remaining points (with raster values equaling 0) were removed from consideration.

Discussion

In this chapter, information has been presented about how lidar data were processed and visualized for the project in order to identify ring-midden features. Recorded sites with ring middens were examined in a GIS to identify ring-midden features in the lidar data, and samples of those features were profiled. Profile measurements were used to morphometrically characterize ring-midden features. The ring-midden-site data were then subsequently used to evaluate environmental associations and to create a locational model of ring-midden sensitivity. An approach to automated identification of potential ring-midden features in the lidar data was also developed. The sensitivity model and AFI routine were used to design and guide the digital survey for ring middens, which is discussed in Chapter 4.

CHAPTER 4

Digital Survey, Field Verification, and Model Refinement

Introduction

In this chapter, information is presented on how the digital survey of ring-midden features was conducted using lidar data collected for the project. The digital-survey results are discussed and analyzed, and the methods and results of the field-verification effort, aimed at ground-truthing a sample of digitally identified ring middens, are presented. That discussion is followed by a presentation of the efforts aimed at refining a locational model of ring-midden sensitivity based on the results of the digital survey.

Digital-Survey Design

The locational model of ring-midden sensitivity was used to develop a sample of areas to be digitally surveyed for potential ring-midden features as part of the project. For the purposes of collecting and organizing lidar data for the project, Surdex divided each of the three study areas into a grid of square tiles measuring 2,000 by 2,000 feet (610 by 610 m) (see Chapter 1). The tile index supplied by Surdex for the three study areas was used as a sampling frame for selecting land parcels for digital survey using the results of the locational model. Survey sample tiles were selected on the basis of the percentage of land area within each tile that consisted of high- or low-sensitivity zone.

For each tile in each of the three study areas, we calculated the percentage area covered by high-sensitivity zone and the percentage area covered by low-sensitivity zone (Table 5). We then identified, per study area, which tiles had the largest percentages of high-sensitivity zone and which tiles had minorities of high-sensitivity zone. We then selected a random sample of tiles based on the percentage of high-sensitivity zone in each tile, such that 75 percent of tiles in each study area survey sample had large percentages of high-sensitivity zone, and the remaining 25 percent of the sample tiles consisted of primarily low-sensitivity zone. Tiles that had been inspected during an initial pilot study were removed from consideration, to allow us to cover more area and avoid re-inspecting areas that had already been documented and inspected for ring middens.

The sample-selection process resulted in an approximately 19.8 percent sample for digital survey from the Azotea Mesa study area and a 17.2 percent sample from the Box Canyon study area (Table 6). Because of the much larger size and low archaeological sensitivity of the Upper Rio Felix study area in comparison to the Azotea Mesa and Box Canyon study areas, a 10 percent sample of the Upper Rio Felix study area was selected for digital survey. Overall, in terms of acreage, 32 percent of the surveyed area consisted of high-sensitivity zone, and 68 percent consisted of low-sensitivity zone.

In total, 359 lidar tiles were digitally surveyed, covering a total of 32,965 acres (Figures 30–32). The digital survey resulted in the identification of 511 potential ring-midden features (254 potential ring middens identified during digital survey in the Azotea Mesa study area, 155 in the Box Canyon study area, and 102 in the Upper Rio Felix study area), as well as 25 features that could potentially be confused with ring middens because of similarities in morphology. In total, 33 (6.5 percent) of the potential ring-midden features identified during the sample survey were located within the boundaries of previously recorded sites; most of those were located within the Azotea Mesa study area, where survey has been more extensive and many sites with ring middens have been recorded. The remaining ring middens identified during digital survey were located outside the boundaries of previously recorded sites.

Table 5. Proportions of High-Sensitivity Zone in Tiles Characterized as Predominately High Sensitivity or Predominately Low Sensitivity, by Study Area

Study Area	High-Sensitivity Tiles			Low-Sensitivity Tiles		
	Minimum Proportion per Tile of High-Sensitivity Zone	Maximum Proportion per Tile of High-Sensitivity Zone	Average Proportion per Tile of High-Sensitivity Zone	Minimum Proportion per Tile of High-Sensitivity Zone	Maximum Proportion per Tile of High-Sensitivity Zone	Average Proportion per Tile of High-Sensitivity Zone
Azotea Mesa	0.50	0.97	0.65	—	0.28	0.14
Box Canyon	0.37	0.87	0.53	—	0.27	0.07
Upper Rio Felix	0.27	0.93	0.43	—	0.23	0.01

Table 6. Sensitivity-Model Statistics for Lidar Tiles Selected for Digital Survey, by Study Area

Study Area	Count of Surveyed Tiles with Large Proportions of High-Sensitivity Zone	Count of Surveyed Tiles with Small Proportions of High-Sensitivity Zone	High-Sensitivity Acreage	Low-Sensitivity Acreage	Total Sample Acreage	Digital-Survey-Sample Proportion of the Study Area	Study Area Total Acreage
Azotea Mesa	62	20	3,561.1	3,968.1	7,529.2	0.198	37,962.1
Box Canyon	75	15	3,737.8	4,526.7	8,264.5	0.173	47,842.2
Upper Rio Felix	140	47	5,522.2	11,649.6	17,171.8	0.100	171,534.2
Total	277	82	12,821.1	20,144.4	32,965.5	0.128	257,338.5

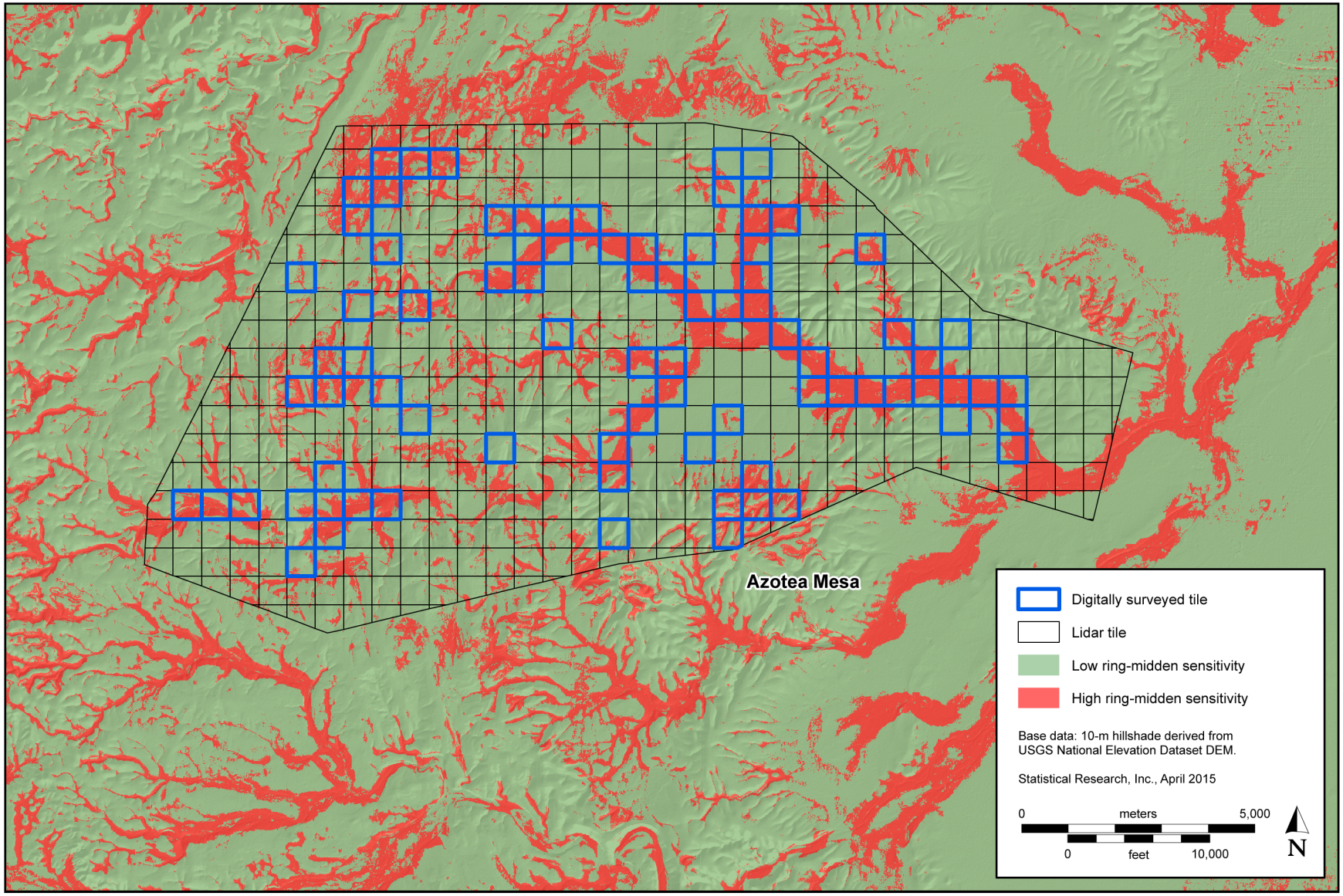

Figure 30. Map showing the locations of survey tiles selected for digital survey in the Azotea Mesa study area.

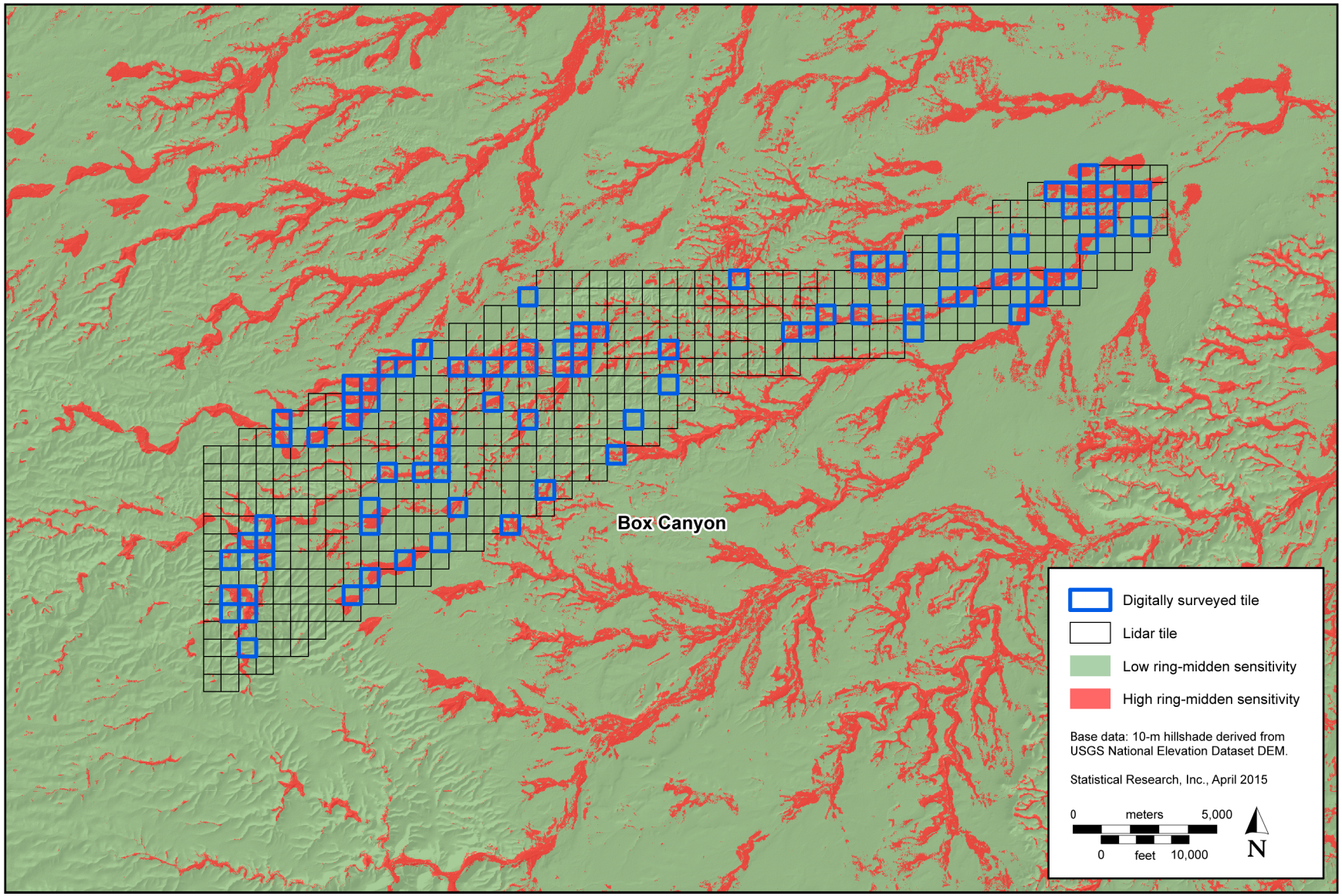

Figure 31. Map showing the locations of survey tiles selected for digital survey in the Box Canyon study area.

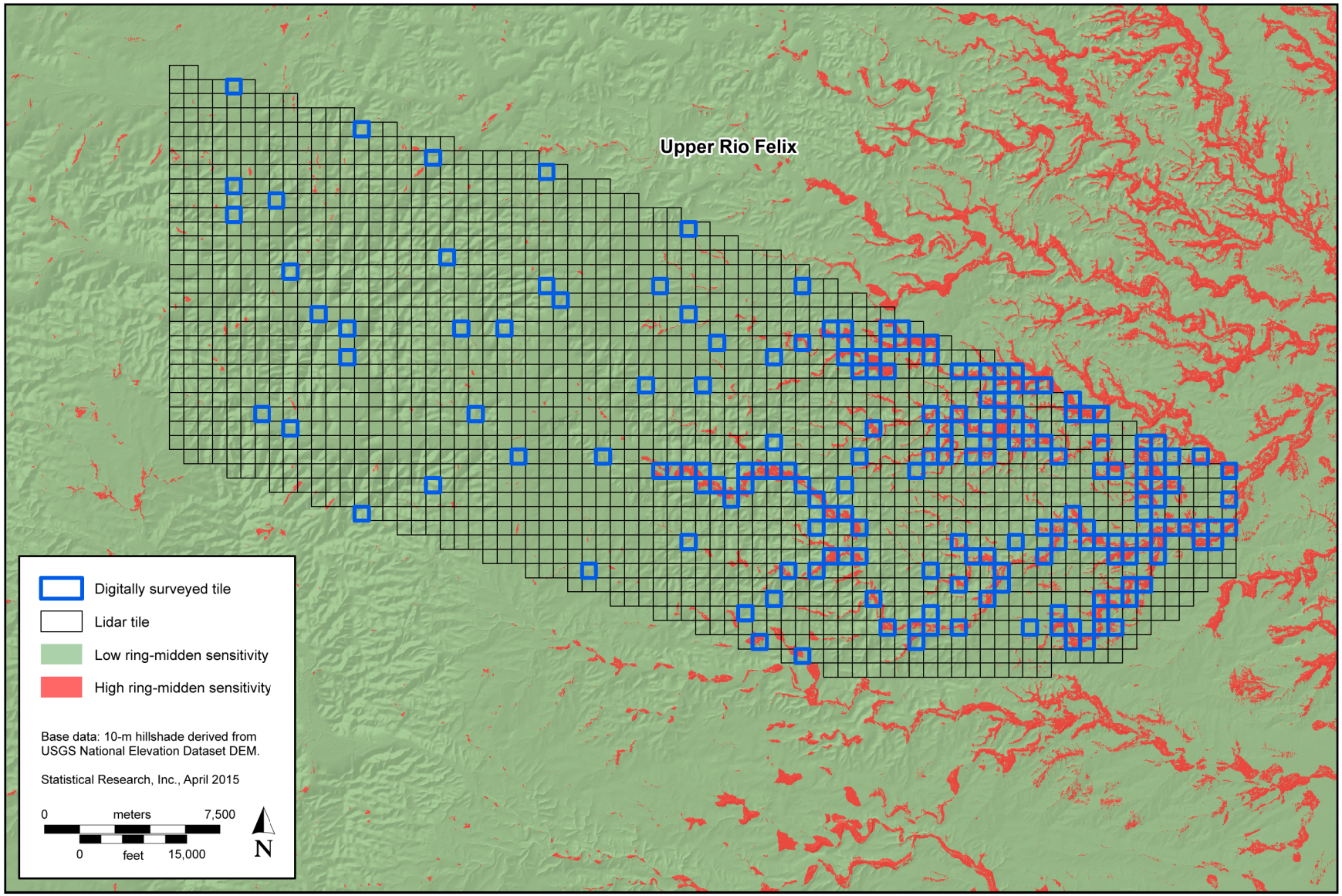

Figure 32. Map showing the locations of survey tiles selected for digital survey in the Upper Rio Felix study area.

Digital-Survey Methods

The digital survey was designed to follow a systematic approach (see Appendix C). For each of the tiles selected as survey tiles, we used the lidar point cloud LAS data to generate a DEM, using the approach discussed in Chapter 3. The DEM was then used to generate LRM, TPI, and hillshade layers for each survey tile. The DEM, LRM, and TPI were also used to develop a series of layers used in our AFI process, ultimately resulting in a point layer representing possible ring-midden locations. All of these layers were created using automated, systematic procedures and were generated using batch-processing techniques and Python scripts developed for the project.

To survey an individual tile, the LRM, TPI, hillshade, and AFI centroid layers were loaded into ArcMap and visualized using the same color and display schemes. Once loaded, the surveyor first searched for ring middens at the scale of the entire tile. At that scale, prominent ring middens can be readily identified in the LRM and/or TPI layers. Any potential ring middens identified at that scale were then closely examined. If the feature had characteristics that conformed to our expectations for ring-midden morphology or that could be confused with those of a ring midden, an elliptical polygon was created to encompass the feature. The polygon was then attributed with data regarding feature-shape characteristics and how well defined the feature appeared in the lidar data. For each of these attributes, attribute states were recorded, according to a series of predefined categories (see Appendix C).

The following categories were used for the feature-definition variable: (1) well defined, (2) moderately defined, (3) faint, (4) indistinct, and (5) not applicable. The category of *indistinct* was intended to be used when a possible feature was present near other, more-definitive ring-midden features but there was minimal feature definition. The *not applicable* category was intended for features that could be confused with ring middens and were recorded only for comparative purposes.

The shape variable consisted of the following categories: closed ring, open ring, irregular/discontinuous ring, ring with mounded lobe, and atypical. The last category was reserved mostly for features that had unusual shape characteristics, such as exhibiting rectilinearity or having an especially deep depression in the center. The *ring with mounded lobe* category was intended for a ring midden that had a large mound attached to one side of the ring. Rings of this type were observed in multiple locations during preliminary feature characterization and were distinctive and recurrent enough to warrant a special shape category. Examples of each definition and shape category were provided to the surveyor prior to digital survey, in order to attribute polygons in a consistent manner. The digital surveyor, Monica Murrell, is an experienced field archaeologist who has conducted intensive field investigations in many parts of New Mexico, including the Permian Basin, and has documented multiple ring middens in the field. Ms. Murrell also has a background in GIS and geoarchaeology. She was thus an excellent choice to conduct the digital survey. Having the survey conducted by a single individual further served to ensure consistency in the results.

The RFQ for the project noted that a ring-midden feature often has one side that is higher than the opposing side, as discussed in Chapters 1 and 3. Morphometric characterization (presented in Chapter 3) confirmed that to be the case. The RFQ requested that the high side of each feature be identified. To record that information consistently, we first explored the possibility of dividing each feature into sections of the compass rose and identifying which section of the compass rose contained the highest portion of the feature. This approach to identifying the high side of each feature proved to be difficult to consistently apply, however. As an alternative approach, the surveyor drew a line from the approximate center of each feature to the "center of gravity" of the high side of the feature, or the area of the discard midden where the highest-elevation cells in the LRM were concentrated. That line was then used to calculate the azimuth from the approximate center of the feature to the center of the high side. The azimuth was calculated for each line using the Polyline_GetAzimuth tool in EasyCalculate10 for ArcGIS, a collection of free measurement tools (http://www.ian-ko.com/free/EC10/EC10_main.htm, accessed January 14, 2015).

Once the entire tile had been reviewed at the scale of a survey tile and any ring middens spotted at that scale had been identified with polygons and attributed, the digital surveyor then proceeded to survey the tile at approximately 1/9 the scale of the tile. Survey began in the northwestern corner of the tile. At that

scale, the surveyor examined the LRM and hillshade as well as the AFI centroids, because AFI centroids are sometimes helpful in identifying subtle features. Potential ring middens identified at this scale that had not been recorded at the broader scale were closely examined. Polygons were created for features considered to be potential ring middens or features that could be confused with ring middens, following the same process as above. Once an area of a tile had been examined, the surveyor panned across the survey tile in regular, east–west transects, in order to closely inspect the entire tile.

Survey Results

The survey resulted in the identification of 536 features. Excluding features with shapes inconsistent with our expectations for the shape of a ring midden (n = 25), 254 potential ring middens were identified during digital survey in the Azotea Mesa study area, 155 in the Box Canyon study area, and 102 in the Upper Rio Felix study area. Based on the survey acreage in each of the three study areas, the number of features discovered demonstrated a steep cline in ring-midden density, with the highest density in the Azotea Mesa study area and the lowest density in the Upper Rio Felix study area (Figure 33).

Ring-Midden Areal Extent

Ring middens also vary considerably in size among the three study areas. On average, the largest ring middens were found in the Azotea Mesa study area, and the smallest were located in the Upper Rio Felix study area (Figure 34). Like ring-midden density, the average, median, and maximum sizes of ring middens decrease dramatically between the Azotea Mesa and Upper Rio Felix study areas (Table 7). Further, the coefficient of variation of ring-midden size, although high for all three study areas, was lowest for the Azotea Mesa study area and highest for the Upper Rio Felix study area. So, as we move from the Azotea Mesa study area to the Upper Rio Felix study area, ring middens get smaller in size (from a surface perspective), less frequent, and also comparably more variable in size.

There are a variety of scenarios that could potentially explain differences in the ring-midden-areal-extent data among the study areas. These differences could relate to variation among the study areas in

(a) the intensity of earth-oven use (if we assume that larger ring middens and higher densities of ring middens are related to more-intensive or more-frequent use of earth ovens),

(b) the types or quantities of materials that were processed in earth ovens, or

(c) differences in visibility or obtrusiveness resulting from differences in disturbance, sedimentation, and/or vegetation.

Disturbance processes could potentially explain differences in size among the study areas, at least in part, if we assume that disturbance processes bury portions of features, making the surface-exposed portion of a feature smaller; displace materials from the discard middens, making ring middens appear smaller from a surface perspective; and also, perhaps, contribute to greater variation in size as observed from a surface perspective.

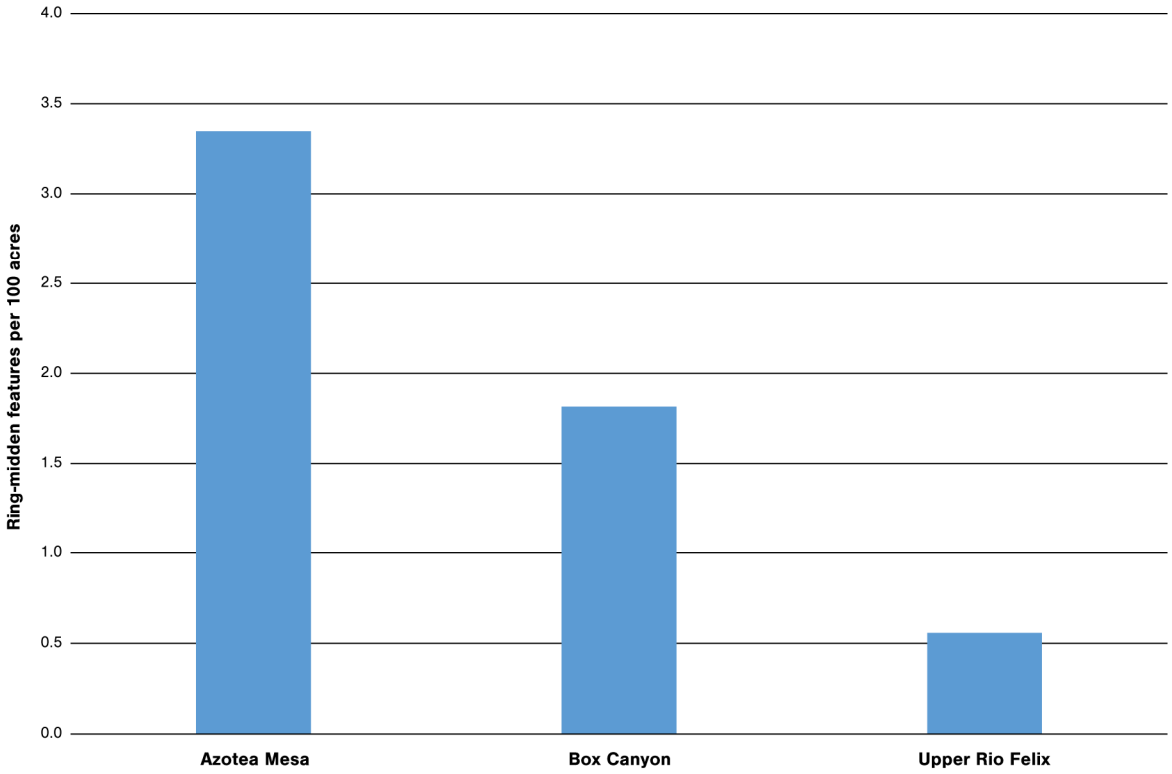

Figure 33. Ring-midden densities based on the digital-survey results, by study area.

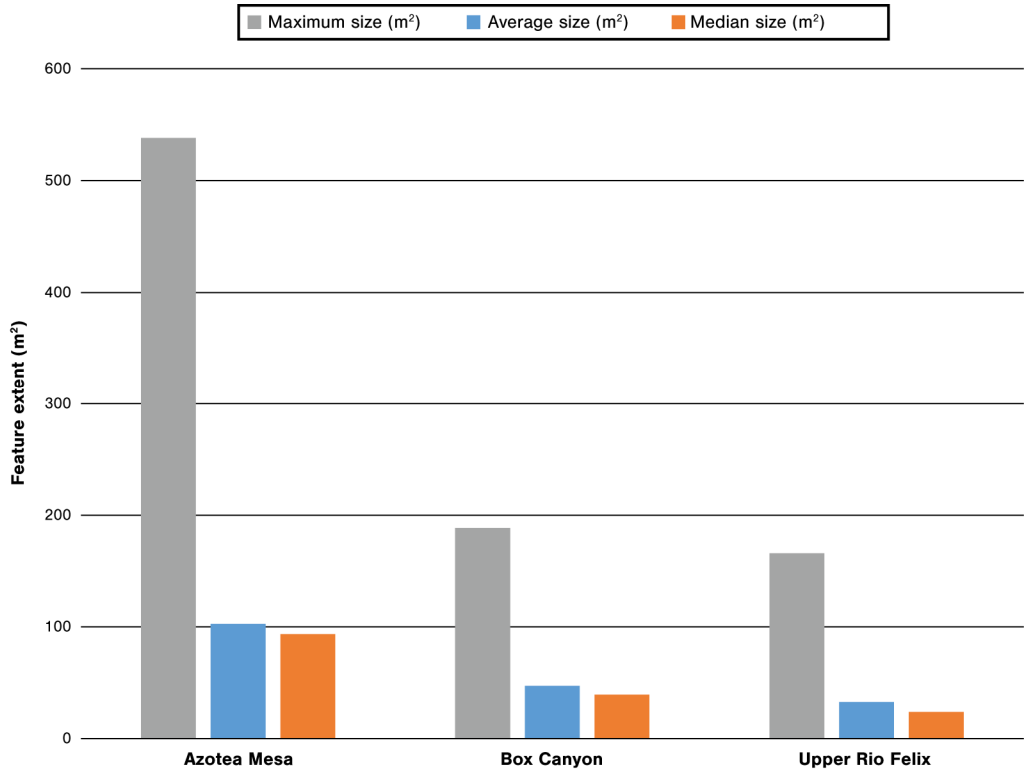

Figure 34. Maximum, average, and median ring-midden areal extents (m^2) based on the digital-survey results, by study area.

Table 7. Statistics for Ring-Midden Areal Extent, by Study Area

Statistic	Study Area		
	Azotea Mesa	Box Canyon	Upper Rio Felix
Count	252	150	81
Average size (m^2)	102.7	47.2	34.3
Median size (m^2)	93.6	39.2	24.7
Minimum size (m^2)	6.2	3.1	6.5
Maximum size (m^2)	538.1	188.6	165.9
Standard deviation	65.9	35.6	27.8
Coefficient of variation (%)	64.1	75.5	81.2

Ring-Midden Shape

Another rather stark difference between the study areas is in ring-midden shape. Ring middens are typically circular to elliptical in plan view. One way to monitor whether ring middens are closer to circular or elliptical in shape is to calculate a shape index. In order to compare the shapes of ring middens, we used an index created by Heilen (2005) that measures how much a polygon shape departs from circularity. To do this, we used the polygon area as calculated in ArcGIS to estimate the length of the radius of a circle with the same area:

$$r_a = \sqrt{(a / \pi)},$$

where r_a = radius and a = polygon area. We then calculated the radius that would be obtained using the perimeter of the shape if the shape of the polygon were a circle:

$$r_p = p/(2\pi).$$

To calculate the index, we then divide r_a by r_p:

$$\text{Shape Index} = r_a / r_p$$

A value close to 1 indicates that the shape closely approximates a circle, and a value above 1 indicates that the shape departs from circularity.

The shape index indicated that there were two regimes for ring middens: low index values, which indicated ring middens approximately circular in shape, and distinctively higher index values, which indicated ring middens more elliptical in shape (Figure 35). Intriguingly, ring middens in the Azotea Mesa study area are predominately closer to circular in shape than those in the Upper Rio Felix study area, which are more oblong, or elliptical, in shape. The Box Canyon study area includes a mixture of ring middens that either approach circularity or are more elliptical in shape. Moreover, the average shape index was lowest for the Azotea Mesa study area and highest for the Upper Rio Felix study area. That pattern held across shape and definition categories, suggesting that it was not the result of differences among specific shape or definition categories. However, there did appear to be an indirect relationship between ring-midden size and the shape index (Figure 36), with the shape index decreasing (approaching circularity) as ring-midden size increased, suggesting that ring middens more closely approach a circular shape as their sizes increase. Perhaps as a ring midden increased in size from repeated use of an earth oven, it tended to become more circular in shape. If so, whether a ring midden is more circular or more elliptical in shape could be related to the frequency of

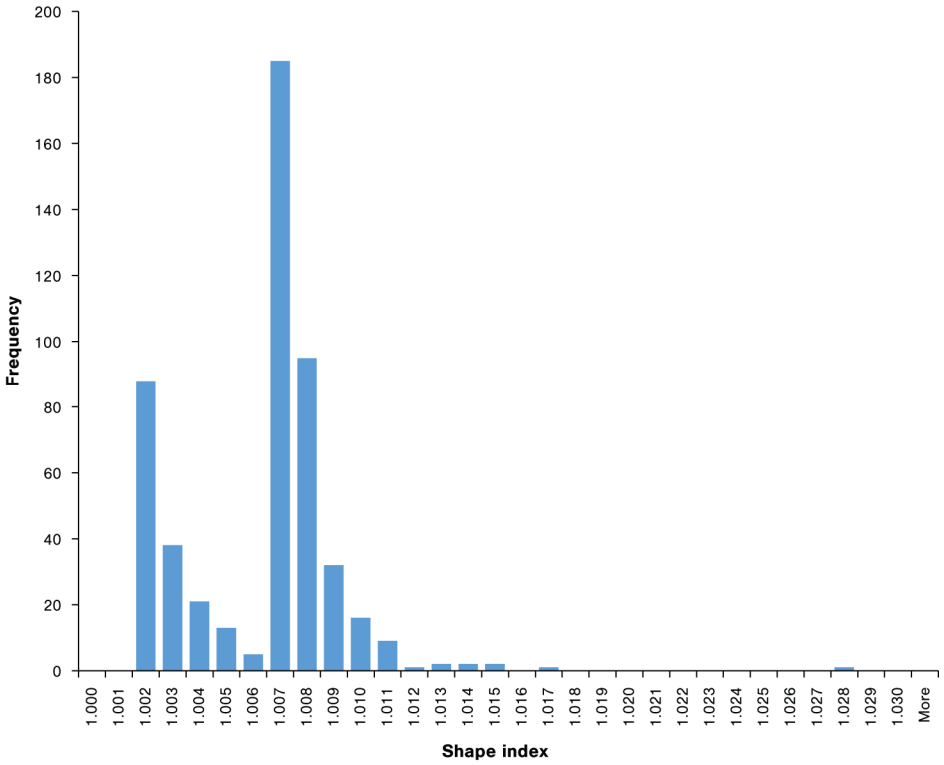

Figure 35. Frequency distribution of digitally identified ring-midden features, by shape, according to the shape index.

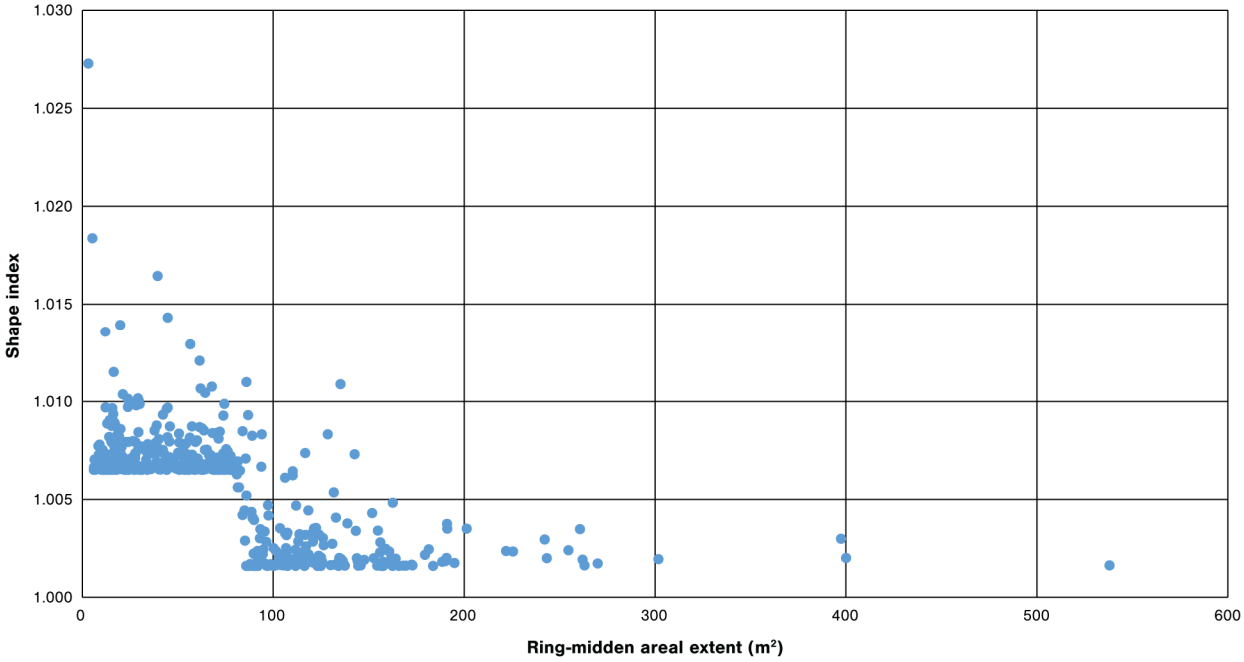

Figure 36. The relationship between shape (according to the shape index) and areal extent for digitally identified ring middens.

earth-oven use. In other words, with fewer uses, discarded heating elements (FCR) and earthen packing material could have tended to be raked out to one side or to a few locations surrounding a ring midden, but as the oven was repeatedly used and cleaned out, discarded earth-oven contents could have come to be more evenly spread around the periphery of the earth oven, resulting in a more circular ring. It has been reported that Apache groups discarded clean-out materials by preferentially tossing materials in intercardinal directions, which could lead to a more irregular and discontinuously defined ring with multiple apparent openings. Disturbance processes can also distort or truncate portions of a ring. In other words, as a ring-midden feature is increasingly disturbed, it may also appear to decrease in size, when viewed from a surface perspective, and appear more elliptical in plan view, as portions of the discard midden get buried or displaced.

Other shape characteristics of ring-midden features also vary among the study areas (Table 8; Figures 37–39). As discussed above, we characterized each ring midden during the digital survey as (1) a closed or mostly closed ring, (2) an open ring, (3) an irregular/discontinuous ring, (4) a ring with a mounded lobe attached to one side, or (5) atypical (e.g., a borrow pit, *charco*, or rectilinear feature). Closed rings were found at similar relative frequencies among the three study areas. However, open rings become more frequent relative to other shapes as one goes from Azotea Mesa to Upper Rio Felix, as do features with atypical shapes. By contrast, rings with irregular, discontinuous shapes and ring middens with mounded lobes are most frequent in the Azotea Mesa study area and decrease in frequency as one goes from Azotea Mesa to Upper Rio Felix. Possibly, the relatively high incidence of ring middens with mounded lobes in the Azotea Mesa study area is also related to more intensive, repeated use of earth ovens. Ring middens with mounded lobes are typically large and very well defined, in comparison to other types of ring middens. For example, no more than 25 percent of ring middens of other shape categories were categorized as well defined, but 65 percent of ring middens with mounded lobes were categorized as well defined, and 21 percent were categorized as moderately well defined (Figure 40). One possible explanation is that they were used so repeatedly that it was no longer practical to continue to add oven-clean-out material to the annular ring, leading to the discard of clean-out material in a pile outside the ring midden. When viewed using intensity data, these mounded lobes tend to have high intensity values, suggesting that the lidar pulse is reflecting comparatively bare ground. This could indicate that these mounded lobes consist primarily of stone that was removed from earth ovens and placed in a large pile outside the annular ring or that large stockpiles of stone intended for planned future use of a ring midden were piled up next to a ring-midden feature. Or the mounded lobes could represent the filling in of formerly used ring-midden features with materials from adjacent ring middens.

Table 8. Shape Characteristics of Digitally Identified Ring Middens, by Study Area

Shape	Azotea Mesa		Box Canyon[a]		Upper Rio Felix[a]		Total[a]	
	No. of Features	Percentage of Study Area Features	No. of Features	Percentage of Study Area Features	No. of Features	Percentage of Study Area Features	No. of Features	Percentage of Total Features
Closed ring	83	31.9	47	29.0	35	31.3	165	30.9
Open ring	59	22.7	51	31.5	40	35.7	150	28.1
Irregular/discontinuous ring	88	33.8	43	26.5	18	16.1	149	27.9
Ring with mounded lobe	22	8.5	9	5.6	3	2.7	34	6.4
Atypical	8	3.1	12	7.4	16	14.3	36	6.7
Total ring middens	252	96.9	150	92.6	96	85.7	498	93.3
Total features	260	100.0	162	100.0	112	100.0	534	100.0

[a] Two features could not be assigned shape attributes, one in Box Canyon and one in Upper Rio Felix.

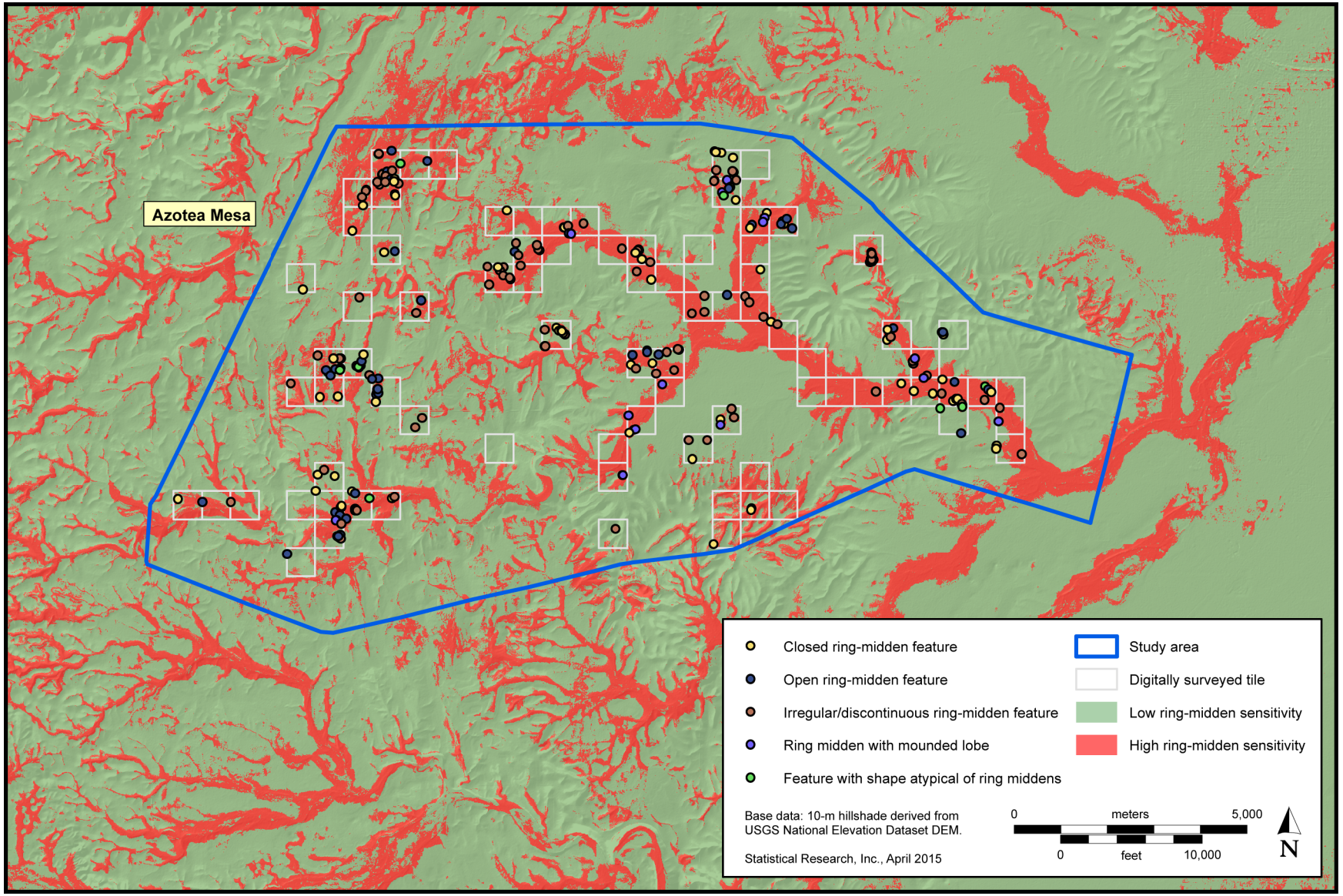

Figure 37. Map showing the results of digital survey in the Azotea Mesa study area, by feature shape.

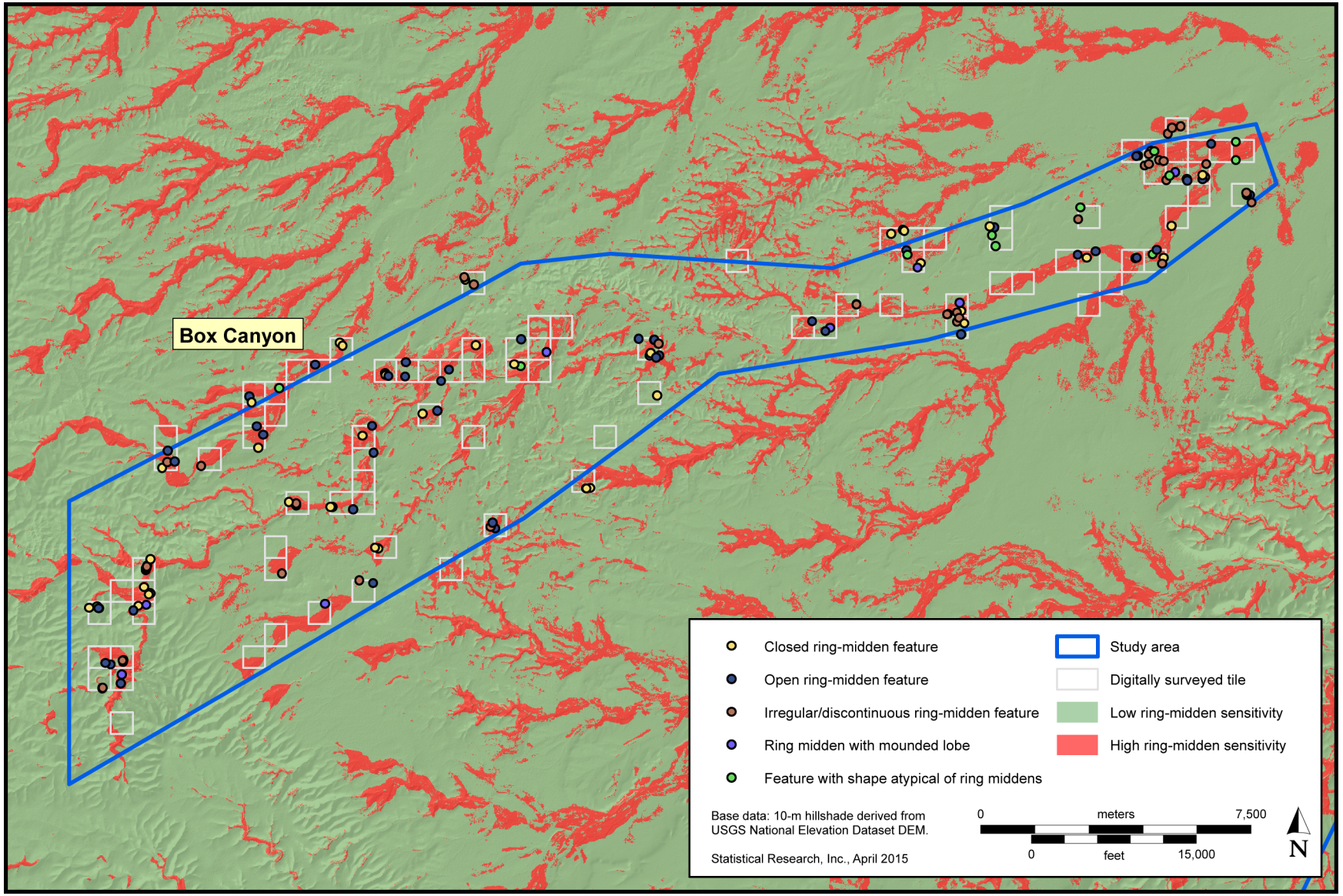

Figure 38. Map showing the results of digital survey in the Box Canyon study area, by feature shape.

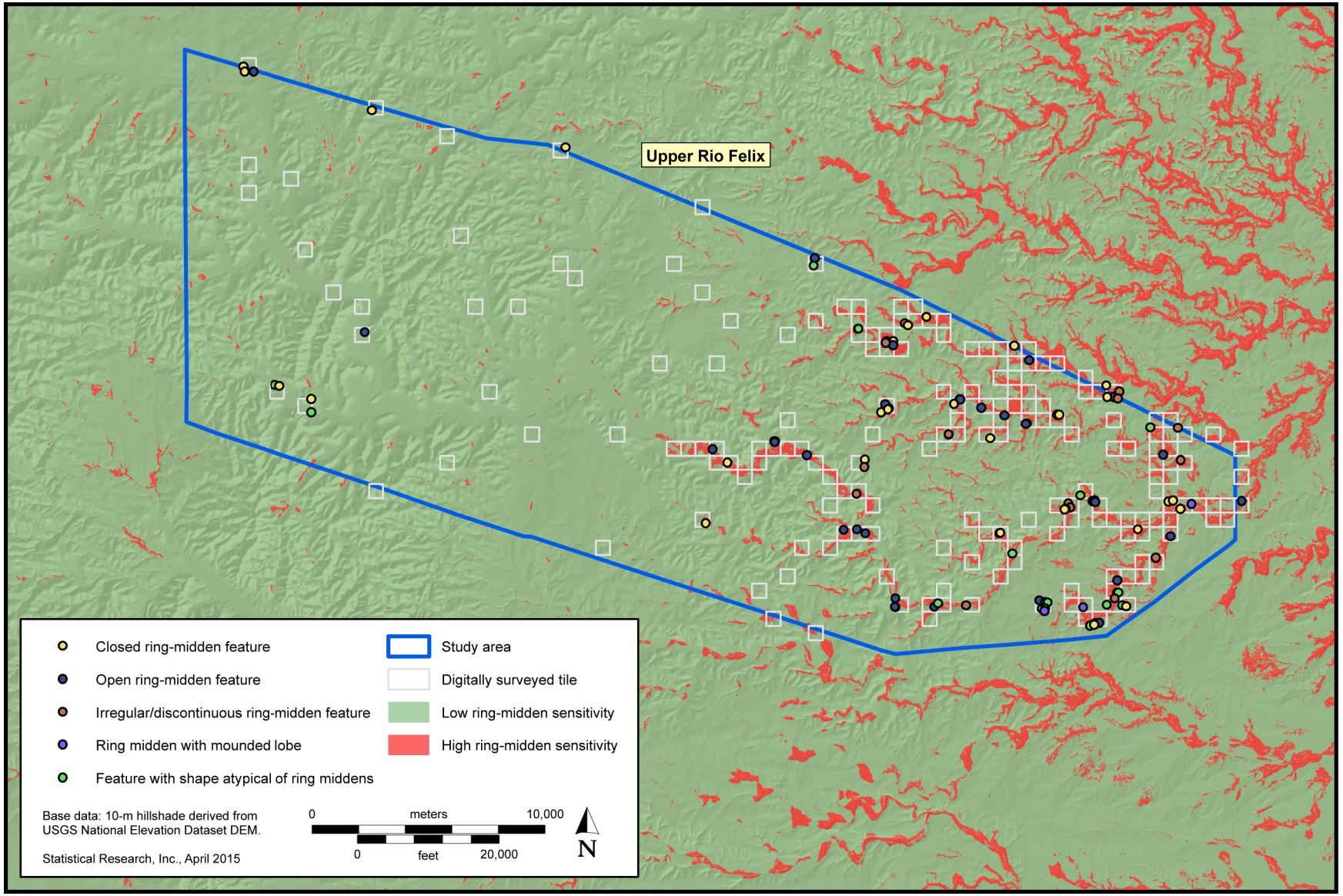

Figure 39. Map showing the results of digital survey in the Upper Rio Felix study area, by feature shape.

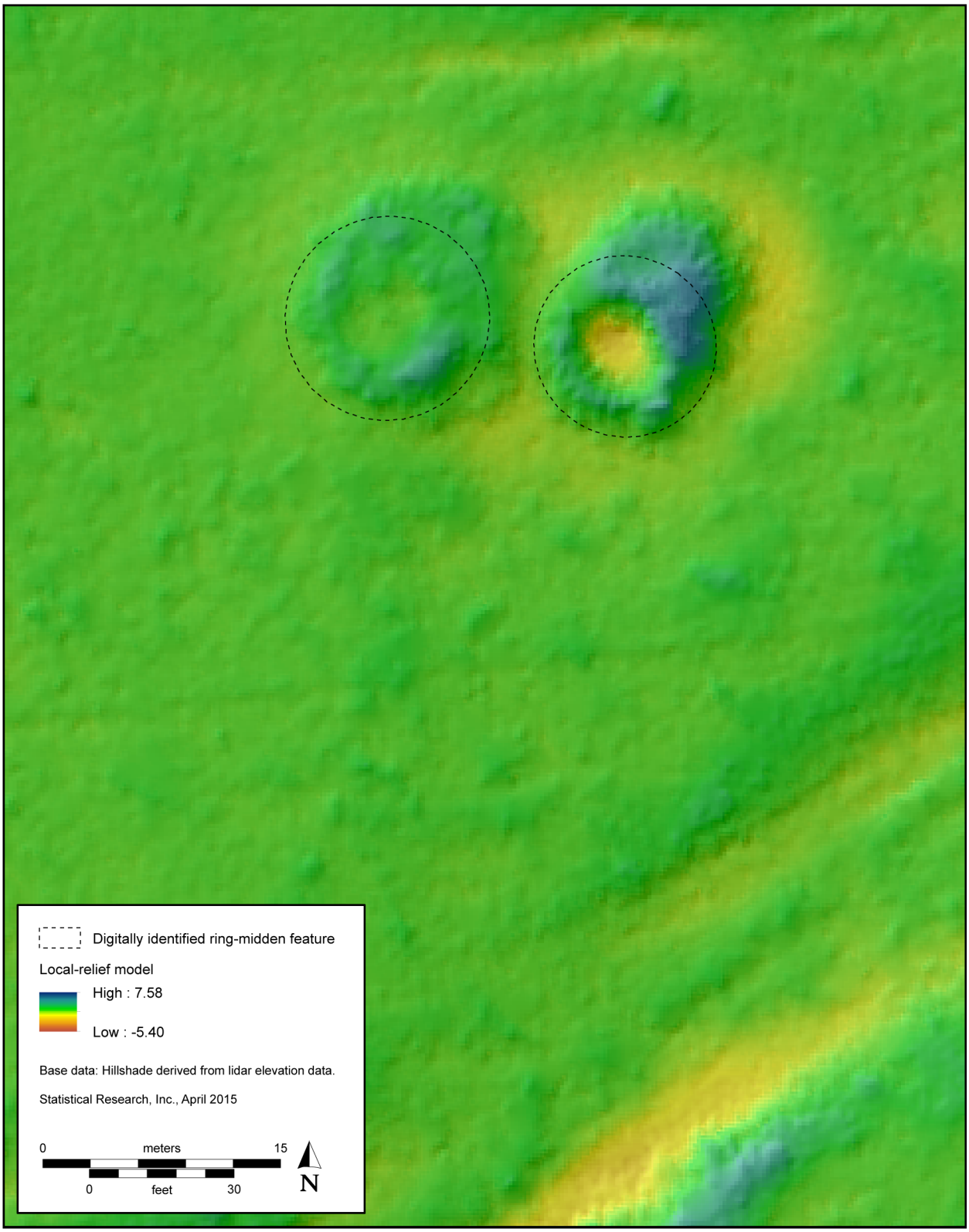

Figure 40. Map showing two features identified during digital survey in the Azotea Mesa study area (Tile 0401) as ring middens with mounded lobes.

How well a ring-midden shape is defined is likely related to how obtrusive and visible the feature is, but it may also relate to the frequency of use, disturbance processes, or cultural variation in discard patterns (Figures 41–43). For example, as an earth oven was used, more rocks were cleaned out with each use and added to the annular ring, leading to a more distinctive and well-defined surface feature. We attributed ring middens identified during digital survey as (1) well defined, (2) moderately well defined, (3) subtly defined, (4) faint but possible, and (5) not likely to be a ring midden but recorded for comparative purposes. Ring middens were most often well defined in the Azotea Mesa study area and were least often well defined in the Upper Rio Felix study area (Table 9). By comparison, ring middens were most often moderately well defined in the Upper Rio Felix study area and least often moderately well defined in the Azotea Mesa study area, although that pattern was not as pronounced as the pattern for well-defined ring middens. There was not a clear trend for subtly defined ring middens. Features identified as faint but possible ring middens are comparatively more common in the Azotea Mesa study area and least common in the Upper Rio Felix study area. Differences among study areas for the categories of *well defined* and *moderately well defined* conformed to our hypothesis that earth ovens were most intensively used in the Azotea Mesa study area and least intensively used in the Upper Rio Felix study area and/or were least affected by disturbance processes in the Azotea Mesa study area and most affected by disturbance processes in the Upper Rio Felix study area.

Ring-Midden High Side

Investigators have noted that ring middens tend to have one side that is higher than the opposing side, but the reasons behind that pattern are unclear. The high sides of the features were patterned across the three study areas (Table 10). In the Azotea Mesa study area, the high side tended to be located along the eastern side of the feature, but sometimes it was on the northwestern side. In the Box Canyon study area, the high side was most often on the southeastern side of the feature. In the Upper Rio Felix study area, the high side tended to be on either the southeastern or the northwestern side of the feature.

The aspects of the land surfaces on which ring middens were situated tended toward the east and southeast in all three study areas and ranged from northeast to southwest for most ring-midden locations (Figure 44). In general, these data suggest that the high side of a ring-midden feature tends to be on the downslope side of the feature. Perhaps more materials from earth ovens were raked or tossed downslope to create the annular ring than were distributed upslope. However, this does not explain why, in the Upper Rio Felix study area, a substantial number of ring-midden features have their high sides on the northwestern sides, when most of the land surfaces on which they are situated trend downward in the opposite direction. Disturbance processes could potentially explain the pattern in the Upper Rio Felix study area, if the downslope portions of the ring middens were more heavily affected by erosional or sedimentary processes.

Ring-Midden Elevation

Elevation is an environmental characteristic that appears to be related to earth-oven use. Comparison of ring-midden size with elevation further suggests that ring-midden size decreases as elevation increases (Figure 45). The relationship between elevation and earth-oven use may be the result of the effects of elevation on the abundance and availability of fuel, rock, and/or the food resources processed in earth ovens, or it could relate to disturbance processes that bury or remove portions of a feature, as discussed above.

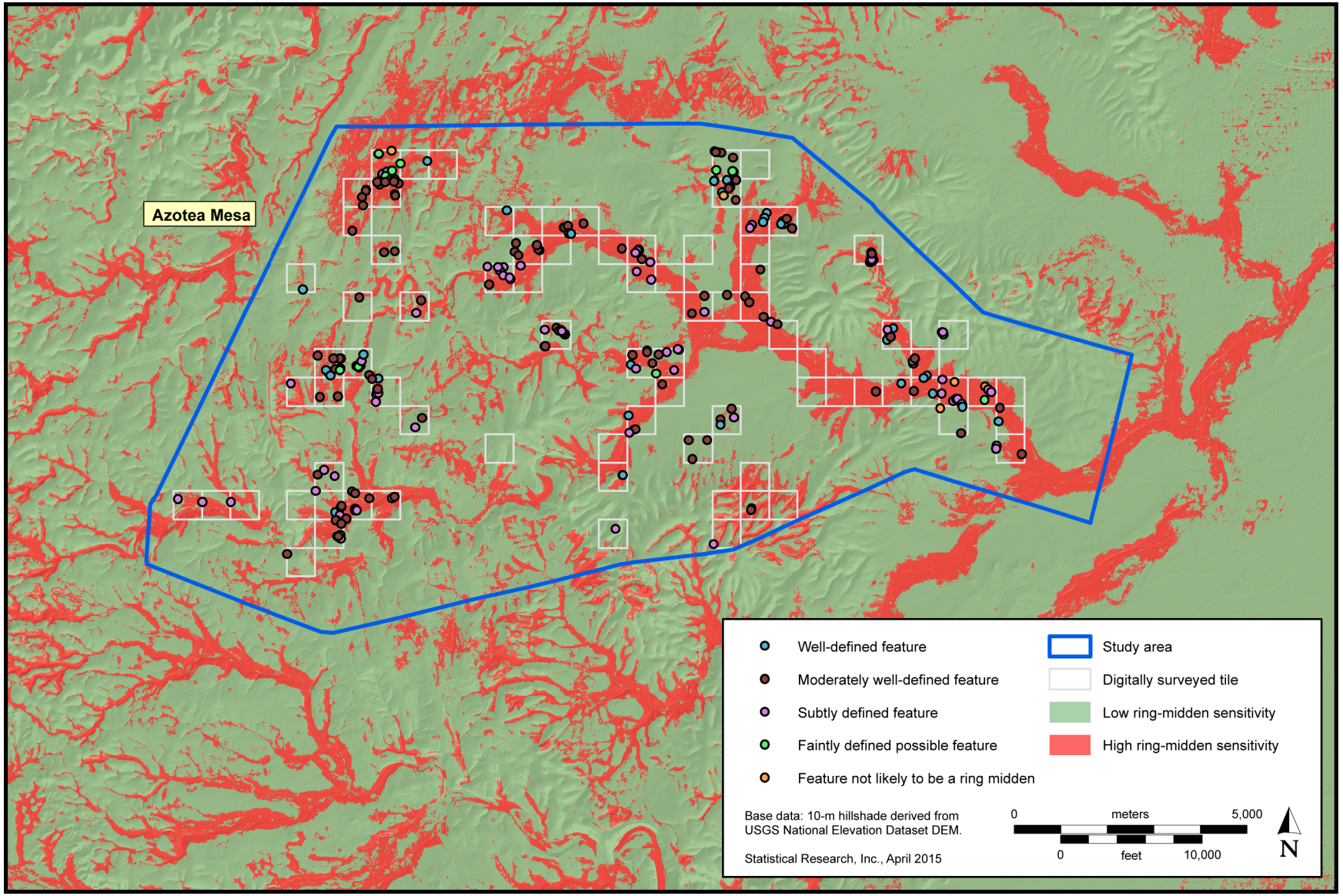

Figure 41. Map showing the results of digital survey in the Azotea Mesa study area, by feature definition.

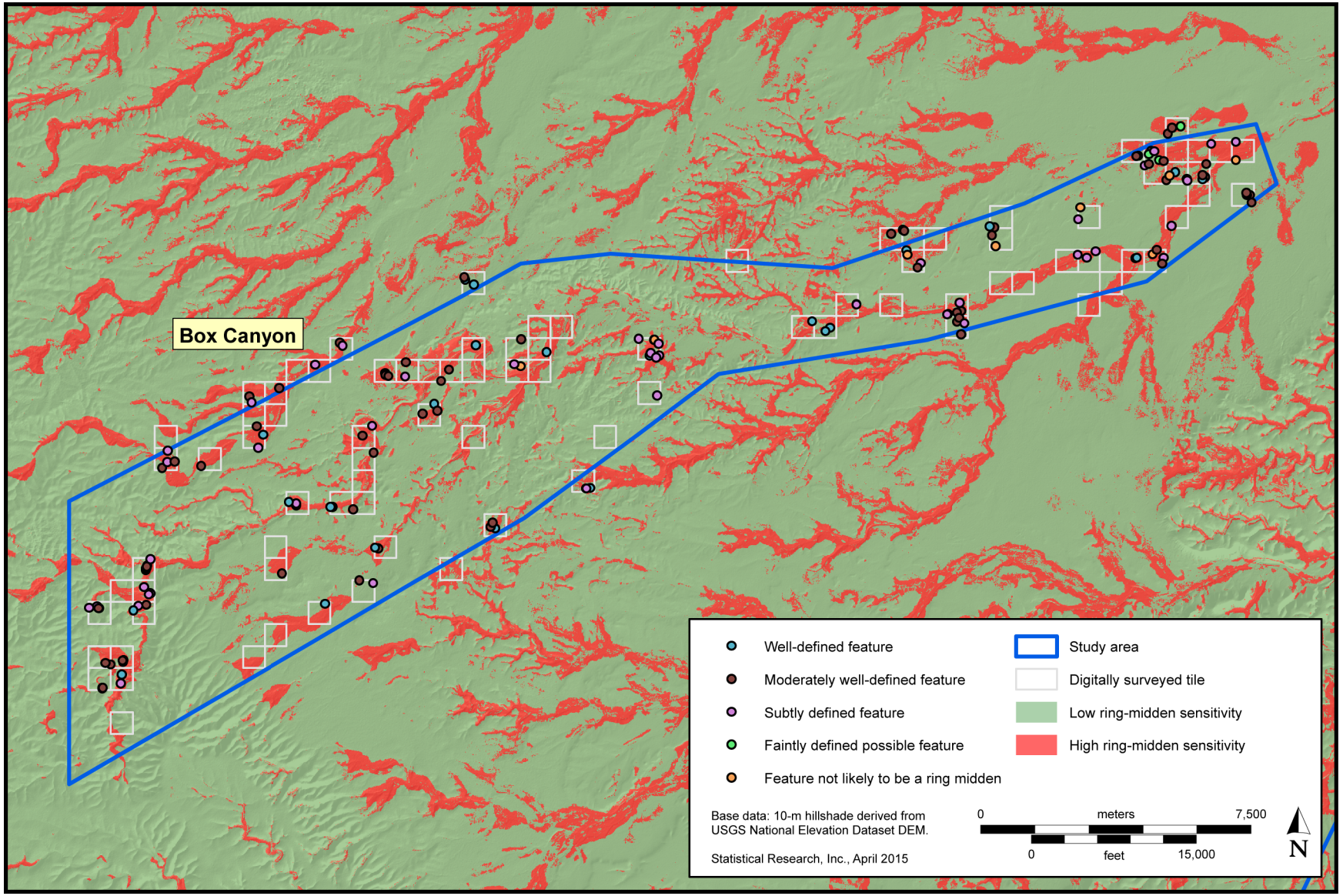

Figure 42. Map showing the results of digital survey in the Box Canyon study area, by feature definition.

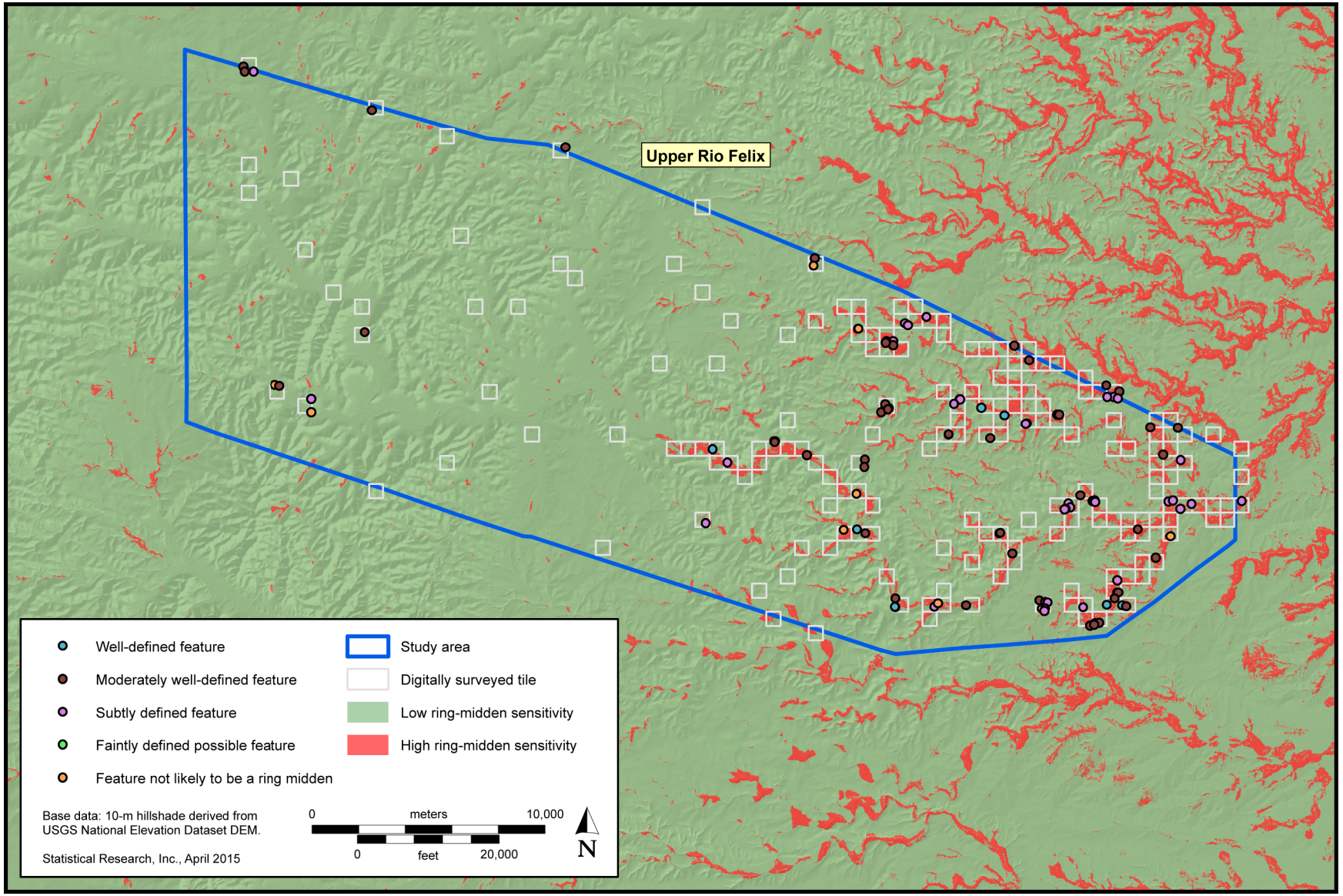

Figure 43. Map showing the results of digital survey in the Upper Rio Felix study area, by feature definition.

Table 9. Degrees of Feature Definition for Digitally Identified Ring Middens, as Observed in the Lidar Data, by Study Area

Degree of Definition	Azotea Mesa		Box Canyon		Upper Rio Felix		Total	
	No. of Features	Percentage of Study Area Features	No. of Features	Percentage of Study Area Features	No. of Features	Percentage of Study Area Features	No. of Features	Percentage of Total Features
Well defined	60	23.1	27	16.6	15	13.3	102	19.0
Moderately well defined	114	43.8	74	45.4	55	48.7	243	45.3
Subtle	68	26.2	48	29.4	31	27.4	147	27.4
Faint but possible	12	4.6	6	3.7	1	0.9	19	3.5
Not interpreted as a ring midden	6	2.3	8	4.9	11	9.7	25	4.7
Total ring middens	254	97.7	155	95.1	102	90.3	511	95.3
Total features	260	100.0	163	100.0	113	100.0	536	100.0

Table 10. Distribution of the High-Side Azimuths of Ring-Midden Features Identified during Digital Survey, by Study Area

Intercardinal Azimuth of Ring-Midden High Side	Azotea Mesa		Box Canyon		Upper Rio Felix		Total	
	No. of Ring Middens	Percentage of Study Area Ring Middens	No. of Ring Middens	Percentage of Study Area Ring Middens	No. of Ring Middens	Percentage of Study Area Ring Middens	No. of Ring Middens	Percentage of Total Ring Middens
North	21	8.3	15	10.0	5	5.2	41	8.2
Northeast	36	14.3	16	10.7	6	6.3	58	11.6
East	60	23.8	26	17.3	10	10.4	96	19.3
Southeast	38	15.1	40	26.7	22	22.9	100	20.1
South	15	6.0	10	6.7	7	7.3	32	6.4
Southwest	20	7.9	7	4.7	6	6.3	33	6.6
West	15	6.0	16	10.7	16	16.7	47	9.4
Northwest	47	18.7	20	13.3	24	25.0	91	18.3
Total	252	100.0	150	100.0	96	100.0	498	100.0

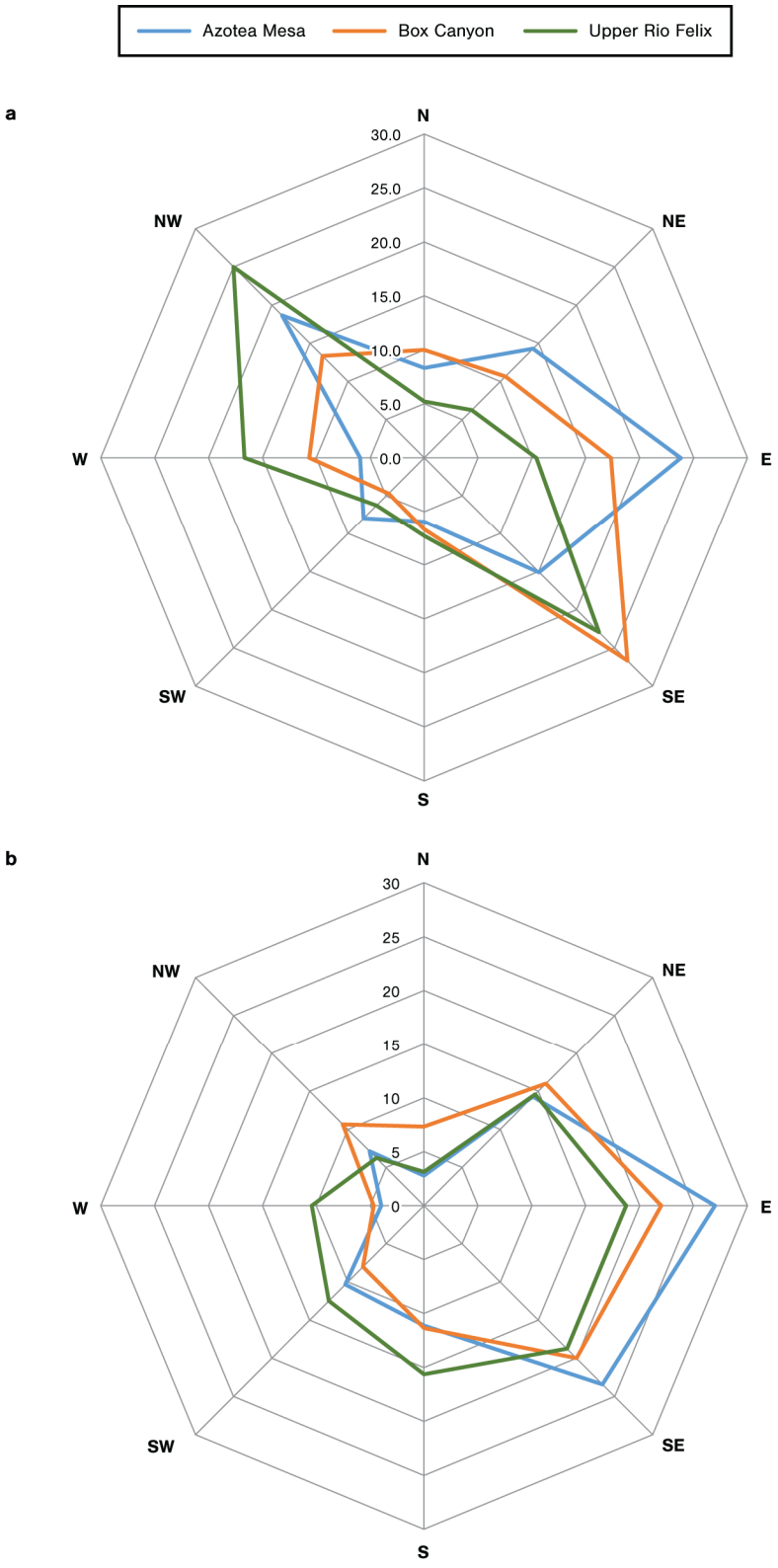

Figure 44. Comparison of (a) the azimuths of the high sides of digitally identified ring-midden features and (b) the aspects of the land surfaces on which digitally identified ring-midden features are located.

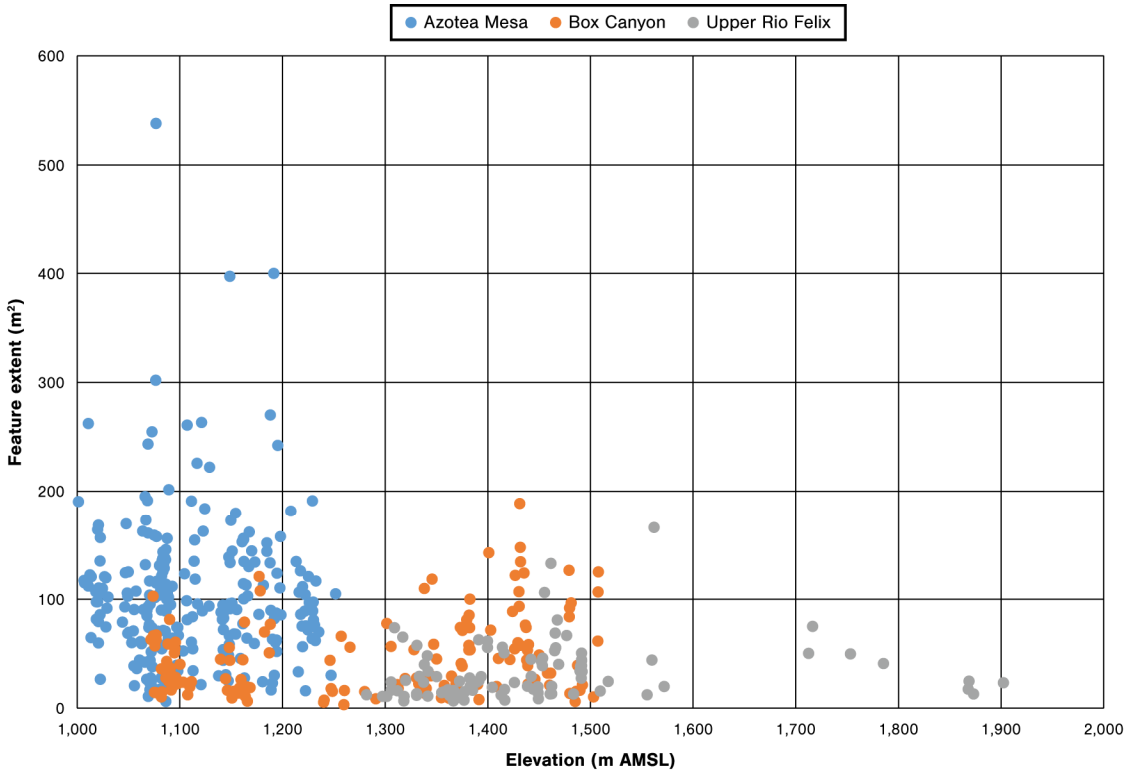

Figure 45. Relationships between ring-midden size (as calculated from digital-survey data) and elevation.

Clustering of Ring-Midden Features

Many of the potential ring-midden features identified during both the pilot study and the digital survey appeared to cluster in space (Figures 46 and 47). It is fairly common, in other words, for potential ring-midden features to be located within tens of meters of one or more similar features. This clustering suggests that people repeatedly revisited the same locations to process foods in earth ovens. It could also be the case that multiple earth ovens were used simultaneously, in some cases. To gain some insight into these issues, we performed nearest-neighbor hierarchical spatial clustering in CrimeStat 4.0 (Levine 2015), using a fixed distance of 100 m, to identify clusters of ring middens in close proximity to each other. We experimented with using fixed distances of 50 and 200 m, but a fixed distance of 50 m broke up clusters that we would consider to be relatively discrete into more than one cluster, and a fixed distance of 200 m tended to organize widely separated individual features into clusters. The fixed distance of 100 m was most successful in identifying clusters of features that we might consider to be associated with the same landform and place and within which any of the potential ring-midden features could be readily seen and accessed. The minimum number of features included in a cluster was two.

This exercise resulted in the identification of a total of 87 clusters of potential ring-midden features. Clusters, when defined in this way, consisted of anywhere from 2 to 11 ring-midden features. Roughly 50 percent of potential ring-midden features were located in clusters of 2 or more features each, and the remaining 50 percent of features could be considered isolated, though potentially clustering at broader scales. The majority of clusters consisted of just 2 potential ring-midden features each, and 93 percent of clusters contained 5 or fewer features each (Figure 48). Clustered ring-midden features were comparatively more common in the Azotea Mesa study area, where 59 percent of features were located within a

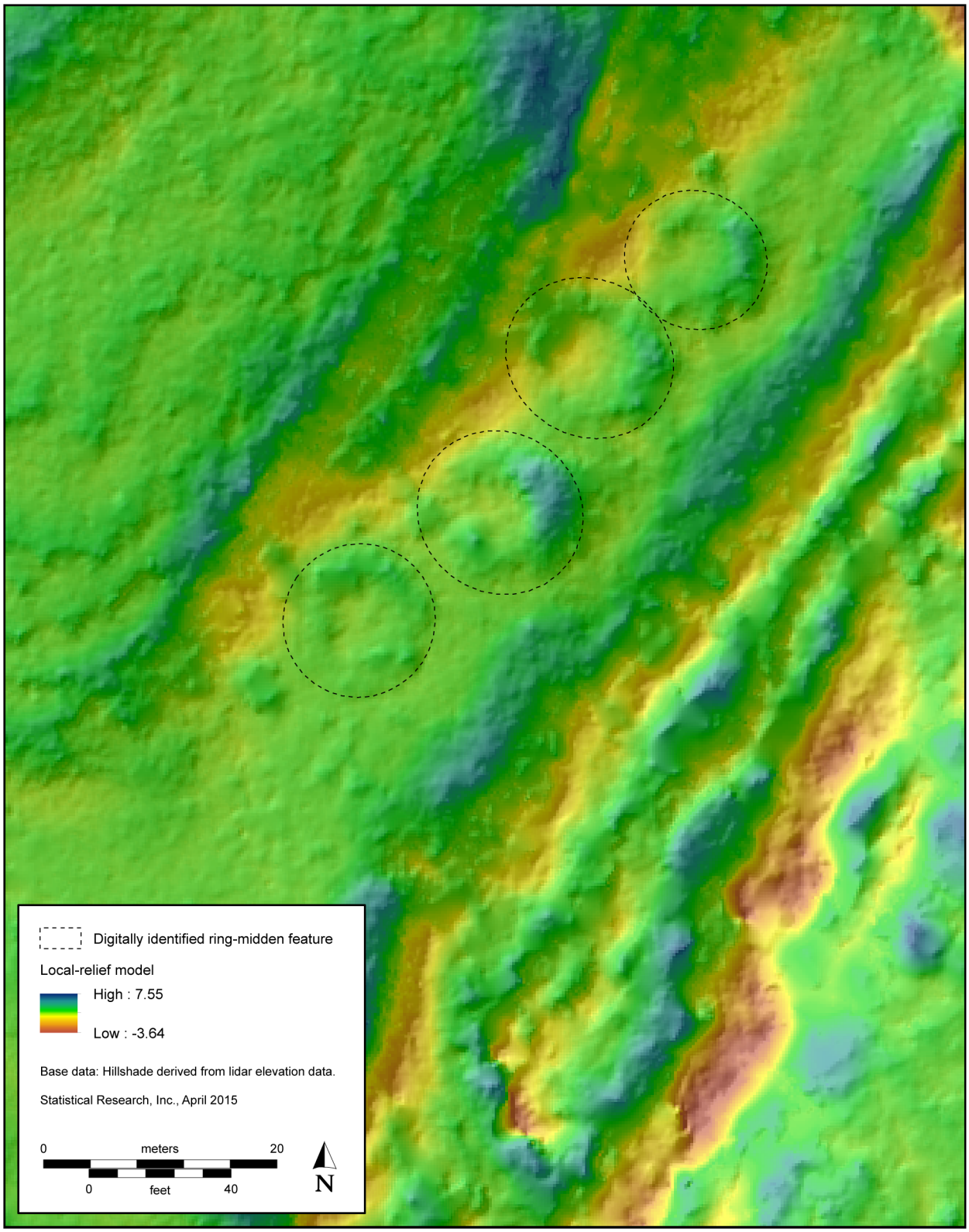

Figure 46. Map showing the linear cluster of four potential ring-midden features identified during digital survey as distributed along a narrow terrace in the Azotea Mesa study area (Tile 0370).

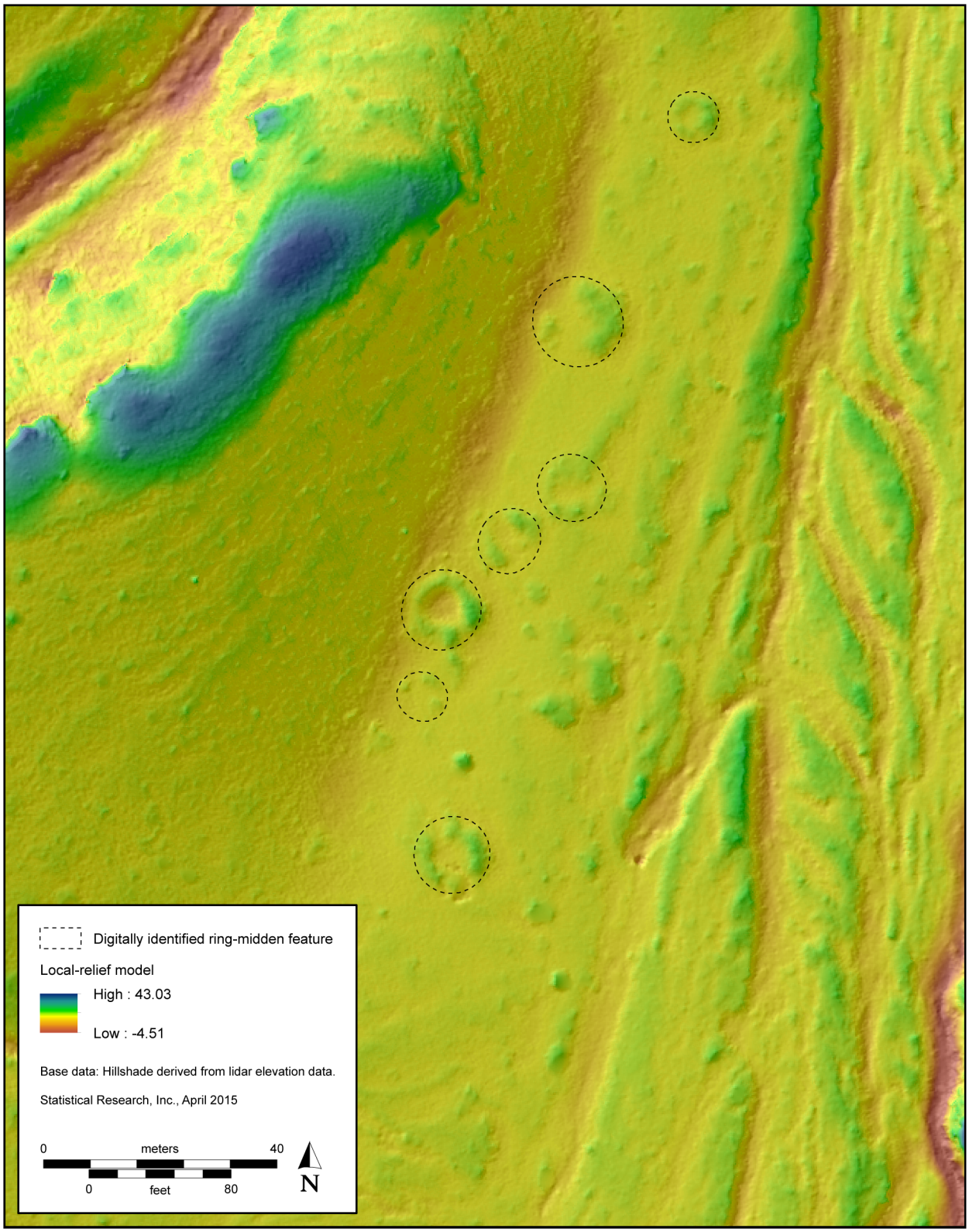

Figure 47. Map showing the linear cluster of four potential ring-midden features identified during digital survey as distributed along a narrow terrace in the Box Canyon study area (Tile 0425).

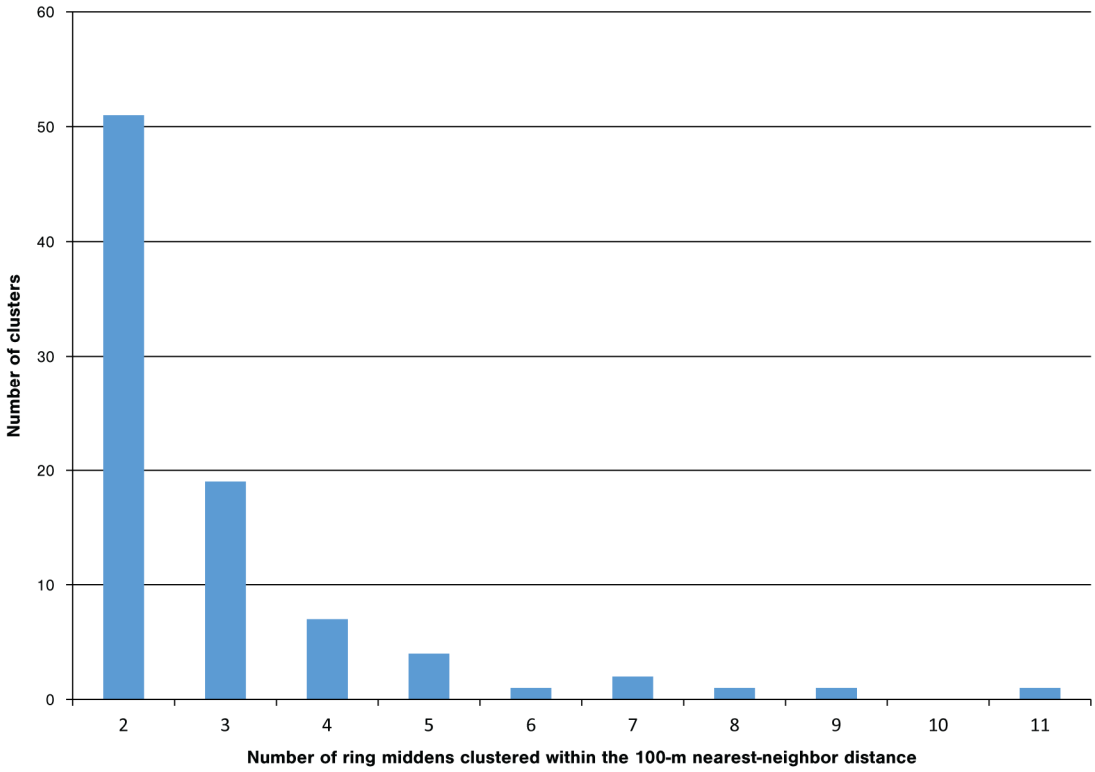

Figure 48. Frequency diagram showing the number of clusters of two or more ring-midden features identified during digital survey, based on nearest-neighbor hierarchical clustering analysis using a fixed distance of 100 m.

cluster of 2 or more features. By contrast, in both the Box Canyon and Upper Rio Felix study areas, approximately 41 percent of features were located within feature clusters. These data suggest that (1) ring-midden features in the study area are often located in proximity to each other, (2) ring middens in the study area commonly are present in clusters of 2–5 features but may also occur in clusters with larger numbers of features, (3) clusters are most common in the Azotea Mesa study area, and (4) on average, the largest clusters are located in the Azotea Mesa study area, and the smallest are located in the Upper Rio Felix study area. Because we probably cannot reliably detect ring middens with low profiles using the lidar data, it is likely the case that this analysis underestimates the degree of clustering and that some clusters of ring-midden features contain much larger numbers of features than have been documented here.

To further evaluate clustering in ring-midden features, we calculated average nearest-neighbor distances using only those features within clusters of two or more features, based on the results of the nearest-neighbor hierarchical clustering analysis, because if we used all the features to calculate nearest-neighbor distances, we would get results that included isolate features that could be separated by unsurveyed area, because we sample surveyed the study areas, and the resulting data did not cover the three study areas in their entirety. In other words, nearest-neighbor distances between isolated features could be inflated based on the digital-survey data, because those data include distances between features that could be separated by unsurveyed space (where intervening features may be located but were not documented). Moreover, such distances do little to advance our understanding of how closely ring-midden features tend to be situated where we see them as clustered. Nearest-neighbor distances were calculated using the Average Nearest Neighbor tool in ArcGIS 10.2.

Nearest-neighbor distances for clustered features were similar among the three study areas. Overall, ring-midden features within clusters tended to be located within an average of 39 m of the closest ring-midden feature. The z score, probability, and expected distances for each study area, and for all features

overall, suggest that ring-midden features were located much closer to each other than would be expected, although we are excluding isolated features from the analysis (because of the problems noted above), and expected distances were still affected by distances between survey tiles. In any case, these data indicate that when ring-midden features are clustered together on the same landform, they tend to be located within a fairly regular center-to-center distance of other ring-midden features. Possibly, that distance could correspond to the practical distance within which to situate ring middens, or some other component of fine-scale spatial behavior. Ring middens, of course, are sometimes situated more closely together than the average nearest-neighbor distance, such as in the cases of ring middens that nearly touch or intersect one another.

Intersecting Rings

Intersecting ring middens are sometimes considered to indicate the passage of time. As adjacent ring middens grow in size through repeated use of their associated earth ovens, the annular rings created as a result of clean-out of closely situated earth ovens may expand to the point that they intersect each other. Although it was relatively common for multiple ring middens identified during digital survey to cluster in proximity to each other, it was comparatively rare that any of these clusters of ring middens included intersecting features. Overall, ring middens that intersect were rare in the digital-survey data. To identify intersecting ring middens, we used an add-in tool available for ArcGIS 10, called Find Overlapping Features, which identifies cases in which polygons in an individual polygon layer intersect (http://www.arcgis.com/home/item.html?id=968e6a55a11640d2b9cfa211104d3811, accessed March 8, 2015).

We used this tool and a polygon layer representing digitally identified ring middens to isolate ring middens that intersected with each other. There were, in total, 10 intersections occurring in 8 different locations. In one case, a series of 4 ring middens arranged in a line intersected with each other. In all other cases, whether occurring as only 2 features or within a larger cluster of features, no more than 2 ring middens intersected. In a few cases, 2 intersecting ring middens were isolated and did not apparently occur in association with other ring middens, and in the remaining cases, intersecting ring middens occurred within larger clusters of ring middens. Only one of the cases of intersecting ring middens occurred within a recorded site. In all other cases, intersecting ring middens were not located inside the boundaries of previously recorded sites.

The majority of cases of intersecting ring middens occurred in the Azotea Mesa study area; two occurred in the Box Canyon study area, and only one occurred in the Upper Rio Felix study area. A variety of conditions appear to have resulted in intersecting ring middens. For the most part, they appear to occur in areas where they are tightly clustered and/or where the available space to place a ring midden is constrained (such as on a narrow terrace at the base of a steep hill). Many were located near drainages, often near confluences, and many were located at the eastern base of a hill or ridge. These appear to have been preferred settings for many of the ring middens discovered during digital survey, which might explain why most ring middens that intersect fulfill these locational characteristics: because they are among the more common locational settings for ring middens.

One such case of intersecting ring middens was in the Azotea Mesa study area, in Tile 022. There, a cluster of five potential ring middens was identified; four of these apparent middens intersect with each other along a line. Three of the intersecting ring middens are well defined, and a fourth is subtly defined and much less prominent in the lidar data. These features intersect to the extent that their annular rings are abutting and merging with the rings of adjacent features. The potential ring middens are all distributed in a linear fashion that follows the course of a nearby drainage.

Another case of intersecting features involved two features in Tile 070 in the Azotea Mesa study area, located at the southern end of LA 43440 (the “Richard Brown” site). These two rings are approximately 12 m north of a small drainage and are also located near the confluence of several drainage segments. Although both of the features have roughly similar horizontal extents, one of these rings (Feature 46) is better defined and has a much more pronounced and vertically prominent ring than the feature that intersects it (Feature 47), suggesting that Feature 46 was the more intensively used of the two. The most prominent and voluminous portions of both rings were noted where the two rings intersect, which could indicate that clean-out material from both ovens was deposited in that area. No other potential ring-midden features were

identified during digital survey in the immediate vicinity of these two intersecting rings, but a possible ring midden was located just outside the boundaries of LA 43440, approximately 90 m northeast of the two intersecting ring middens.

Another case of intersecting features involved two features within a larger cluster of at least nine features located on the southern side of a drainage and clustering around the eastern, southern, and northeastern sides of a small knoll. The two intersecting features (Features 82 and 85) were located on the southern edge of the cluster, at the base of the hill. One of the features (Feature 82) is considerably larger and better defined than the other feature. There appeared to be a small gap in the two rings in the area where they intersect, which could suggest simultaneous use of the associated earth ovens, should the gap represent pedestrian access between the two earth ovens during feature use.

Another case of intersecting features involved Features 226 and 227. No other ring middens were apparent in the vicinity. The two rings are both well defined, with prominent annular rings, and both were identified as having mounded lobes. The northernmost of the two rings has a large mound adjoining the northeastern side of the ring. The rings were located on an alluvial terrace at the eastern base of a ridge, approximately 28 m west of a drainage. On the opposite side of the drainage, approximately 130 m south of the two intersecting features, is a large, rectilinear feature measuring approximately 14 by 20 m. A large, circular feature with an approximately 11-m diameter abuts this rectilinear feature on its northern side. Although the feature has some characteristics that overlap with those of potential ring-midden features, it was not identified during digital survey as either a potential ring midden or a feature with overlapping characteristics that could be confused with those of a ring midden.

Another case of intersecting features is two features (Features 235 and 236) located within a linear cluster of four closely situated potential ring-midden features in Tile 0340 in the Azotea Mesa study area. Multiple other clusters of potential ring-midden features were identified in the general vicinity during digital survey. The cluster containing the two intersecting features was also located approximately 540 m northwest of a large site, LA 43442, named Sue's Shelter Caves. The features were located on a terrace or ledge above a drainage, on the southeastern side of a hill, near the confluence of two drainages. The two northernmost features in the cluster of four were close enough to each other that they appeared to minimally intersect, such that their annular rings were slightly merged. The location of these rings appeared to be within a confined space just large enough to fit the rings. The limited space likely accounted for the slight intersection of the two rings.

Feature Profiles

In order to understand more about the morphology of potential ring-midden features identified during digital sample survey, we selected from each of the three study areas a random sample of surveyed tiles that contained potential ring-midden features. Selecting the sample by survey tile allowed us to profile clusters of ring middens located in individual tiles as well as to obtain samples from a variety of different settings in the three study areas. Obtaining the profiles for features located within a random selection of survey tiles also allowed for more efficient data development, because multiple features could be profiled in quick succession using the same tile-based GIS layers, rather than requiring the analyst to locate individual features across the entire study area and load the GIS layers associated with the features in order to generate a profile.

The sample consisted of a total of 154 prospective features: 69 in the Azotea Mesa study area, 44 in the Box Canyon study area, and 41 in the Upper Rio Felix study area (Tables 11 and 12). This resulted in a sample percentage of 27 in both the Azotea Mesa and Box Canyon study areas. The sample percentage in the Upper Rio Felix study area was larger (36 percent), because that study area had a larger number of features that were not considered likely to be ring middens and were recorded only for comparative purposes. We wanted to include some of these non-ring-midden features but also capture a sufficient sample of features in the Upper Rio Felix study area that could more confidently be identified as ring-midden features. The larger sample percentage in the Upper Rio Felix study area was thus due to the inclusion of a comparatively large sample of non-ring-midden features from that study area.

Table 11. Distribution of the Random Sample of Digitally Identified Features Profiled, by Feature Definition and Study Area

Study Area	Well Defined		Moderately Well Defined		Faint but Possible		Indistinct		Likely Not a Ring Midden		Total	
	No. of Features Profiled	Percentage of Digital-Survey Sample	No. of Features Profiled	Percentage of Digital-Survey Sample	No. of Features Profiled	Percentage of Digital-Survey Sample	No. of Features Profiled	Percentage of Digital-Survey Sample	No. of Features Profiled	Percentage of Digital-Survey Sample	No. of Features Profiled	Percentage of Digital-Survey Sample
Azotea Mesa	12	20.0	34	29.8	19	27.9	1	8.3	3	50.0	69	26.5
Box Canyon	8	29.6	18	24.3	13	27.1	3	50.0	2	25.0	44	27.0
Upper Rio Felix	3	20.0	15	27.3	13	41.9	1	100.0	9	81.8	41	36.3
Total	23	22.5	67	27.6	45	30.6	5	26.3	14	56.0	154	28.7

Table 12. Distribution of the Random Sample of Digitally Identified Features Profiled, by Feature Shape and Study Area

Study Area	Closed Ring		Open Ring		Irregular, Discontinuous Ring		Ring with Mounded Lobe		Atypical Shape		Total	
	No. of Features Profiled	Percentage of Digital-Survey Sample	No. of Features Profiled	Percentage of Digital-Survey Sample	No. of Features Profiled	Percentage of Digital-Survey Sample	No. of Features Profiled	Percentage of Digital-Survey Sample	No. of Features Profiled	Percentage of Digital-Survey Sample	No. of Features Profiled	Percentage of Digital-Survey Sample
Azotea Mesa	30	36.1	10	16.9	21	23.9	5	22.7	3	37.5	69	26.5
Box Canyon	9	19.1	14	27.5	14	32.6	4	44.4	3	25.0	44	27.0
Upper Rio Felix	16	45.7	13	32.5	7	38.9	—	—	5	31.3	41	36.3
Total	55	33.3	37	24.7	42	28.2	9	26.5	11	30.6	154	28.7

When compared to the pilot sample described in Chapter 3 that was used to initially characterize potential ring-midden features observed in the lidar data, the spans of ring middens identified during the digital survey had a broader range, varying from 2.8 to 17.9 m across (compared to 5.6–15.0 m in the pilot sample) (Table 13). The average span for the profiled digital-survey sample (8.7 m), however, was smaller than that of the pilot sample (10.8 m). The coefficient of variation was also substantially larger in the profiled digital-survey sample than in the pilot sample. The difference was largely due to the fact that ring-midden size decreases as one goes from the Azotea Mesa study area to the Upper Rio Felix study area, and there is more metric variation across that cline than was evident in the pilot sample. By contrast, the profiled digital-survey sample from the Azotea Mesa study area had a very similar average span when compared to the pilot-survey sample, which makes sense, because the pilot sample consisted entirely of ring middens in the Azotea Mesa and Box Canyon study areas. Further, the profiled digital-survey sample showed that the average, median, minimum, and maximum spans of ring middens all decline from Azotea Mesa to Upper Rio Felix, which is consistent with the similar decline in feature area discussed above. Features interpreted to be something other than ring middens had some of the broadest spans but also could be quite small. There did not appear to be a clear relationship between ring-midden span and shape. However, well-defined and moderately well-defined ring middens tended to have a somewhat broader span than more subtly defined ring middens.

Average and maximum profile heights were calculated for profiled ring-midden features (Table 14). The average height of ring middens recorded during digital survey ranged from 2.6 to 42.0 cm, averaging 10.4 cm. The maximum height varied from 6.5 to 88.5 cm, averaging 24.2 cm. The average height of ring middens tended to be largest in the Azotea Mesa study area and smallest in the Upper Rio Felix study area, which is consistent with our hypothesis that earth ovens may have been most intensively used in the Azotea Mesa study area and least intensively used in the Upper Rio Felix study area. However, the maximum profile height tended to be greater in the Box Canyon study area than in the Azotea Mesa study area, though not by a large amount.

Table 13. Statistics on the Estimated Spans of Digitally Identified Features, as Calculated from Profile Data, by Study Area

Ring-Midden Statistic	Azotea Mesa	Box Canyon	Upper Rio Felix	Total	Comparative Features
Mean span (m)	10.83	7.26	6.15	8.69	10.44
Median span (m)	11.09	6.99	5.50	8.81	10.30
Standard deviation	2.70	2.65	2.43	3.33	5.40
Minimum span (m)	3.63	3.83	2.84	2.84	4.14
Maximum span (m)	17.92	13.50	12.90	17.92	20.70
Coefficient of variation	0.25	0.36	0.39	0.38	0.52
Total ring middens	66	42	32	140	14

Table 14. Statistics for the Estimated Heights of Digitally Identified Features, as Calculated from Profile Data, by Study Area

Feature Statistic	Azotea Mesa		Box Canyon		Upper Rio Felix		All Ring Middens		Non-Ring-Midden Features	
	Average	Maximum	Average	Maximum	Average	Maximum	Average	Maximum	Average	Maximum
Mean profile height (cm)	10.7	24.1	10.5	25.9	9.8	22.1	10.4	24.2	23.0	53.1
Median profile height (cm)	8.4	19.5	9.4	21.3	8.0	18.4	8.7	20.0	20.5	43.7
Standard deviation	7.6	16.1	6.0	15.4	6.3	14.1	6.8	15.4	13.8	36.7
Minimum profile height (cm)	3.3	6.6	2.9	6.9	2.6	6.5	2.6	6.5	7.9	12.5
Maximum profile height (cm)	42.0	88.4	29.6	67.3	28.5	61.3	42.0	88.4	58.9	149.1
Total features	66	66	42	42	32	32	140	140	14	14

Feature size, average profile height, maximum profile height, span, and estimated above ground feature volume all decrease with elevation. For each of these variables, small ring middens are present across elevations, but the range and maximum values all decrease as elevation increases. A possible reason for this is that earth-oven use was less intensive at higher elevations. This does not necessarily mean that fewer resources were acquired or processed at higher elevations but, more likely, that the fuel-saving characteristics of earth ovens was less important with increases in elevation, because of a greater availability of fuelwood at higher elevations. Another explanation, which is not exclusive of the fuel-availability hypothesis, is that resources were more often processed repeatedly in earth ovens that were located closer to residential bases at lower elevations, and more-distant earth ovens in higher-elevation settings were used less often. Similarly, these same measures indicative of earth-oven use decrease as distance to streams increases, particularly average height and maximum profile height, suggesting that earth-oven use was more intensive close to streams and less intensive farther away from streams. This suggests that plants growing along streams were likely important as fuel and perhaps also that the availability of water was important to earth-oven use (e.g., for use in steaming earth-oven contents). Rock suitable for use as heating elements may also be concentrated in streams and may be particularly concentrated at drainage confluences.

Field-Verification Approach

As Gallagher and Joseph (2008:204) observed, "LiDAR is by no means a stand-alone method of data-gathering that can independently distinguish natural from cultural features. Interpretations made from LiDAR data need to be verified in the field." Thus, this project included a field-verification component, albeit one that could only field check a small sample of features.

Ground-truthing efforts focused on recording clusters of ring middens with different attributes, so that a maximal number of ring middens with different characteristics could be observed and recorded during the allotted field time (Figures 49–53). SRI visited undocumented clusters of ring-midden features in the Box Canyon and Upper Rio Felix study areas and a previously recorded site in the Azotea Mesa study area (LA 130591) where a large number of ring-midden features had been noted. The two clusters in the Upper Rio Felix and Box Canyon study areas were newly recorded during the ground-truthing efforts as LA 181701 and LA 181702, respectively; LA 130591 was updated (see Appendix D).

During the ground-truthing efforts, we had hoped to also visit two unusual features that were identified during digital survey as ring middens with mounded lobes. Each of these was identified during digital survey as a well-defined ring with a large mounded area extending several meters beyond the outer edge of the ring. Some evidence from the lidar data suggests that these mounded lobes may in some cases consist primarily of mounded rock or bare sediment. In total, 33 such features were identified during digital survey, the majority of them in either the Azotea Mesa or Box Canyon study area. Unfortunately, roads that could be used to access the two features of this type that we had selected to visit were impassable. Despite multiple attempts to access these features, we were unable to observe an example of these unusual features on the ground, to gain a better understanding of feature characteristics.

Fieldwork was conducted on April 21–25, 2015, and ground-truthing efforts equaled, in total, 8 10-hour person days. Attributes recorded for each of the investigated features included feature type; metric dimensions (length, width, and height); whether a central depression was present; the abundance, size, and dominant lithology of associated FCR; types of vegetation that grow in and around the feature; soil characteristics inside and outside the feature (texture and Munsell color); and documentation of any apparent stockpiles of rock adjacent to the feature. Photographic documentation of the features included both profiles and overhead plan views.

Field conditions at each of the sites ranged from minimum to dense vegetation cover, and ground visibility was most obscured by a thick cover of spring annuals and forbs within the newly documented LA 181701, in the Upper Rio Felix study area. Also, periodic inundation had resulted in the partial burial of most of the features in silt, as well as the dispersal of many of the ring-midden features ground-truthed within the Upper Rio Felix study area. Ring middens visited at LA 130591, in the Azotea Mesa study area,

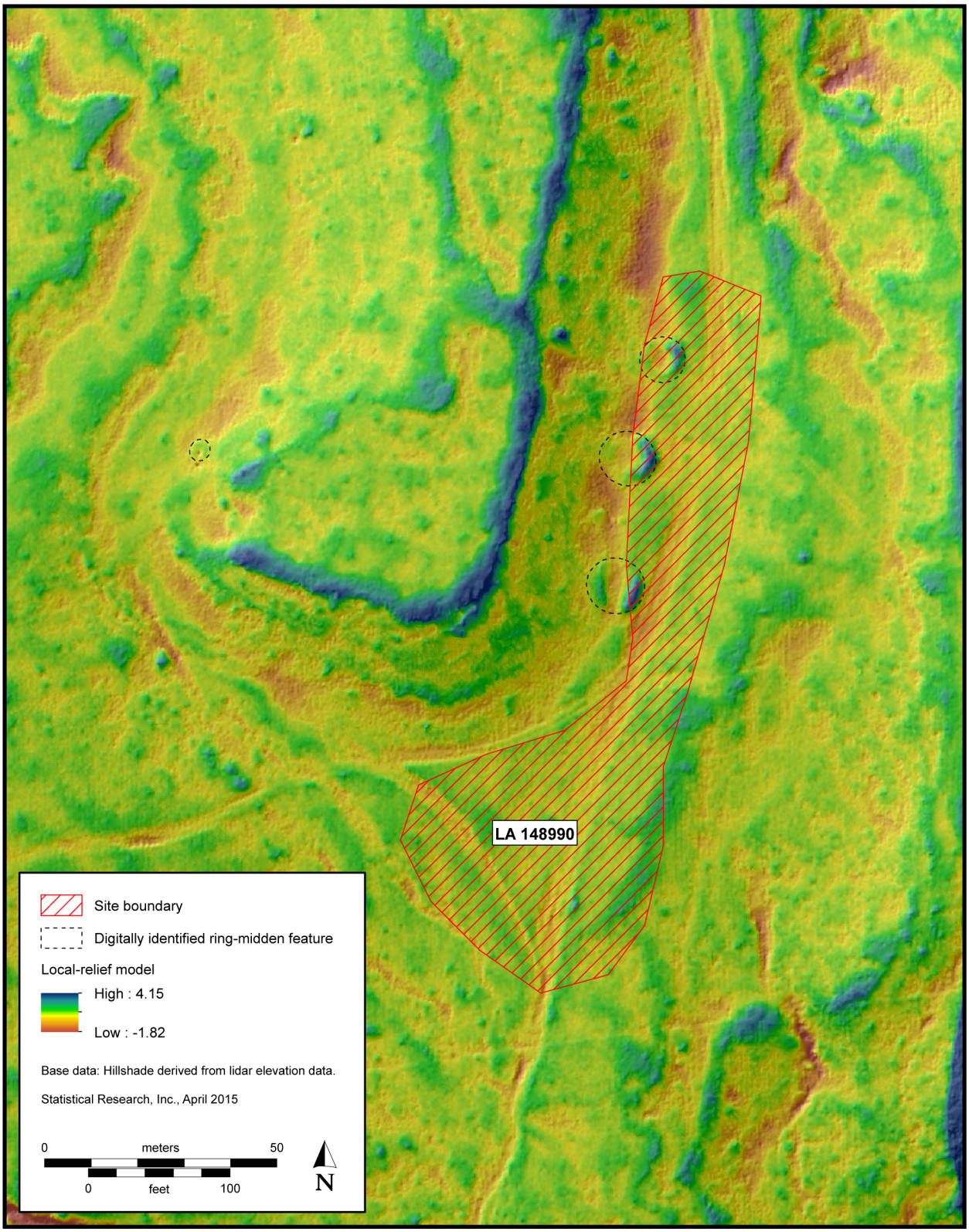

Figure 49. Map showing the locations of the four features identified during digital survey in the Azotea Mesa study area (Tile 0198) that were selected for field verification.

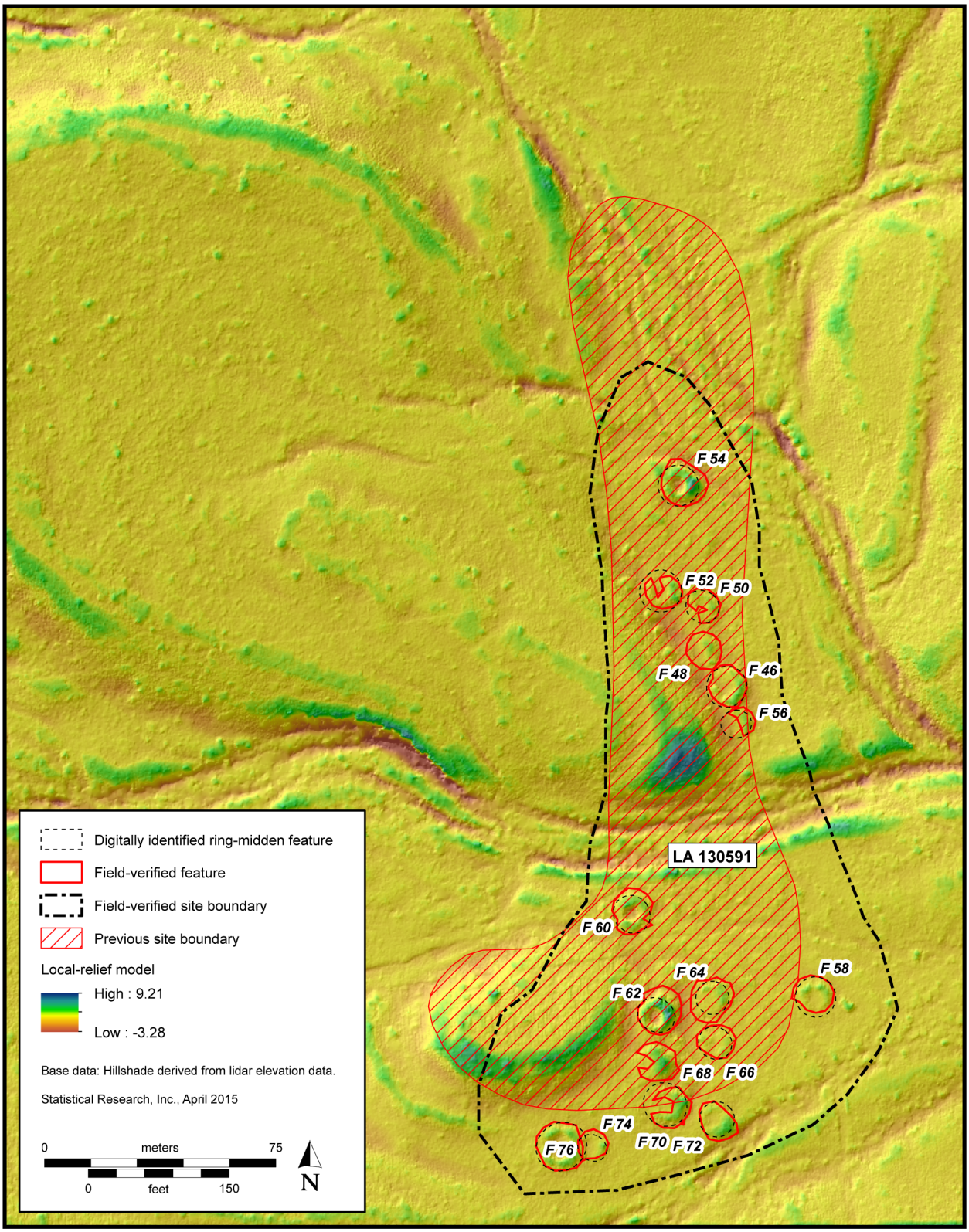

Figure 50. Map showing the locations of the 14 features identified during digital survey in the Azotea Mesa study area (Tile 0104) that were selected for field verification.

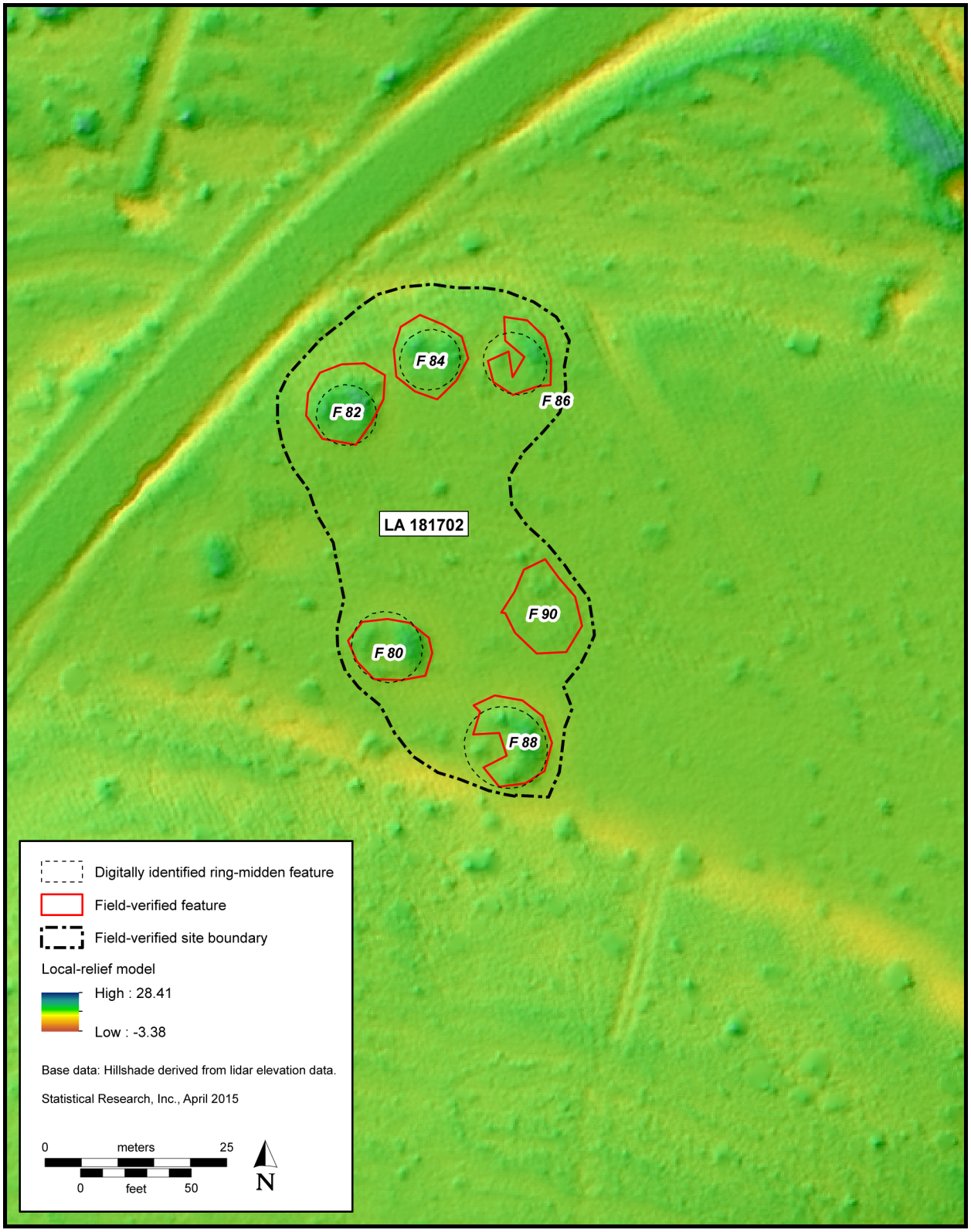

Figure 51. Map showing the locations of the five features identified during digital survey in the Box Canyon study area (Tile 0368) that were selected for field verification, along with the locations of all features documented during field verification.

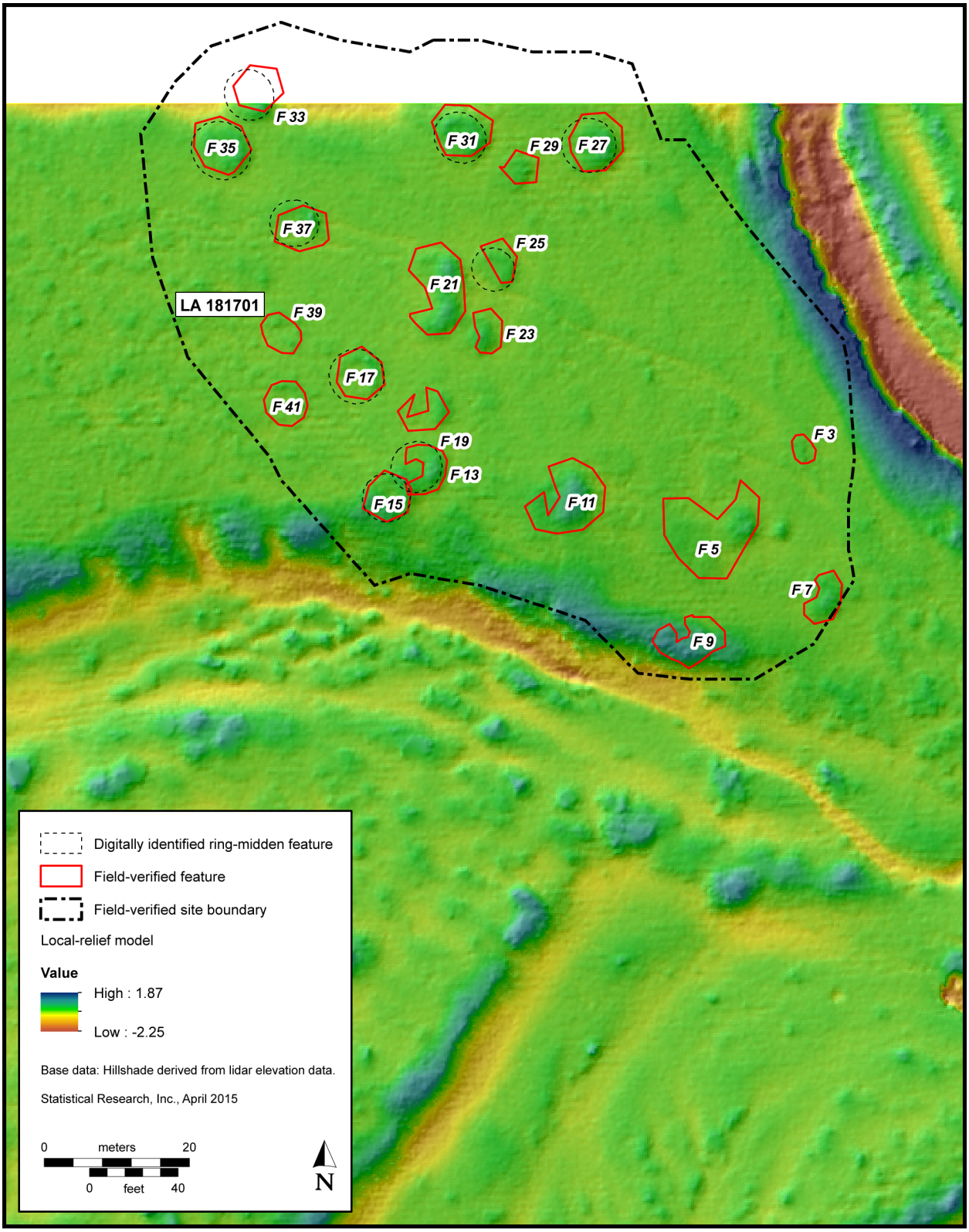

Figure 52. Map showing the locations of nine of the features identified during digital survey in the Upper Rio Felix study area (Tile 1199) that were selected for field verification, along with the locations of all features documented during field verification.

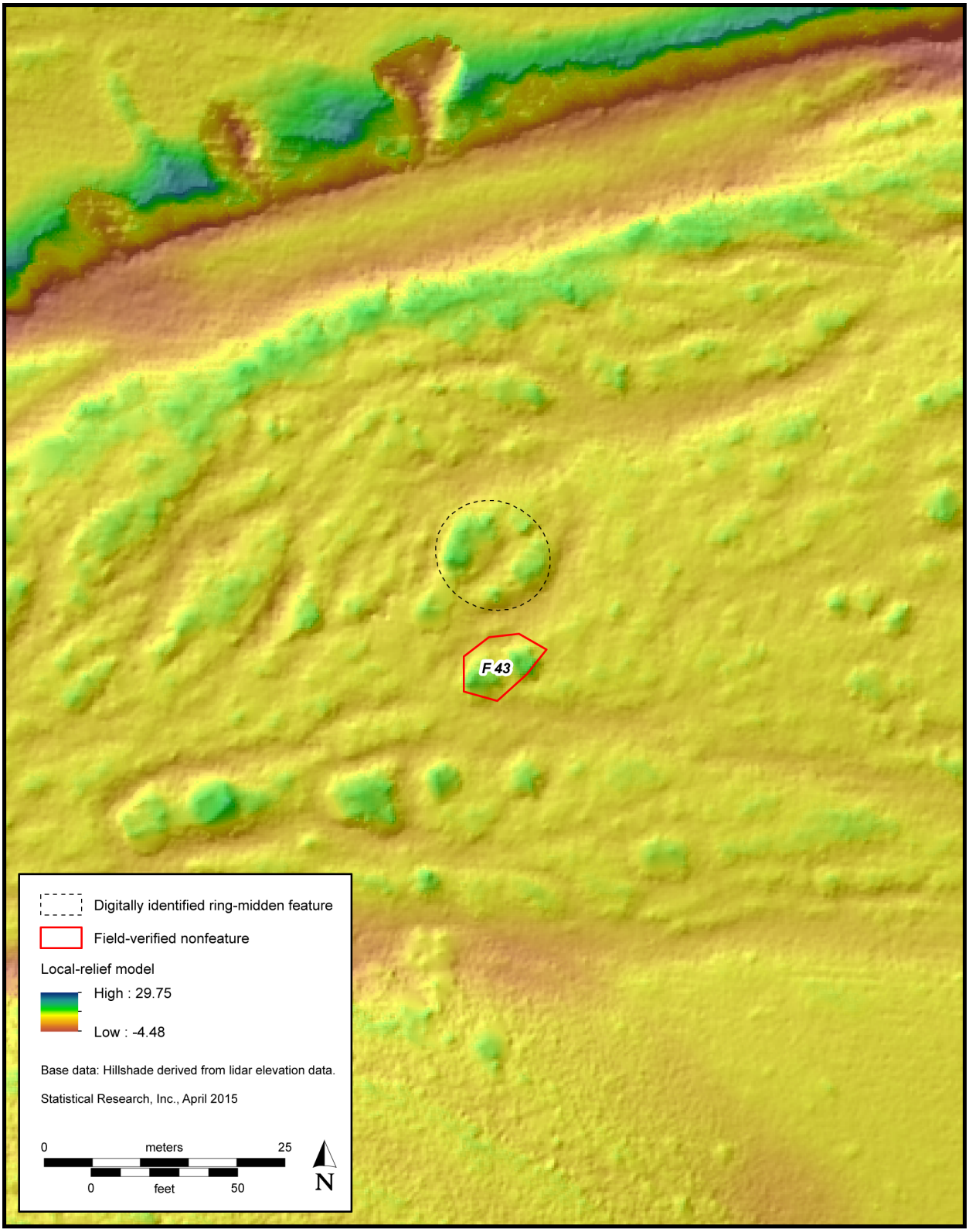

Figure 53. Map showing the location of one of the features identified during digital survey in the Upper Rio Felix study area (Tile 1400) that was selected for field verification.

were the best preserved and did not exhibit any appreciable evidence of modern disturbances. Most of the features investigated within the Box Canyon study area at LA 181702 were intact; however, one of the newly recorded features was located within a modern two-track that bisects the site. Additionally, there was evidence that the site area had been used for modern camping activities, based on the presence of glass bottles and a recently used campfire ring.

In total, 43 features were recorded during the fieldwork efforts (Table 15). All of the features identified during the lidar survey were verified as ring middens, with the exception of a single natural feature with morphological characteristics that could be confused with those of a ring midden. This feature was recorded during the digital survey only for comparative purposes. When examined in the field, the anomaly was shown to consist of a large clump of vegetation deposited along the Rio Felix floodplain.

Fourteen of the features recorded during the fieldwork had not been originally identified during the lidar digital survey. Most of them were at the newly recorded LA 181701, in the Upper Rio Felix study area. The 11 new features found within the Upper Rio Felix study area were comparatively much smaller (6 m or less) in size and less obtrusive in height than the adjacent lidar-identified features. Moreover, 3 of these features could only be described as FCR middens and lacked the morphological and structural characteristics of ring-midden features. All of the newly recorded features in this area had been moderately to highly disturbed by floodplain erosion/deposition that had resulted in displacement and partial burial of the features within alluvium. Similarly, the newly identified feature at LA 181702, in the Box Canyon study area, was located entirely within a roadbed and had been almost completely flattened, leaving behind only a minimally perceptible, circular distribution of FCR on the ground surface. The 2 features at LA 130591 that had not been identified during the digital survey did not include completely enclosed circular rings but, rather, raised berms that were only slightly detectable in plan view.

Overall, the field-verification efforts indicated that the lidar survey was highly successful in identifying ring-midden features but failed to detect features of very low relief and/or heavily disturbed features. With the exception of one isolated feature visited for comparative purposes that was revealed not to be a feature, all of the lidar-identified ring-midden features visited during ground-truthing were verified as ring-midden features. Remarkably, the feature locations and extents as recorded during the field-verification efforts were quite similar to those recorded for the same features during digital survey. However, the heights, as estimated using 3-D profile data, had been consistently underestimated, suggesting that ring-midden vertical dimensions tended to be larger than we had estimated using the lidar data.

The field-verification efforts suggested that the failure to detect ring-midden features during digital survey could be attributed to a small number of factors. As discussed above, features that went unrecognized in the lidar data had been mostly disturbed and lacked the relief necessary to be detected confidently using lidar data. This suggests that ring-midden densities were likely underestimated as a result of the digital survey, particularly in the Upper Rio Felix study area, where disturbance processes appear to have had a pronounced effect on the obtrusiveness and visibility of ring-midden features observed using the lidar data.

Admittedly, the sample of ring middens visited in the field was comparatively small (only 5.7 percent of digitally identified ring-midden features). It is likely that some of the potential ring-midden features identified during digital survey are not, in fact, ring-midden features, but we have no way of documenting that without further field checks. The field-verification efforts suggested that many of the potential ring-midden features identified during digital survey will turn out to be ring middens when field checked, but it is also likely that at least some of the digitally identified features will turn out to be features of other types or, in a few cases, not features at all.

Table 15. Attributes Recorded for the Sample of Features Identified during Digital Survey That Were Ground-Truthed, by Study Area

LA Site No.	Field Site No.	PD No.	Digital-Survey Feature No.	Ring Midden?	Central Depression?	Length (m)	Width (m)	Height (cm)	Average Length of FCR (cm)	Sediment Texture	Munsell Color
					Azotea Mesa Study Area						
130591	SRI-44	46	79	yes	yes	13.00	14.0	60	6.3	silty fine sand	5YR 4/1
130591	SRI-44	48		yes	yes	11.00	9.0	20	6.0	silty fine sand	5YR 4/3
130591	SRI-44	50	90	yes	yes	7.00	8.0	20	5.3	silty fine sand	5YR 4/3
130591	SRI-44	52	78	yes	yes	10.00	10.4	30	6.0	silty fine sand	5YR 4/3
130591	SRI-44	54	77	yes	yes	12.00	12.3	200	6.3	ashy silt loam	10YR 1/3
130591	SRI-44	56	80	yes	yes	9.50	8.5	15	5.0	silty fine sand	5YR 4/3
130591	SRI-44	58	87	yes	yes	10.00	10.5	30	5.6	silty fine sand	5YR 4/1
130591	SRI-44	60	84	yes	yes	11.00	11.0	100	6.0	silty fine sand	7.5YR 4/1
130591	SRI-44	62	81	yes	yes	12.00	12.6	200	5.3	silty fine sand	7.5YR 4/1
130591	SRI-44	64	89	yes	no	9.00	11.0	20	5.6	silty fine sand	5YR 4/3
130591	SRI-44	66	88	yes	no	9.50	10.5	5	5.6	silty fine sand	5YR 6/3
130591	SRI-44	68		yes	no	9.50	8.5	100	6.3	silty fine sand	5YR 4/3
130591	SRI-44	70	83	yes	no	9.00	10.0	5	6.0	silty fine sand	5YR 4/3
130591	SRI-44	72	86	yes	yes	11.00	11.0	20	5.1	silty fine sand	5YR 4/3
130591	SRI-44	74	85	yes	yes	9.00	9.0	10	7.0	silty fine sand	5YR 4/3
130591	SRI-44	76	82	yes	yes	14.00	14.0	70	6.0	silty fine sand	5YR 4/3
					Box Canyon Study Area						
181702	SRI-78	80	370	yes	yes	9.30	9.6	95	7.3	fine sandy loam	5YR 6/3
181702	SRI-78	82	371	yes	yes	10.50	11.5	70	6.3	fine sandy loam	5YR 6/3
181702	SRI-78	84	373	yes	yes	9.00	9.0	35	6.3	ashy fine sandy loam	5YR 4/2
181702	SRI-78	86	372	yes	yes	7.90	7.5	45	8.0	fine sandy loam	5YR 4/3
181702	SRI-78	88	369	yes	yes	10.00	10.0	95	7.6	ashy fine sandy loam	5YR 4/4
181702	SRI-78	90		yes	no	9.30	9.5	10	4.6	fine sandy loam	5YR 4/4
					Upper Rio Felix Study Area						
181701	SRI-1	3		no	no	2.80	3.5	20	6.6	silt loam	5YR 4/3

LA Site No.	Field Site No.	PD No.	Digital-Survey Feature No.	Ring Midden?	Central Depression?	Length (m)	Width (m)	Height (cm)	Average Length of FCR (cm)	Sediment Texture	Munsell Color
181701	SRI-1	5		yes	no	12.50	8.0	40	7.6	silt loam	5YR 4/3
181701	SRI-1	7		yes	yes	6.75	5.5	30	8.6	silt loam	5YR 4/3
181701	SRI-1	9		yes	no	6.00	9.5	20	6.0	silt loam	5YR 4/3
181701	SRI-1	11		yes	yes	8.50	9.5	35	6.6	silt loam	5YR 4/3
181701	SRI-1	13	479	yes	yes	7.00	7.0	30	7.0	silt loam	5YR 4/3
181701	SRI-1	15	474	yes	yes	7.50	7.0	20	7.0	silt loam	5YR 4/3
181701	SRI-1	17	473	yes	yes	6.00	6.5	10	6.0	silt loam	5YR 4/3
181701	SRI-1	19		yes	yes	6.00	5.5	15	7.3	silt loam	5YR 4/3
181701	SRI-1	21		yes	yes	9.00	12.0	35	6.6	ashy silt loam	7.5YR 4/1
181701	SRI-1	23		yes	no	7.00	5.0	15	6.6	silt loam	5YR 4/3
181701	SRI-1	25	475	yes	yes	6.00	6.0	10	6.0	silt loam	5YR 4/3
181701	SRI-1	27	476	yes	no	6.90	6.9	10	6.3	silt loam	5YR 4/3
181701	SRI-1	29		no	no	5.00	5.0	20	8.0	silt loam	5YR 4/3
181701	SRI-1	31	472	yes	yes	9.50	8.0	40	8.0	silt loam	5YR 4/3
181701	SRI-1	33	478	yes	no	7.50	8.0	45	8.0	silt loam	5YR 4/3
181701	SRI-1	35	471	yes	yes	6.80	8.6	30	6.0	silt loam	5YR 4/3
181701	SRI-1	37	477	yes	yes	5.40	7.0	30	8.0	silt loam	5YR 4/3
181701	SRI-1	39		yes	yes	6.00	6.6	15	6.6	silt loam	5YR 4/3
181701	SRI-1	41		yes	yes	6.50	7.0	30	5.3	silt loam	5YR 4/3
Isolate		43	487	no	no	6.50	8.0	200			

Model Testing

To test the locational model of ring-midden sensitivity, we calculated the number of digitally identified ring middens that fell within the low-sensitivity zone of the model and the number of digitally identified ring middens that fell within the high-sensitivity zone. Calculation of the Gain statistic using these data showed that the model, when tested with the digital-survey data, had a low to moderate Gain (Table 16). Gain was highest for the Upper Rio Felix study area and lowest for the Box Canyon study area. Although the majority of ring middens were found in the high-sensitivity zone, particularly in the Azotea Mesa study area, large proportions of ring middens were also found in the low-sensitivity zone. Visual inspection of the distribution of ring middens with respect to sensitivity zones indicated that although some ring middens that fell within the low-sensitivity zone were located just outside the high-sensitivity zone, others were at some distance from the high-sensitivity zone. Some were located in very different settings than had been predicted by the model, such as on tablelands and in a variety of landscape positions distant from larger streams or stream confluences. Clearly, substantial numbers of ring middens identified through digital survey were located in landscape positions that had not been adequately predicted by the sensitivity model.

The inability of the model to place these ring middens in the high-sensitivity zone could, in part, have to do with existing survey areas' not being adequately representative of the environmental zones within the three study areas. A lack of variables that adequately capture ring-midden setting may also be a factor. In some ways, the model appears to be effective in capturing ring middens located in settings where survey has occurred, but it does not appear to capture ring middens located in other kinds of settings.

Experimentation with model refinement proved to be difficult. Using a combination of the digital-survey data and data available from pedestrian survey did not result in a model that performed especially well, despite the testing of additional predictor variables and multiple attempts at developing models using different subsamples of the data. These results imply that ring middens may be located in a variety of unexpected environmental settings for which we need more data to understand.

Finding that the preliminary model did not perform as well as we would have liked is not necessarily a bad thing, because it suggests that ring middens are not located in any one particular kind of environmental setting. In other words, there may be greater variability in ring-midden location than previously suspected. A greater diversity of environmental settings in which ring middens are found could mean that there was greater variability in where and how earth ovens were used. With additional data, there may be some potential for further differentiating earth-oven use according to environmental setting. If that is the case, such an understanding would improve our ability to study and interpret this resource.

Because we have no way of knowing the temporal or cultural affiliations of ring middens identified through digital survey, it may also be the case that environmental changes through time affected ring-midden location but are not adequately represented by the current suite of environmental variables used to model ring-midden location. Developing a better understanding of how environmental changes may have effected ring-midden use would likely improve our ability to predict ring-midden location more effectively.

Overall, these results suggest a need to refine the model with additional variables and survey data. A useful approach to refining the model may be to perform additional sample digital survey, particularly in the low-sensitivity zone, in order to derive a larger data set that more adequately captures a greater variety of environmental settings. Additional survey data would likely allow us to gain a more nuanced understanding of how ring-midden location varies across the three study areas.

Despite the somewhat disappointing performance of the preliminary model and the difficulties encountered in attempting to refine the model with the available data, it was worthwhile to calculate the ring-midden density per sensitivity zone and study area and to use those values to estimate the numbers of ring middens that could be located within the three study areas (Table 17). Density calculations indicated that digitally identified ring middens were present at greater densities in the high-sensitivity zone than in the

Table 16. Results of the Digital Survey with Respect to the Preliminary Locational Model

Study Area	Ring Middens Identified in Low-Sensitivity Zone	Ring Middens Identified in High-Sensitivity Zone	Total Ring Middens	Proportion of Identified Ring Middens in High-Sensitivity Zone	Proportion of Surveyed Area That is High Sensitivity	Gain
Azotea Mesa	81	173	254	0.68	0.47	0.31
Box Canyon	62	93	155	0.60	0.45	0.25
Upper Rio Felix	50	52	102	0.51	0.32	0.37
Total	193	318	511	0.62	0.39	0.37

Note: Data for the Azotea Mesa and Box Canyon study areas are for ring middens identified during the digital survey.

Table 17. Estimated Ring-Midden Densities and Projected Numbers of Ring Middens within Each Study Area, by Sensitivity Zone

Study Area	Ring Middens per Acre in Low-Sensitivity Zone	Ring Middens per Acre in High-Sensitivity Zone	Study Area Low-Sensitivity Acres	Study Area High-Sensitivity Acres	Estimated No. of Ring Middens in Low-Sensitivity Zone	Estimated No. of Ring Middens in High-Sensitivity Zone	Total Estimated No. of Ring Middens
Azotea Mesa	0.0204	0.0486	28,638.6	9,469.9	585	460	1,045
Box Canyon	0.0137	0.0249	33,861.3	7,363.4	464	183	647
Upper Rio Felix	0.0043	0.0094	153,248.7	9,390.8	658	88	746
Total	0.0096	0.0248	215,748.6	26,224.1	2,067	650	2,717

Note: Data for the Azotea Mesa and Box Canyon study areas are for ring middens identified during the digital survey.

low-sensitivity zone. Overall, ring-midden density was approximately 2.6 times higher in the high-sensitivity zone than in the low-sensitivity zone. The data also suggest that, in absolute numbers, there could be several times more ring middens in the low-sensitivity zone than in the high-sensitivity zone, particularly in the Upper Rio Felix study area, where ring middens had not been previously recorded by pedestrian survey and little was known about ring-midden distribution prior to the current project.

Though admittedly rough estimates, the density calculations imply that there may be more than 2,700 ring middens within the three study areas. Estimates are likely to improve with more-refined modeling of ring-midden location, but they also suggest that there are many more ring middens in the three study areas than have been recorded. These results underscore the value of digital survey. With the data and methods developed for the current project, it is now possible to develop a much more comprehensive understanding of ring-midden location than would be possible using pedestrian survey methods alone.

CHAPTER 5

Discussion and Conclusions

Ring middens are absolutely fascinating archaeological features. Archaeologists have been studying ring middens for nearly a century (see Chapter 1). Over the years, they have been identified in many areas in New Mexico and Texas through pedestrian survey, and some have been subjected to excavation and specialized studies. Varieties of typologies have been developed for documenting and studying ring middens, and multiple interpretations have been advanced regarding how they were used in different times and contexts and what they tell us about behavioral and environmental changes. Although much has been learned through these investigations, many questions have also been raised, and there is a great deal left to learn.

Recently, archaeologists have begun to conceptualize ring middens as manifestations of an ancient technology that has been used in many parts of the world for thousands of years: the earth oven (Black and Thoms 2014). In this view, it was the repeated cleaning and refurbishment of earth ovens that resulted in the formation of the annular discard middens we associate with ring middens. Ring middens in southeastern New Mexico are intriguing examples of hot-rock cookery as it was implemented in western North America. Long before people experimented with or invested in agriculture, they were experimenting with using hot rocks to cook foods in ways that allowed greater use of lower-ranked food sources and extraction of more nutrients from the environment.

Thoms (2008, 2009) has hypothesized that hot-rock cookery in western North America was a response to food crises. As food sources were depleted or became insufficient to support growing populations, people had to find new ways to extract more nutrients from the environment. They needed to invest more in food-processing technologies, and they needed to look to new food sources to support themselves. The use of hot rocks to cook foods is interpreted to represent a kind of carbohydrate revolution, as people came to look to roots, geophytes, and small seeds to fill in the dietary gaps.

The appearance of large ring middens in a region is taken to be one form of evidence of resource intensification, because their use signifies the attempt to derive a greater quantity of subsistence resources per unit area, often in response to social and environmental pressures, such as population packing or drought. In other words, as the population in the region increased and more readily available subsistence resources were depleted, earth ovens were used to make greater use of food resources, such as agave and sotol, that required extended cooking time to detoxify and render them digestible. Periods of drought that suppressed the availability of more easily attained wild resources or decreased agricultural productivity may have also spurred the use of earth ovens. By retaining and slowly radiating heat from heated rocks, earth ovens also make better use of limited fuel resources than do open fires, particularly when fuel resources are depleted in a region as a result of drought or increased settlement and land use.

In some areas of southeastern New Mexico, such as in the foothills of the Guadalupe and Sacramento Mountains, survey has indicated that ring-midden features are very numerous and often are present in clusters of several. The density of these features, as revealed through survey, suggests that there may be thousands more of them on BLM lands than have been documented by survey. In order to manage and study these resources, the BLM will need to gain a better understanding of where these features are located, where they may be most threatened by disturbance or land use, and where we are more or less likely to find them through archaeological survey efforts.

One of the great advantages to the study of ring middens is that they are highly visible on the landscape. Ring middens have a unique, recognizable shape consisting of an aboveground annular midden surrounding a central depression or pit. To date, most ring middens have been discovered by archaeologists who walked

across a survey area in regularly spaced transects to closely inspect the ground surface, in search of archaeological remains. Yet because the BLM administers large areas of land in southeastern New Mexico, and only a small percentage of that land has been surveyed for archaeology, there are a great many more ring middens on BLM lands than can practically be identified through pedestrian survey.

To conduct a digital survey for ring middens, SRI hired Surdex to obtain aerial lidar data for each of the three study areas examined during the project: Azotea Mesa, Box Canyon, and Upper Rio Felix. Those data were then used by SRI, along with data on the locations of recorded ring-midden features, to develop an approach to identifying ring-midden features in digital lidar data using GIS software. The locations of recorded sites with ring-midden features were used to develop an approach to visualizing (or recognizing) ring-midden features in a GIS using the lidar data and to create a locational model to predict where (within the three study areas) ring middens were more or less likely to be located. Observations made about the size and shape characteristics of recorded ring middens were then used to create an automated GIS method for identifying features with shapes and sizes similar to those of ring middens in the lidar data. Based on the results of the locational model, a sample of survey areas was selected from the three study areas and subjected to systematic digital survey. The digital survey was conducted within a GIS by an archaeologist who systematically inspected the lidar data for each survey area using a variety of visualization techniques. Each location that had been identified via our AFI method as potentially containing a ring midden was also closely inspected during the survey.

Once the survey was complete, a sample of areas where potential ring-midden features had been identified was chosen for field verification. These efforts focused on ground-truthing clusters of features that were of diverse sizes, shapes, and conditions, to evaluate how effective the digital survey was in identifying ring-midden features. The results of the field verification confirmed that each feature digitally identified as a potential ring-midden feature was, in fact, a ring-midden feature. In areas where disturbance was common, however, ring-midden features that had very low relief or had their shapes altered by disturbance were not properly identified during the digital survey. Overall, these efforts suggest that digital survey using lidar data to find ring-midden features is effective but that features that have been disturbed and/or are of very limited relief are likely to be missed by digital survey.

Visualization of the Lidar Data

Visualization refers to the data and methods used to observe patterns in remotely sensed data, such as lidar data. The classified LAS file can be visualized and processed using a number of commercial software programs, such as ArcGIS for Desktop, Erdas Imagine, Exelis ENVI, Global Mapper, and Rapidlasso LAStools. After the classified LAS file has been imported into any of the abovementioned software packages, it can be used to produce a number of GIS layers to represent models of the land surface as well as models that represent buildings or other features, such as power lines or road features (Figure 54).

The most common product created using the classified LAS files is a DEM, a grid of uniformly sized cells, each with its own elevation, that together represent a model of the elevation of the land surface measured by the lidar system. Although DEMs often are made using only those points in the LAS file that are classified as bare ground, doing so can have the effect of erasing archaeological features, because some points corresponding to small archaeological features that protrude above the land surface are sometimes misclassified as low vegetation. Thus, for the current project, DEMs for individual survey areas were made using points classified as either bare ground or low vegetation. Based on the typical size and shape characteristics of ring-midden features and the resolution of the lidar data, DEMs were made for the project using a grid-cell size of 0.25 by 0.25 m, because it was determined that this resolution would be sufficient to recognize the ring-midden shapes in the data.

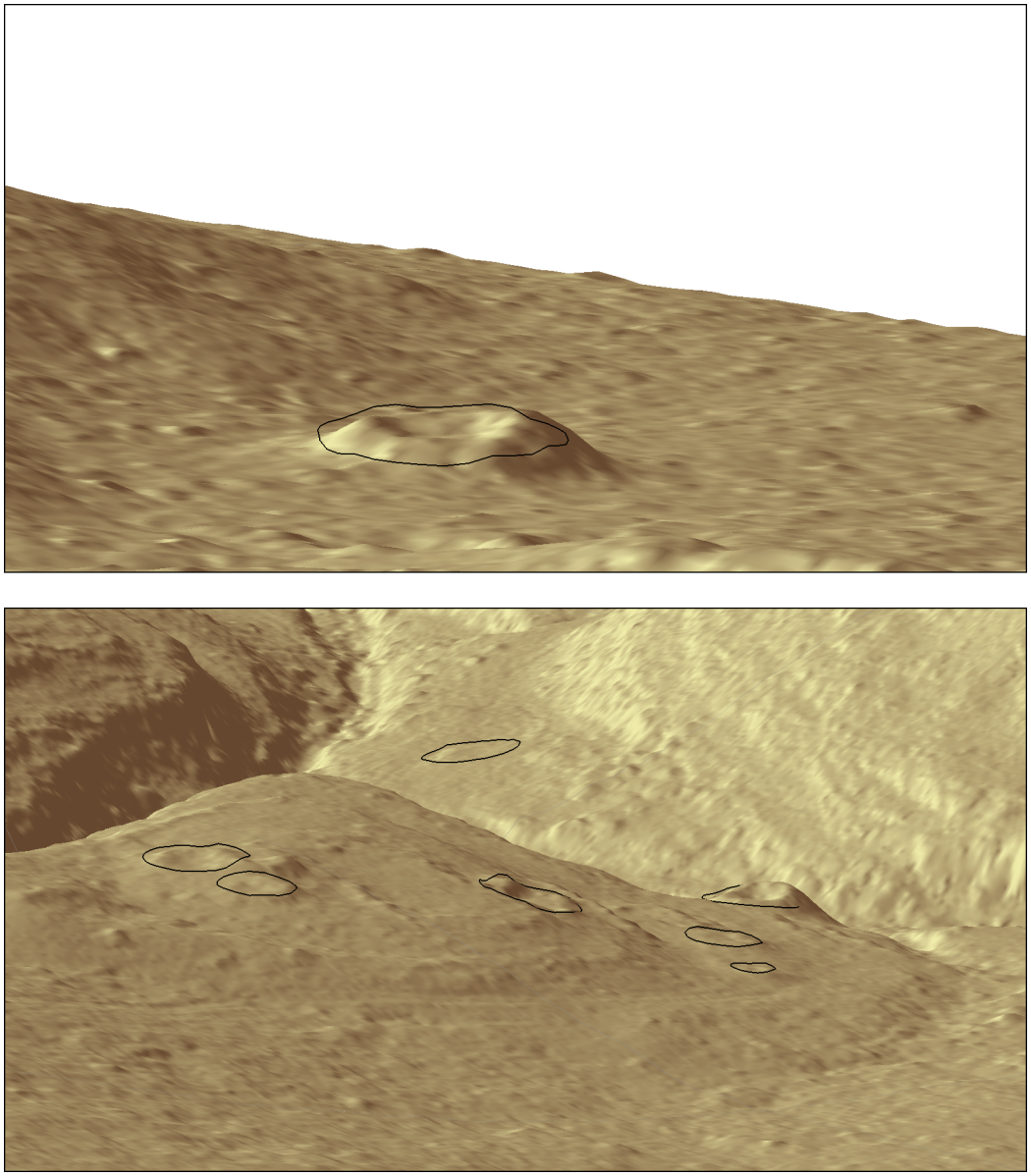

Figure 54. Three-dimensional renderings of ring middens identified in the Azotea Mesa study area during the digital survey.

By itself, a DEM is not very useful for identifying archaeological features. The DEM must be transformed into other representations of the land surface that can be used to more clearly distinguish different characteristics of that surface, such as slope and aspect. One of the most common GIS layers derived from a DEM is a hillshade. A hillshade is made by modeling a light source, like the sun, such that it is shining on the land surface from a specific angle and direction. The modeled light source, along with elevation data from the DEM, is used to create a surface that looks like a landscape when viewed from above, as though from a plane. Hillshades are commonly used to identify archaeological features using lidar data, but like DEMs, they have limitations.

When visualizing lidar data to look for archaeological features, it is useful to also create layers that make different characteristics of those features stand out more clearly, in order to distinguish the features from background noise. We experimented with a variety of visualization techniques to find the ones that would work best in visualizing ring-midden features in the three study areas. We found that, in addition to hillshades, two kinds of representations of the land surfaces worked well in visualizing ring-midden features: TPI layers and LRMs.

TPI layers use elevation values within a neighborhood of grid cells to identify whether a specific grid cell is high or low with respect to the grid cells around it. Grid cells that have the highest topographic positions are identified with a value of 1, and those with the lowest topographic positions are identified with a value of 0. Grid cells that fall between the highest and lowest positions are given values between 0 and 1, based on where they lie between the minimum and maximum values in a neighborhood of grid cells. When calculated using neighborhoods of a size similar to the size of a ring-midden feature, the ring portion of the feature stands out as having a high topographic position, with values close to 1. The central portion of the feature and the area immediately outside the feature typically have values closer to 0. This allowed us to clearly identify a ring-like shape in the lidar data and to hone in on potential ring-midden features during digital survey.

What an LRM essentially does is go through a series of transformations of the elevation data to identify general trends in the terrain, to create a generalized terrain surface that lacks the small, local undulations in relief that may correspond to archaeological features. That generalized terrain surface is then subtracted from the original DEM, resulting in a surface that identifies small-scale, local changes in relief. Particularly when viewed in combination with a hillshade, an LRM makes the high and low portions of a ring midden stand out more starkly, allowing these features to be more clearly recognized.

Ring-Midden Modeling

In addition to processing the lidar data to be better able to see ring-midden features when viewed in a GIS, we created two models to help find ring-midden features in the lidar data. The first was a locational model of ring-midden sensitivity. This model was created by statistically evaluating the relationship between sites with ring middens and environmental variables, in comparison to surveyed locations where no sites had been found. The environmental variables that were examined included soil attributes, distance to water, distance to stream confluences, elevation, slope, aspect, topographic position, and various measures of topographic ruggedness and relief. These variables were evaluated in terms of the degree of influence they have on ring-midden location.

Analysis of the relationship between site location and environmental variables indicated that in comparison to nonsite locations, sites with ring middens tend to be closer to streams and confluences and are located at lower elevations above water than nonsite locations. Also, sites with ring middens more often tend to be located at lower midslope positions and in areas of lower relief, topographic ruggedness, and slope than nonsite locations. The greatest observed differences in locational attributes between sites with ring middens and nonsite locations were in cost distance to major streams, cost distance to streams, and elevation above water.

Using the most important environmental variables, a sample of ring-midden sites and nonsite locations, and a sophisticated modeling method called Random Forests, a statistical model was created. The Random Forests method essentially takes a sample of sites and nonsite locations and a sample of the variables used to predict sites and nonsite locations and creates a decision tree that specifies the conditions under which sites are expected or not expected to be present. The algorithm performs this process of sampling variables and cases thousands of times, resulting in the creation of thousands of individual decision-tree models, which are then statistically compared, to arrive at a model that combines the best aspects of all the individual decision trees. The result is a model that performs best based on a robust analysis of all the cases and variables used to create the model.

The resulting statistical model was then used to create a sensitivity map, which divided the study areas into zones of high and low potential for ring-midden sites. The ability of the sensitivity map to identify environmental zones where ring middens were likely to be located was then tested, using a sample of ring-midden sites and surveyed nonsite locations that had not been used to create the underlying statistical model. Measures of model performance indicated that the model appeared to work well in differentiating zones within the study areas where ring-midden sites were more or less likely to be present.

In addition to the statistical model, we also created a process for filtering the lidar data to identify specific topographic conditions that meet the shape and size characteristics of ring middens, and we refer to this process as AFI. The locational model discussed above identified broad zones where environmental conditions suggested that ring middens were likely or not likely to be present. The AFI process, by contrast, attempted to identify individual ring-midden features by finding local topographic conditions that matched those for ring middens. These kinds of models are difficult to develop, because they have a tendency to identify large numbers of locations where multiple conditions are met that suggest a ring-midden feature could be present but where no such features are actually located (false positives). However, they can be useful in narrowing the search for features, when faced with examining large amounts of remotely sensed data.

To develop the model, we evaluated the size and shape characteristics of ring-midden features and developed a series of expectations about where in the lidar data such characteristics were met. Some of these expectations were based on a series of measurements of known ring middens we made in a GIS, by generating 3-D profiles of the features. To derive the measurements, we used a sample of known ring middens to create two 3-D profiles in a GIS for each ring-midden feature. We then used the 3-D-profile data to generate a series of measurements quantifying the size and shape of different aspects of each ring midden, such as height, span, difference in height between the central depression and the highest portions, and estimated aboveground volume. We also identified a number of conditions under which topographic characteristics can be confused with those associated with ring-midden features but ring-midden features are unlikely to be present. Essentially, areas that are rugged or on steep slopes were identified as conditions under which ring middens were unlikely to be present and could be ruled out as potentially containing ring middens. With these expectations and conditions, we then created an automated process using computerized script that generated a series of layers in a GIS, evaluated a series of conditions, and then output a layer of point locations where potential ring middens could be located.

A common problem in this kind of automated feature extraction is in striking the right balance between, on the one hand, finding a lot of features that may or may not be the kinds being searched for and, on the other hand, being very strict and limiting in identifying potential features. Oftentimes, such processes identify many more potential features than actually are present. As a result, there tend to be large numbers of false positives in such approaches. Because we wanted to be conservative in not ruling out potential ring-midden locations, we created the process so that it would cast a wide net in searching for potential ring-midden features. The resulting process was successful in identifying many of the ring-midden features in our sample of known ring middens, but it also identified large numbers of potential features that, after close examination, are not likely to be ring-midden features. In any case, the approach demonstrated some promise for being able to identify ring-midden features and could likely be improved to reduce the number of false positives.

Digital-Survey Approach

One major purpose of this project was to conduct a digital survey for ring middens in the three study areas using the lidar data collected for the project. Although digital survey can be conducted faster and with less cost than field survey, the study areas selected for the project were still quite large and would have required more effort to fully survey than could be performed with the current project funding. However, the methods for visualizing ring middens developed during the current project could, with additional effort, be applied across the entire study area. The purpose of the current project was to collect appropriate lidar data, test whether ring middens could be located using the lidar data, develop methods for visualizing ring middens using the lidar data, predict where they were likely to be located, conduct a sample survey of the three study areas, and ground-truth a sample of digitally identified features to test whether the digital identification approach was effective.

For the purposes of collecting and organizing lidar data for the project, Surdex divided each of the three study areas into a grid of square tiles measuring 2,000 by 2,000 feet (610 by 610 m). The tile index supplied by Surdex for the three study areas was used as a sampling frame for selecting land parcels for digital survey using the results of the locational model. To conduct the sample survey, we used the locational model to identify survey tiles in which ring middens were more or less likely to be present. We then identified tiles in each study area that had large and small percentages of high-sensitivity zone. Using these data, we then selected survey tiles for digital survey, such that 75 percent of survey tiles contained large percentages of high-sensitivity zone, in which ring middens were most likely to be found, and the remaining 25 percent had comparatively low percentages of high-sensitivity zone. The sample-selection process resulted in an approximately 19.8 percent sample for digital survey from the Azotea Mesa study area and a 17.2 percent sample from the Box Canyon study area. Because of the much larger size and low archaeological sensitivity of the Upper Rio Felix study area, a 10 percent sample was selected for digital survey there.

The digital survey was designed to follow a systematic approach. For each of the tiles selected for survey, we used the lidar point cloud LAS data to generate a DEM, using the approach discussed above. The DEM was then used to generate LRM, TPI, and hillshade layers for each survey tile. The DEM, LRM, and TPI were also used to develop a series of layers used in our AFI process, ultimately resulting in a point layer that represented possible ring-midden locations. All of these layers were created using automated, systematic procedures and were generated using computerized scripts developed specifically for the project.

To survey an individual tile, the LRM, TPI, hillshade, and AFI centroid layers were loaded into ArcMap and visualized using the same color and display schemes. Once the layers were loaded, the surveyor first searched for ring middens at the scale of the entire tile. At that scale, prominent ring middens can be readily identified in the LRM and/or TPI layers. Any potential ring middens identified at that scale were then closely examined. If the feature had characteristics that conformed to our expectations for ring-midden morphology or that could be confused with those of a ring midden, an elliptical polygon was created in a GIS to delineate the feature. The polygon was then attributed with data regarding shape characteristics and how well defined the feature appeared in the lidar data. For each of these attributes, attribute states were recorded, according to a series of predefined categories.

The following categories were used for the feature-definition variable: (1) well defined, (2) moderately defined, (3) faint, (4) indistinct, and (5) not applicable. The category of *indistinct* was intended to be used when a possible feature was present near other, more-definitive ring-midden features but there was minimal feature definition. The *not applicable* category was intended for features that could be confused with ring middens and were recorded only for comparative purposes.

The shape variable consisted of the following categories: closed ring, open ring, irregular/discontinuous ring, ring with mounded lobe, and atypical. The last category was reserved mostly for features that had unusual shape characteristics, such as exhibiting rectilinearity or having an especially deep depression in the center. The *ring with mounded lobe* category was intended for a ring midden that had a large mound attached to one side of the ring. Rings of this type were observed in multiple locations during preliminary feature characterization and were distinctive and recurrent enough to warrant a special shape category.

Examples of each definition and shape category were provided to the surveyor prior to digital survey, in order to attribute polygons in a consistent manner.

Another piece of information that was gathered about the digitally identified ring middens was the location of the high side of each feature, because investigators have noted that ring middens tend to have one side that is higher than the other. Our measurements of ring-midden dimensions that were made using 3-D-profile data confirmed that to be the case. To gather information on the location of the high side for each digitally identified ring midden, we used a GIS tool that measures the azimuth of a line. A line was drawn from the center of each feature to the center of the highest portion, and the azimuth of that line was then calculated, using the GIS tool, to develop the necessary data.

Digital-Survey Results

In total, 359 lidar tiles were digitally surveyed, covering a total of 32,965 acres. The digital survey resulted in the identification of 511 potential ring-midden features (254 in the Azotea Mesa study area, 155 in the Box Canyon study area, and 102 in the Upper Rio Felix study area), as well as 25 features that could potentially be confused with ring middens because of similarities in morphology. In total, 33 (6.5 percent) of the potential ring-midden features identified during the digital sample survey were located within the boundaries of previously recorded sites, most of them within the Azotea Mesa study area, where survey has been more extensive and many sites with ring middens have been recorded. The remaining ring middens identified during digital survey were located outside previously recorded site boundaries, greatly increasing our knowledge of where ring middens are located in the three study areas. Based on the survey acreage in each of the three study areas, the number of features discovered in each study area demonstrated a steep cline in ring-midden density, with the highest density in the Azotea Mesa study area and the lowest density in the Upper Rio Felix study area.

Ring-Midden Size

Ring middens vary considerably in size among the three study areas. The largest ring middens were found in the Azotea Mesa study area, and the smallest were located in the Upper Rio Felix study area. The ring-midden-size data suggest substantial differences among the study areas in (a) the intensity of earth-oven use, (b) the types or quantities of materials processed in earth ovens, or (c) visibility and obtrusiveness. Disturbance processes could potentially explain differences in size among the study areas, at least in part, if we assume that disturbance processes have buried portions of features and displaced materials from the discard middens, making the surface-exposed portions of the features appear smaller.

Ring-Midden Definition

How well a ring-midden shape is defined is likely related to how obtrusive and visible the feature is but may also relate to frequency of use, disturbance processes, or cultural variation in discard patterns. Ring middens were most often well defined in the Azotea Mesa study area and least often well defined in the Upper Rio Felix study area. By contrast, ring middens were most often moderately well defined in the Upper Rio Felix study area and less often moderately well defined in the Azotea Mesa study area, although that pattern was not as pronounced as the pattern for well-defined ring middens. There was not a clear trend for subtly defined ring middens. Features identified as faint but possible ring middens were comparatively more common in the Azotea Mesa study area and least common in the Upper Rio Felix study area. Differences among study areas for the categories of *well defined* and *moderately well defined* conformed to our hypotheses that earth ovens were most intensively used in the Azotea Mesa study area and least intensively

used in the Upper Rio Felix study area and/or were least affected by disturbance processes in the Azotea Mesa study area and most affected by disturbance processes in the Upper Rio Felix study area.

Ring-Midden Shape

Ring-midden shape also varies among the study areas. Closed rings were found at similar relative frequencies in the three study areas. However, open rings become more frequent than other shapes as one goes from the Azotea Mesa study area to the Upper Rio Felix study area, as do features with atypical shapes. By contrast, rings with irregular, discontinuous shapes and ring middens with mounded lobes are most frequent in the Azotea Mesa study area and decrease in frequency as one goes from there to the Upper Rio Felix study area. These differences could potentially relate to how ring middens were used, but they could also relate to disturbance processes, with open rings more often affected by disturbance processes. Perhaps discontinuous rings are also more affected by disturbance processes or are more often simply vegetation. An interesting result regarding shape was the relatively high incidence of ring middens with mounded lobes in the Azotea Mesa study area. Perhaps the presence of ring middens with these shapes is related to more intensive and repeated use of earth ovens and/or the stockpiling of materials for use in earth ovens.

Ring-Midden High Side

Investigators have noted that ring middens tend to have one side that is higher than the opposing side, but the reasons behind that pattern are unclear. Presumably, it is related in some fashion to how earth ovens were cleaned out. The high side of each feature was patterned in the three study areas. In the Azotea Mesa study area, the high side tended to be located along the eastern side of the feature but was sometimes on the northwestern side. In the Box Canyon study area, the high side was most often on the southeastern side of the feature. In the Upper Rio Felix study area, the high side tended to be on either the southeastern or the northwestern side of the feature.

The aspect of the land surface on which ring middens are situated tended toward the east and southeast in all three study areas and ranged from northeast to southwest for most ring-midden locations. In general, these data suggest that the high side of a ring-midden feature tends to be on the downslope side. Perhaps more materials from earth ovens were raked or tossed downslope to create the annular ring than were distributed upslope. However, that does not explain why, in the Upper Rio Felix study area, the high sides of a substantial number of ring-midden features are on the northwestern sides, when most land surfaces on which they are situated trend downward in the opposite direction. Disturbance processes could potentially explain that pattern, if the downslope portions were more heavily affected by erosional or sedimentary processes.

Ring-Midden Clustering

Two really fascinating things about ring-midden features are their spatial distribution and environmental associations. For example, as a result of this project, we have observed that ring middens tend to cluster at multiple scales. If you find a ring-midden feature in one location, it is not uncommon to find another ring midden, or even several other ring middens, nearby. Moreover, ring middens tend to cluster at broader scales, along individual drainages and drainage segments as well as in broad landscape zones. These different scales of clustering likely have to do with a number of interacting social and environmental factors that could vary according to scale. Clusters of two or more ring-midden features located within tens of meters of each other are common in the study area. Clustering is most common in the Azotea Mesa study area and is somewhat less common in the other two study areas. Intriguingly, average nearest-neighbor distances are quite similar among the three study areas, suggesting a similar underlying pattern among the study areas in the placement and spacing of ring middens.

Intersecting Rings

Intersecting ring middens are of interest to the study of ring middens in that they are sometimes considered indicators of the passage of time. Although it was relatively common for multiple ring middens identified during the digital survey to cluster in proximity to each other, it was comparatively rare that ring-midden features intersected. In a number of cases in which they did intersect, they appeared to do so because multiple ring middens had been placed in an area where space was limited, causing them to be more closely packed.

Feature Profiles

Despite the widespread presence of ring middens, minimal effort has been made to characterize their dimensions in a systematic manner. Most descriptions of ring-midden dimensions either apply to one or a few ring-midden features intensively investigated as part of a mitigation project or are anecdotal and lack supporting data. Investigators have certainly measured ring-midden features and provided some characterizations of their size, but rarely have they attempted to calculate statistics on ring-midden dimensions using a large and representative sample. For the first time, this project has allowed for morphometric characterization of ring middens for a large sample of those that could be identified using lidar data. Moreover, the data were developed for all of the ring middens using identical protocols and procedures and were based on measurement data acquired using identical methods and instruments. It must be kept in mind, however, that the measurements obtained were limited by the precision and accuracy of the lidar data and thus are not identical to measurements made on the ground using standard field measurement devices. Potentially, some variation in ring-midden dimensions could be used to derive inferences about cultural and natural formation processes. For example, the overall size of a ring midden, particularly ring-midden volume, could be related to how intensely or frequently ring middens were used or, in some cases, could be related to differential effects of disturbance processes.

In order to understand more about the morphology of potential ring-midden features identified during the digital sample survey, we selected a random sample of surveyed tiles that contained potential ring-midden features from each of the three study areas. When measured using the 3-D-profile data, feature size, average profile height, maximum profile height, span, and estimated aboveground feature volume all decreased with elevation. A possible reason is that earth-oven use was less intensive at higher elevations. That does not necessarily mean that fewer resources were acquired or processed at higher elevations but, more likely, that the fuel-saving characteristics of earth ovens was less important with increases in elevation because of a greater availability of fuelwood at higher elevations. Another explanation, which is not exclusive of the fuel-availability hypothesis, is that resources were more often processed repeatedly in earth ovens located closer to residential bases, at lower elevations, and more-distant earth ovens, in higher elevation settings, were less often used. Similarly, these same measures decreased as the distance to streams increased, particularly average height and maximum profile height, suggesting that earth-oven use was more intensive near streams and less intensive farther away from streams. This suggests that plants growing along streams were likely important as fuel and perhaps also that the availability of water was important to earth-oven use (e.g., for use in steaming).

Field Verification

To test the validity of the digital-survey results, areas containing digitally identified ring-midden features were inspected in the field. The field-verification efforts focused on recording clusters of ring middens with different attributes, so that a maximal number of ring middens with different characteristics could be observed and recorded during the allotted field time. In total, 43 features were recorded during the fieldwork efforts. Fourteen of the features recorded had not originally been identified during the lidar digital survey,

and 11 of those were found at a newly recorded site in the Upper Rio Felix study area. These features were much smaller in size and had substantially lower relief than nearby features that had been identified during digital survey. Moreover, 3 of these features, though containing FCR, were not consistent in shape or other characteristics used to define ring-midden features. All of the newly recorded features identified during the field-verification efforts either had been disturbed from floodplain erosion or deposition or, in a few cases, had very low relief and uncharacteristic shapes.

Overall, the field-verification efforts indicated that the lidar survey was highly successful in identifying ring-midden features but failed to detect heavily disturbed features and features of very low relief. These results suggest that lidar data can be successfully used to identify large numbers of ring middens on BLM land in southeastern New Mexico that would otherwise be unrecorded and could be recorded using digital methods more quickly and at a lower cost than would be achieved through pedestrian survey. This finding allows the BLM not only to better manage and protect these fascinating and important resources but also to understand a great deal about how they are distributed across the landscape, how they vary in shape and size, and how they were used to support indigenous populations of the ancient past and more recent times.

Model Testing

Testing of the ring-midden sensitivity model using data from the digital survey suggested that it worked moderately well but suffered from a number of limitations. Experimentation with refining the model suggested that model refinement would benefit from a larger sample that covered a greater variety of environmental contexts. The model worked well to delineate contexts in which ring middens have been found through pedestrian survey but not contexts that appeared to have been less well represented by survey. The greater variety of environmental settings in which ring middens were found in the digital survey suggests that there may have been greater diversity in ring-midden placement and use than had been suspected. This suggests that a substantial amount can be learned by further study of the spatial distribution of ring middens and comparisons based on field observations among ring middens found in different environmental contexts. Black and Thoms (2014:216) argued that "oven pits develop into long-term facilities" (such as ring middens) in three sets of conditions: (1) places where sediments are shallow or difficult to excavate, such as very rocky or indurated sediments; (2) places accessible to attractive resources; and (3) peripheral areas of "favored residential sites." Developing variables that better meet these expectations could help not only to develop better models of ring-midden sensitivity but also to interpret their spatial distribution in the three study areas. For example, one factor that was not explicitly modeled due to the lack of appropriate spatial data was the location of potential source areas where suitable rocks to use in an earth oven could be obtained. Although all rings are located in areas of limestone or dolomite bedrock, not all locations have suitable rocks eroded on the surface that can be used and no example of mining rocks for heating has been recorded. Information about rocks on the surface is not readily available in the lidar data or in other spatial data used to model ring midden location, but this may have been a factor in ring-midden location. Perhaps, the fact that ring middens tend to be located near drainage confluences could relate to this factor if suitable rocks tend to concentrate in such locations along a drainage network.

What We Have Learned

This project has been more successful than anticipated. At the outset, it was unknown whether ring middens could confidently be identified in lidar data. Experimentation with visualization techniques and comparison of lidar data with existing records of sites where ring middens have been documented suggested that there was good potential to identify ring middens using lidar data. Additional analysis showed that there was

good potential to make observations on their size, shape, and degree of definition. Modeling of ring-midden location showed that ring middens tended to be located near streams and stream confluences and in relatively flat areas at low topographic positions, at the bases of hills. Digital survey for ring middens indicated that large numbers of ring middens are likely to be present in many areas that have yet to be surveyed and that there are distinct differences in ring-midden size, shape, degree of definition, and clustering among the study areas. The field-verification efforts showed that all of the ring middens identified in the digital data and visited in the field were, in fact, ring middens, demonstrating that the digital-survey results are a good reflection of the distribution of ring middens in the study area.

The field-verification efforts suggested that the failure to detect ring-midden features during digital survey could be attributed to a small number of factors. As discussed above, features that went unrecognized in the lidar data had been mostly disturbed and lacked the relief necessary to detect them confidently using lidar data. This suggests that the ring-midden densities resulting from the digital survey are likely underestimated, particularly in the Upper Rio Felix study area, where disturbance processes appear to have had a pronounced effect on the obtrusiveness and visibility of ring-midden features, as observed using the lidar data. Moreover, the field-verification efforts suggested that some of the differences between study areas in ring-midden density, size, and other characteristics potentially resulted from differences in disturbance among the study areas but may also be attributable to differences in how ring middens were used in different areas. These efforts suggest that digital survey is useful for planning and scoping studies in areas where ring middens are prevalent, but are not suitable as an alternative survey method for section 106 compliance due to limitations in regard to recognizing low-relief ring middens, features of other types, and artifact scatters. Nonetheless, the identification of ring middens using digital methods can be an important means for identifying where some sites are located and where additional archaeological resources not recognized in the digital data may be present.

A great deal more can be learned from the data developed for this project by further analyzing the distribution of ring middens with respect to other sites and environmental variables. With some additional effort, the portions of the three study areas that were not digitally surveyed during the current project can be surveyed using the data and methods developed for this project. Also, many of the locations where ring middens have been digitally identified should be visited, to perform additional ground-truthing efforts and to record the sites as they appear on the ground. Overall, the project has shown that modern digital technology can be used to study ancient earth-oven technology and to shed light on this fascinating and important heritage resource managed by the BLM.

APPENDIX A

Lidar Acquisition Information

LiDAR ACQUISITION REPORT

Project:	Carlsbad, NM LiDAR Project
Client:	Statistical Research, Inc.
SRI Project No.:	12PB02
Date:	27-March-2014
Submitted by:	Cornell Rowan, Project Manager

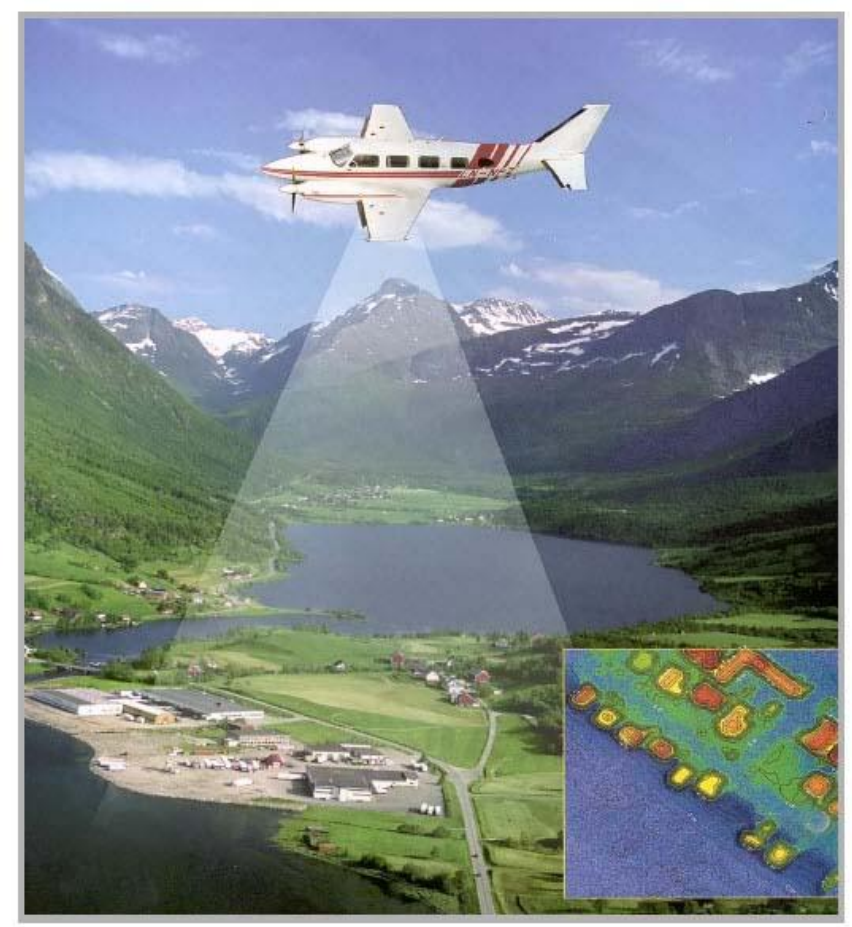

Project Overview

Statistical Research, Inc. contracted with Surdex Corporation in the fall of 2013 to collect high resolution LiDAR elevation data over three localities west and northwest of Carlsbad, New Mexico. The data collection was to be accomplished in December 2013, or January or February of 2014.

- Azotea Mesa Study Area = 54 square miles
- Box Canyon Study Area = 64 square miles
- Upper Rio Felix Study Area = 254 square miles

On January 07, 2014 there was a failed attempt to begin the aerial LiDAR data acquisition phase of the project. Due to the specs and data collection requirements for the project, the crew was unable to stall the aircraft to the required speed to collect the 15 points per meter as required. The aerial LiDAR acquisition officially started on February 14, 2014 and ended March 14, 2014. Windy and/or rainy days were the only two elements that delayed the data collection.

LiDAR Data Acquisition

The Leica ALS 70 HP SP3 Sensor was used to acquire the data in leaf-off, snow-free conditions. The data acquisition was performed at an approximate altitude of 900 meters above ground level with a 55% overlap between flight-lines to collect a minimum of 15 points per meter for all three study areas. Acquisition of all three study areas required 355 flight-lines that totals approximately 3,748 flight-line miles.

The flight crew was guided by a GPS controlled flight management system, which displays the flight plan; including altitude, heading, cross track deviation and PDOP. During the flight mission, the system operator monitored flight management data and the laser information, to ensure a successful mission. During each flight mission, GPS base stations were strategically placed within 25 miles of all flights to guarantee usable Airborne GPS data.

Calibration tie flights to ensure the accuracy of the data were also acquired at each of the three study areas. The calibration flights consisted of two sets of parallel lines flown in opposite directions, each set perpendicular to the project flight-lines. The calibration lines are flown across the project flight-lines to check for any horizontal or vertical offset.

All data collected in the aircraft, including AbGPS, IMU (inertial measurement unit, i.e. rotational angles); laser ranges; were recorded onto 72 GB removable hard drives and 1 GB flash memory cards. Upon landing, the system operator removed all storage devices from the LIDAR system and the GPS receivers. At the end of each flight day, all data was copied to a second set of data drives for archival purposes. Two copies of all data are maintained throughout our entire acquisition and product development process.

Azotea_Mesa_Output_ADJ.TXT

\\FLIGHTS\Flight Data\New_Mexico\Carlsbad\survey data\combinedPoints_CK_Shots.txt

Number	Easting	Northing	Known Z	Laser Z	Dz
20	552509.582	3588012.993	1127.376	1127.550	+0.174
21	551665.871	3585228.584	1184.702	1184.830	+0.128
33	559617.577	3581547.932	1065.955	1066.050	+0.095
29	554072.965	3580290.137	1126.898	1126.980	+0.082
28	550402.823	3578487.246	1196.488	1196.570	+0.082
25	548145.499	3579968.455	1214.363	1214.430	+0.067
35	566470.242	3580474.447	996.131	996.190	+0.059
26	551720.965	3580051.967	1154.007	1154.040	+0.033
22	549724.737	3582894.430	1282.272	1282.300	+0.028
34	561059.474	3582316.388	1044.935	1044.890	-0.045
32	560001.194	3583937.731	1043.342	1043.280	-0.062
30	557353.836	3580829.305	1092.736	1092.630	-0.106
24	556250.053	3582878.856	1098.857	1098.600	-0.257
23	554717.211	3583088.006	1130.469	1130.110	-0.359

Average dz	-0.006
Minimum dz	-0.359
Maximum dz	+0.174
Average magnitude	0.113
Root mean square	0.144
Std deviation	0.149

UTM coordinates, ground-measured elevation values, LIDAR elevation values, and error statistics for GPS locations used as LIDAR control points in the Azotea Mesa project area.

Box_Canyon_Output_ADJ.TXT

F:\New_Mexico\Box_Canyon\CK_Data\adjusted meters.txt

Number	Easting	Northing	Known Z	Laser Z	Dz
20	519622.637	3595994.750	1389.816	1389.900	+0.084
19	516977.751	3593906.606	1431.408	1431.480	+0.072
8	545476.363	3602286.991	1076.025	1076.090	+0.065
7	538241.188	3598015.747	1160.626	1160.680	+0.054
13	525279.381	3598251.071	1337.989	1338.040	+0.051
16	520186.947	3592397.964	1411.591	1411.620	+0.029
15	522275.946	3590930.110	1383.488	1383.510	+0.022
3	542441.078	3599498.751	1106.430	1106.430	+0.000
4	540809.833	3599217.014	1122.830	1122.830	+0.000
1	543364.511	3599269.762	1099.578	1099.570	-0.008
6	539677.185	3598573.494	1136.591	1136.580	-0.011
9	546462.232	3601701.105	1072.661	1072.650	-0.011
2	543234.023	3599603.982	1098.735	1098.710	-0.025
11	532422.244	3598591.307	1247.246	1247.220	-0.026
12	533873.863	3597334.659	1193.589	1193.560	-0.029
10	536915.048	3598741.354	1161.631	1161.590	-0.041
5	540701.563	3600498.255	1123.962	1123.920	-0.042
14	526028.133	3593116.299	1362.275	1362.210	-0.065
18	516241.114	3589485.177	1482.008	1481.910	-0.098
17	518507.855	3590618.029	1440.503	1440.380	-0.123

Average dz	-0.005
Minimum dz	-0.123
Maximum dz	+0.084
Average magnitude	0.043
Root mean square	0.054
Std deviation	0.055

UTM coordinates, ground-measured elevation values, LIDAR elevation values, and error statistics for GPS locations used as LIDAR control points in the Box Canyon project area.

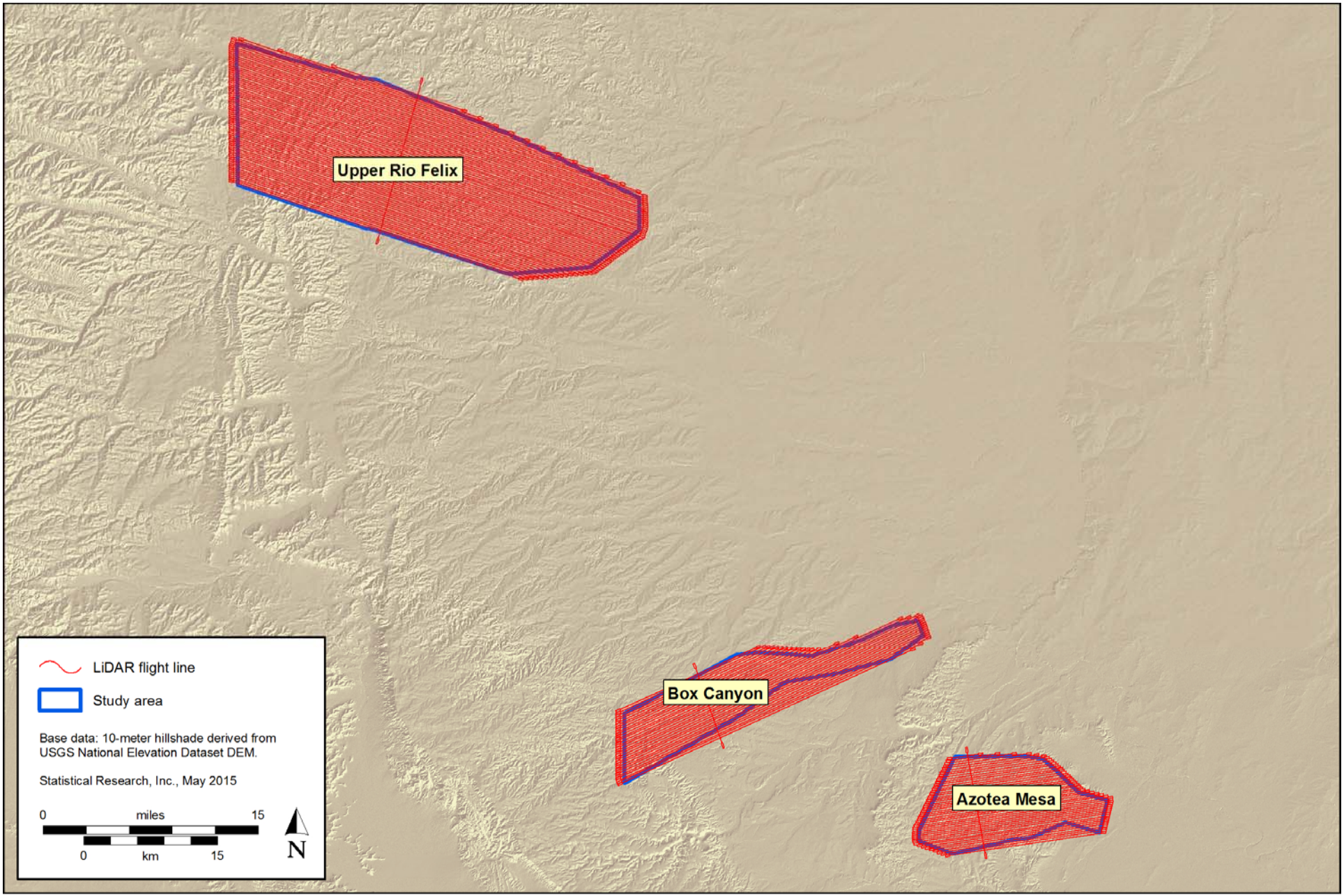
Upper Rio Felix
Box Canyon
Azotea Mesa
LiDAR flight line
Study area
Base data: 10-meter hillshade derived from USGS National Elevation Dataset DEM.
Statistical Research, Inc., May 2015
0
miles
15
0
km
15
N

APPENDIX B

Python Scripts Developed for Batch Processing of Geographic Information Systems Data

Python Script for Batch-Creation of Local Relief Model Rasters

```
# ---------------------------------------------------------------------------
# LocalReliefModel.py
# Created on: 2014-12-03 11:27:20.00000
# Created by: Adam Byrd, Statistical Research, Inc.
# Description: Script for batch creation of local relief model rasters
# ---------------------------------------------------------------------------

# Import arcpy modules
import arcpy
from arcpy import env
from arcpy.sa import *

arcpy.env.overwriteOutput = 1

# Check out any necessary licenses
arcpy.CheckOutExtension("spatial")
arcpy.CheckOutExtension("3D")

# Script arguments
inputRasters = arcpy.GetParameterAsText(0)


Set_cellsize_of_input_DEM = arcpy.GetParameterAsText(1)
if Set_cellsize_of_input_DEM == '#' or not Set_cellsize_of_input_DEM:
    Set_cellsize_of_input_DEM = "CELLSIZE 1" # provide a default value if unspecified
else:
    Set_cellsize_of_input_DEM = "CELLSIZE " + str(Set_cellsize_of_input_DEM)

Low_Pass_window_shape_and_extent = arcpy.GetParameterAsText(2)
if Low_Pass_window_shape_and_extent == '#' or not Low_Pass_window_shape_and_extent:
    Low_Pass_window_shape_and_extent = "Rectangle 25 25 MAP" # provide a default value if unspecified

Output_Folder = arcpy.GetParameterAsText(3)

# Local variables:
neighborhood = NbrRectangle(10, 10, "MAP")
rasterList = str(inputRasters)
rasterFiles = rasterList.split(";")

for Input_DEM in rasterFiles:
    arcpy.AddMessage("Start")
    desc = arcpy.Describe(Input_DEM)
    DEMname = desc.file
    DEMname = DEMname[:-4]
    arcpy.CreateFolder_management(Output_Folder, DEMname)
```

```
    tempFolder = Output_Folder + "//" + DEMname
    arcpy.AddMessage("Calculating Focal Statistics")
    # Process: Focal Statistics
    outFocalStatistics = FocalStatistics(Input_DEM, neighborhood, "MEAN", "DATA")
    outFocalStatistics.save(tempFolder + "//smoothedDEM.tif")
    smoothed_DEM = tempFolder + "//smoothedDEM.tif"
    # Process: Minus
    arcpy.AddMessage("Calculating Minus")
    outMinus = Minus(Input_DEM, smoothed_DEM)
    outMinus.save(tempFolder + "//Difference.tif")
    Difference = tempFolder + "//Difference.tif"

    # Process: Contour
    arcpy.AddMessage("Calculating Contour")
    break_lines = tempFolder + "//contour.shp"
    Contour(Difference, break_lines, "10000", "0", "1")


    # Process: Extract by Mask
    arcpy.AddMessage("Calculating Extract By Mask")
    arcpy.Copy_management(Input_DEM, tempFolder + "//inputDEM.tif")
    Input_DEM = tempFolder + "//inputDEM.tif"
    outExtractByMask = ExtractByMask(Input_DEM, break_lines)
    outExtractByMask.save(tempFolder + "//sim_elev.tif")
    simplified_elevation_raster = tempFolder + "//sim_elev.tif"

    # Process: Raster to Point
    arcpy.AddMessage("Calculating Raster to Point")
    elevation_points = tempFolder + "//elevation_points.shp"
    arcpy.RasterToPoint_conversion(simplified_elevation_raster, elevation_points, "Value")

    # Process: Create TIN
    arcpy.AddMessage("Calculating Create TIN")
    TIN = tempFolder + "//TIN"
    arcpy.CreateTin_3d(TIN, "", "'" + elevation_points + "' GRID_CODE Mass_Points <None>",
"DELAUNAY")

    # Process: TIN to Raster
    arcpy.AddMessage("Calculating TIN to raster")
    DTM = tempFolder + "//DTM.tif"
    arcpy.TinRaster_3d(TIN, DTM, "FLOAT", "NATURAL_NEIGHBORS",
Set_cellsize_of_input_DEM, 1)

    # Process: Parse Path
    #arcpy.AddMessage("Calculating Parse Path")
    #arcpy.ParsePath_mb(Input_DEM, "NAME")

    # Process: Minus (2)
    arcpy.AddMessage("Calculating 3D Minus")
    LRM = Output_Folder + "//LRM_" + DEMname + ".tif"
    arcpy.Minus_3d(Input_DEM, DTM, LRM)
```

Python Script for Batch-Creation of Automated Feature Identification Layers

```
# ---------------------------------------------------------------------------
# AutomatedFeatureIdentification.py
# Created on: 20145-02-20
# Created by: Nahide Aydin, Statistical Research, Inc.
# Description: Script for batch creation of automated feature identification layers
# ---------------------------------------------------------------------------


import os
import arcinfo
import arcpy
from arcpy.sa import *
import glob
arcpy.CheckOutExtension("Spatial")

#Filepath of input workspace MUST BE FILLED IN
inws = ''

#Filepath of output workspace MUST BE FILLED IN
outws = ''

try:
# get list of .las files
  arcpy.env.overwriteOutput = True
  lrm_dir = os.path.join(inws, 'lrm')
  tpi_dir = os.path.join(outws, 'tpi')
  if not os.path.exists(tpi_dir):
   os.makedirs(tpi_dir)
  mask_dir = os.path.join(outws, 'mask')
  if not os.path.exists(mask_dir):
   os.makedirs(mask_dir)
  centroid_dir = os.path.join(outws, 'centroids')
  if not os.path.exists(centroid_dir):
   os.makedirs(centroid_dir)
  fileNames = glob.glob(os.path.join(lrm_dir, '*.tif'))

  for fileName in fileNames:
    fileName = os.path.basename(fileName)[16:23]
    print fileName
    baseTPI = inws + '\\tpi\\tpi_mixed_' + fileName + '.tif'
    if os.path.isfile(outws + '\\tpi\\tpi_conditions_' + fileName + '.tif'):
       continue
    innerFocalStatMean = FocalStatistics(inws + '\\tpi\\tpi_mixed_' + fileName + '.tif', NbrAnnulus(3,6,
"MAP"),"MEAN", "DATA")
```

```
   innerReClass = Reclassify(innerFocalStatMean, "VALUE", RemapRange([[0, 0.27, 0], [0.27, 0.33, 2],
[0.33, 0.4, 3], [0.4, 0.49, 4], [0.49, 1, 3]]),"DATA")
   outerFocalStatMean = FocalStatistics(inws + '\\tpi\\tpi_mixed_' + fileName + '.tif',
NbrAnnulus(6,9,"MAP"),"MEAN", "DATA")
   outerReClass = Reclassify(outerFocalStatMean, "Value", RemapRange([[0,0.07,2], [0.07,0.12,3],
[0.12,0.17,4], [0.17,0.23, 3], [0.23,1,0]]), "DATA")
   SumInOut = innerReClass + outerReClass
   SumInOutReClass = Reclassify(SumInOut, "Value", RemapRange([[0,5,0], [5,8,1]]), "DATA")
   SumInOutReClass.save(outws + '\\tpi\\tpi_conditions_' + fileName + '.tif')
   print "TPI Conditions Raster " + fileName + " saved"
   SlopePercent = Slope(inws + '\\lrm\\LRM_FilteredDEM_'+ fileName+'.tif', "PERCENT_RISE")
   SlopePercentFocalStatMean = FocalStatistics(SlopePercent, NbrCircle(9, "MAP"), "MEAN",
"DATA")
   SlopePercentFocalStatMeanReClass = Reclassify(SlopePercentFocalStatMean, "Value",
RemapRange([[0, 2.4, 0], [2.4,12,1], [12,10000,0]]), "DATA")
   LRMReClass = Reclassify(inws+'\\lrm\\LRM_FilteredDEM_'+ fileName+'.tif', "Value",
RemapRange([[-100,-0.25,0], [-0.25,0.15,1], [0.15,100,0]]), "DATA")
   LRMReClass.save(outws + '\\tpi\\LRMReClass_' + fileName + '.tif')
   LRMReClassExpand = Expand(LRMReClass, 2,0)
   DEMFocalRange = FocalStatistics(inws+'\\dem\\FilteredDEM_'+ fileName+'.tif',NbrCircle(9, "MAP"),
"RANGE", "NODATA")
   DEMFocalRangeReClass = Reclassify(DEMFocalRange, "VALUE", RemapRange([[0,2,1],
[2,100,0]]), "DATA")
   FinalMasked = SlopePercentFocalStatMeanReClass * LRMReClassExpand *
DEMFocalRangeReClass
   FinalMasked.save(outws + '\\mask\\final_mask' + fileName + '.tif')
   AFEblobs = FinalMasked * SumInOutReClass
   AFEblobs.save(outws + '\\mask\\afeBlobs' + fileName + '.tif')
   print "Masked Raster " + fileName + " saved"

   FinalMaskedExpand = Expand(AFEblobs, 5,1)
   Raster2Poly = outws + '\\mask\\rasterPly' + fileName + '.shp'
   arcpy.RasterToPolygon_conversion(FinalMaskedExpand, Raster2Poly, "NO_SIMPLIFY", "VALUE")
   Raster2PolySelect = outws + '\\mask\\rasterPly_sel_' + fileName + '.shp'
   arcpy.Select_analysis(Raster2Poly, Raster2PolySelect, '"GRIDCODE" = 1')
   cursor = arcpy.da.SearchCursor(Raster2PolySelect, "SHAPE@XY")
   centroid_coords = []
   for feature in cursor:
      centroid_coords.append(feature[0])
   point = arcpy.Point()
   pointGeometryList = []
   for pt in centroid_cords:
      point.X = pt[0]
      point.Y =  pt[1]
      pointGeometry = arcpy.PointGeometry(point)
      pointGeometryList.append(pointGeometry)
   arcpy.CopyFeatures_management(pointGeometryList, outws + '\\centroids\\centroids' + fileName +
'.shp')

#Additionally false positive removal steps
   focalMeanTPI = FocalStatistics(baseTPI, NbrCircle(2.5, "MAP"), "MEAN", "DATA")
```

```
    RCfocalMeanTPI = Reclassify(focalMeanTPI, "VALUE", RemapRange([[0,0.35,1], [0.35,1,0]]),
"DATA")
    extractPoints = outws + '\\centroids\\centroidsExt' + fileName + '.shp'
    extractValues = ExtractValuesToPoints(outws + '\\centroids\\centroids' + fileName + '.shp',
RCfocalMeanTPI, extractPoints)
    extractPointsFinal = outws + '\\centroids\\centroidsFinal' + fileName + '.shp'
    arcpy.Select_analysis(extractPoints, extractPointsFinal, '"RASTERVALU" = 1')

#Cleanup
    print "Deleted raster objects."
    del baseTPI
    del innerFocalStatMean
    del innerReClass
    del outerFocalStatMean
    del outerReClass
    del SumInOut
    del SlopePercent
    del SlopePercentFocalStatMean
    del SlopePercentFocalStatMeanReClass
    del LRMReClass
    del LRMReClassExpand
    del DEMFocalRange
    del DEMFocalRangeReClass
    del FinalMasked
    del AFEblobs
    del FinalMaskedExpand
    del focalMeanTPI
    del RCfocalMeanTPI
    print "DONE"
except arcpy.ExecuteError:
    print arcpy.GetMessages()
finally:
    arcpy.RefreshCatalog(outws)
    import gc
    gc.collect()
    arcpy.Delete_management("in_memory")
```

APPENDIX C

Digital Survey Methods

Ring-Midden Identification

The digital survey approach involved the visual inspection of a sample of individual tiles generated from the lidar data by means of geographic information system (GIS) software. GIS layers inspected during the digital survey included a hillshade, local-relief models (LRMs), topographic-position indexes (TPIs), and the automated feature identification (AFI) centroids that were generated for each individual tile. First, the hillshade for each individual tile was inspected at the scale of the entire tile to identify prominent ring-midden-like features. Each potential feature identified at this scale was more closely inspected at a smaller scale to determine if it exhibited attributes consistent with ring-midden morphology. Next, the hillshade, LRM, and TPI layers were viewed, with the hillshade displayed over the LRM with a transparency set at 60 percent, to delineate the polygon. All potential ring middens were marked by drawing an elliptical polygon encapsulating the feature around the outside lower edge of the ring-midden feature. Definition and shape attributes were entered into the shapefile attribute table for each ring-midden polygon recorded during the digital survey (Tables C.1 and C.2).

Figures C.1 and C.2 provide examples of both definition and shape attributes used during the digital survey.

Each tile was then visually scanned at the scale of $^1/_9$ of the tile beginning with the northwest corner of the tile. All potential ring-midden features were closely examined and were identified by creating polygons with shape and definition attributes. The tile was then panned from west to east and inspected, and visible ring middens were recorded. This process was repeated moving from west to east and north to south until each $^1/_9$ section was completely examined.

The azimuth was determined by recording the high side of each ring-midden feature. For each feature, a polyline was created starting from the center of the ring-midden depression and extending to the highest portion of the rock berm. The polylines were used to calculate the azimuth of each feature via the polyline_get_azimuth tool in ArcGIS.

Ring-Midden Profiles

A random subsample of ring-midden features identified during the digital survey was selected to generate a sample of ring-midden profiles, or contours, using digital elevation models (DEMs) generated from the lidar data. Profiles were drawn to capture both the major and the minor axes of the sampled features. The profile lines were drawn to bisect each feature by means of intercardinal azimuths (northwest to southeasat; southwest to northeast). Each profile line was created via a polyline shapefile. Profile 1 extended from the northwest to the southeast axis, starting in the northwestern quadrant; Profile 2 extended along the southwest–northeast axis, starting in the southwestern quadrant of the feature. Profile lines were generated by means of the ArcGIS 3-D Analyst Interpolate Line tool. Then, *x*- and *y*-coordinate data generated from the interpolated profile lines were viewed and downloaded into an Excel file via the Profile Graph function. These resulting *x*/*y* data were then used to calculate a series of metric statistics and profile graphs for each sampled feature.

Table C.1. Definition Attributes of Ring Middens

Definition Code	Interpretation
1	well defined
2	moderately well defined
3	faint but possible
4	indistinct
5	probably not a ring midden but recorded for comparative purposes

Table C.2. Shape Attributes of Ring Middens

Shape Code	Interpretation
1	closed ring (closed ring with small openings)
2	open ring
3	irregular discontinuous ring
4	ring with mounded lobe
5	atypical

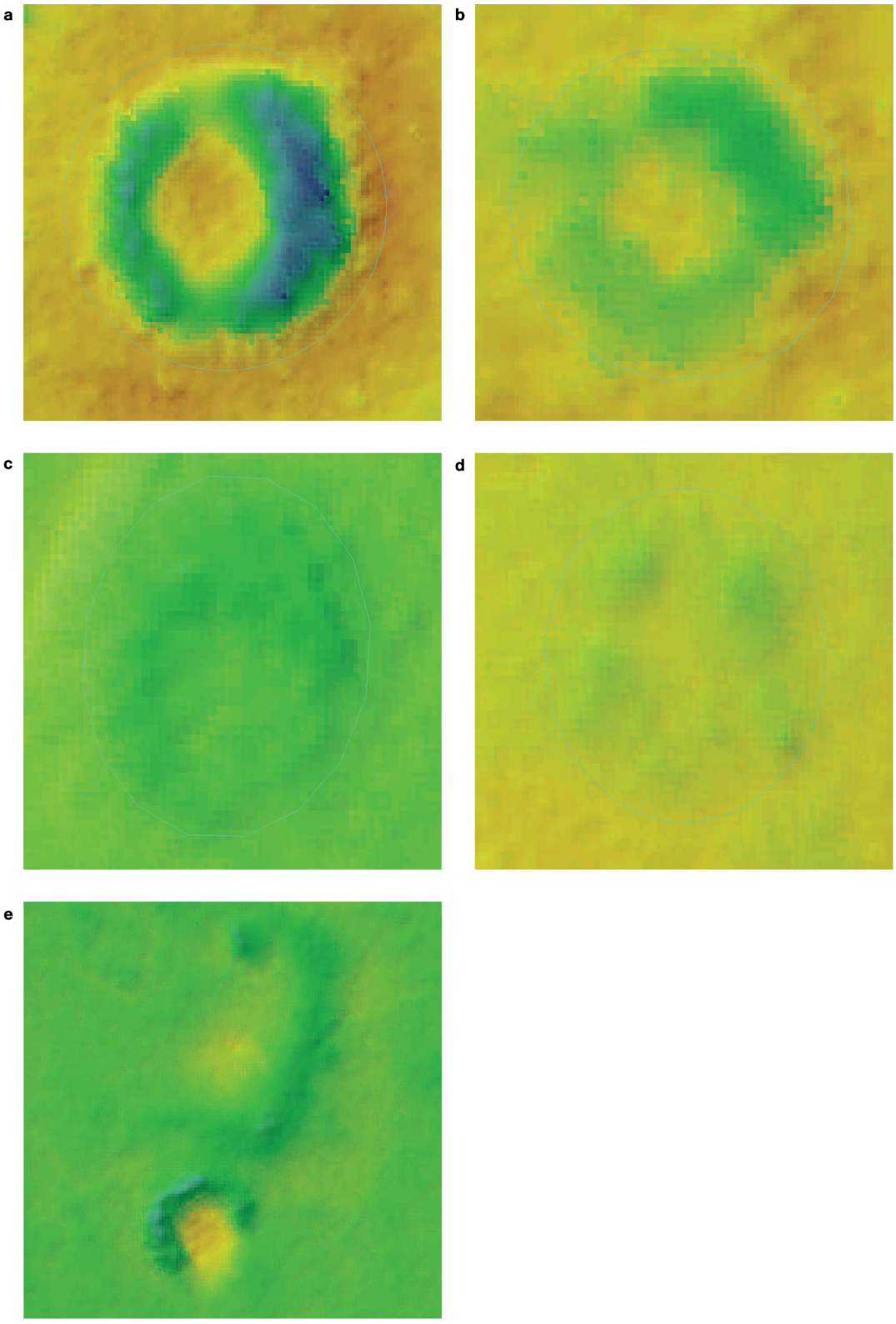

Figure C.1. Examples of definition attributes used during the digital survey: (*a*) Definition Code 1: well defined; (*b*) Definition Code 2: moderately well defined; (*c*) Definition Code 3: faint but possible; (*d*) Definition Code 4: indistinct; (*e*) Definition Code 5: probably not a ring midden but recorded for comparative purposes.

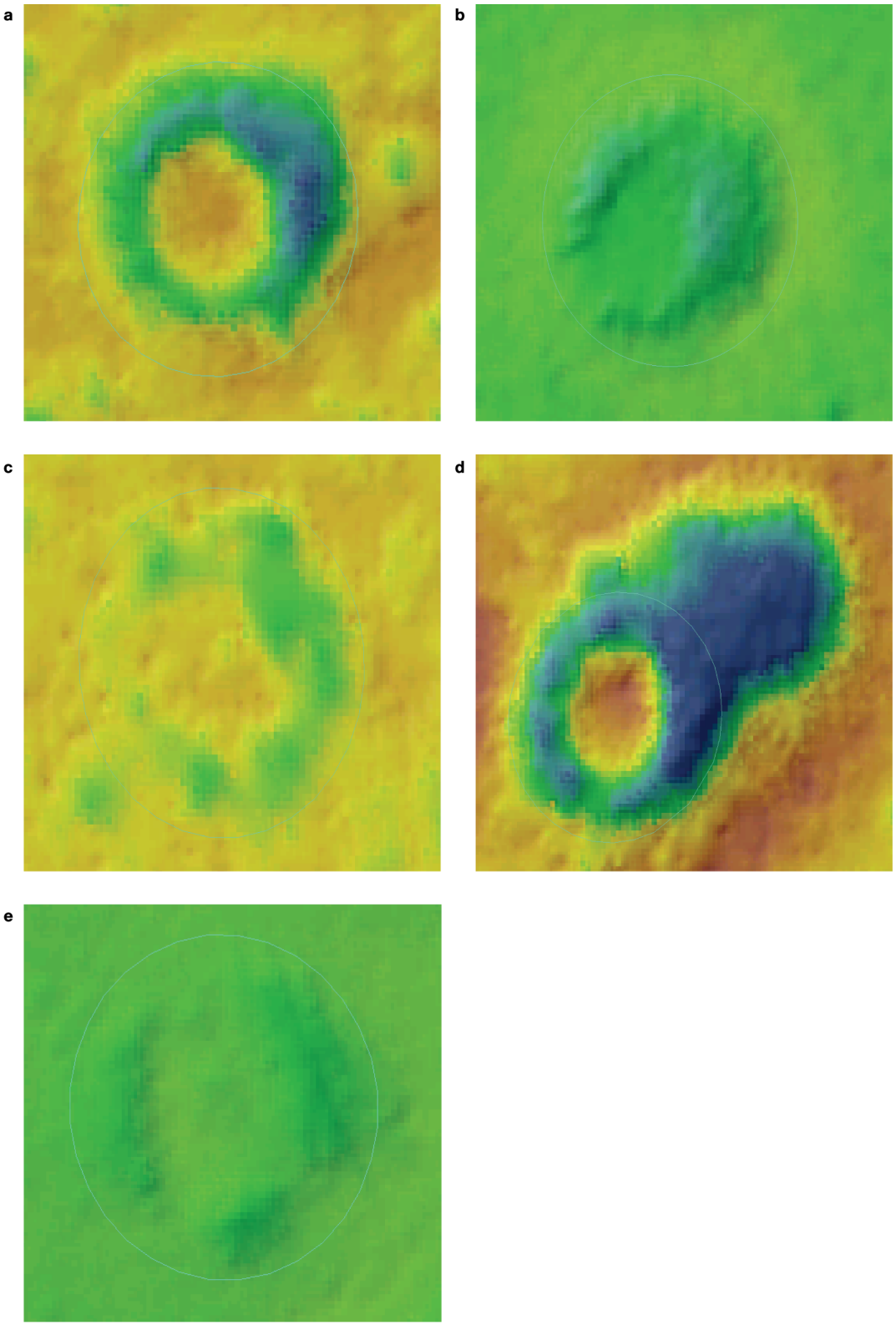

Figure C.2. Examples of shape attributes used during the digital survey: (*a*) Shape Code 1: closed ring; (*b*) Shape Code 2: open ring; (*c*) Shape Code 3: irregular discontinuous ring; (*d*) Shape Code 4: ring with mounded lobe; (*e*) Shape Code 5: atypical.

Site Descriptions Resulting from Field-Verification Efforts

Upper Rio Felix Study Area

LA 181701 (SRI-1)

Site Setting

LA 181701 is situated along a Holocene-aged terrace located at the confluence of Rio Felix and two south-trending unnamed tributaries, one of which originates from Scotty Canyon. The site has been subject to periodic inundation, and thick alluvial silt deposits blanket the terrace surface. A broad, Pleistocene-aged strath terrace cut into San Andres formation limestone borders the extent of the Rio Felix floodplain and its associated tributary drainages. Vegetation in this area is typical of desert scrubland; it includes desert holly (*Atriplex hymenelytra*), desert willow (*Chilopsis linearis*), croton (*Croton*), rainbow cactus (*Echinocereus pectinatus*), claretcup cactus (*Echinocereus triglochidiatus*), cholla (*Cylindropuntia*), tabosa grass (*Hilaria mutica*), soaptree yucca (*Yucca elata*), Torrey yucca (*Yucca treculeana*), and various forbs. The diversity and density of succulent-scrub species increase along the limestone uplands bordering the floodplain; the terrace surface is dominated by grasses and forbs because of the thick silt accumulations deposited across this area. The site is moderately intact, having suffered some degree of erosion that has resulted in the dispersal of many of the ring-midden features. Most of the features exhibit a moderate degree of disarticulation, and many are buried by thick accumulations of silt. Additional modern disturbances within this area include livestock grazing.

Site Description

LA 181701 is a specialized-activity area or roasting locale dating to the Formative period. This area probably was episodically revisited, and only intermittently occupied, throughout Formative times. The site consists of a dense concentration of sizable roasting features situated along the lowermost terrace formed between two unnamed tributaries that converge with Rio Felix immediately to the south. In total, 20 features have been recorded in association with LA 181701, including both ring middens and fire-cracked-rock (FCR) middens. FCR is the most ubiquitous material present across the site surface; only a handful of associated artifacts have been documented among the features. The paucity of artifacts, most of which consist of retouched tools, suggests that the site did not support any sort of long-term occupational events; rather, it probably was visited specifically for the purposes of resource procurement and processing.

FCR middens recorded at the site are very likely to be the disarticulated remains of ring-midden features. Most of the ring middens recorded at the site lack a clear definition because many are partially buried in silt and dispersed by alluvial erosion. Furthermore, many of the features situated along the edges of the terrace have been further eroded downslope as a result of down-cutting processes. Only one of the ring middens (Feature 21) includes associated datable deposits; another ring midden (Feature 33) includes an intact slab-lined hearth. No associated charcoal or ash was observed within the confines of the feature with the intact hearth, however, and this ring midden has partially eroded down the slope of the terrace edge.

Features

Feature 3 is an FCR midden that measures 280 cm north–south and 350 cm east–west and extends 20 cm above the ground surface. It is composed of an estimated 125 burned-limestone fragments. The FCR midden is ovate in plan, and no central depression is evident. A trowel probe used to assess characteristics of the associated deposits indicated that it lacks any evidence of datable material. The feature exhibits a moderate degree of modern impact, and an ant mound is present within the center of the midden where a depression would be expected. No artifacts were documented in direct association with the feature.

Feature 5 is a ring midden that measures 1,250 cm north–south and 800 cm east–west and extends 40 cm above the ground surface. It is composed of an estimated 2,550 burned-limestone fragments. The midden is characterized by a semicircular berm of FCR that is open to the north; it lacks a well-defined central depression. A trowel probe used to assess characteristics of the associated deposits indicated that it lacks any evidence of datable material. The feature exhibits a high degree of modern impact from alluvial erosion and is mostly buried in silt. No artifacts were documented in direct association with the feature.

Feature 7 is a ring midden that measures 675 cm north–south and 550 cm east–west and extends 30 cm above the ground surface. It is composed of an estimated 400 burned-limestone fragments. The midden is characterized by a semicircular rock berm that is open to the northwest; it contains a slight central depression. A trowel probe used to assess characteristics of the associated deposits indicated that it lacks any evidence of datable material. The feature exhibits a low degree of modern impact from alluvial erosion and has been partially displaced down the slope of the terrace edge. No artifacts were documented in direct association with the feature.

Feature 9 is a ring midden that measures 600 cm north–south and 950 cm east–west and extends 20 cm above the ground surface. It is composed of an estimated 2,000 burned-limestone fragments. The midden is characterized by a semicircular rock berm of FCR that is open to the north; it lacks a well-defined central depression. A trowel probe used to assess characteristics of the associated deposits indicated that it lacks any evidence of datable material. The feature exhibits a high degree of modern impact from alluvial erosion resulting in dispersal by inundation, and the southern portion of the feature is displaced down the slope of the terrace edge. No artifacts were documented in direct association with the feature.

Feature 11 is a ring midden that measures 850 cm north–south and 950 cm east–west and extends 35 cm above the ground surface. It is composed of an estimated 3,000 burned-limestone fragments. The midden is characterized by a semicircular rock berm that is open to the west; it has a slight central depression. A trowel probe used to assess characteristics of the associated deposits indicated that it lacks any evidence of datable material. The feature exhibits a moderate degree of modern impact from alluvial erosion resulting in dispersal by inundation. No artifacts were documented in direct association with the feature.

Feature 13 (FID 479) is a ring midden that measures 700 cm in diameter and extends 30 cm above the ground surface. It is composed of an estimated 1,000 burned-limestone fragments. The midden is characterized by a semicircular rock berm that is open to the west; it has a slight central depression. A trowel probe used to assess characteristics of the associated deposits indicated that it lacks any evidence of datable material. The feature exhibits a moderate degree of modern impact from alluvial erosion resulting in dispersal by inundation and is also partially buried in alluvial silt. No artifacts were documented in direct association with the feature.

Feature 15 (FD 474) is a ring midden that measures 750 cm north–south and 700 cm east–west and extends 20 cm above the ground surface. It is composed of an estimated 2,500 burned-limestone fragments. The midden is characterized by a circular enclosed ring with a central depression and is appended to the southwestern edge of Feature 13. A trowel probe used to assess characteristics of the associated deposits indicated that it lacks any evidence of datable material. The feature exhibits a moderate degree of modern impact from inundation and is partially buried in alluvial silt. Two undifferentiated brown ware body sherds were documented in direct association with the feature.

Feature 17 (FID 473) is a ring midden that measures 600 cm north–south and 650 cm east–west and extends only 10 cm above the ground surface. It is composed of an estimated 3,000 burned-limestone fragments. The midden is characterized by a circular enclosed ring with a slight central depression. A trowel

probe used to assess characteristics of the associated deposits indicated that it lacks any evidence of datable material. The feature exhibits a moderate degree of modern impact, and inundation has mostly buried the feature in silt. No artifacts were documented in direct association with the feature.

Feature 19 is a ring midden that measures 600 cm north–south and 550 cm east–west and extends only 15 cm above the ground surface. It is composed of an estimated 2,050 burned-limestone fragments. The midden is characterized by a semicircular rock berm open to the north, with a slight central depression. A trowel probe used to assess characteristics of the associated deposits indicated that it lacks any evidence of datable material. The feature exhibits a moderate degree of modern impact, and inundation has mostly buried the feature in silt. No artifacts were documented in direct association with the feature.

Feature 21 is a ring midden that measures 1,200 cm north–south and 900 cm east–west and extends 35 cm above the ground surface. It is composed of an estimated 5,000 burned-limestone fragments. The midden is characterized by a semicircular rock berm open to the west, with a central depression. A trowel probe used to assess characteristics of the associated deposits indicated that the feature contains datable material, and dark organic material probably cleaned out from the central depression is present along the rock berm. The feature exhibits a moderate degree of modern impact, and inundation has mostly buried it in silt. Artifacts documented in direct association with the feature include 3 undifferentiated brown ware sherds, a chert biface flake, and a limestone retouched flake.

Feature 23 is a FCR midden that measures 700 cm north–south and 500 cm east–west and extends approximately 15 cm above the ground surface. It is composed of an estimated 500 burned-limestone fragments. This FCR midden is appended to the eastern edge of Feature 21. This feature may be an eroded ring midden or may just be a dump of rocks associated with the use of Feature 21. A trowel probe used to assess characteristics of the associated deposits indicated that it lacks any evidence of datable material. The feature exhibits a high degree of modern impact, and inundation has mostly buried the feature in silt. No artifacts were documented in direct association with the feature.

Feature 25 (FID 475) is a ring midden that measures 600 cm in diameter and extends only 10 cm above the ground surface. It is composed of an estimated 800 burned-limestone fragments. The midden is characterized by an enclosed ring, with only a very slight central depression. A trowel probe used to assess characteristics of the associated deposits indicated that it lacks any evidence of datable material. The feature exhibits a moderate degree of modern impact, and inundation has mostly buried the feature in silt. No artifacts were documented in direct association with the feature.

Feature 27 (FID 476) is a ring midden that measures 690 cm in diameter and extends only 10 cm above the ground surface. It is composed of an estimated 450 burned-limestone fragments. The midden is characterized by a circular distribution of FCR lacking any observable central depression. A trowel probe used to assess characteristics of the associated deposits indicated that it lacks any evidence of datable material. The feature exhibits a moderate degree of modern impact, and inundation has mostly buried the feature in silt. No artifacts were documented in direct association with the feature.

Feature 29 is a FCR midden that measures 500 cm in diameter and extends approximately 40 cm above the ground surface. It is composed of an estimated 300 burned-limestone fragments. The feature may be the remains of an eroded ring midden. A trowel probe used to assess characteristics of the associated deposits indicated that it lacks any evidence of datable material. The feature exhibits a high degree of modern impact, and inundation has mostly buried the feature in silt. No artifacts were documented in direct association with the feature.

Feature 31 (FID 472) is a ring midden that measures 950 cm north–south and 800 cm east–west and extends approximately 40 cm above the ground surface. It is composed of an estimated 1,500 burned-limestone fragments. The midden is characterized by an enclosed ring, with only a very slight central depression. A trowel probe used to assess characteristics of the associated deposits indicated that it lacks any evidence of datable material. The feature exhibits a moderate degree of modern impact from inundation. No artifacts were documented in direct association with the feature.

Feature 33 (FID 478) is a ring midden that measures 750 cm north–south and 800 cm east–west and extends approximately 45 cm above the ground surface. It is composed of an estimated 3,000 burned-limestone fragments. An intact slab-lined hearth is preserved within the center of the midden, but it lacks a

central depression. A trowel probe used to assess characteristics of the associated deposits indicated that it lacks any evidence of datable material. The feature exhibits a moderate degree of modern impact from inundation, and FCR has been displaced downslope along the northern edge of the terrace. No artifacts were documented in direct association with the feature.

Feature 35 (FID 471) is a ring midden that measures 680 cm north–south and 860 cm east–west and extends approximately 30 cm above the ground surface. It is composed of an estimated 3,500 burned-limestone fragments. The midden is characterized by an enclosed ring with a central depression. A trowel probe used to assess characteristics of the associated deposits indicated that it lacks any evidence of datable material. The feature exhibits a moderate degree of modern impact from inundation. No artifacts were documented in direct association with the feature.

Feature 37 (FID 477) is a ring midden that measures 540 cm north–south and 700 cm east–west and extends approximately 30 cm above the ground surface. It is composed of an estimated 3,500 burned-limestone fragments. The midden is characterized by an enclosed ring with a central depression. A trowel probe used to assess characteristics of the associated deposits indicated that it lacks any evidence of datable material. The feature exhibits a moderate degree of modern impact from inundation. A single chert scraper was documented in direct association with the feature.

Feature 39 is a ring midden that measures 600 cm north–south and 660 cm east–west and extends approximately 15 cm above the ground surface. It is composed of an estimated 750 burned-limestone fragments. The midden is characterized by an enclosed ring with a slight central depression. A trowel probe used to assess characteristics of the associated deposits indicated that it lacks any evidence of datable material. The feature exhibits a moderate degree of modern impact from inundation. No artifacts were documented in direct association with the feature.

Feature 41 is a ring midden that measures 650 cm north–south and 700 cm east–west and extends approximately 30 cm above the ground surface. It is composed of an estimated 2,000 burned-limestone fragments. The midden is characterized by an enclosed ring with a slight central depression. A trowel probe used to assess characteristics of the associated deposits indicated that it lacks any evidence of datable material. The feature exhibits a moderate degree of modern impact from inundation. A chert biface was documented in direct association with the feature.

Artifacts

Tens of artifacts were observed among this dense concentration of roasting features; most of the lithic items are retouched tools. Lithic tools include a small variety of formal bifaces (one of which is a small preform suitable for an arrow-sized point); a tabular knife; a scraper; and an informal, elongated retouched flake exhibiting marginally invasive retouch, which appears to have functioned as a knife. The few tools at the site, such as the tabular knife and the knifelike retouched flake, have been previously interpreted as associated with succulent-processing activities. The paucity of debitage found among the features suggests that lithic tools probably were transported to the site as finished items rather than being manufactured on-site. Raw materials observed among the lithics include both undifferentiated cherts and a single piece of San Andres "fingerprint" chert, as well as locally available limestone. Only a single piece of ground stone, consisting of an indeterminate metate fragment, was recorded. Ceramic artifacts consist of a handful undifferentiated brown ware body sherds, indicating that the site dates generally to the Formative period, between A.D. 200 and 1450.

Site Summary

LA 181701 is a specialized-activity site consisting of a Formative period temporal component. Twenty large roasting features (ring middens and FCR middens), accompanied by a low-density scatter of lithic and ceramic artifacts, were recorded at the site. Among the scant artifacts is a prevalence of lithic tools

associated with plant-processing activities. Diagnostic artifacts associated with the site indicate a general Formative period temporal affiliation.

Many of the features exhibit impacts from periodic inundation along the floodplain, including both the displacement of ring-midden berms and partial burial in alluvial silt. Consequently, only one of the ring middens contains organic materials suitable for radiometric dating. However, features might include datable deposits that are concealed by alluvial silt. Furthermore, recent investigations of large earth-oven features within the western foothills of the Sacramento Mountains revealed that residential structures have been identified in direct association with FCR middens (Ward and Vierra 2011). This site contains the largest number and diversity of ring-midden features among sites from the three study areas and has the potential to yield additional information relevant to various general and Formative period research questions relating to chronology, subsistence, and settlement, including the following (Hogan 2006):

- When was the site occupied?
- What plant food resources were collected, processed, and/or consumed by the sites inhabitants?
- What seasonal variation was there in the procurement of food resources?
- What were the subsistence resource staples?
- What areas were the foci of subsistence activities?
- What was the relative contribution of hunting, gathering, and cultivation?
- Could the available mix of food resources in the area support a year round occupation, or would resources in other areas have to be exploited at some point in the annual round?
- What were the annual rounds of Ceramic period hunter-gatherers in the different parts of the region?
- Was residential or logistical mobility employed in the procurement of wild plant resources?

Therefore, LA 181701 is recommended eligible for listing in the National Register of Historic Places (NRHP), under Criterion d.

Azotea Mesa Study Area

LA 130591 (SRI-44)

Site Setting

LA 130591 is situated along a series of Holocene-aged terraces located at the coalescence of two unnamed tributaries of Little McKittrick Draw. The north–south-trending drainage is bordered by a steep terrace strath cut into San Andres formation limestone. Hackberry Hills are located immediately to the east, and McGruder Hill is situated directly southwest, of the site. Vegetation in this area is typical of Chihuahuan desert scrubland and includes juniper (*Juniperus*), mesquite (*Prosopis*), acacia (*Senegalia*), soaptree yucca, Torrey yucca, lechuguilla (*Agave lecheguilla*), sotol (*Dasylirion*), rainbow cactus, claretcup cactus, cholla, Christmas cholla (*Cylindropuntia leptocaulis*), pincushion cactus (*Mammillaria*), prickly pear (*Opuntia*), broom snakeweed (*Gutierrezia sarothrae*), pepperweed (*Lepidium*), silver desert-thorn (*Lycium berlandieri*), beargrass (*Nolina*), and various forbs. A large diversity of succulent-scrub species is present across the limestone talus slopes bordering the floodplain. The site is well preserved, with no evidence of any substantive disturbances. Most of the features are intact; only a few appear to have been minimally eroded, and some include animal burrows present within the central depression.

Site Description

LA 130591 is a specialized-activity locale including a concentration of large roasting features with diagnostic artifacts suggestive of a Late Formative period temporal affiliation. The site probably was episodically revisited, representing only intermittent occupations, spanning throughout Formative times. A dense concentration of sizable ring middens and FCR features is present across the terraces. In total, 16 ring-midden features were recorded, in addition to 8 previously recorded small FCR concentrations that were not investigated during the course of the Statistical Research, Inc. (SRI), site update. FCR is by far the most ubiquitous material present across the site surface; only a few scattered lithic and ceramic artifacts were observed among the features. The paucity of artifacts, most of which consist of retouched tools, suggests that the site did not support any sort of long-term occupational events; rather, it probably was visited specifically for the purposes of resource procurement and processing. This site includes a large diversity of succulent-shrub species that probably were targeted by prehistoric populations inhabiting this area. Most of the ring middens recorded at the site are well preserved; some of them have sizable berms obtruding 1–2 m above the ground surface. Half of the ring middens (Features 46, 50, 52, 54, 58, 60, 62, and 74) include associated organic deposits suitable for radiometric dating.

Features

Feature 46 (FID 79) is a ring midden that measures 1,300 cm north–south and 1,400 cm east–west and extends approximately 60 cm above the ground surface. It is composed of an estimated 10,000 burned-limestone fragments. The midden is characterized by an enclosed ring with a deep central depression. A trowel probe used to assess characteristics of the associated deposits indicated that it contains datable material. The feature exhibits a low degree of modern impact. No artifacts were documented in direct association with the feature.

Feature 48 is a ring midden that measures 1,100 cm north–south and 900 cm east–west and extends approximately 20 cm above the ground surface. It is composed of an estimated 8,000 burned-limestone fragments. The midden is characterized by an enclosed ring with a central depression. A trowel probe used to assess characteristics of the associated deposits indicated that it lacks any evidence of datable material. The feature exhibits a moderate degree of modern impact, the noted disturbance consisting of an animal burrow present within the central depression. A single chert uniface was documented in direct association with the feature.

Feature 50 (FID 90) is a ring midden that measures 700 cm north–south and 800 cm east–west and extends approximately 20 cm above the ground surface. It is composed of an estimated 9,000 burned-limestone fragments. The midden is characterized by a semicircular rock berm open to the southeast with a central depression. A trowel probe used to assess characteristics of the associated deposits indicated that it contains datable material. The feature exhibits a moderate degree of modern impact. No artifacts were documented in direct association with the feature.

Feature 52 (FID 78) is a ring midden that measures 1,000 cm north–south and 1,040 cm east–west and extends approximately 30 cm above the ground surface. It is composed of an estimated 13,000 burned-limestone fragments. The midden is characterized by a semicircular rock berm open to the north with a central depression. A trowel probe used to assess characteristics of the associated deposits indicated that it contains datable material. The feature exhibits a low degree of modern impact. No artifacts were documented in direct association with the feature.

Feature 54 (FID 77) is a sizable, well-preserved ring midden that measures 1,200 cm north–south and 1,230 cm east–west and extends around 200 cm above the ground surface. It is composed of an estimated 30,000 burned-limestone fragments. The midden is characterized by an enclosed ring with a central depression. A trowel probe used to assess characteristics of the associated deposits indicated that it contains datable material. The feature exhibits a low degree of modern impact with a recent animal burrow present within the central depression. No artifacts were documented in direct association with the feature.

Feature 56 (FID 80) is a ring midden that measures 950 cm north–south and 850 cm east–west and extends only 15 cm above the ground surface. It is composed of an estimated 7,000 burned-limestone fragments. The midden is characterized by a semicircular berm open to the west with a central depression. A trowel probe used to assess characteristics of the associated deposits indicated that it lacks any evidence of datable material. The feature exhibits a moderate degree of modern impact. A single quartzite retouched piece was documented in direct association with the feature.

Feature 58 (FID 87) is a ring midden that measures 1,000 cm north–south and 1,050 cm east–west and extends approximately 30 cm above the ground surface. It is composed of an estimated 9,000 burned-limestone fragments. The midden is characterized by an enclosed ring with a central depression. A trowel probe used to assess characteristics of the associated deposits indicated that it contains datable material. The feature exhibits a moderate degree of modern impact. No artifacts were documented in direct association with the feature.

Feature 60 (FID 84) is a well-preserved ring midden that measures 1,100 cm in diameter and extends approximately 100 cm above the ground surface. It is composed of an estimated 17,000 burned-limestone fragments. The midden is characterized by an enclosed ring with a central depression. A trowel probe used to assess characteristics of the associated deposits indicated that it contains datable material. The feature exhibits a low degree of modern impact. No artifacts were documented in direct association with the feature.

Feature 62 (FID 81) is a sizable ring midden that measures 1,200 cm north–south and 1,260 cm east–west and extends an impressive 200 cm above the ground surface. It is composed of an estimated 30,000 burned-limestone fragments. The midden is characterized by an enclosed ring with a central depression. A trowel probe used to assess characteristics of the associated deposits indicated that it contains datable material. The feature exhibits a low degree of modern impact. No artifacts were documented in direct association with the feature.

Feature 64 (FID 89) is a ring midden that measures 900 cm north–south and 1,100 cm east–west and extends approximately 20 cm above the ground surface. It is composed of an estimated 30,000 burned-limestone fragments. The midden is characterized by an enclosed ring with no central depression. A trowel probe used to assess characteristics of the associated deposits indicated that it lacks any evidence of datable material. The feature exhibits a moderate degree of modern impact. A chert retouched flake and a piece of limestone angular debris were documented in direct association with the feature.

Feature 66 (FID 88) is a ring midden that measures 950 cm north–south and 1,050 cm east–west and extends only 5 cm above the ground surface. It is composed of an estimated 10,000 burned-limestone fragments. The midden is characterized by an enclosed ring with no central depression. A trowel probe used to assess characteristics of the associated deposits indicated that it lacks any evidence of datable material. The feature exhibits a high degree of modern impact and appears to be heavily eroded. A quartzite retouched piece was documented in direct association with the feature.

Feature 68 is a terraced ring midden that measures 950 cm north–south and 850 cm east–west and extends approximately 100 cm above the ground surface along the terraced edge. It is composed of an estimated 9,000 burned-limestone fragments. The midden is characterized by a semicircular rock berm open to the east with no central depression. A trowel probe used to assess characteristics of the associated deposits indicated that it lacks any evidence of datable material. The feature exhibits a moderate degree of modern impact. A Three Rivers Red-on-terracotta body sherd was documented in direct association with the feature.

Feature 70 (FID 83) is a ring midden that measures 900 cm north–south and 1,000 cm east–west and extends only 5 cm above the ground surface. It is composed of an estimated 10,000 burned-limestone fragments. The midden is characterized by a semicircular rock berm open to the east with no central depression. A small stockpile of limestone rocks was also recorded along the southeastern edge of the berm. A trowel probe used to assess characteristics of the associated deposits indicated that it lacks any evidence of datable material. The feature exhibits a moderate degree of modern impact. No artifacts were documented in direct association with the feature.

Feature 72 (FID 86) is a ring midden that measures 1,100 cm in diameter and extends approximately 20 cm above the ground surface. It is composed of an estimated 8,000 burned-limestone fragments. The midden is characterized by an enclosed ring with a central depression. A trowel probe used to assess characteristics

of the associated deposits indicated that it lacks any evidence of datable material. The feature exhibits a moderate degree of modern impact. No artifacts were documented in direct association with the feature.

Feature 74 (FID 85) is a ring midden that measures 900 cm in diameter and extends approximately 10 cm above the ground surface. It is composed of an estimated 8,000 burned-limestone fragments. The midden is characterized by an enclosed ring with a central depression and was constructed along the eastern edge of Feature 76, thereby sharing a berm with the larger adjacent feature. A trowel probe used to assess characteristics of the associated deposits indicated that it contains datable material. The feature exhibits a low degree of modern impact. No artifacts were documented in direct association with the feature.

Feature 76 (FID 82) is a sizable and well-preserved ring midden that measures 1,400 cm in diameter and extends approximately 70 cm above the ground surface. It is composed of an estimated 50,000 burned-limestone fragments. The midden is characterized by an enclosed ring with a central depression and shares a berm with the smaller, adjacent Feature 74. A trowel probe used to assess characteristics of the associated deposits indicated that it lacks any evidence of datable material. The feature exhibits a low degree of modern impact. No artifacts were documented in direct association with the feature.

Artifacts

Fewer than ten artifacts were observed, most of which consist of flaked stone tools along with a few ceramic sherds. FCR figures most prominently among the lithic materials recorded at the site. The retouched tools include a uniface, a few retouched flakes, and a single core flake. The lack of any substantial debitage suggests that tools were brought to the site as finished items. Raw materials include undifferentiated chert, quartzite, and limestone. The ceramic artifacts include a single undifferentiated brown ware body sherd and a Three Rivers Red-on-terracotta body sherd reflecting a Late Formative period component, dating to A.D. 1125–1300. A few fragments of sun-colored-amethyst glass were also recorded at the site, representing an isolated historical-period manifestation.

Site Summary

LA 130591 is a specialized-activity site representing a Late Formative period temporal component. Sixteen large ring middens, accompanied by a low-density scatter of lithic and ceramic artifacts, were recorded at the site. Eight additional FCR concentrations previously recorded at the site were not investigated during the SRI update. Among the scant artifacts is a prevalence of lithic tools representing an emphasis on wild-plant processing. Prehistoric populations probably targeted the rich diversity of succulent-scrub species growing along the limestone canyon edges as an abundant source of wild-food resources. Diagnostic artifacts associated with the site indicate a Late Formative period temporal affiliation.

Many of the features are well preserved, with sizable berms, and half of the ring middens contain organic materials suitable for radiometric dating. Recent investigations of large earth-oven features within the western foothills of the Sacramento Mountains revealed that residential structures have been identified near FCR middens (Ward and Vierra 2011), and habitation structures may be located near the site. This site has the potential to yield additional information relevant to various general and Formative period research questions relating to chronology, subsistence, and settlement, including the following (Hogan 2006):

- When was the site occupied?
- What plant food resources were collected, processed, and/or consumed by the sites inhabitants?
- What seasonal variation was there in the procurement of food resources?
- What were the subsistence resource staples?
- What areas were the foci of subsistence activities?
- What was the relative contribution of hunting, gathering, and cultivation?
- Could the available mix of food resources in the area support a year round occupation, or would resources in other areas have to be exploited at some point in the annual round?

- What were the annual rounds of Ceramic period hunter-gatherers in the different parts of the region?
- Was residential or logistical mobility employed in the procurement of wild plant resources?

Therefore, LA 130591 is recommended eligible for listing in the NRHP, under Criterion d.

Box Canyon Study Area

LA 181702 (SRI-78)

Site Setting

LA 181702 is situated along the southern Holocene-aged terrace surface of Box Canyon Draw. A steep, Pleistocene-aged strath terrace cut into San Andres formation limestone borders the northern extent of Box Canyon near the site. The southern margin of the canyon wall is more gradual in relief. Vegetation in this area is typical of Chihuahuan desert scrubland and includes juniper, mesquite, soaptree yucca, Torrey yucca, Spanish dagger (*Yucca baccata*), slim-footed agave (*Agave gracilipes*), Parry's agave (*Agave parryi*), sotol, rainbow cactus, claretcup cactus, cholla, Christmas cholla, pincushion cactus, prickly pear, broom snakeweed, beargrass, and various forbs. This site includes the highest diversity of succulent-scrub species growing along the floodplain and adjacent Pleistocene-aged limestone terrace. The site is moderately intact, having suffered some degree of disturbance from modern camping and a two-track road that has heavily impacted one of the ring-midden features. The integrity of the remaining features has not been severely compromised by modern disturbances. A recently used campfire ring made of stacked limestone and a few scattered modern brown-glass bottles are also present at the site.

Site Description

LA 181702 is a specialized-activity locale characterized by a circular concentration of large roasting features with a few associated diagnostic artifacts suggestive of a Late Formative period temporal affiliation. The immediate site area may have been episodically revisited, representing a series of intermittent specialized uses, spanning throughout Formative times. However, several rockshelters are visible along the northern canyon escarpment, and these natural features may have been used for habitation during prehistoric times. Accordingly, this site contains the largest density of lithic debitage, reflecting a slightly greater diversity of domestic activities than the other investigated ring-midden sites. In total, six ring-midden features were recorded at the site. FCR is by far the most ubiquitous material present across the site surface; only tens of lithic and ceramic artifacts were observed among the features. The paucity of artifacts found among the features suggests that the immediate site area did not support long-term occupational events; rather, it probably was visited specifically for the purposes of resource procurement and processing. This site includes a large diversity of succulent-shrub species that probably were targeted by prehistoric populations inhabiting this area. Most of the ring middens recorded at the site are well preserved; some of them include sizable berms obtruding almost 1 m above the ground surface. Notably, one of the ring middens has been heavily disturbed by a modern two-track that bisects the site. It is mostly flattened and was noted only by the presence of a circular distribution of FCR only very slightly obtruding from the modern surface. Half of the ring middens (Features 80, 84, and 88) include associated organic deposits suitable for radiometric dating.

Features

Feature 80 (FID 370) is a ring midden that measures 930 cm north–south and 960 cm east–west and extends approximately 95 cm above the ground surface. It is composed of an estimated 15,000 burned-limestone fragments. The midden is characterized by an enclosed ring with a central depression. A trowel probe used to assess characteristics of the associated deposits indicated that it contains datable material. The feature exhibits a moderate degree of modern impact. Artifacts documented in direct association with the feature include 3 chert core flakes, 2 pieces of chert angular debris, a silicified-wood core flake, and 2 undifferentiated brown ware body sherds, one of which exhibits a red surface treatment that suggests that it may be an El Paso decorated sherd.

Feature 82 (FID 371) is a ring midden that measures 1,050 cm north–south and 1,150 cm east–west and extends approximately 70 cm above the ground surface. It is composed of an estimated 17,000 burned-limestone fragments. The midden is characterized by an enclosed ring with a central depression. A trowel probe used to assess characteristics of the associated deposits indicated that it lacks evidence of datable material. The feature exhibits a low degree of modern impact. Artifacts documented in direct association with the feature include 3 chert core flakes and a single piece of chert angular debris.

Feature 84 (FID 373) is a ring midden that measures 900 cm in diameter and extends approximately 35 cm above the ground surface. It is composed of an estimated 10,000 burned-limestone fragments. The midden is characterized by an enclosed ring with a central depression. A trowel probe used to assess characteristics of the associated deposits indicated that it contains datable material. The feature exhibits a moderate degree of modern impact. Artifacts documented in direct association with the feature include 2 chert core flakes, a limestone core flake, a chert indeterminate flake fragment, and a quartzite tabular knife.

Feature 86 (FID 372) is a ring midden that measures 790 cm north–south and 750 cm east–west and extends 45 cm above the ground surface. It is composed of an estimated 10,000 burned-limestone fragments. The midden is characterized by a semicircular rock berm open to the east and includes a central depression. A trowel probe used to assess characteristics of the associated deposits indicated that it lacks any evidence of datable material. The feature exhibits a moderate degree of modern impact. Artifacts documented in direct association with the feature include a chert retouched flake and an undetermined sandstone metate fragment.

Feature 88 (FID 369) is a ring midden that measures 1,000 cm in diameter and extends 95 cm above the ground surface. It is composed of an estimated 12,000 burned-limestone fragments. The midden is characterized by a semicircular rock berm open to the east and includes a central depression. A trowel probe used to assess characteristics of the associated deposits indicated that it contains datable material. The feature exhibits a low degree of modern impact. Artifacts documented in direct association with the feature include a chert core, a chert core flake, a limestone retouched flake, and a limestone tabular knife.

Feature 90 is a heavily disturbed ring midden that measures 930 cm north–south and 950 cm east–west and extends 10 cm above the ground surface in some places around the remaining portions of the berm. It is composed of an estimated 1,500 burned-limestone fragments still visible on the surface. The midden is characterized by an enclosed ring with no central depression. The feature has been mostly flattened by use of a two-track road, within which the feature was found. A trowel probe used to assess characteristics of the associated deposits indicated that it lacks any evidence of datable material. The feature exhibits a high degree of modern impact and is almost completely flattened as a result of being driven over. A single piece of chert angular debris was documented in direct association with the feature.

Artifacts

Artifacts at the site number in the tens; most of them consist of flaked stone debitage along with a few retouched tools and ceramic sherds. FCR figures most prominently among the lithic materials recorded at the site. The retouched tools include a few retouched flakes and tabular knives. The lack of any substantial debitage indicates that tools may have been brought to the site mostly as finished items. The handful of debitage found among the features is entirely representative of core-reduction activities. Raw materials include undifferentiated chert, San Andres “fingerprint” chert, quartzite, limestone, and silicified wood.

The ceramic artifacts include two undifferentiated brown ware body sherds, one of which has a red surface treatment that suggests that it may be an El Paso decorated sherd. The presence of a decorated El Paso brown ware ceramic provides a tentative date range of the Middle to Late Formative period, sometime between A.D. 1050 and 1450.

Site Summary

LA 181702 is a specialized-activity site that appears to reflect a Middle to Late Formative period temporal component. In total, six large ring middens accompanied by a low-density scatter of lithic and ceramic artifacts were recorded at the site. Among the scant artifacts are a few flaked stone tools representing an emphasis on wild-plant-processing activities that took place at the site. Prehistoric populations probably targeted the rich diversity of succulent-scrub species growing along the floodplain and adjacent limestone canyon walls as an abundant source of wild-food resources. Diagnostic artifacts associated with the site are suggestive of a Middle to Late Formative period temporal affiliation.

Most of the features are well preserved, with sizable berms, and half of the ring middens contain organic materials suitable for radiometric dating. Recent investigations of large earth-oven features within the western foothills of the Sacramento Mountains revealed that residential structures have been identified in direct association with FCR middens (Ward and Vierra 2011), and habitation structures may be located near the site. Furthermore, natural rockshelters observed along the northern canyon wall could have been used for prehistoric occupation. This site has the potential to yield additional information relevant to various general and Formative period research questions relating to chronology, subsistence, and settlement, including the following (Hogan 2006):

- When was the site occupied?
- What plant food resources were collected, processed, and/or consumed by the sites inhabitants?
- What seasonal variation was there in the procurement of food resources?
- What were the subsistence resource staples?
- What areas were the foci of subsistence activities?
- What was the relative contribution of hunting, gathering, and cultivation?
- Could the available mix of food resources in the area support a year round occupation, or would resources in other areas have to be exploited at some point in the annual round?
- What were the annual rounds of Ceramic period hunter-gatherers in the different parts of the region?
- Was residential or logistical mobility employed in the procurement of wild plant resources?

Therefore, LA 181702 is recommended eligible for listing in the NRHP, under Criterion d.

References Cited

Hogan, Patrick F.

2006 *Development of Southeastern New Mexico Regional Research Design and Cultural Resource Management Strategy*. Report No. 185-849. Office of Contract Archeology, University of New Mexico, Albuquerque. Submitted to USDI Bureau of Land Management, New Mexico State Office, Santa Fe.

Ward, Christine G., and Bradley J. Vierra (editors)

2011 *Mitigation of Three Archaeological Sites in the New IBCT Training Area, East McGregor Range, Fort Bliss Military Reservation, Otero County, New Mexico*. Technical Report 11-34. Statistical Research, El Paso, Texas.

REFERENCES CITED

Adams, Karen R., Susan Smith, and Chad Yost
2011 Subsistence Analysis. In *Mitigation of Three Archaeological Sites in the New IBTC Training Area, East McGregor Range, Fort Bliss Military Installation, Otero County, New Mexico*, edited by Christine G. Ward and Bradley J. Vierra, pp. 245–262. Historic and Natural Resources Report No. 10-24. Technical Report 11-34. Statistical Research, El Paso, Texas.

American Society for Photogrammetry and Remote Sensing (ASPRS)
2008 LAS Specification Version 1.2. Electronic document, http://www.asprs.org/a/society/committees/standards/asprs_las_format_v12.pdf, accessed May 18, 2015.

Amick, Daniel S.
1995 Patterns of Technological Variation among Folsom and Midland Projectile Points in the American Southwest. *Plains Anthropologist* 40:23–38.

Amick, Daniel S., and Paul D. Lukowski
2006 Late Pleistocene and Early Holocene Projectile Points at Fort Bliss, Southern Tularosa Basin, New Mexico and West Texas. *Current Research in the Pleistocene* 23:75–79.

Anderson, David G., and Kenneth E. Sassaman
1996 *The Paleoindian and Early Archaic Southeast*. University of Alabama Press, Tuscaloosa.

Anderson, Sally
1993 Archaic Period Land Use in the Southern Tularosa Basin, New Mexico. In *Preliminary Investigations of the Archaic in the Region of Las Cruces, New Mexico*, edited by Richard S. MacNeish, pp. 48–67. Historic and Natural Resources Report No. 9. Cultural Resources Management Branch, Directorate of Environment, U.S. Army Air Defense Artillery Center, Fort Bliss, Texas.

Beckett, Patrick H., and Richard S. MacNeish
1994 The Archaic Chihuahua Tradition of South-Central New Mexico and Chihuahua, Mexico. In *Archaic Hunter-Gatherer Archaeology in the American Southwest*, edited by Bradley J. Vierra, pp. 335–372. Contributions in Anthropology, vol. 13, no. 1. Eastern New Mexico University, Portales.

Black, Stephen L., and Darrell G. Creel
1997 The Central Texas Burned Rock Midden Reconsidered. In *Hot Rock Cooking on the Greater Edwards Plateau: Four Burned Rock Midden Sites in West Central Texas*, edited by Stephen L. Black, Linda W. Ellis, Darrell G. Creel, and Glenn T. Goode, pp. 269–314. Studies in Archeology No. 22, vol. 1. Archeology Studies Program Report No. 2. Texas Department of Transportation, Environmental Affairs Division, Austin. Texas Archeological Research Laboratory, University of Texas, Austin.

Black, Stephen L., Linda W. Ellis, Darrell G. Creel, and Glenn T. Goode
1997 *Hot Rock Cooking on the Greater Edwards Plateau: Four Burned Rock Midden Sites in West Central Texas*. Texas Archeological Research Laboratory, University of Texas, Austin.

Black, Stephen L., and Alston V. Thoms
2014 Hunter-Gatherer Earth Ovens in the Archaeological Record: Fundamental Concepts. *American Antiquity* 79(2):204–226.

Bofinger, Jörg, and Ralf Hesse
2011 As Far as the Laser Can Reach. . . Laminar Analysis of LiDAR Detected Structures as a Powerful Instrument for Archaeological Heritage Management in Baden-Württemberg, Germany. In *Remote Sensing for Archaeological Heritage Management*, edited by David C. Cowley, pp. 163–173. Occasional Paper No. 5. Europae Archaeologia Consilium (EAC), Brussel, Belgium.

Bohrer, Vorsila L.
2007 Behavioral Ecology, Optimal Foraging, and the Diet Breadth Model. In *Preceramic Subsistence in Two Rock Shelters in Fresnal Canyon, South Central New Mexico*, edited by Vorsila L. Bohrer, pp. 135–144. University of Arizona Press, Tucson.

Breiman, Leo
2001 Random Forests. *Machine Learning* 45:5–32.

Brown, David E. (editor)
1994 *Biotic Communities: Southwestern United States and Northwestern Mexico*. University of Utah Press, Salt Lake City.

Bureau of Land Management (BLM)
2008 *Memorandum of Agreement (MOA) among U.S. Department of the Interior, Bureau of Land Management New Mexico State Office (BLM); and New Mexico State Historic Preservation Officer (SHPO); and Advisory Council on Historic Preservation (ACHP) Concerning Improved Strategies for Managing Historic Properties within the Permian Basin, New Mexico*. BLM MOA NM-930-2008-003. Bureau of Land Management, New Mexico State Office, Santa Fe.

Cable, John S.
1996 Haw River Revisited: Implications for Modeling Terminal Late Glacial and Early Holocene Hunter-gatherer Settlement Systems in the Southeast. In *The Paleoindian and Early Archaic Southeast*, edited by David G. Anderson, and Kenneth E. Sassaman, pp. 107–148. University of Alabama Press, Tuscaloosa.

Carmichael, David
1986 *Archaeological Survey in the Southern Tularosa Basin of New Mexico*. Historic and Natural Resources Report No. 3. Project No. 79-01. Environmental Management Office, Directorate of Engineering and Housing, U.S. Army Air Defense Artillery Center, Fort Bliss, Texas. Publications in Anthropology 10. Centennial Museum, University of Texas, El Paso.

Carpenter, John P., Guadalupe Sánchez, and María Elisa Villalpando C.
2005 The Late Archaic/Early Agricultural Period in Sonora, Mexico. In *The Late Archaic across the Borderlands: From Foraging to Farming*, edited by Bradley J. Vierra, pp. 13–40. Texas Archaeology and Ethnohistory Series. University of Texas Press, Austin.

Castetter, Edward F.
1935 *Uncultivated Plants Used as Sources of Food.* Ethnobiological Studies in the American Southwest, Vol 1. Bulletin No. 266. University of New Mexico, Albuquerque.

Challis, Keith, Paolo Forlin, and Mark Kincey
2011 A Generic Toolkit for the Visualization of Archaeological Features on Airborne LiDAR Elevation Data. *Archaeological Prospection* 18:279–289.

Challis, Keith, and Andy J. Howard
2013 The Role of Lidar Intensity Data in Interpreting Environmental and Cultural Archaeological Landscapes. In *Interpreting Archaeological Topography—Airborne Laser Scanning, Aerial Photographs and Ground Observation*, edited by Rachel Opitz and David C. Cowley, pp. 163–172. Oxbow, Oxford.

Collins, Michael B.
1999 Clovis and Folsom Lithic Technology on and near the Southern Plains: Similar Ends, Different Means. In *Folsom Lithic Technology*, edited by Daniel S. Amick, pp. 12–38. Archaeological Series No. 12. International Monographs in Prehistory, Ann Arbor, Michigan.

Condon, Peter C.
2006 Paleoamerican Stone Selection at Blackwater Locality No. 1: Alibates Silicified Dolomite and Edwards Plateau Chert Frequency Analysis. *Current Research in the Pleistocene* 23:94–95.

Corley, John A.
1965 A Proposed Eastern Extension of the Jornada Branch of the Mogollon. *Bulletin of the Lea County Archaeological Society* 1:30–36.

Creel, Darell G.
1999 Assessing the Relationship between Burned Rock Midden Distribution and Archaic Subsistence in West Central Texas. In *The Burned Rock Middens of Texas: An Archaeological Symposium*, edited by Thomas R. Hester, pp. 33–44. Studies in Archeology No. 13. Texas Archeological Research Laboratory, University of Texas, Austin. Jointly Published by the Texas Archaeological Research Laboratory and the Council of Texas Archeologists.

Cummings, Linda Scott, and Peter Kováčik
2013 *Macrofloral, Phytolith, and Starch Analyses, and AMS Radiocarbon Dating for the Permian Basin MOA, New Mexico*. Technical Report No. 13-050. PaleoResearch Institute, Golden, Colorado. Prepared for the U.S. Department of the Interior Bureau of Land Management, New Mexico Field Office, Carlsbad, New Mexico.

Dering, Phillip J.
1997 Macrobotanical Remains: Appendix D. In *Hot Rock Cooking on the Greater Edwards Plateau: Four Burned Rock Midden Sites in West Central Texas*, edited by Stephen L. Black, Linda W. Ellis, Darrell G. Creel, and Glenn T. Goode, pp. 571–600. Studies in Archeology No. 22. Texas Archeological Research Laboratory, University of Texas, Austin.

2003 Appendix B: Plant Remains from Sites 41BR392, 41BR500, and 41BR522 Located on Camp Bowie, Brown County, Texas. In *Archeological Testing of Four Sites on Camp Bowie, Brown County, Texas*, edited by Jason D. Weston and Raymond P. Mauldin. Archaeological Survey Report No. 335. Center for Archaeological Research, University of Texas, San Antonio.

2007 Assessment of Botanical and Faunal Assemblages from the Paleoindian and Early Archaic Components on the Periphery of the Southern Plains. *Bulletin of the Texas Archaeological Society* 78:177–195.

2011 Plant Remains from Middens in the Sacramento Mountains. In *Burned Rock Middens of the Southern Sacramento Mountains*, edited by Myles R. Miller, Tim B. Graves, Moira Ernst, and Michael Stowe, pp. 229–248. Fort Bliss Cultural Resources Report No. 09-28. GMI Report No. 782EP. Geo-Marine, El Paso, Texas.

Devereux Benjamin J., Gabriel S. Amable, and P. Crow
2008 Visualisation of LiDAR Terrain Models for Archaeological Feature Detection. *Antiquity* 82(316):470–479.

Dick-Peddie, William A.
1993 *New Mexico Vegetation: Past, Present and Future*. 1st ed. University of New Mexico Press, Albuquerque.

Driver, Harold E., and William C. Massey
1957 *Comparative Studies of North American Indians*. Transactions of the American Philosophical Society, New Series, Vol. 47, Part 2. American Philosophical Society, Philadelphia.

Freeman, Elizabeth, and Tracey Frescino
2009 *ModelMap: Modeling and Map Production Using Random Forest and Stochastic Gradient Boosting*. U.S. Department of Agriculture Forest Service, Rocky Mountain Research Station, Ogden, Utah.

Funk, R. E.
1978 Post-Pleistocene Adaptations. In *Northeast Handbook of North American Indians*, vol. 15, edited by Bruce G. Trigger, pp. 16–27. William C. Sturtevant, general editor, Smithsonian Institution, Washington, D.C.

GIS in the Rockies
2012 Introduction to Lidar: Geospatial Solutions. Electronic document, http://www.slideshare.net/GISITR/gis-in-therockiesintrotolidarworkshop2012, accessed May 18, 2015.

Green, F. Earl
1963 The Clovis Blades: An Important Addition to the Llano Complex. *American Antiquity* 29:145–165.

Greer, John W.
1965 A Typology of Midden Circles and Mescal Pits. *Southwestern Lore* 31(3):41–55.

Hall, Stephen A.
2002 *Field Guide to the Geoarchaeology of the Mescalero Sands, Southeastern New Mexico*. New Mexico Historic Preservation Division and the U.S. Department of the Interior, Bureau of Land Management, New Mexico State Office, Santa Fe.

Hammatt, H. H.
1976 The Gore Pit Site: An Archaic Occupation in Southwestern Oklahoma and a Review of the Archaic Stage in the Southern Plains. *Plains Anthropologist* 21:245–277.

Hard, Robert J., Raymond P. Mauldin, and Gerry R. Raymond
1996 Mano Size, Stable Carbon Isotope Ratios, and Macrobotanical Remains as Multiple Lines of Evidence of Maize Dependence in the American Southwest. *Journal of Archaeological Method and Theory* 3:253–318.

Hard, Robert J., and John R. Roney
2005 The Transition to Farming on the Rio Casas Grandes and in the Southern Jornada Mogollon Region in the North American Southwest. In *The Late Archaic across the Borderlands: From Foraging to Farming*, edited by Bradley J. Vierra, pp. 141–186. Texas Archaeology and Ethnohistory Series. University of Texas Press, Austin.

Haukos, David A.
1997 *Common Flora of the Playa Lakes*. Texas Tech University Press, Lubbock.

Hawley, John W.
1986 Physiographic Provinces and Landforms of New Mexico. In *New Mexico in Maps*, edited by Jerry L. Williams, pp. 23–31. 2nd ed. University of New Mexico Press, Albuquerque.

Heilen, Michael
2005 *An Archaeological Theory of Landscapes.* Ph.D. dissertation, Department of Anthropology, University of Arizona. UMI Press, Ann Arbor, Michigan.

2014 Memorandum: Progress on GAPP Screening Tool Demo for Norrisville Township and Surrounding Townships, Harrison County, Ohio. Submitted to Gas and Preservation Partnership, Washington, D.C. Manuscript in possession of the author.

Heilen, Michael P., and Jeffrey A. Homburg
2006 Modeling Soil Quality in Ancient Agricultural Landscapes of Southeastern Arizona. Poster presented at the Archaeological Sciences in the Americas Conference 2006, Tucson, Arizona.

2007 Assessing Soil Quality in Ancient Agricultural Landscapes of Southern Arizona. Poster presented at the International Annual Meeting of the American Society of Agronomy–Crop Science Society of American–Soil Science Society of America, New Orleans, Louisiana.

Heilen, Michael P., Phillip O. Leckman, Adam Byrd, Jeffrey A. Homburg, and Robert A. Heckman
2013 *Archaeological Sensitivity Modeling in Southern New Mexico: Automated Tools and Models for Planning and Management*. Technical Report 11-26. Statistical Research, Tucson, Arizona.

Hesse, Ralf
2010 LiDAR-derived Local Relief Models—A New Tool for Archaeological Prospection. *Archaeological Prospection* 17:67–72.

Hester, James J.
1972 *Blackwater Locality No. 1: A Stratified, Early Man Site in Eastern New Mexico*. Publication No. 8. Fort Burgwin Research Center, Southern Methodist University, Ranchos de Taos, New Mexico.

Hester, Thomas R. (editor)
1999 *The Burned Rock Middens of Texas: An Archaeological Symposium*. Studies in Archeology No. 13. Texas Archeological Research Laboratory, University of Texas, Austin. Jointly Published by the Texas Archaeological Research Laboratory and the Council of Texas Archeologists.

Hogan, Patrick F.
2006 *Development of Southeastern New Mexico Regional Research Design and Cultural Resource Management Strategy*. Report No. 185-849. Office of Contract Archeology, University of New Mexico, Albuquerque. Submitted to the U.S. Department of the Interior Bureau of Land Management, New Mexico State Office, Santa Fe.

Holliday, Vance T.
1997 *Paleoindian Geoarchaeology of the Southern High Plains*. Texas Archaeology and Ethnohistory Series. University of Texas Press, Austin.

Howard, Margaret Ann
1999 Burned Rock Midden Excavations, Hearths and Botanical Remains. In *The Burned Rock Middens of Texas: An Archaeological Symposium*, edited by Thomas R. Hester, pp. 45–70. Studies in Archeology No. 13. Texas Archeological Research Laboratory, University of Texas, Austin. Jointly Published by the Texas Archaeological Research Laboratory and the Council of Texas Archeologists.

Hughes, Jack T., and Patrick S. Willey
1978 *Archeology at Mackenzie Reservoir*. Archeological Survey Report No. 24. Texas Historical Commission, Austin.

Irwin-Williams, Cynthia
1973 *The Oshara Tradition: Origins of Anasazi Culture*. Contributions in Anthropology, vol. 5, no. 1. Paleo-Indian Institute, Eastern New Mexico University, Portales.

Jelinek, Authur J.
1967 *A Prehistoric Sequence in the Middle Pecos Valley, New Mexico*. Anthropological Paper No. 31. Museum of Anthropology, University of Michigan, Ann Arbor.

Katz, Susana R., and Paul R. Katz
1985a *The Prehistory of the Carlsbad Basin, Southeastern New Mexico*. Bureau of Reclamation, Southwest Regional Office, Amarillo, Texas.

1985b *The History of the Carlsbad Basin, Southeastern New Mexico: Technical Report of Historic Archaeological Investigations in the Brantley Project Locality*. Incarnate Word College, San Antonio. Submitted to the U.S. Department of the Interior, Bureau of Reclamation, Southwest Regional Office, Amarillo, Texas.

1993 *Archaeological Overview of Southeastern New Mexico*. New Mexico Historic Preservation Division, Santa Fe.

Katz, Susana R., and Paul Katz (editors)
2001 *The Archaeological Record of Southern New Mexico: Sites and Sequences of Prehistory*. Project No. 35-99-1426419. HSR Environmental Services, Santa Clara, California.

Kokalj, Žiga, Krištof Oštir, and Klemmen Zakšek
2011 Application of Sky-view Factor for the Visualization of Historic Landscape Features in Lidar-derived Relief Models. *Antiquity* 85(327):263–273.

Kokalj, Žiga, Klemmen Zakšek, and Krištof Oštir
2013 Visualizations of Lidar Derived Relief Models. In *Interpreting Archaeological Topography—Airborne Laser Scanning, Aerial Photographs and Ground Observation*, edited by Rachel Opitz and David C. Cowley, pp. 100–114. Oxbow, Oxford.

Kvamme, Kenneth L.
1988a Using Existing Archaeological Survey Data for Model Building. In *Quantifying the Present and Predicting the Past: Theory, Method, and Application of Archaeological Predictive Modeling*, edited by W. James Judge and Lynne Sebastian, pp. 301–323. U.S. Department of the Interior, Bureau of Land Management, Denver, Colorado.

1998b Development and Testing of Quantitative Models. In *Quantifying the Present and Predicting the Past: Theory, Method, and Application of Archaeological Predictive Modeling*, edited by W. James Judge and Lynne Sebastian, pp. 325–428. U.S. Department of the Interior, Bureau of Land Management, Denver, Colorado.

Lehmer, Donald J.
1948 *The Jornada Branch of the Mogollon*. Social Science Bulletin No. 17. University of Arizona, Tucson.

Leslie, Robert H.
1978 Projectile Point Types and Sequences of the Eastern Jornada-Mogollon, Extreme Southeastern New Mexico. In *Transactions of the 13th Regional Archaeological Symposium for Southeastern New Mexico and West Texas*, pp. 81–157. Midland, Texas.

1979 The Eastern Jornada Mogollon: Extreme Southeastern New Mexico (A Summary). In *Jornada Mogollon Archaeology: Proceedings of the First Jornada Conference*, edited by Patrick H. Beckett and Regge N. Wiseman, pp. 179–199. New Mexico Historic Preservation Division, Santa Fe.

Levine, Ned
2015 *CrimeStat*: A Spatial Statistics Program for the Analysis of Crime Incident Locations (v 4.02). Ned Levine & Associates, Houston, Texas, and the National Institute of Justice, Washington, D.C. August.

Lillesand, Thomas, and Ralph W. Kiefer
1999 *Remote Sensing and Image Interpretation*. 4th ed. John Wiley and Sons, New York.

Louderback, Lisbeth A., Bruce M. Pavlik, and Amy M. Spurling
2013 Ethnographic and Archaeological Evidence Corroborating Yucca as a Food Source, Mojave Desert, USA. *Journal of Ethnobiology* 33(2):281–297.

MacNeish, Richard S. (editor)
1993 *Preliminary Investigations of the Archaic in the Region of Las Cruces, New Mexico*. Historic and Natural Resources Report No. 9. Directorate of Environment, Cultural Resources Management Branch, U.S. Army Air Defense Artillery Center, Fort Bliss, Texas.

Mera, H. P.
1938 "Mescal Pits"—Misnomer. *Science* 77:168–169.

Miller, Myles R., Tim B. Graves, Moira Ernst, and Michael Stowe
2011 *Burned Rock Middens of the Southern Sacramento Mountains*. Fort Bliss Cultural Resources Report No. 09-28. GMI Report No. 782EP. Geo-Marine, El Paso, Texas.

Miller, Myles R., Tim B. Graves, and Melinda Landreth
2012 *Further Investigations of Burned Rock Middens and Associated Settlements: Mitigation of Three Sites for the IBTC, Fort Bliss, Otero County, New Mexico*. Fort Bliss Cultural Resources Report No. 10-21. GMI Report No. 790EP. Geo-Marine, El Paso, Texas.

Miller, Myles R., and Nancy A. Kenmotsu
2004 Prehistory of the Eastern Trans-Pecos and Jornada Mogollon Regions of West Texas. In *The Prehistory of Texas*, edited by T. K. Pertulla, pp. 205–265. Texas A&M University Press, College Station.

Miller, Myles R., Nancy Kenmotsu, and Mel Landreth (editors)
2009 *Significance and Research Standards for Prehistoric Archaeological Sites at Fort Bliss: A Design for the Evaluation, Management, and Treatment of Cultural Resources*. Report No. 697EP. Geo-Marine, El Paso, Texas. Cultural Resources Report No. 05-16. Directorate of Public Works, Environmental Division, Cultural Resources Branch, U.S. Army Air Defense Artillery Center, Fort Bliss, Texas.

Miller, Myles R., and M. Steven Shackley
1998 New Interpretations of Obsidian Procurement and Movement in the Jornada Mogollon Region of West Texas, Southern New Mexico, and Northern Chihuahua. Paper presented at the annual meeting of the Texas Archaeological Society, Waco.

Millward, Sarah A.
2010 Thermal Features in Southeastern New Mexico: An Economic Analysis. Unpublished Masters thesis, Eastern New Mexico University, Portales New Mexico.

National Oceanographic and Atmospheric Administration Coastal Services Center
2012 Lidar 101: An Introduction to Lidar Technology, Data, and Applications. Electronic document, http://coast.noaa.gov/digitalcoast/_/pdf/lidar101.pdf, accessed May 18, 2015.

Nayegandhi, Amar
2007 Lidar Technology Overview. Electronic document, http://www.google.com/url?sa=t&rct=j&q=&esrc=s&source=web&cd=1&cad=rja&uact=8&ved=0CB4QFjAA&url=http%3A%2F%2Flidar.cr.usgs.gov%2Fdownloadfile2.php%3Ffile%3DNayegandhi_Lidar_Technology_Overview.pdf&ei=r69kVfHPIsvQtQW_lICgCA&usg=AFQjCNHGOs1PSIyFva8slXP61Agi227iWg&bvm=bv.93990622,d.b2w, accessed May 18, 2015.

O'Laughlin, Thomas C.
1980 *The Keystone Dam Site and Other Archaic and Formative Sites in Northwest El Paso, Texas*. Publications in Anthropology No. 8. Centennial Museum, University of Texas, El Paso.

Opler, M. E.
1969 *Apache Odyssey: A Journey between Two Worlds*. Holt, Reinhart and Wilson, New York.

Petraglia, Michael D.
2002 The Heated and the Broken: Thermally Altered Stone, Human Behavior, and Archaeological Site Formation. *North American Archaeologist* 23:241–269.

Prasad, Anantha M., Louis R. Iverson, and Andy Liaw
2006 Newer Classification and Regression Tree Techniques: Bagging and Random Forests for Ecological Prediction. *Ecosystems* 9:181–199.

Pratt, Boyd C., Dan Scurlock, and Vernon J. Glover
1989 *Llano, River, and Mountains: The Southeast New Mexico Regional Overview*. New Mexico Historic Preservation Division, Santa Fe.

Prewitt, Elton R.
1991 Burned Rock Middens: A Summary of Previous Investigations and Interpretations. In *The Burned Rock Middens of Texas: An Archaeological Symposium*, edited by Thomas R. Hester, pp. 25–32. Studies in Archeology No. 13. Texas Archeological Research Laboratory, University of Texas, Austin. Jointly Published by the Texas Archaeological Research Laboratory and the Council of Texas Archeologists.

Quigg, Mike, Mark Sechrist, and Grant Smith
2002 *Testing and Data Recovery of Burned Rock Features in Sites on Otero Mesa, New Mexico*. Fort Bliss Cultural Resources Report No. 99-14. TRC Mariah Associates, El Paso Texas. TRC Report No. was not stipulated.

Railey, Jim A., John Rissetto, and Matthew Bandy (editors)
2009 *Synthesis of Excavation Data for the Permian Basin Mitigation Program*. SWCA Environmental Consultants, Albuquerque, New Mexico. Prepared for the U.S. Department of the Interior Bureau of Land Management, Carlsbad Field Office, Carlsbad, New Mexico.

R Development Core Team
2008 *R: A Language and Environment for Statistical Computing*. R Foundation for Statistical Computing, Vienna, Austria.

Reeves, C. C., Jr.
1972 Tertiary-Quaternary Stratigraphy and Geomorphology of West Texas and Southeastern New Mexico. In *Guidebook of East-Central New Mexico: New Mexico Geological Society Twenty-Third Field Conference, September 28, 29, and 30, 1972*, edited by Vincent Cooper Kelley and Frederick D. Trauger, pp. 108–117. New Mexico Geological Society, Socorro.

Scurlock, Dan
1998 *From the Rio to the Sierra: An Environmental History of the Middle Rio Grande Basin*. General Technical Report No. RMRS-GTR-5. Rocky Mountain Research Station, Fort Collins, Colorado.

Sebastian, Lynne, and Signa Larralde
1989 *Living on the Land: 11,000 Years of Human Adaptation in Southeastern New Mexico: An Overview of Cultural Resources in the Roswell District, Bureau of Land Management*. Cultural Resources Series No. 6. U.S. Department of the Interior Bureau of Land Management, New Mexico State Office, Santa Fe.

Shelley, Phillip H.
1994 Review of the Archaic Archaeology of the Llano Estacado and Adjacent Areas of New Mexico. In *Archaic Hunter-Gatherer Archaeology in the American Southwest*, edited by Bradley J. Vierra, pp. 372–404. Contributions in Anthropology, vol. 13, no. 1. Eastern New Mexico University, Portales.

Simpson, Sean
2010 Holocene Thermal Feature Types in Archaeological Sites of the Mescalero Sands Environment, New Mexico. Unpublished Masters thesis, University of Nevada, Reno.

Stanford, Dennis J.
1991 Clovis Origins and Adaptations: An Introductory Perspective. In *Clovis: Origins and Adaptations*, edited by Robson Bonnichson and Karen L. Turnmire, pp. 1–14. Center for the Study of the First Americans, Oregon State University, Corvallis.

Statistical Research, Inc.
2013 *Quotation to Conduct Aerial LIDAR Survey of Three Localities West and Northwest of Carlsbad, New Mexico, Vol. 1: Technical Quotation*. Request for Quotations No. L13PS00947. Statistical Research, Albuquerque, New Mexico. Submitted to the U.S. Bureau of Land Management, Denver, Colorado.

Štular, Benjamin, Žiga Kokalj, Krištof Oštir, and Laure Nuniger
2012 Visualization of Lidar-derived Relief Models for Detection of Archaeological Features. *Journal of Archaeological Science* 39:3354–3360.

Suhm, Dee Ann
1960 A Review of Central Texas Archeology. *Bulletin of the Texas Archeological Society* 29:63–67.

Tagg, Martyn D.
1996 Early Cultigens from Fresnal Shelter, Southeastern New Mexico. *American Antiquity* 61:311–324.

Thoms, Alston V.
2008 Ancient Savannah Roots of the Carbohydrate Revolution in South-Central North America. *Plains Anthropologist* 53:121–136.

2009 Rocks of Ages: Propagation of Hot-rock Cookery in Western North America. *Journal of Archaeological Science* 36(3):573–591.

Tuan, Yi-Fu, Cyril E. Everard, Jerold G. Widdison, and Iven Bennett
1973 *The Climate of New Mexico*. New Mexico State Planning Office, Santa Fe.

Turner, Ellen Sue, and Thomas R. Hester
1993 *A Field Guide to Stone Artifacts of Texas Indians*. 2nd ed. Texas Monthly Field Guide Series. Gulf Publishing, Houston.

Upham, Steadman, Richard S. MacNeish, Walton C. Galinat, and Christopher M. Stevenson
1987 Evidence Concerning the Origin of Maize de Ocho. *American Anthropologist* 89:410–419.

U.S. Department of Agriculture
1995 *Soil Survey Geographic (SSURGO) Data Base: Data Use Information*. Miscellaneous Publication 1527. U.S. Department of Agriculture, Natural Resources Conservation Service, National Soil Survey Center. National Cartography and GIS Center, Fort Worth, Texas.

U.S. Environmental Protection Agency
2006 *National Hydrography Dataset Plus (NHDPlus)*. U.S. Environmental Protection Agency, Washington, D.C.

Vierra, Bradley J.
2007 Early Agriculture on the Southeastern Periphery of the Colorado Plateau: A Case of Diversity in Tactics. In *Archaeology without Borders: Contact, Commerce, and Change in the U.S. Southwest and Northwestern Mexico*, edited by Maxine E. McBrinn and Laurie D. Webster, pp. 71–88. University Press of Colorado, Boulder.

Vierra, Bradley J. (editor)
2005 *The Late Archaic across the Borderlands: From Foraging to Farming*. Texas Archaeology and Ethnohistory Series. University of Texas Press, Austin.

Vierra, Bradley J., Margaret A. Jodry, M. Steven Shackley, and Michael J. Dilley
2012 Late Paleoindian and Early Archaic Foragers in the Northern Southwest. In *From the Pleistocene to the Holocene: Human Organization and Cultural Transformations in Prehistoric North America*, edited by C. Britt Bousman and Bradley J. Vierra, pp. 171–196. Texas A&M Press, College Station.

Vierra, Bradley J., and Christine G. Ward
2012 *Mitigation of Three Archaeological Sites along and near El Paso Draw in the New Mexico IBTC Training Area, East McGregor Range, Fort Bliss Military Reservation, Otero County, New Mexico*. Historic and Natural Resources Report No. 11-14. Technical Report 12-56. Statistical Research, El Paso, Texas.

Wandsnider, Luann
1997 The Roasted and the Boiled: Food Composition and Heat Treatment with Special Emphasis on Pit-Hearth Cooking. *Journal of Anthropological Archaeology* 16:1–48.

Ward, Christine G., and Bradley J. Vierra
2011 *Mitigation of Three Archaeological Sites in the New IBTC Training Area, East McGregor Range, Fort Bliss Military Installation, Otero County, New Mexico*. Historic and Natural Resources Report No. 10-24. Technical Report 11-34. Statistical Research, El Paso, Texas.

Williams, Jerry L. (editor)
1986 *New Mexico in Maps*. 2nd ed. University of New Mexico, Albuquerque.